THE UNIVERSITY *of* EDINBURGH

Direction finding during mouse renal development

C-HONG CHANG

Doctor of Philosophy

Centre for Integrative Physiology

School of Biomedical Sciences

The University of Edinburgh

2014

Table of Contents

Declaration

I declare that:

(a) this thesis was composed by me;

(b) the work presented here is my own otherwise clearly stated; and

(c) the work has not been submitted for any other degree or professional qualification

_____

C-Hong Chang

Acknowledgements

I would like to express my gratitude to my supervisor Prof. Jamie Davies for his insightful advice and encouragement to write my thesis. I also want to thank his support for me to have several publications during the past enjoyable years. I am also grateful to my thesis committee members, Prof. Ian Mason and Dr. John West, for their helpful comments for my project.

I also want to thank Davies lab members who have brought an enthusiastic environment which helped me to concentrate on my project. Special thanks go to Dr. Melanie Lawrence and Christopher Mills for their invaluable comments on my thesis. I expand my appreciation to Dr. Elise Cachat, Weijia Liu, Dr. Roland Partridge and Kim martin for their support to my experiments. I thank to GUDMAP members, Dr. Jane Armstrong, Dr. Jane Brennan, and Sue Lloyd-MacGilp, for their kind help to use GUDMAP database and for, more importantly, an enjoyable chat with them.

I also want to stress the help kindly given by Viv Allison and Louise Dunn for histological techniques. Gratitude also goes to Dr. Owen Sansom (Beaton Institute) for giving me Lgr5-EGFP mouse embryos and Dr. Nicholas Ferreri (Department of Pharmacology, New York Medical College, US) for sending me raTAL cells.

I thank to my parents, Bong Woo Chang and Yeong Shin Lim, for their unlimited support and patience. At last, my deep gratitude goes to my wife Ga Hyun Kim, my son Seung Hu Chang, and my sister Seo Yeon Chang. Without my family, it would have been impossible to finish this work.

Abbreviations

ADH	antidiuretic hormone
ADP	adenosine diphosphate
Ang	angiopoietins
ATP	adenosine triphosphate
°	angle
°C	degrees centigrade
Bmp	bone marrow protein
CAM	chorioallantoic membrane
cAMP	cyclic adenosine monophosphate
cAR1	cAMP receptor 1
CD	collecting duct
CD1	mouse strain
cGMP	cyclic guanosine monophosphate
cm	centimetre
cond	conditioned medium
ctrl	control
d	day(s)
DAPI	4´,6-diamidino-2-phenylindole
2D	two dimensional
2DE	two-dimensional gel electrophoresis
DT	distal tubule
E	embryonic days
ECM	extracellular matrix
EDTA	ethylenediaminetetraacetic acid
EGF	epidermal growth factor
EGFP	enhanced green fluorescent protein
Ena/VASP	Enabled/vasodilator-stimulated phosphoprotein
FBS	foetal bovine serum
FITC	fluorescein isothiocyanate
GA-1000	gentamycin sulphate and amphotericin B
GAG	glycosaminoglycan

GAP	GTPase-activating protein
GDNF	glial-derived neural growth factor
GDP	guanosine diphosphate
Gfrα1	Gdnf family receptor alpha 1
Gm	glomerulus
GTP	guanosine triphosphate
GTPase	GTP-binding protein
GUDMAP	genitourinary developmental molecular anatomy project
h	hour(s)
HBP	heparin-binding protein
HSr	heparin-Separopore resin
IHC	immunohistochemistry
KCM	kidney culture medium
Lgr5	Leucine-rich repeat-containing G-protein coupled receptor 5
LIMK	LIM kinase
LoH	loop(s) of Henle
LV	low volume
Mdk	midkine
MEM	minimum essential medium
MET	mesenchymal-to-epithelial transition
µm	micrometer
MGI	mouse genome informatics
min	minute(s)
MM	metanephric mesenchyme
mm	millimetre
mM	millimolar
MSP	macrophage stimulating protein
Mt	matrix
mV	millivolt
NC	neighbouring cells
nm	nanometer
P	postnatal day
PBS	phosphate buffer saline
PDGFC	platelet-derived growth factor, C polypeptide

PFA	paraformaldehyde
PGC	Primordial germ cell
PI	propidium iodide
PI3K	phosphoinositide 3-kinase
PIP_2	phosphatidylinositol 4,5-bisphosphate
PIP_3	Phosphatidylinositol 3,4,5-triphosphate
P/S	penicillin/streptomycin
PT	proximal tubule
PTEN	Phosphatase and tensin homologue
Ptn	pleiotrophin
raTAL	rat thick ascending limb of Henle's loop
REBM	renal epithelial basal medium
REGM	renal epithelial growth medium
RMA	robust multi-array average
Robo	Roundabout
ROMK	renal outer medullary potassium channel
RPE	retinal pigment epithelial
RT	room temperature
RTK	receptor tyrosine kinase
RV	renal vesicle
σ	standard deviation
SEM	standard error of mean
Sema	semaphorin
sGC	Soluble guanylyl cyclase
SHH	sonic hedgehog
siRNA	small interfering ribonucleic acid
Smo	smoothened
Spry1	sprouty homolog 1
T3	triiodothronine
TBPS	0.1% Triton X-100 in PBS
TE	Trypsin EDTA
THP	Tamm-Horsfall protein
Tie	Tyrosine kinase with immunoglobulin-like loops and epidermal growth factor homology domain

TGFβ	transforming growth factor beta
TRITC	tetramethylrhodamine
UB	ureteric bud(s)
UC	ureteric bud cyst(s)
Umod	uromodulin
VE	vascular endothelial
VEGF	vascular endothelial growth factor
VEGFR	vascular endothelial growth factor receptor
WASP	Wiskott-Aldrich syndrome protein
WAVE	WASP-family verprolin homology protein
Wnt	Wingless-type MMTV integration site family

List of figures and tables

Abstract

The adult kidney consists of hundreds of thousands of fine epithelial tubules as functional units called nephrons. Nephrons have U-shaped tubules: loops of Henle that descend from the cortex to the medulla. This radial arrangement is critical to maintain water homeostasis in the kidney. Although Henle's loops are crucial to renal physiology, the cue(s) they uses to navigate to the medulla are not understood. In this thesis, I investigate how the loop of Henle elongates during mouse renal development and show that it is probably guided to the medulla by diffusible, heparin-binding molecules.

I used immumohistochemistry (IHC) on cryosections of embryonic kidneys to study the natural anatomy of the Henle's loop. I used a low-volume culture system to allow embryonic kidneys (both natural and tissue-engineered) to form loops of Henle *ex vivo* and manipulated their direction of growth. Time-lapse imaging of Lgr-5 EGFP embryonic kidneys demonstrated the movement of the apex of the loop which suggested the idea of guidance cue(s) acting on the loop of Henle. Cut-and-paste experiments showed that loops appeared to be attracted to maturing collecting duct. Co-culture with an exogenous tubule inducer suggested the embryonic spinal cord as another source to attract the loops. Using raTAL (rat thick ascending loop of Henle) and 6TA2 (embryonic collecting duct cells) cell lines, I designed and performed a cell migration assay to test whether raTAL was attracted to 6TA2 cells. raTAL cells were notably attracted to 6TA2 cells compared to other cell lines. raTAL cells were also attracted to 6TA2-conditioned medium, which indicated that raTAL cells were attracted by secreted molecule(s). To begin to characterise those secreted molecule(s), heparin-binding protein-coated beads were used in the cell migration system and showed that at least one critical guidance factor is heparin-binding.

From this study, I found that the apex of the Henle's loop does move and loops are attracted by secreted molecule(s) possibly from the collecting duct. Although target molecule(s) were unidentified, this study provides the first mechanistic information about the guidance of the loop of Henle. Moreover, this was the first study of guidance of epithelial tubule shafts (rather than tips) adding to our understanding of general tubule morphogenesis.

1 Chapter 1 Introduction to cell migration, kidney development, and the loop of Henle

1.1 Introduction

Patterning a complex organ is a highly elaborate process mediated by coordinated mechanisms to eventually construct its functional structures. In order to produce functional structures, individual cells or/and groups of cells have to undergo major biological processes such as cell differentiation, proliferation, cell death, and cell migration (Gilbert, 2013).

The main focus of this thesis is guidance of tube migration during development. In the few systems that have been well-studied, cell migration occurs at a tip region of a tube by sequence of orchestrated steps. Vascular sprouting is, for instance, led by its tip cell. Whereas cues guiding navigation at the tip region are relatively well understood, how a middle of a bent tube navigates remains to be determined.

The kidney is a great model to study this with respect to its unique U-shaped component, the loop of Henle (LoH). Therefore, I aim to use this system to study the guidance cue(s) underlying directional growth of the bend of a tube.

In this review chapter, I will present an account of our general understanding of guidance cues that mediate cell migration, followed by overview of mouse kidney development and, finally, development of the LoH.

1.2 Overview of cell navigation

Cell migration, a term that also refers to cell movement, is one of fundamental behaviours of cells. Cell migration plays crucial roles such as embryogenesis, immune responses and regeneration processes (Friedl and Weigelin, 2008, Kurosaka and Kashina, 2008, Friedl and Gilmour, 2009). In contrast, cell migration can also contribute to abnormal development. In cancer, for instance, cell migration aids cancer cell spreading, which eventually gives rise to cancer metastasis (Wells, 2006, Leong et al., 2012). However, both normal and abnormal cases provide valuable information to understand cell migration.

In terms of the number of cells that migrate, cell migration can broadly be classified into solitary or collective cell migration. Solitary cells migrate individually. A widely studied example is the migration of primordial germ cells (PGCs) towards the prospective gonad in zebrafish, mouse, and *Drosophila* models (Kunwar et al., 2006). Better examples include leukocyte extravasation to peripheral tissue for immune function, and hematopoietic stem cell migration from bone marrow to blood circulation, and neuronal migration in the nervous

system (Wright et al., 2001, Friedl and Weigelin, 2008, Cooper, 2013). In contrast to individual cell migration, collective cells migrate as a group, such as a two-dimensional (2D) sheet, coupled by cell-cell interactions while they migrate. I will review this later.

1.2.1 Mechanisms underlying individual cell migration

In order to move, a sequence of steps (the cell motility cycle) takes place at the leading edge of a cell (reviewed in Bravo-Cordero et al., 2013). A cell becomes polarized and shows protrusions as its initial response to guiding molecules. These protrusions take the formation of lamellipodia or filopodia (Mejillano et al., 2004). Their formation is triggered by small guanosine triphosphate (GTP)-binding proteins (GTPases) acting on actin polymerization (Ridley, 2001, Raftopoulou and Hall, 2004). The actin-based protrusions are stabilized by connecting the extracellular matrix (ECM) and the actin cytoskeleton. This adhesion also plays a role to pull on the cell body (Cramer, 2013). Finally, both actomyosin contractility and disassembled adhesion at the cell rear cause the retraction of the trailing edge of the cell (Cramer, 2013).

Although the overall structures of lamellipodia vary between different cell types, lamellipodia generally have a thin sheet structure composed of highly branched actin filament networks constructed by actin polymerization (Welch and Mullins, 2002). The protrusion can be illustrated by the 'Treadmilling model' (reviewed by Pollard and Borisy, 2003). Once a receptor of a cell receives extracellular stimuli, the receptor activates small GTPases of the Rho family and phosphatidylinositol 4,5-bisphosphate (PIP_2) followed by activating Wiskott-Aldrich syndrome protein (WASP)/WASP-family verprolin homology protein (WAVE) (Figure 1-1). WASP/WAVE recruits Arp2/3 complex and an ATP-actin monomer (Figure 1-1). The actin polymerization initiates by this Arp2/3 complex by its binding to the side or the barbed end of a pre-existing (old) actin filament to assemble new actin filaments (Figure 1-1) (Welch and Mullins, 2002, Pollard and Borisy, 2003). When the barbed end of filaments become free by Brownian motion (bending), the newly branched filaments form by adding actin to their ends and these elongated filaments spring back to their original position (Mogilner and Oster, 1996). This is so-called 'elastic Brownian ratchet' eventually pushes the membrane and results in the membrane protrusion (Mogilner and Oster, 1996). The elongation ceases when the barbed end of branches is capped by capping proteins (Cooper and Sept, 2008) (Figure 1-1). The capping proteins also bind to wrongly positioned branches to inhibit incorrect branching (Cooper and Sept, 2008). When

the actin filaments get older by ATP hydrolysis, ADF/cofilin facilitates dephosphorylation of actin filaments and reduces ADP-bound actins at the pointed ends of the filaments to actin monomers (Pavlov et al., 2007) (Figure 1-1). These ADP-actin monomers then become ATP-actin monomers by the exchange of ADP for ATP catalyzed by profilin (Witke, 2004) (Figure 1-1). These ATP-actin monomers are recycled for new actin polymerization (Figure 1-1). Therefore, membrane protrusion relies on the actin polymerization, uncapping new ends of filaments, and severing older ends of filaments (Condeelis, 1993, Zigmond, 1996).

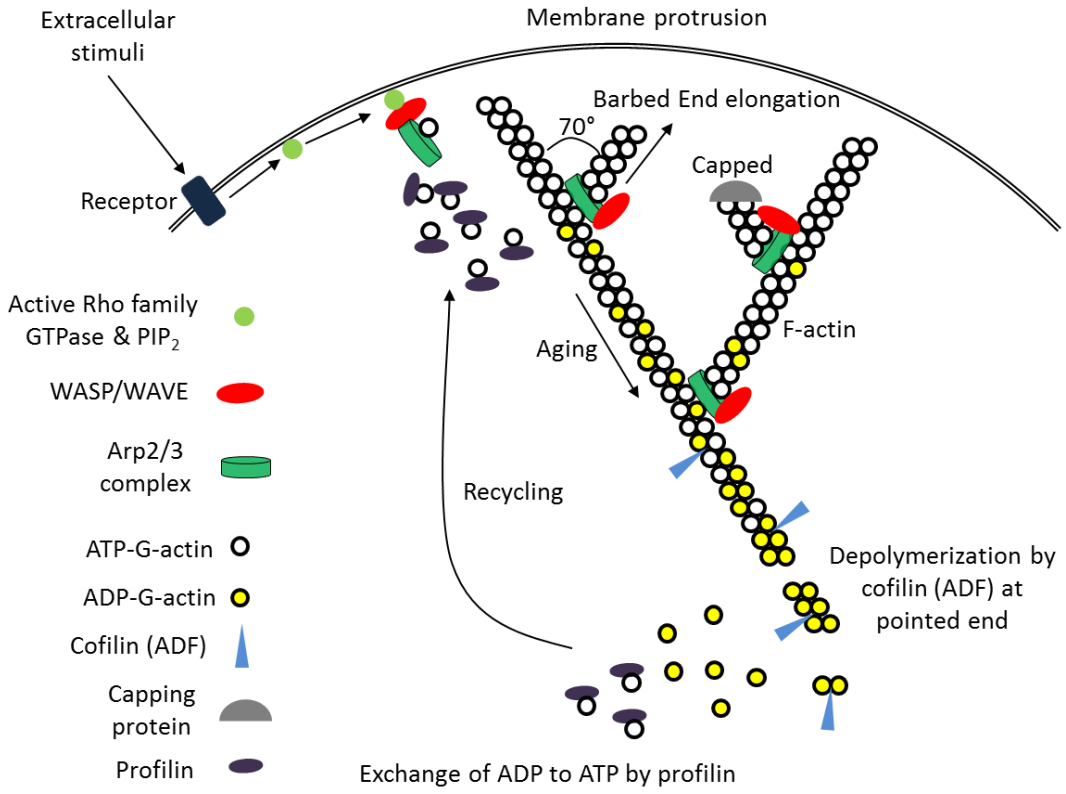

Figure 1-1 A simplified diagram of treadmilling model for cell membrane protrusion by actin polymerization and depolymerization (Redrawn and modified from a figure in Pollard and Borisy, 2003).

Filopodia are another protrusive structure seen at the leading edge of migrating cells, reaching beyond lamellipodia. Filopodia are morphologically different from lamellipodia. They have long and thin finger-like structures composed of parallel bundles of unbranched F-actins (Mattila and Lappalainen, 2008). Similar to lamellipodia, filopodial protrusion is also thought to be mediated by a filament treadmilling model (Welch and Mullins, 2002, Ridley et al., 2003). However, the Arp2/3 complex and the capping proteins are almost

absent in filopodial tips, suggesting the use of different proteins such as the enabled/vasodilator-stimulated phosphoprotein (Ena/VASP) family protein MENA, fascin, and Irsp53 to form a bundle of unbranched long filaments (Krause et al., 2003, Vignjevic et al., 2006). Ena/VASP proteins inhibit end capping and branching by binding at the barbed end (Krause et al., 2003). Fascin and Irsp53 are actin-bundling proteins that might increase the stiffness of filopodia to push the membrane efficiently (Welch and Mullins, 2002, Vignjevic et al., 2006).

Both lamellipodia and filopodia are regulated by central regulators, the Rho family small GTPase proteins; Rac, and Cdc42 (Nobes and Hall, 1995, Raftopoulou and Hall, 2004, Heasman and Ridley, 2008). Rho family GTPases proteins are regulated by binding to GTP (active form) or GDP (inactive form) (Jaffe and Hall, 2005). The active form of Rho GTPases binds to downstream molecules to regulate lamellipodia and filopodia (Heasman and Ridley, 2008). Rac and Cdc42 are major GTPases proteins regulating the cell protrusions (Nobes and Hall, 1995, Raftopoulou and Hall, 2004). One of downstream targets for Rac is WAVE complex which activates Arp2/3 to proceed actin polymerization for lamellipodia (Heasman and Ridley, 2008) (Figure 1-2). Cdc42 also mediates actin polymerization via WASP or Irsp53 to form filopodia (Krugmann et al., 2001) (Figure 1-2). Rac and Cdc42 both can induce actin polymerization by activating mDia2 (Heasman and Ridley, 2008) (Figure 1-2). In addition, Rac and Cdc42 shares Ser/Thr kinase PAK to LIM kinase (LIMK) pathway to inhibit cofilin activation to regulate actin turnover for lamellipodia and filopodia respectively (Edwards et al., 1999) (Figure 1-2).

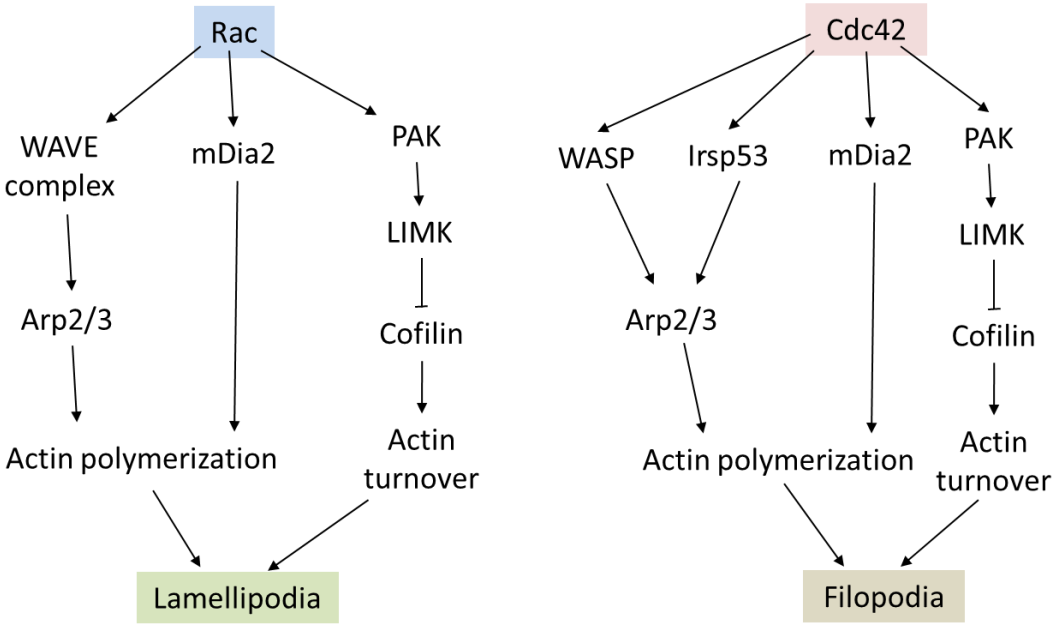

Figure 1-2 Rho GTPases associated pathways to form lamellipodia and filopodia (Image adapted and redrawn from Heasman and Ridley, 2008).

In order for cells to advance forward in response to a cue, cells have to protrude at the leading edge and to pull the cell body and to retract the trailing edge. Importantly, cell matrix adhesion between actin cytoskeleton and the substratum plays a role of a "molecular clutch" during cell locomotion (Hu et al., 2007, Le Clainche and Carlier, 2008). This adhesion is mediated by a transmembrane receptor family, integrin heterodimers that consist of α and β subunits (Ivaska, 2012). When the integrin is activated by binding to extracellular ligands, it gives rise to conformational changes of the receptors to cluster integrin (Cluzel et al., 2005). The integrin clustering begins intracellular signaling including small GTPases activation, which eventually determines the adhesion site (Cluzel et al., 2005). The integrin is in an active form predominantly at the site where the adhesion occurs (Ridley et al., 2003). If this molecular clutch (integrin) is disengaged from the actin cytoskeleton, the cell cannot protrude since the force produced by actin elongation is expended on retrograde flow (Figure 1-3). Conversely, if the clutch is engaged with the actin assembly, cell protrusion takes place by the force from the actin polymerization acting at the leading edge of the cell (Figure 1-3). The molecular clutch also regulates cell body traction and the tail retraction by myosin II with actin filaments (actomyosin) tension that is transmitted to the focal adhesion (Ivaska, 2012) (Figure 1-3).

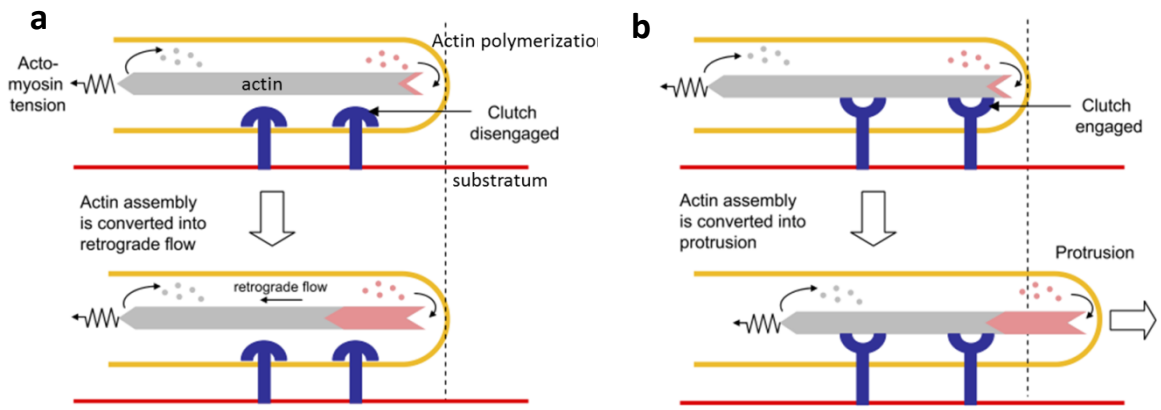

Figure 1-3 Adhesions between the substratum and actin assembly for cell advance (Image adapted and modified from Le Clainche and Carlier, 2008)

As a final step for cell locomotion, adhesions at the cell rear should be disassembled. As a cell advances at the leading edge by protrusion, the actomyosin-generated tension (myosin II-based contractile force) at the rear increases and is sufficient to release the adhesion between the integrin and the actin filament (Cramer, 2013). Other forces can also drive the retraction of the rear. A study in fibroblasts reported that, instead of myosin II-motor-based force, actin filament depolymerisation establishes retraction at the rear (Mseka and Cramer, 2011). Another study in nematode worm sperm cells reported that the force originating from macrophage stimulating protein (MSP) depolymerisation drives rear retraction (these cells lack actin and motor proteins) (Shimabukuro et al., 2011). Therefore, both myosin II-based contractility and actin disassembly are thought to drive retraction at the cell rear.

1.2.2 Types of guidance cues

In order for cells to migrate using the highly organized motility machinery described in the previous section, guidance cue(s) are required to trigger cells' locomotion by activating signaling pathways that regulate the actomyosin cytoskeleton. In many cases, cells migrate in response to external sources of guidance cue(s). When cells exposed to an either symmetrical or asymmetrical cue tend to show random (non-directional) locomotion, the phenomenon is called chemokinesis (Petrie et al., 2009). In contrast, if cells detect asymmetrical environmental cues and they display directional locomotion, it is directional migration such as chemotaxis (Petrie et al., 2009). These asymmetrical environmental cues can be broadly divided in to ECM and soluble molecules. Among many types of guidance cues, contact guidance, haptotaxis, and durotaxis (mechanotaxis) are ECM-dependent

guiding cues. Chemotaxis is a soluble molecule-mediated guiding cue. In this section, I will review the guidance cues that induce directional locomotion of cells.

1.2.2.1 Contact guidance

Cells can migrate directionally by contact guidance. Contact guidance applies when the topographical structure of surrounding cells, namely ECM, controls cellular morphology and migration (Curtis and Wilkinson, 1997). Specifically, cells follow the fibre density-based geometries. If a low density of fibres is present, cells find it difficult to detect the fibres, giving rise to unidirectional (random) migration (Petrie et al., 2009). Conversely, a high density of fibres, especially when the fibres are aligned, can navigate directional cell migration (Petrie et al., 2009). An example of contact guidance has been reported in Xenopus laevis gastrula, where mesodermal cell locomotion was promoted by aligned ECM fibrils (Nakatsuji and Johnson, 1982). An *in vitro* approach has been made in another study, using neurons from Xenopus spinal cord and rat hippocampus: here a topographic factor artificially generated by grooved quartz played a path-defining role for neurons to establish their polarity and migration (Rajnicek et al., 1997). Most other *in vitro* bioengineering studies consistent with contact guidance have made an effort to recapitulate fibres or a fibre-based network to study contact guidance. These studies suggest that physical contact with structures having topographical features can induce and facilitate directional cell locomotion.

1.2.2.2 Haptotaxis

Haptotaxis is the guidance of cells by a gradient of chemotactic molecules bound to the substratum. The more ligands are bound to the substratum, the stronger adhesive interaction is present between the cell and ECM. Like contact guidance, haptotaxis also directs cell migration through contact with ECM. However, haptotaxis relies on the gradient of adhesive of interaction between integrin and ECM (Lara Rodriguez and Schneider, 2013). A great study to demonstrate haptotaxis was carried out by Suter et al. in *Aplysia* neurons (Suter et al., 1998). In order to see how physical interaction between the cell surface and a substrate affects directional motility of the neuronal growth cone, they coated a silica bead with a homophilic adhesion molecule, apCAM that is also expended by the cell surface (Suter et al., 1998). Then, the bead was placed on the top of the growth cone to mimic interaction between the cell surface and the substrate (Figure 1-4). When the bead was unrestrained, it was carried back by retrograde actin flow (Figure 1-4). However, if the bead was held by a

micro-needle to recapitulate physical interaction between the growth cone to the substrate, after few minutes a new protrusion formed beyond the bead and the central domain, including microtubules, actomyosins, was also steered towards the bead (Figure 1-4) (Suter et al., 1998). This demonstrated haptotaxis by illustrating its feature, navigating cells towards where the stronger mechanical force to the substrate takes place.

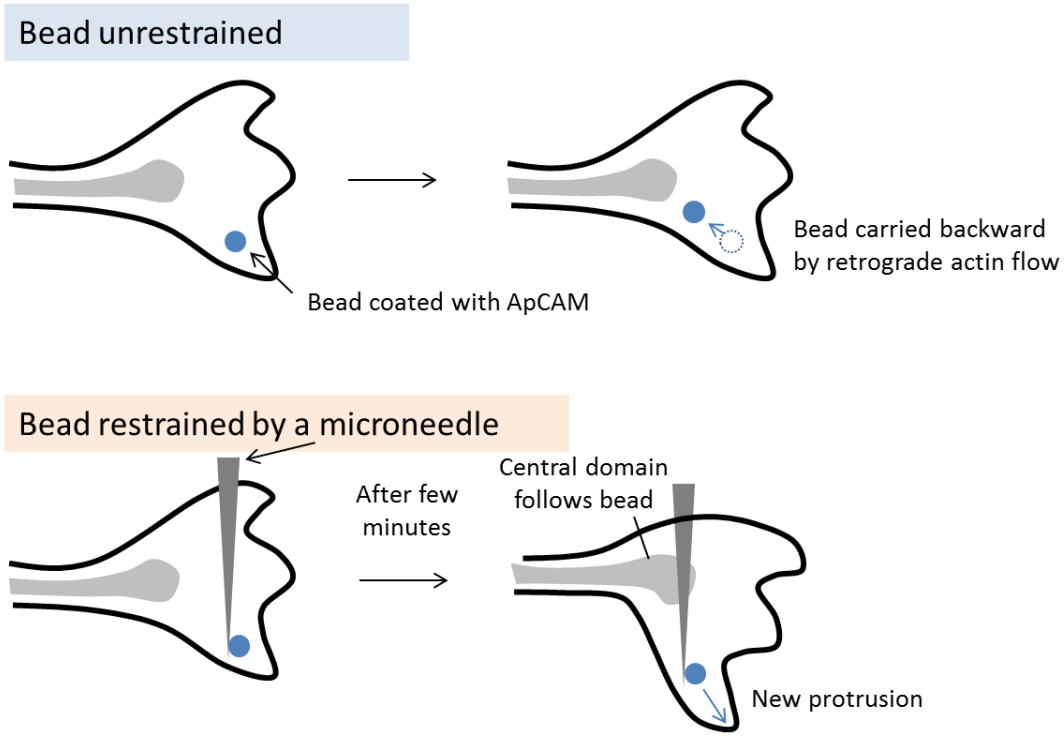

Figure 1-4 An example of demonstrating Haptotaxis (Image modified and redrawn from Rorth, 2011, Davies, 2013b)

1.2.2.3 Durotaxis

Durotaxis (mechanotaxis) occurs when cells preferentially migrate towards more rigid substrate than other. Durotaxis and haptotaxis basically share a concept of using net physical interactions between the cell and the substrate. Durotaxis differs from haptotaxis in terms of that durotaxis uses a gradient of rigidity to navigate cells whilst haptotaxis uses a gradient of adhesiveness to guide cells. One of the pieces of evidence to demonstrate durotaxis has come from a study of fibroblasts cultured in type I collagen-coated elastic polyacrylamide gel (Lo et al., 2000). A gradient of the pliability was induced in the polyacrylamide gel by adding different amounts of the bis-acrylamide cross-linker (Lo et al., 2000). In this environment,

fibroblasts directed their locomotion towards relatively rigid regions by stronger traction forces on them (Lo et al., 2000). Other studies using different cell types and different kinds of substrates, such as a microfabricated substrate, have also demonstrated durotaxis (Saez et al., 2007, Tse and Engler, 2011, Lara Rodriguez and Schneider, 2013).

1.2.2.4 Chemotaxis

Chemotaxis is the guidance cue of navigating cells by diffusible chemotactic factors. Consistent with the essential role of chemotaxis in aspect of development including angiogenesis, neurogenesis, and embryogenesis, chemotaxis might be one of the most studied mechanisms of navigation (Lamalice et al., 2007, Raz and Mahabaleshwar, 2009, Cooper, 2013). Chemotaxis works in a similar way as haptotaxis does in that they both use a graded external input to direct cells' locomotion bias. However, cells in chemotaxis are navigated by diffusible (soluble) chemotactic factors whilst haptotaxis is mediated by the factors that are bound to the substratum.

How chemotaxis steers directional cell locomotion has been well studied in the model *Dictyostelium discoideum* (*D. discoideum*) (reviewed by Newell et al., 1990, Vicker and Grutsch, 2008, Wang et al., 2011, Davies, 2013a). Due to its simplicity, *D. discoideum* is a favorable system to study chemotaxis (Charest and Firtel, 2010). During the life cycle of *D. discoideum*, cells undergo an aggregation process before forming fruiting bodies. These aggregating cells use chemotaxis to migrate towards aggregation centres (Vicker and Grutsch, 2008).

D. discoideum also begins to move by protrusions, termed pseudopods, at the leading edge, and uropods at the rear and these make *D. discoideum* to determine its directional movement (Van Haastert, 2010). In order for cells to be polarized and protrude under chemotaxis, they have to sense and amplify a shallow gradient external cue, and internally convert the cue to cell locomotion. Cyclic adenosine monophosphate (cAMP) in a shallow gradient initiates chemotaxis by binding to cAMP receptor 1 (cAR1), a G-protein coupled receptor (Saxe et al., 1991). cAR1 stimulates heterotrimeric G-proteins which activate phosphoinositide 3-kinase (PI3K). PI3K then phosphorylates phosphatidylinositol 4,5-bisphosphate (PIP_2) to phosphatidylinositol 3,4,5-triphosphate (PIP_3) that is one of the important second messengers to mediate actin polymerization. Therefore, cAMP is a fine trigger to initiate the signaling cascade via its effectors to migrating cell movement. However, cells need to amplify a shallow gradient of cAMP to an internal steep gradient, thereby becoming polarized and

protruding towards a region of slightly higher cAMP. The problem can partly be resolved by amplifying the internal signaling through a downstream effector of cAR1, PI3K. Although the receptor for cAMP is dispersed around the cells in proportion to a gradient of cAMP, the downstream effectors of the receptor, PI3K and its effector PIP_3 are relatively more localized at the up-gradient edge (Parent et al., 1998, Funamoto et al., 2002). Hence, this asymmetrical distribution of such effectors promotes actin proliferation preferentially at the up-gradient edge. Another way can also lead to inhomogeneous distribution of a steep gradient. Opposite in function to PI3K, the protein phosphatase and tensin homologue (PTEN) dephosphorylates PIP_3 into PIP_2 and PTEN localizes towards the rear when cells sense a gradient of cAMP (Iijima and Devreotes, 2002). Since PTEN is activated by a PIP_2-dependent way, decreasing PIP_2 by PI3K at the leading edge results in less PTEN at the leading edge, which makes more asymmetric to distribution of PIP_3 (PIP_3 is produced at the leading edge and degraded at the rear) (Iijima et al., 2004). In addition to this steep gradient of the cAMP downstream effectors to promote pseudopod extension at the leading edge, inhibiting other protrusions at the lateral and the rear might be essential for efficient chemotactic movement. This is mediated by cGMP produced by soluble guanylyl cyclase (sGC) which is activated by cAMP stimulation (Veltman et al., 2008). cGMP inhibits pseudopodia through regulating myosin II, an actin-based motor protein, which is present in the lateral and the rear (Bosgraaf et al., 2002). As myosin II plays an inhibitory role for lateral and rear pseudopodia, pseudopodia can be confined to the leading edge for efficient chemotactic locomotion of cells.

Chemorepulsion is an opposite concept to chemoattraction but is also an example of chemotaxis. Whereas cells that undergo chemoattraction migrate towards a diffusible attractant, cells in chemorepulsion move away from a diffusible repellent. This repulsive locomotion, in addition to attractive cell movement, is also important for cells to navigate to their correct target by keeping them away from a region that should not be occupied (Nguyen Ba-Charvet et al., 1999). Thus, both chemoattraction and chemorepulsion contribute to development of the nervous system by guiding axon growth cones (Bagnard et al., 2000).

One of major signaling pathways that underlie chemorepulsion is the Slit-Roundabout (Robo) pathway. The Slit family is evolutionarily conserved protein family initially identified as a molecule implicated with the midline glia development and later found to repel midline axons in *Drosophila* (Rothberg et al., 1990, Battye et al., 1999). The repulsion begins by the diffusible Slit binding to the Robo, the receptor family protein (Andrews et al., 2007) (Figure 1-5). Subsequently, the Robo activates GTPase-activating protein (GAP)

which dephosphorylates Cdc42-GTP (active) to Cdc42-GDP (inactive) (Figure 1-5). This leads to relatively less Cdc42-GDP resulting in less actin polymerization through WASP activating Arp2/3 (refer to 1.2.1) at the region that faces a higher gradient of the Slit (Figure 1-5). In contrast, the other part of the cell, that encounters a lower gradient of the Slit, has more of Cdc42-GTP that promotes actin polymerization, thereby repelling the cell from a higher Slit environment to a lower (Figure 1-5).

Class III semaphorins also play a repulsive role in the central and peripheral nervous systems (Puschel et al., 1995, Van Vactor and Lorenz, 1999). Neuropilin / plexin is the receptor complex through which semaphroin III can signal (Kolodkin et al., 1997, Rohm et al., 2000). Neuropilin is a semaphorin III-binding subunit and plexin is a signal transduction subunit (Rohm et al., 2000). It was noted that semaphorin III signaling through a functional receptor, plexin, inhibits axonal growth cones via direct-binding to Rac1, suggesting semaphorin III is a repellent (Jin and Strittmatter, 1997, Vikis et al., 2000, Hu et al., 2001). At the same time, plexin activates RhoA which consequently promotes actomyosin filament polymerization (Hu et al., 2001). Therefore, the semaphorin III-plexin pathway suppresses the actin protrusion but promotes actomyosin formation which renders the semaphorin III-confronted region of the cell to be the trailing edge.

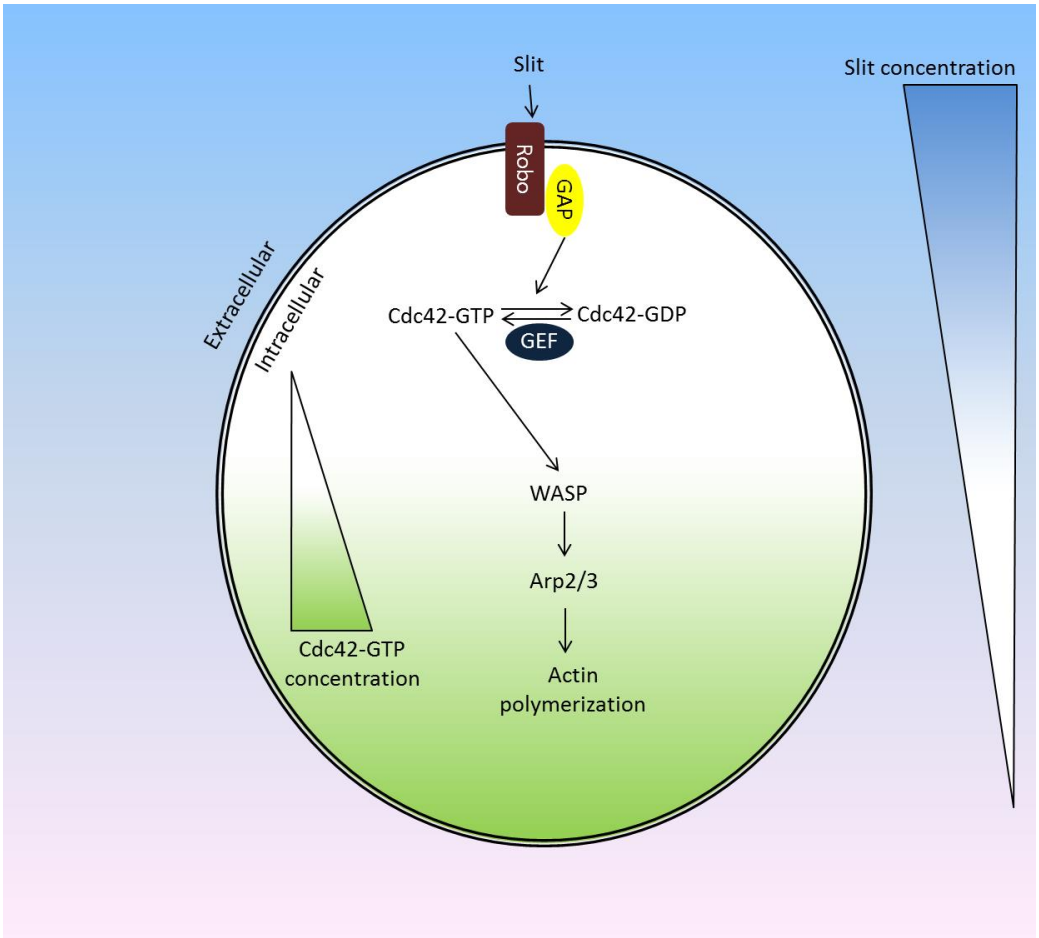

Figure 1-5 Chemorepulsive model by slit-stimulated signaling pathway (Image modified from Wong et al., 2001).

1.2.2.5 Galvanotaxis

Galvanotaxis, also called electrotaxis, is the cue driving the cellular movement by a gradient of electric field. Depending on physiological conditions, epithelial cells produce transepithelial potential differences in a range of a few millivolts (mV) to tens of mV (Mycielska and Djamgoz, 2004). Cells can use these potential differences as a guide to migrate towards the cathode or the anode. Cells such as bovine aortic vascular endothelial cells, human karatinocytes, and amphibian neural crest cells predominantly move towards the cathode (Cooper and Keller, 1984, Sheridan et al., 1996, Li and Kolega, 2002). However, some cells, such as rabbit corneal endothelial cells and human vascular endothelial cells move towards the anode (Chang et al., 1996, Zhao et al., 2004). Since cells are unlikely have exclusive cellular components to direct the galvanotatic cell movement, galvanotaxis should

be implicated with intracellular signaling pathways to modulate eventually cytoskeletal rearrangements (Mycielska and Djamgoz, 2004).

A much studied candidate molecule to regulate galvanotaxis might be Ca^{2+}. The resting potential of the cell membrane is negative (Figure 1-6). However, if the cell exposed to a direct current electric field, the region facing the anode becomes hyperpolarized resulting in a passive influx of Ca^{2+} (Figure 1-6). Increased [Ca^{2+}] at the region of the cell facing the anode gives rise to the cell contraction by Ca^{2+}/calmodulin-mediated myosin II regulation (Tansey et al., 1992) (Figure 1-6). On the other region of the cell that faces the cathode has relatively low [Ca^{2+}] which can cause actin polymerization by releasing actin severing proteins at the barbed end (Onuma and Hui, 1988, Welch and Mullins, 2002) (Figure 1-6). Therefore, asymmetrical [Ca^{2+}] in the cell consequently leads the cell to move towards the cathode by pushing from the cell rear by actomyosin contraction and leading by protrusion.

This mechanism can be affected by the distribution of voltage-gated ion channels and the capability of cells to store Ca^{2+} (Mycielska and Djamgoz, 2004). However, a [Ca^{2+}]-dependent way and/or other proteins that regulate galvanotatic movement of cells are sufficient to demonstrate that cell locomotion can be steered by an electric field.

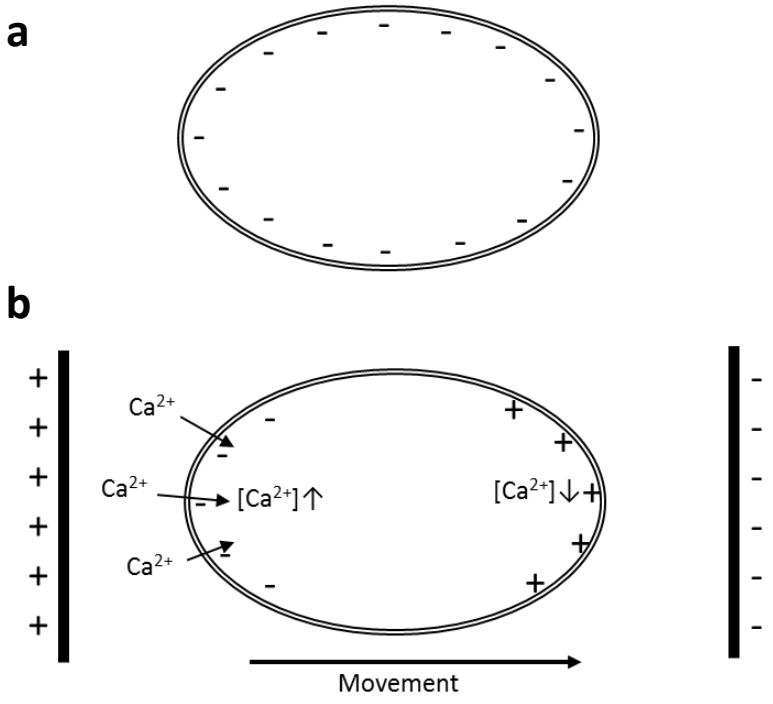

Figure 1-6 Ca^{2+}-dependent galvanotaxis (Image modified from Mycielska and Djamgoz, 2004). (a) Resting membrane potential of a cell is negative. (b) A cell influenced by a DC electric field shows hyperpolarized membrane towards the anode and depolarized membrane towards the cathode.

1.2.3 Collective cell migration

As a second mode of cell movement during development, cells can move in groups, termed as 'collective cell migration'. Both individually and collectively migrating cells share key processes to promote their locomotion. These cyclical processes are polarization, protrusion at the leading edge of the cell, actomyosin-based contraction, and disassembled adhesions at the cell rear as described in the previous section (refer to 1.2.1) (Ridley et al., 2003, Rorth, 2011). However, one major feature of collective migration differs from solitary migration is that cells in collective migration maintain cell-cell cohesion throughout their journey, thereby migrating as a single unit (Weijer, 2009, Friedl and Gilmour, 2009, Ilina and Friedl, 2009). The cohesion between cells is achieved by adherens junction proteins such as cadherins, alpha-catenin, and gamma-catenin linked to actin cytoskeleton network (Meng and Takeichi, 2009, Vicente-Manzanares et al., 2009). These adherens junction proteins allow cells to be strongly connected and to efficiently communicate each other via signaling crosstalk throughout their directional locomotion. Another important feature of collective migration is that there is a leading cell(s) at the front of the group and many follower cells at the rear (Friedl and Gilmour, 2009, Aman and Piotrowski, 2010). The role of the tip cells is to sense external guidance cues and to promote cytoskeletal rearrangement in response to those cues (Friedl and Gilmour, 2009). Since this cytoskeletal action at the tip cells is greater than it at the stalk cells, the tip cells naturally lead the stalk cells (Friedl and Gilmour, 2009). In addition, altering surrounding ECM is also one of important features of collective migration. Cells in collective migration confront a relatively high mechanical constraint compared to individually migrating cells. Therefore, collective cells need to make an enough space (path) for the group to migrate through by remodeling ECM and decreasing mechanical resistance of surrounding tissues (Lu et al., 2011). One of ways to remodel ECM is degrading ECM using proteases such as metalloproteinases that are localized on the tip cell surface (Cawston and Young, 2010). In order to obtain the least resistance from surrounding ECM, the leading cells synthesize the basement membrane materials including laminins and type IV collagen to provide a smooth path for the following cells (Lu et al., 2011). Therefore, these distinct features allow collective cell migration to distinguish from individual cell migration.

Collective migration plays a critical role during developmental and regenerative processes. Evidence to support this comes from collective migration of the border cell clusters towards the oocyte in the *Drosophila* egg chamber, convergent extension of the Malpighian tubules

in the *Drosophila*, migration of the lateral line primordium to become a sensory system in the zebrafish, neural crest migration from the dorsal neural tube throughout the embryo in vertebrates, and angiogenic sprouting to form a vasculature network in vertebrates (Skaer, 2003, Ghysen and Dambly-Chaudiere, 2007, Poukkula et al., 2011, Theveneau and Mayor, 2012, Wimmer et al., 2012). I will discuss and focus on collective migration that underlies tubes because the loop of Henle, the main topic of this thesis, is a tube-based tissue with an inner lumen, akin to the structure of blood vessels.

Unlike vasculogenesis, which is an initial step to form vascular networks from endothelial precursor cells, angiogenesis is the process that forms a new vascular tube from a pre-existing vessel. This occurs in both cases of morphogenesis and regeneration (Woolf, 2003, Patan, 2004, Arima et al., 2011). Angiogenic sprouting is the first step of angiogenesis, and sprouting is associated with collective migration. Angiogenic sprouting is well described in the retina model of neonatal mice (Gerhardt et al., 2003, Uemura et al., 2006, Stahl et al., 2010). Prior to the retinal angiogenesis, the retina is avascular and thus hypoxic. This hypoxia stimulates vascular endothelial growth factor (VEGF) expression (Liu et al., 1995, Forsythe et al., 1996). Evidence from in situ hybridization for VEGF mRNA suggests that VEGF expression is confined mainly to the peripheral region of the retina during its development (Figure 1-7) (Ng, 2008). In response to a gradient of VEGF along the radial axis of the retina, angiogenic sprouts emerge from a capillary ring residing at the embryonic retina centre and migrate towards the peripheral retina by chemoattraction (Figure 1-7) (Gerhardt, 2008). These angiogenic outgrowths are led by tip cells and VEGF specifies these tip cells. Follower cells are inhibited from being tips by Delta/Notch signaling (Figure 1-7) (Hellstrom et al., 2007). In this way, only tip cells can lead outgrowth (Figure 1-7). Following cells guided by tip cells in sprouts are termed stalk cells, and these stalk cells and the tip cell are bridged by vascular endothelial (VE)-cadherin (Figure 1-7) (Vestweber, 2008).

Unlike tip cells, stalk cells are proliferative and they form a lumen in a sprout (Figure 1-7). An early study using irradiation to suppress cell proliferation suggested that sprouting can take place in absence of cell division (Ausprunk and Folkman, 1977). This study evidently indicates that angiogenic sprouting is predominantly driven by the pulling force of tip cells rather than by pushing from stalk cells (Ausprunk and Folkman, 1977). However, a later finding that stalk cells generally show polarized cell division along the sprouting axis to support the sprout elongation highlights the importance of proliferation during migration (Zeng et al., 2007).

In addition, tip cells produce filopodial protrusions whilst stalks do not (Gerhardt et al., 2003). Multiple filopodial protrusions and their orientation towards the source of VEGF in the tip cell are also stimulated by VEGF (Gerhardt et al., 2003). This is supported by demonstrating co-localization of vascular endothelial growth factor receptor 2 (VEGFR2 or Flk-1) in both the body of tip cells and their filopodia (Gerhardt et al., 2003).

Once the retina is sufficiently vascularized, blood that comes through new vessels provides oxygen giving rise to down-regulation of VEGF expression thereby ceasing sprouting angiogenesis (Liu et al., 1995, Forsythe et al., 1996).

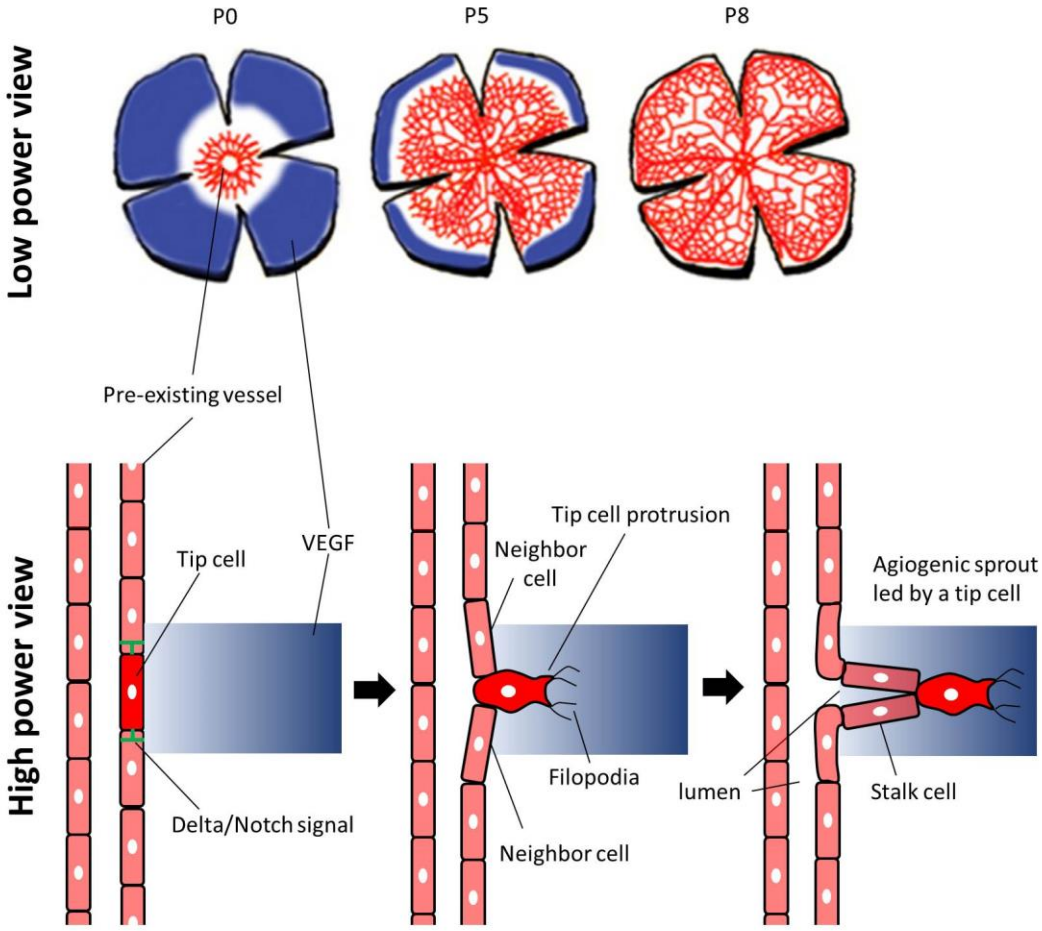

Figure 1-7 Collective migration in the retinal angiogenic sprouting (Image adapted and modifed from Rorth, 2009, Aman and Piotrowski, 2010). A low power view depicts mouse retinal angiogenesis from P0 to P8. Blue indicates a gradient of VEGF and red indicates angiogenic vasculatures. A high power view depicts in detail how the sprout forms by collective migration.

An additional example of tubular collective migration is convergent extension of the Malpighian tubule elongation in the *Drosophila*. The Malpighian tubules are the excretory system in the Drosophila akin to the mammalian renal tubules (Skaer, 2003). There are two pairs of the Malpighian tubules in the *Drosophila*; two anterior tubules and two posterior tubules (Figure 1-8). I will mainly discuss the development of those anterior looped-tubules due to their morphological resemblance to the shape of the Henle's loop (Figure 1-8).

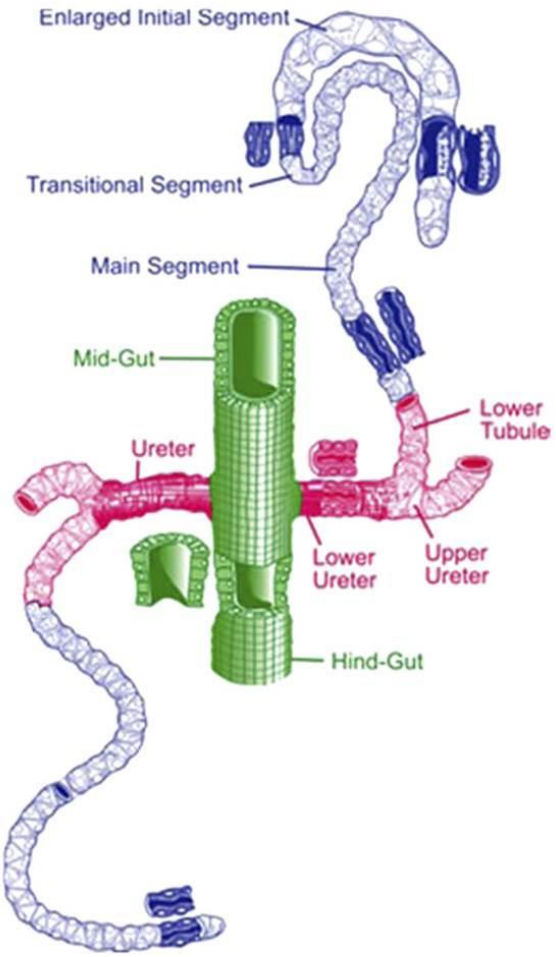

Figure 1-8 An illustration of the Malpighian tubules in the Drosophila (Image adopted from Singh et al., 2007).

In the *Drosophila*, the Malpighian tubules originate from the hindgut primordium sprouting as four anlage buds (reviewed in Skaer, 2003, Weavers and Skaer, 2013). These anterior buds then grow to form tubes by their tip cells expressing EGF to stimulate cell division of neighboring cells (Sudarsan et al., 2002, Jung et al., 2005). This tip cell-regulated tube growth is somewhat analogous to it of the angiogenic sprouting (Figure 1-7). After completion of cell division in the tubules, they commence to lengthen and to become

narrower (Skaer, 2003). The tip cell anchorage of the anterior tubule to the alary muscle renders the middle of the looped tubule moving forward (Figure 1-9) (Weavers and Skaer, 2013). The loop extends towards the region where Decapentapegic (Dpp) resides and it consequently reaches its invariant destination in the gastric caeca closely located to the ventral nerve cord (Figure 1-9) (Skaer, 2003, Weavers and Skaer, 2013).

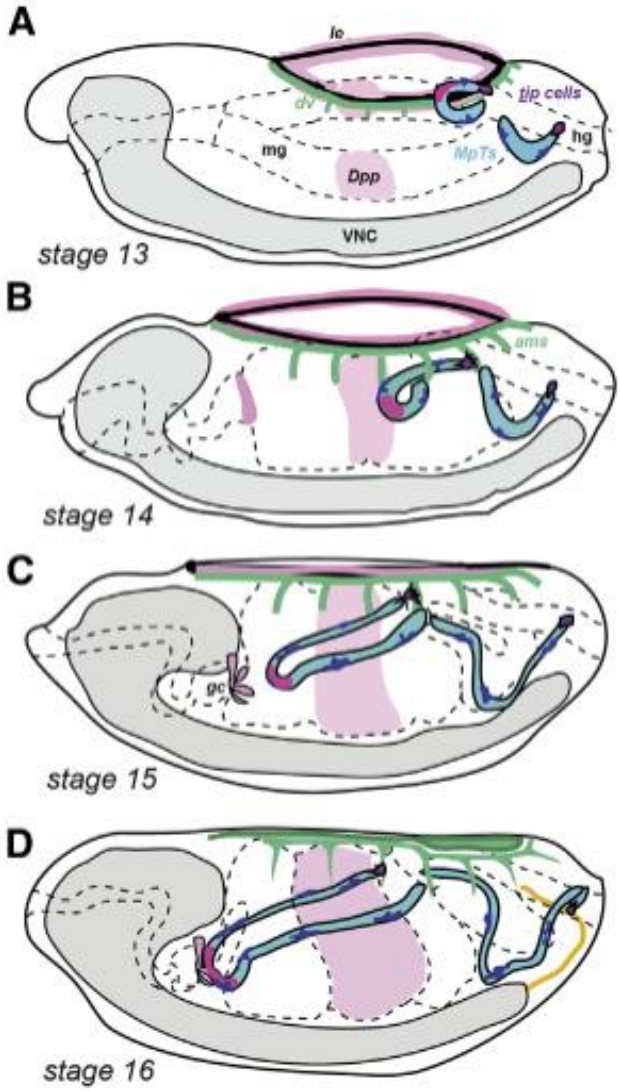

Figure 1-9 Convergent extension of the Malpighian anterior tubule (Image adopted from Weavers and Skaer, 2013). An anterior tubule (blue) lengthens during the Drosophila embryonic stage 13 to 16. (A-B) Since the tip cell at the distal end of the tubule is anchored to the alary muscle, the tubule becomes looped and the middle of the tubule navigates in response to Dpp (pink) guidance cues. (C-D) The tubule consequently reaches the gastric caeca at stage 16 (le; leading edge, mg; midgut, hg; hindgut, ams; alary muscles. VNC; ventral nerve cord, gc; gastric caeca).

In this section and the previous sections, I have briefly reviewed mechanisms underlying individual cell migration and collective cell migration. For collective migration, I focused especially on angiogenic collective sprouting and convergent extension of the *Drosophila* Malpighian tubule to illustrate how the end and the middle of insect renal tubules navigate. However, how the middle of a bent tube in mammalian kidney is navigated remains to be determined.

1.3 Overview of mammalian kidney development

The developing kidney is a great place to study navigation of a middle region of a bent tubule. This bent tubule is the loop of Henle (LoH) which I will discuss in detail later. Since the LoH is one of many components in the kidney, I will briefly review the origin and general development of the kidney in this section.

There are three different types of kidneys during mammalian renal development; two transient kidneys, the pronephros and the mesonephros which eventually degenerate, and the final permanent functional kidney, the metanephros (Figure 1-10). These kidneys originate from the intermediate mesoderm (nephrogenic cord), located between the paraxial somatic mesoderm and the lateral plate mesoderm (reviewed by Dressler, 2009). Precursors of the nephric duct (Wolffian duct) form from the intermediate mesoderm at near E22 in humans and E8.0 in mice (Vetter and Gibley, 1966, Saxén, 1987, Davidson, 2008). These precursors then form an epithelial tube by a mesenchymal-to-epithelial transition (MET) and the tube elongates caudally towards the cloaca (Figure 1-10). Molecular fate mapping in the embryonic mouse reveals that this later elongation of the nephric duct is driven by its cell migration/proliferation rather than by recruitment of new cells (Mugford et al., 2008).

Only a few of the pronephric tubules form from the rostral region of the nephric duct, and the tubules and the rostral part of the nephric duct undergo apoptotic degeneration short after they formed (Pole et al., 2002) (Figure 1-10). While the rostral nephric duct degenerates, the lower part of the nephric duct remains and proliferates to form the mesonephros and the metanephros (Figure 1-10).

The mouse mesonephros arises from the middle part of the nephric duct at approximately E9 (Sainio, 2003) (Figure 1-10). In the mouse mesonephros, approximately 18 mesonephric tubules with proximal glomeruli form, with a morphology that resembles metanephric

nephrons (Vize et al., 2003, Davidson, 2008). Mesonephric tubules can be divided into cranial and caudal tubules based on their connection to the nephric duct (Sainio, 2003) (Figure 1-10). Only cranial tubules are linked to the nephric duct and the other tubules, the caudal tubules, are not connected to the nephric duct (Figure 1-10). Degeneration of the mesonephros occurs at E14.5 and almost all cranial and caudal tubules disappear within 24h (Smith and Mackay, 1991).

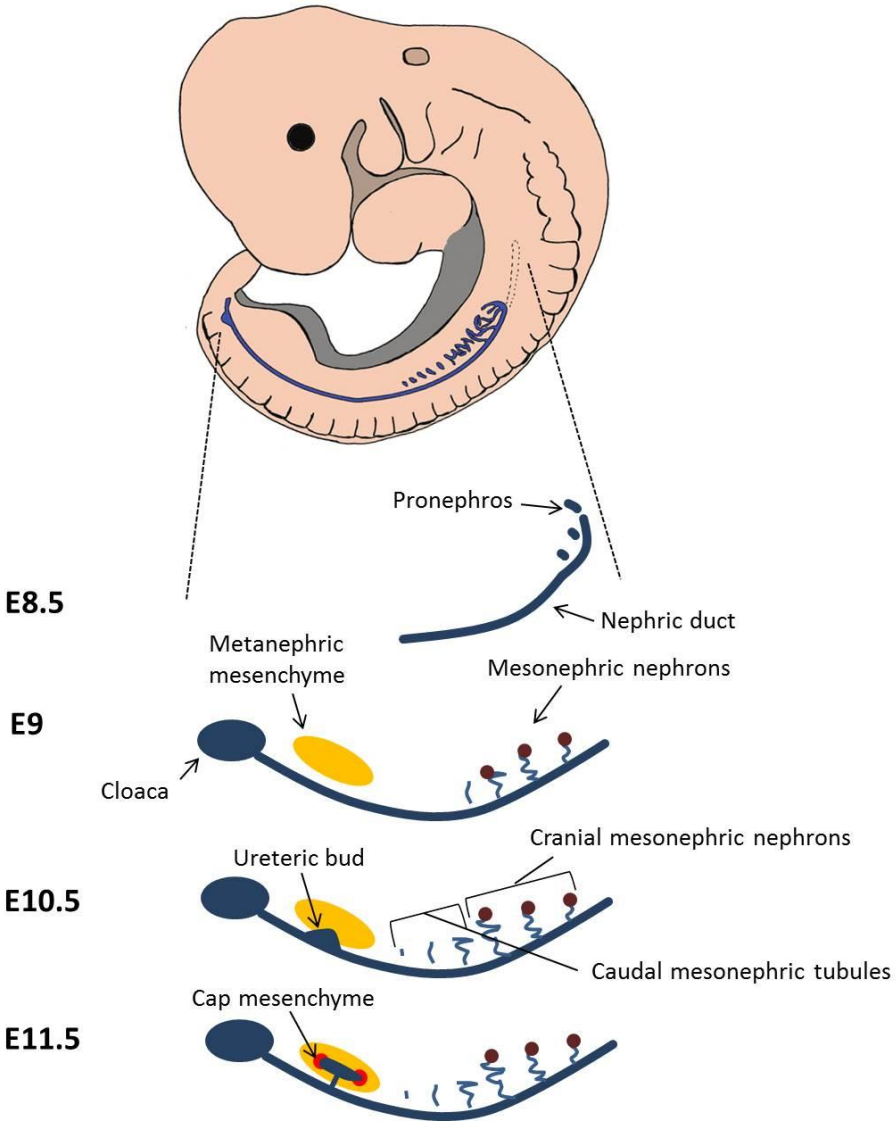

Figure 1-10 Origin of the kidney (Image adapted and modified from Davidson, 2008, Dressler, 2009).

The permanent functional kidney, the metanephros, begins to develop from the caudal part of the intermediate mesoderm when the metanephric blastema becomes demarcated at E10 in mice, E11 in rats, and E28 in humans (Vize et al., 2003). In response to an inductive signal from the metanephric mesenchyme, ureteric bud (UB) outgrowth from the nephric duct occurs and invades the metanephric mesenchyme at E10.5 (Figure 1-10, 1-11). The metanephric mesenchyme provides progenitor cells which later become the nephrons of the metanephric kidneys. The UB, in turn, undergoes arborization, branching repeatedly taking place in its tip region (terminal bifurcation) to form the collecting duct system. The UB tips induce metanephric mesenchyme to condense to form a cap composed of self-renewing mesenchymal progenitor cells, also termed 'cap mesenchyme,' morphologically distinguishable from the peripheral 'loose' mesenchyme (Figure 1-10, 1-11). Extensive studies of cell lineage tracing experiments have demonstrated that all components of the nephron originate from the cap mesenchyme (Herzlinger et al., 1992, Osafune et al., 2006, Kobayashi et al., 2008). Metanephric nephron development begins at E11.5 by forming a pre-tubular aggregate from the cap mesenchyme beneath the UB tips (Figure 1-11). The pre-tubular aggregate becomes an epithelial vesicle by undergoing MET at E12.5 (Figure 1-11). The renal vesicle then grows to form the comma-shaped body followed by the S-shaped body that joins to the collecting duct (CD) (Figure 1-11). As the S-shaped body proliferates, the podocyte that reside in the lower cleft of the S-shape body attract angioblasts to form the glomerulus (Robert and Abrahamson, 2001). Linked to the glomerulus, the proximal tubule, the loop of Henle, and the distal tubule in sequence constitute the nephron and this nephron unit is linked to the collecting duct via the connecting tubule (Figure 1-11).

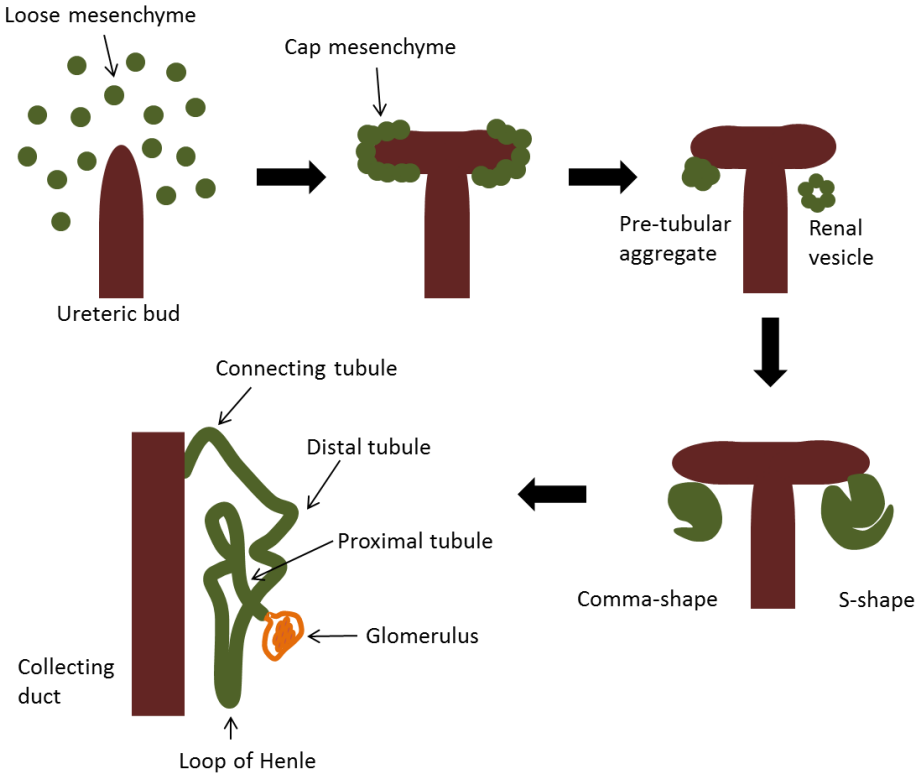

Figure 1-11 Simplified overview of metanephric nephron development (Image modified and redrawn from Saxén, 1987).

1.4 Guidance in the developing kidney

The kidney has a unique and a complex structure and cell migration aids to form those structures. Related to the main focus of this thesis-studying the LoH navigation during kidney development-it is worth illustrating how the other components of the developing kidney develop by guidance cues.

1.4.1 Guidance of the ureteric bud

The development of the metanephric kidney begins when the ureteric bud (UB) outgrowth from the posterior nephric duct is induced (refer to 1.3). The UB sprouts into its nearby mesenchyme blastema and navigates by fine tuning of positive and negative signaling pathways. One of major pathways to promote UB outgrowth and branching is the glial-derived neural growth factor (Gdnf)/Ret receptor tyrosine kinase pathway (reviewed by Costantini, 2010, Song et al., 2011, Little and McMahon, 2012). Gdnf is a neurotrophin that secreted by the metanephric mesenchyme (MM), and it is broadly expressed along the

nephrogenic mesenchyme by E9.5, but is restricted to the metanephric mesenchyme by E10.5 (Hellmich et al., 1996). Ret is the receptor for Gdnf and it is expressed along the nephric duct (Pachnis et al., 1993). Ret is activated by Gdnf binding to the co-receptor, Gdnf family receptor alpha 1 (Gfrα1) (Jing et al., 1996). These three factors play important roles in UB outgrowth and branching , a conclusion that is supported by a study of mutant mice lacking Gdnf, Ret, or Gfrα1, which show failure of UB penetration which gives rise to kidney agenesis (Jain, 2009).

There are molecules that act as regulators of the Gdnf/Ret signaling for the normal UB outgrowth, as sprouting angiogenesis is mediated by regulations including site-specific selection and suppressing its surroundings for the sprouting (refer to 1.2.3). Bone marrow protein-4 (Bmp-4) is one of them, that is absent in the MM but present in the mesenchyme enveloping the nephric duct. It down-regulates Gdnf/Ret signaling (Obara-Ishihara et al., 1999, Costantini, 2010). Since Bmp-4 is inhibited by the MM-expressed gremlin, only a confined region of the nephric duct adjacent to the MM is allowed to respond to Gdnf/Ret (Michos et al., 2007). Slit2/Robo2 signaling also contributes to correct UB guidance towards the MM through restricting Gdnf expression posteriorly (Grieshammer et al., 2004). In addition, sprouty homolog 1 (Spry1), a receptor tyrosine kinase (RTK) antagonist, acts as an intracellular regulator to prevent ectopic outgrowth of the UB by inhibition of Ret (Basson et al., 2006, Basson et al., 2005). Under control of these factors to the Gdnf/Ret signaling, a single UB from the posterior nephric duct will sprout towards the MM.

Although the mechanisms that link between activation of Ret to the UB outgrowth and penetration into the MM are not fully understood, there are several pieces of evidence that UB outgrowth is mediated in part by chemotactic cell migration. As discussed previously, PI3K promotes lamellipodia and filopodia by actin polymerization at the leading edge of migrating cells (refer to 1.2.2.4). Tang et al. demonstrated Gdnf as a chemotactic agent in terms of promoting lamellipodia, filopodia extension and cell motility in Ret-positive MDCK renal epithelial cells in response to a localized Gdnf (Tang et al., 1998). Later, they also reported that PI3K activity was elevated when Gdnf is added to Ret-expressing MDCK cells whilst specific inhibition of PI3K resulted in blocking both chemotactic MDCK cell migration and the Gdnf-sensitive outgrowth of the UB in organ culture (Tang et al., 2002). Opposite to the role of PI3K at the cell leading edge, PTEN aids chemotactic migration by inhibiting PI3K at the lateral and rear of the migrating cell (refer to 1.2.2.4). The study performed by Kim and Dressler reported that loss of PTEN resulted in chemotactic migration defects in MDCK cells and irregular UB branching in organ cultures (Kim and Dressler,

2007). These findings suggest that the factors (PI3K and PTEN), that promote directional cell migration in *Dictyostelium*, may also play a critical role in UB migration.

After UB outgrowth towards the MM, the UB undergoes repetitive bi- or trifurcated branching steps and UB branching is also partly mediated by directional cell migration under the Gdnf/Ret signaling. During the UB branching, Ret is restrictedly localized at the UB branch tip by a positive feedback loop via Wnt11 (Pepicelli et al., 1997, Majumdar et al., 2003). The coordination of Wnt11 and the Gdnf/Ret signaling also plays a role in retaining the proper level of Gdnf expression from the cap mesenchyme, thereby resulting in the UB tip growth towards the cap mesenchyme (Pepicelli et al., 1997, Majumdar et al., 2003).

As discussed before, the actin skeletal network produced by actin polymerization and de-polymerization critically mediates directional cell migration (refer 1.2.1). There was a study that double mutation of cofilin and destrin, the actin depolymerizing proteins, in the UB causes a cell migration defect and thereby resulting in abnormal UB branching and also complete kidney malformation (Kuure et al., 2010).

Collectively, these studies highlight that correct and elaborate guidance cues play a crucial role in the outgrowth of the UB from the nephric duct towards the nearby MM and in UB branching morphogenesis.

1.4.2 Guidance of blood vessels

One of main functions of the kidney is filtering blood, so the adult mammalian kidney must be vascularized. In fact, approximately 20% of the cardiac output flows into the kidney suggesting the importance of the renal vascularization (reviewed in Woolf, 2003). Therefore, guiding blood vessels towards their correct and final destination is an essential process for normal renal vascularization. In this section, I will discuss some of the major blood vessel-guiding events that occur in the kidney. Prior to this, it is necessary to discuss how the developing kidney receives with vascularization.

Compared to studies of the renal vessel development in humans that are merely descriptive, for obvious reasons, the mouse is a useful model to address stage-based renal vascularization since *in vivo* and *ex vivo* manipulations are allowed in the mouse model (reviewed in Woolf, 2003). As described in the previous section 1.3, when the UB invades the nearby MM by E11, capillaries originating from the dorsal aorta appear to encompass the avascular metanephric kidney (reviewed in Woolf and Yuan, 2001, Abrahamson, 2009). As the UB

undergoes several branching steps, capillaries are found to be localized near the stalk of the UB in the hilum and are also dispersed loosely in the MM at E12. In turn, when nephrogenesis takes place beneath the UB tip, displaying serial primitive nephron structures composed of the renal vesicle, the comma-shape body, and the S-shape body (refer to 1.3), scattered endothelial cells and angioblasts (endothelial precursors) are recruited to the lower cleft of the S-shape body to become later the mature glomerulus. From E14, the capillaries that formed around the UB stalk at the hilum develop into renal arteries which cross from the hilum to the corticomedullary junction. They form arterial branches at their ends which link to afferent glomerular capillaries (Woolf and Yuan, 2001, Woolf, 2003). After E15, as both nephrons and capillaries mature, the descending and ascending loops of Henle become associated with the descending and ascending vasa recta at the medulla (Woolf and Yuan, 2001, Woolf, 2003).

Guidance of blood capillaries or endothelial cells is mediated by several growth factors during renal vascularization. As discussed above, endothelial cells that are scattered in the MM need to be guided to the vascular cleft of primitive nephrons. Well-characterized growth factors and their receptors can in part mediate this guiding event. Vascular endothelial growth factor (VEGF) is a well-known chemoattractant for endothelial cells, and Flt-1 and Flk-1 are receptor tyrosine kinases for VEGF (Gerhardt, 2008, Song et al., 2011). VEGF is predominantly expressed by podocytes, distal tubules, and collecting ducts, and Flt-1 and Flk-1 are expressed by glomerular endothelial cells in developing and mature kidneys (Breier et al., 1992, Kitamoto et al., 1997, Baderca et al., 2006). Therefore, Flk-1-positive endothelial cells navigate towards the S-shape cleft (the vascular cleft) in response to podocyte-secreted VEGF (Robert et al., 1998). In addition to Flt-1 and Flk-1, neuropilin-1, which was previously described as a semaphorin III-triggered repellent in axon guidance (refer to 1.2.2.4), is also found to bind VEGF (Soker et al., 1998). The *ex vivo* study performed by Soker et al. reported that cells co-expressing neuropilin-1 and Flk-1 showed increased binding to VEGF and stronger chemotaxis than cells only expressing Flk-1 did (Soker et al., 1998). This suggests that neuropilin-1 is a regulator of endothelial migration through modulating VEGF/Flk-1 binding.

Another growth factor family implicated with blood vessel guidance during renal development might be the angiopoietins. A vascular growth factor family, the angiopoietins include angiopoietin-1 (Ang-1) and angiopoietin-2 (Ang-2) (Woolf et al., 2009, Woolf, 2010). Ang-1 binds to tyrosine kinase with immunoglobulin-like loops and epidermal growth factor homology domain 2 (Tie-2). Ang-2 is also a ligand for Tie-2 but it is a natural

inhibitor for Ang-1-activated Tie-2 (Maisonpierre et al., 1997). In mouse kidney, Ang-1 is expressed by the condensed mesenchyme, the glomerulus, the proximal tubule and the outer medullary tubule at E18-P3, and Ang-2 is expressed by the outer medullary tubule at E18-P1 and later at P3, it is restrictedly expressed by the vasa recta (Yuan et al., 1999). Tie-2 is expressed by the interstitial capillaries at E18-P1, and at P3 it is localized in the glomerulus and the vasa recta (Yuan et al., 1999). These expression patterns in the kidney imply that the role of angiopoietins is mainly maturing and stabilizing renovascularisation (Woolf et al., 2009). In addition, the ex vivo study demonstrated that not Ang-2 but Ang-1 induce chemotactic motility of endothelial cells although neither Ang-1 nor Ang-2 evokes a proliferative effect (Witzenbichler et al., 1998). This can be supportive evidence for Ang-1 acting as a guidance cue during maturation of renovascularisation such as the formation of the vasa recta.

1.5 The loop of Henle

Whilst there are a number of studies that describe how the end of a tube navigates and grows as discussed previously (section 1.2.3), how the apex of the bent tube is guided is largely unknown. The kidney is a great place to investigate this since one of components in the nephron, the loop of Henle (LoH) has a fine U-shape. In this section, I will describe the origin and morphological features of the LoH followed by its structure-associated function in the kidney.

1.5.1 Origin and anatomy of Henle's loop

As briefly reviewed in section 1.3, the nephron originates from the cap mesenchyme surrounding the UB tip and the cap mesenchyme undergoes the mesenchymal-to-epithelial transition (MET) induced by Wnt signaling, thereby forming the renal vesicle (RV) (Carroll et al., 2005). To date, a number of genes that are expressed along the polarized axis of the nephron (the proximal-distal axis) are found in the RV (Georgas et al., 2009). For instance, genes that are restrictedly expressed in the distal region of the RV include *Lhx1, Dll1, Brn1, cadherin1, Dkk1, Jag1*, and *Bmp2* (Cho et al., 1998, Nakai et al., 2003, Kobayashi et al., 2005, Georgas et al., 2009). Since a study of the *Brn1* mutant mouse resulted in defects of the distal tubule and the LoH, the LoH is in part considered as one of the distal region derivatives of the RV (Nakai et al., 2003). The other region, the proximal part of the RV, expresses genes including *cadherin6* and *Wt1* (Cho et al., 1998, Georgas et al., 2009). As the RV morphologically transforms into a comma-shape followed by an S-shape the polarity

becomes morphologically evident. Pax-2 and Pax-8 are known to regulate this transition (polarization) from the RV to the S-shape body (Narlis et al., 2007). In addition, *in vivo* and *ex vivo* studies by Cheng et al. reported that Notch signaling affects the proximal-distal axis pattern between the RV and the S-shape body, thereby later regulating the differentiation of the podocyte, the proximal tubule, and the LoH (Cheng et al., 2007, Cheng et al., 2003). A recent study also reported that Rho-kinase is essentially required for the proximal-distal polarity during the nephron development (Lindstrom et al., 2013). As the S-shaped body proliferates, the lower cleft of it becomes the glomerulus, including the podocyte, the mesangial precursor cells, and the endothelial cells (Quaggin and Kreidberg, 2008). The other end, the distal end is connected to the ureteric bud, but it is not completely clear to define a border between the distal end of the S-shaped body epithelium and the ureteric bud (Cho, 2003). Proximal tubule precursors reside in the middle of those two ends of the S-shaped body. As proliferated, the proximal tubule becomes convoluted and it leads to the long tubule which descends into the medulla and ascends back (Figure 1-10) (Cho, 2003). Finally, this ascending limb is connected to the collecting duct through the convoluted distal tubule (Figure 1-12).

The LoH is the middle segment of the nephron and links the proximal and the distal tubule. According to the morphological distinction and the level in the medulla of the LoH, LoH can be classified into 'short LoH' and 'long LoH' (Figure 1-12) (Kriz and Bankir, 1988, Hallgrimsson, 2003). Short LoH are found in nephrons that commence to form in the outer- or the mid-cortex and the bend of a short LoH appears not to go deeper than the outer medulla (Figure 1-12). In addition, a short LoH has a relatively short thin limb compared to the long LoH (Figure 1-12). The long LoH arises from the nephron that begins to form in the juxtamedullary zone (Figure 1-12). The long LoH is distinguished from the short LoH by its extended thin limbs and the localization of its bend in the inner medulla (Figure 1-12). Since the long LoH has relatively longer thin limbs than the short LoH, the long LoH comprises the descending thin limb, the ascending thin limb, and the ascending thick limb (Figure 1-12). The transition between the proximal tubule and the thin limb appears abrupt in both short- and long-LoH. Proportions of the long LoH among the total number of the LoH in various species are 15% in humans, 18% in mice, 30% in rats, 66% in rabbits, 100% in dogs (Kriz, 1967, Kaissling and Kriz, 1979, Bulger et al., 1979, Hallgrimsson, 2003, Zhai et al., 2006). Regarding structural-functional correlation of the LoH in the kidney, those diverse ratios in different species might reflect their different capability in concentrating urine (Zhai et al., 2006).

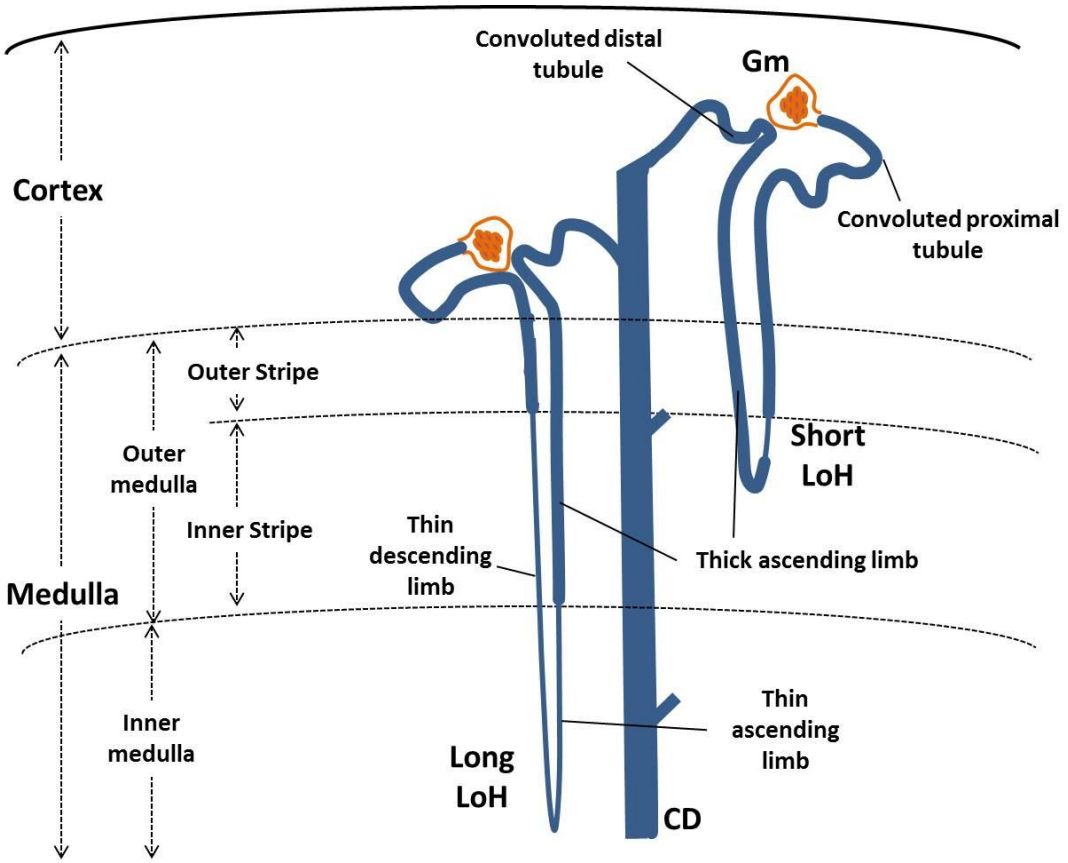

Figure 1-12 Description of a long- and short-loop of Henle (LoH) in mouse kidney (modified from Zhai et al., 2006). The long LoH originates from the juxtamedullary cortex and has its bend located in the inner medulla. The long LoH consists of a thin ascending limb, a thin descending limb, and a thick ascending limb. The short LoH begins to form from the superficial cortex and to have a bend in the outer medulla. The thin descending limb in the short LoH is short. Gm: glomerulus, CD: collecting duct.

1.5.2 Function of Henle's loop

The kidney is an organ that filters and reprocesses body fluids. Since those processes are highly complicated, it cannot simply be explained as a 'biological sieve'. Among many roles of the kidney such as regulating blood pressure and maintaining calcium levels, major roles are to filter unwanted components and reabsorb useful components from body fluids.

Under general circumstances, mammals take in more proteins than they actually require for the use in anabolic processes and thus nitrogen waste from those proteins would accumulate. Mammals excrete approximately 90% of this nitrogen waste as urea though the kidney

(Fenton and Knepper, 2007). Therefore, urea and other toxic wastes from the blood must be filtered and excreted as urine. There are several steps to produce concentrated urine and the LoH plays a principal role in reabsorbing water from urine by building up a hypertonic environment in the medulla.

When the blood flows through the afferent arteriole into the glomerulus, enclosed by the renal capsule (Bowman's capsule), large components, including blood cells, antibodies, and most albumin are retained in the blood (Quaggin and Kreidberg, 2008). However, the filtrate, containing small molecules and ions, is led to the proximal convoluted tubule where reabsorption of useful components, including amino acids, glucose, and mineral ions, into the blood occurs (Christensen and Gburek, 2004). In addition to useful proteins and ions, water is reabsorbed into the blood by passive transport (osmosis).

Subsequently, the filtrate enters the first portion of the LoH, the descending limb of LoH. The descending limb is permeable to water and less permeable to ions (mainly NaCl) (Figure 1-13) (Zhai et al., 2007). In order for the isotonic filtrate, that passes through the descending limb, to equilibrate the hypertonic medullary interstitium, water leaves the filtrate and is finally reabsorbed into the vasa recta, the countercurrent exchanger (Pallone et al., 2003). In this way, the medullary interstitium is still hypertonic and water is persevered. The filtrate that flows via the bend of LoH is the most concentrated so when the filtrate passes through the thin ascending limb of LoH, some of NaCl passively diffuses from the filtrate into the interstitium (Figure 1-13) (Pannabecker, 2012). The thick ascending limb does not have permeability to water since it lacks water channels (Nielsen et al., 2002). However, the thick ascending limb cells have symporters (co-transporter) which are able to transport Na^+, Cl^- and K^+ by active transport from the filtrate into the cells (Kaplan et al., 1996). Then, Na^+ is pumped out of the cells into the interstitium through the Na^+/K^+ ATPase pump (Jorgensen, 1976). This also results in diffusion of K^+ and Cl^- from the cell into the interstitium, but K^+ is reabsorbed into the cells and their lumen through the Na^+/K^+ ATPase pump and the renal outer medullary potassium channel (ROMK) respectively (Unwin et al., 1994). Overall, transportation of NaCl from the filtrate into the interstitium contributes to the hypertonic environment in the medulla (Figure 1-13).

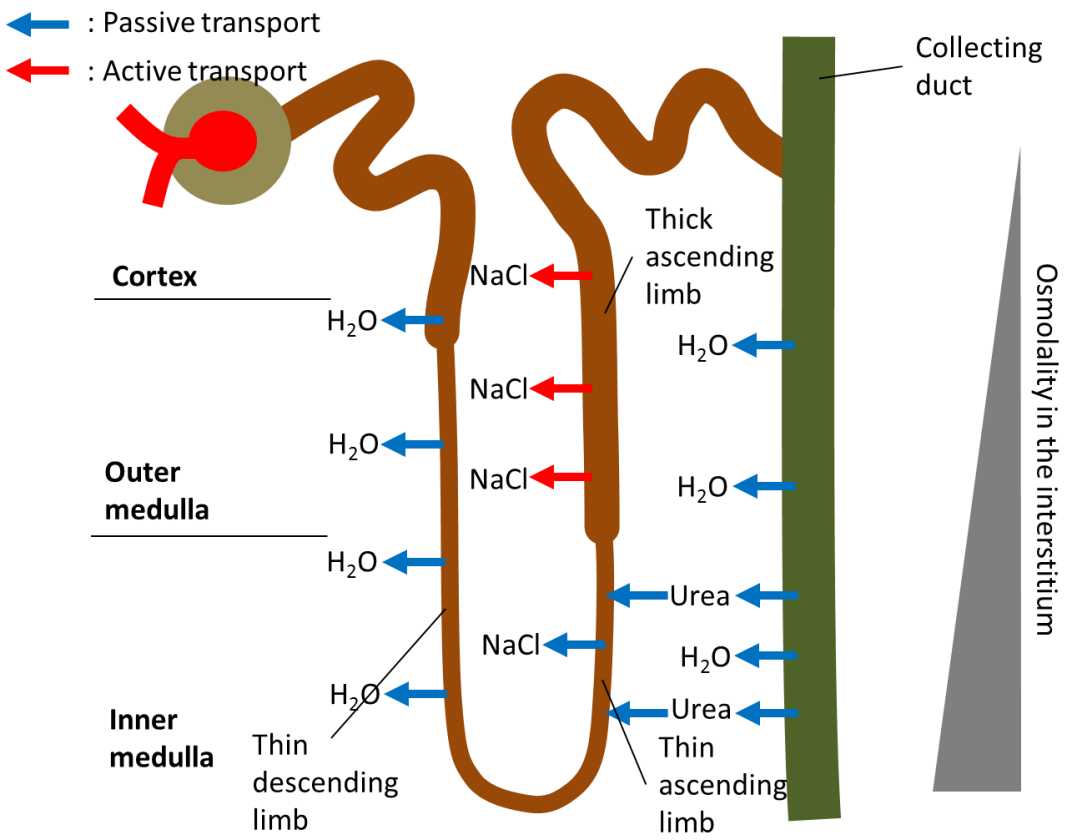

Figure 1-13 Urinary concentrating mechanism of the loop of Henle and the collecting duct (modified and redrawn from Sands, 2012).

Therefore, the filtrate becomes hypotonic and enters the distal convoluted tubule. Secretion of H^+ and K^+ takes place, that is mediated by active transport, from the blood into the distal convoluted tubule to maintain pH and salt homeostasis respectively (Reilly and Ellison, 2000).

Finally, as the filtrate descends through the collecting duct, water is recovered into the hypertonic medullary interstitium (Figure 1-13). Here, water diffuses through aquaporins in the collecting duct walls and these channels are controlled by the antidiuretic hormone (ADH) (Nielsen et al., 1995). Accumulated water in the interstitium is immediately reabsorbed by the countercurrent exchange of the vasa recta, so high tonicity in the medulla retains (Pallone et al., 2003). Since water leaves from the filtrate in the collecting duct, the filtrate (urine) becomes highly concentrated. This leads to diffusion of urea from the collecting duct into the medullary interstitium that also contribute to the hypertonic medulla (Figure 1-13) (Sands et

al., 2011). Urea in the interstitium is recycled by diffusing into the thin descending and mainly into the thin ascending limb (Sands and Layton, 2009).

Overall, the essential function of preserving water and concentrating urine in the kidney is, in part, closely correlated with the distinct anatomy of the LoH. Specifically, the hairpin structure of thin- and thick limbs of LoH in the medulla seems to be major components for generating the hypertonic medullary interstitium. However, to date, no study has focused on how the LoH, a bent tubule, ends up in the medulla.

1.6 Aims of this thesis

I aim to investigate how the loop of Henle (LoH) navigates towards its destination, the medulla, during mouse kidney development. The question arose from two important points that underlie tissue navigation mechanisms and the functional and anatomical importance of the LoH in the kidney. As described previously, there are a number of studies that describe how the end of a complete tube is navigated; for instance, angiogenic sprouting. However, it is almost completely unknown how the middle of a bent tube is guided. From renal anatomical and functional perspectives, the morphological feature of the LoH plays an essential role during kidney development. However, whilst there are many studies that seem to focus on the LoH structure in a descriptive way, the mechanism to produce the structure and arrangement of the LoH in the kidney has not been studied. Therefore, I aim to study guidance of the LoH during mouse renal development and my specific aims are as follows:

First, to study the natural anatomy and arrangment of the LoH during development.

Second, to develop an appropriate culture system to study LoH orientation.

Third, to investigate possible guidance cues pertinent to the LoH by experimental manipulation.

Fourth, to develop a method to screen candidate molecules for LoH guidance activity.

2 Chapter 2: Materials and methods

2.1 Mouse strains

Pregnant CD1 mice were raised, mated, and sacrificed according to a Schedule 1 method (Animal Scientific Procedures Act 1986) by the home office-licensed facility, BRR-HRB, George Square, Edinburgh, EH8 9XD.

2.2 Dissection of embryonic kidneys

E11.5 kidneys were harvested from CD1 mice under a microscope (Zeiss Stemi-2000) as described in Davies (Davies, 2010). The finding of the vaginal plug in the morning was considered as E0.5. An embryo was beheaded, the tail was cut and all the remaining body part was cut in a half along the spinal cord, exposing left and right kidneys. Cutting was carried out using 25-gauge needles in Eagle's Minimum Essential Medium (MEM) (M5650; Sigma). A kidney is located in a region near the Wolffian duct at the level of the hind-limb bud (Figure 2-1) (Davies, 2010). Other stages of embryonic kidneys were also isolated in a similar manner as described above.

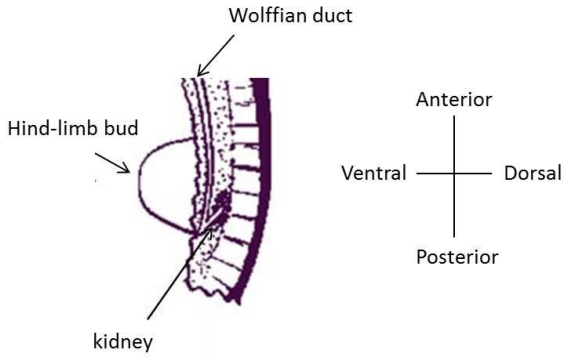

Figure 2-1 Location of E11.5 kidney in the kidney rudiment (Image adopted and modified from Davies, 2010).

2.3 Dissection of embryonic spinal cord

The spinal cord was obtained from E11.5 embryos. For spinal cord isolation, the dorsal region of the trunk was kept and other parts including a head, viscera, and tail were removed by needles. Due to the conspicuous size of the spinal cord, its dorsal part can easily be isolated after opening the canal of the spinal cord. The isolated spinal cord was cut in pieces for the co-culture experiment in Chapter 6.

2.4 Tissue culture methods

2.4.1 Conventional (Saxén-style) culture

In the Saxén system, the isolated kidney was placed on a 5μm pore polycarbonate membrane filter (Millipore) supported by a metal grid. The set of kidney-filter-grid was located in a 35 × 10 mm culture dish (627160; CELLSTAR). The kidney was incubated at the surface of culture medium (KCM) consisting MEM supplemented with 10% foetal bovine serum (FBS) (10108165; Invitrogen) and 1% penicillin/streptomycin (P4333; Sigma). The medium was changed every 2 days.

2.4.2 Low-volume (LV) culture

The low-volume (LV) system was performed by modifying protocols described in Sebinger et al. (Sebinger et al., 2010). Kidneys were grown in a thin film of medium surrounded by a silicone ring (flexiPERM Cone shape A; SARSTEDT).

For glass preparation, microscope slide glasses were cut to 2 cm width by a glass cutter and pieces were washed in 1M HCl for no less than 1h followed by distilled water. They were then oven-dried at 70°C for 20 min. The acid washing step was not only for sterilising the glass, but also for increasing their roughness to make cells easily attach.

Silicone rings were submerged in plenty of distilled water and autoclaved and oven-dried at 70°C for 20 min. By repeating these steps, rings were reusable. The bottom of rings is naturally adhesive to glass. A ring was stuck to a piece of glass, and the set of ring-glass piece was placed on a lid of a small petri dish (35 × 10 mm) (Figure 2-2). To preventing quick drying out of medium, PBS including 1% penicillin/streptomycin was filled in the surrounding area of the lid (Figure 2-2).

A freshly dissected kidney was located in the centre of the ring within KCM confined (Figure 2-2). The KCM volume used in the LV system was 82 μl for the initial 2 days and, afterwards, was 85 μl. KCM was replaced every two days.

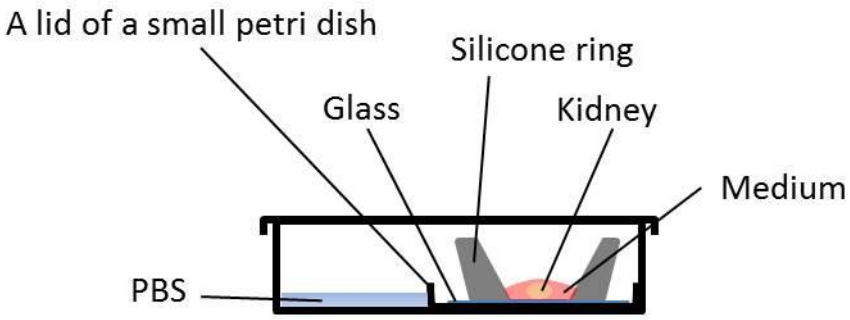

Figure 2-2 Schematic description of modified low-volume system (Image modified and redrawn from Sebinger et al., 2010).

2.5 Drug treatments

For cyclopamine treatment, E11.5 kidneys were pre-incubated in the LV system as described in the section 2.4.2. E11.5 + 7d kidneys were cultured in KCM supplemented with 5µM cyclopamine (Sigma) for 3 days. The concentration of cyclopamine was determined by a previous study (Taipale et al., 2000).

For sodium chlorate ($NaClO_3$) treatment in cultures, E11.5 kidneys were also pre-incubated in the LV system for 4 days followed by being 30 mM sodium chlorate (AnalaR) in KCM for 5 days. This concentration was based on a previous study (Davies et al., 1995).

2.6 Reaggregate culture in the Saxén system followed by the Low-volume system

2.6.1 Isolation of a ureteric bud cyst from kidney reaggregates (Step1)

Kidney reaggregates were obtained by following the methods described above and in Unbekandt and Davies (Unbekandt and Davies, 2010). Freshly isolated 7 kidneys (E11.5) were dissociated by enzymes (1x trypsin/EDTA in PBS) (T4174; Sigma) for 3 min at 37°C followed by being quenched in KCM for 10 min at 37°C in a 500µl tube. After gentle pipetting, dissociated renal cells were filtered through a 40 µm cell strainer (352340; BD Falcon) and centrifuged at 3,000 rpm for 2 min. A reaggregated cell clump (pellet) was then gently detached from the tube and transferred to a filter in the Saxén system using a glass

pipette. The ROCK inhibitor (1.25µM glycyl-H1152-dihydrochloride) (Tocris) was added to KCM for the first 24h and, afterwards, the medium was changed with inhibitor-free KCM. After 3-4 days of incubation in the Saxén system, ureteric bud cysts (UC) were verified by their round shape and lumen, and isolated by manual dissection using needles (Figure 2-3).

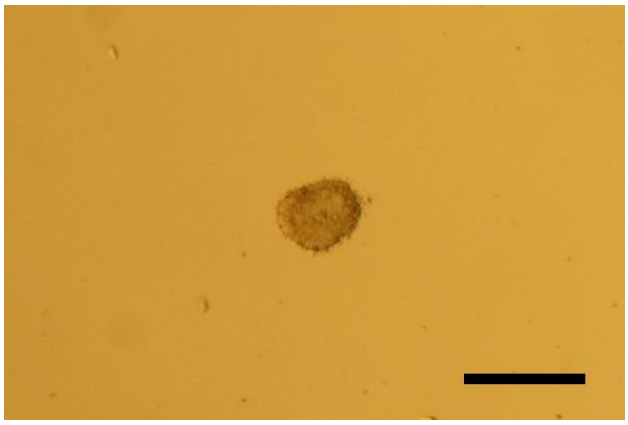

Figure 2-3 A ureteric bud cyst (UC) isolated from a renal reaggregate. The scale bar = 250 µm.

2.6.2 Making metanephric mesenchyme reaggregates (Step 2)

Metanephric mesenchyme (MM) reaggregates were produced as described by Ganeva et al. (Ganeva et al., 2011). To obtain MM reaggregates, 10 to 15 kidneys (E11.5) were isolated as described in the section 2.2. The kidneys were then dissociated by 2x Trypsin/EDTA in MEM for 2min at 37°C and placed in KCM for quenching. The MM were isolated from the ureteric bud and collected in a 500µl tube. The MM were dissociated by gentle pipetting and reaggregated by centrifugation at 3,000 rpm for 2min. The MM pellet was gently detached from the tube by a 200 µl pipette and transferred to a filter in the Saxén system.

2.6.3 Combination of a ureteric bud cyst and mesenchyme reaggregates (Step 3)

The ureteric bud cyst (UC) and the mesenchyme reaggregates were combined and first incubated in the Saxén system for 1-2 days. This process was to make the UC-mesenchyme reaggregates complex solid enough to be cultured in LV system. After 1-2 days of incubation in the Saxén system, the combined culture was transferred to the LV system and cultured for further 5-7 days.

2.7 Cut-and-paste experiments

All cut-and-paste experiments were performed on cultured kidneys in the LV system. The E11.5 kidney was pre-incubated for 7 days before surgical manipulation was applied.

In spinal cord co-culture, a piece of E11.5 spinal cord was obtained as described in section 2.3. Then, the spinal cord was placed next to E11.5+7d kidney and incubated for 3 further days.

For cut-and-paste experiments, it was possible to directly manipulate the kidney since the cortex and medulla regions were clearly defined (Figure 2-4). For the cut-and-paste experiment, a part of the cortex was removed, rotated, and pasted manually using needles. For the cut-only experiment, the entire medulla was removed and discarded.

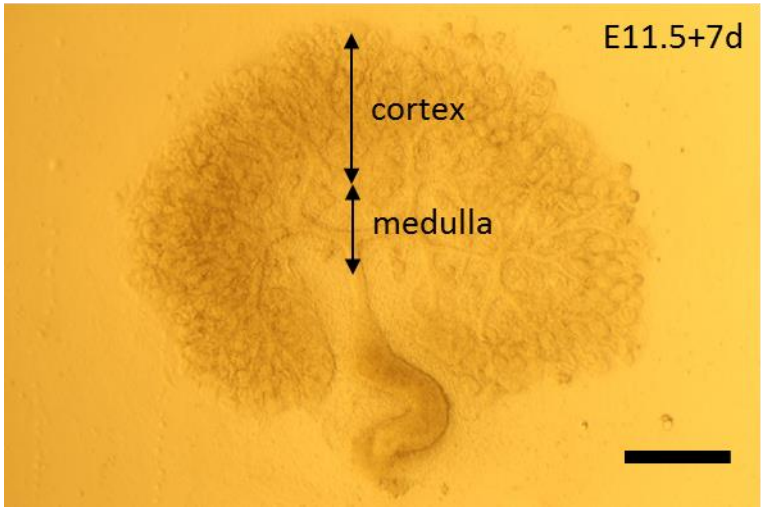

Figure 2-4 A bright-field image of an E11.5+7d kidney in the low-volume system. The scale bar = 500 µm.

2.8 Immunohistochemistry

Tissues were fixed in either 4% PFA or cold methanol for 20 min. In the low-volume (LV) system, the silicone rings were resistant to fixatives (methanol and 4% PFA), which allowed direct fixation and staining in the rings. After fixation, the tissues were rinsed in 1xPBS for 30 min at room temperature. Primary, secondary, and conjugated antibodies used in this thesis are listed in Table 2-1. All antibodies were diluted in PBS. Primary antibodies were applied overnight at 4°C followed by being rinsed in 1xPBS for several hours. Secondary

antibodies were also applied overnight at 4°C. The tissues were washed in 1xPBS for a few hours at room temperature.

Primary antibodies	Working dilution	Company (Catalogue number)
Rabbit anti-laminin	1:100	Sigma (L9393)
Chicken anti-laminin	1:500	Abcam (ab14055)
Mouse anti-calbindin	1:100	Abcam (ab9481)
Mouse anti-pan cytokeratin	1:200	Sigma (C2562)
Rabbit anti-human THP	1:100	Bioquote (bt-590)
Rabbit anti-collagen 18α1	1:100	Sigma (SAB4503213)
Rabbit anti-β-Tubulin III	1:100	Sigma (T2200)

Secondary antibodies	Working dilution	Company (Catalogue number)
Goat FITC anti-chicken	1:100	Abcam (ab97134)
Goat TRITC anti-chicken	1:100	Abcam (ab6874)
Goat FITC anti-mouse	1:100	Sigma (F2012)
Goat TRITC anti-rabbit	1:100	Sigma (T6778)
Sheep FITC anti-rabbit	1:100	CHEMICON (AB7130F)
Horse AMCA anti-mouse	1:100	VECTOR (CI-2000)

Conjugated antibody	Working concentration	Company (Catalogue number)
FITC phalloidin	0.1µg/ml	Sigma (P5282)

Table 2-1 Lists of primary, secondary, conjugated antibodies that are used in this thesis.

2.9 Mounting and imaging

A small amount of a mounting solution (50% PBS: 50% glycerol) was used to cover the specimen. Small pieces of coverslips were then placed at each ends of a glass slide as spacers to prevent crushing of the specimen after it was covered by a long coverslip for imaging. Imaging was performed using a Zeiss Axiovert epifluorescence microscope.

2.10 Time-lapse imaging by lumascope

For time-lapse imaging, E11.5 kidneys were isolated from Lgr5-EGFP-ires-CreERT2 knock-in (Lgr5-ki) embryos (kindly donated by Dr. Owen Sansom from Beaton Institute) (Barker et al., 2007). Lgr5-EGFP kidneys were used because Lgr5 is expressed in the thick ascending

limb of loop of Henle and convoluted distal tubules (Barker et al., 2012). The isolated kidney was set up in a low-volume culture as described in 2.3.2 and was cultured for 7 days when the LoH begins to form. At E11.5 + 7d, the culture was located on an in-incubator microscope, LumaScope (Model 500; etaluma). Images were captured every 15 min for 57 hours from E11.5+7d.

2.11 Histology

2.11.1 Cryosectioning

From E14.5 to E16.5 embryos, kidneys were isolated and fixed in 4% PFA overnight at 4°C. After fixation, the kidneys were rinsed in 1xPBS several times, and cryoprotected in 30% sucrose (S9378; Sigma) in 1xPBS overnight at 4°C. The kidneys were equilibrated in a 1:1 mixture of 30% sucrose/PBS: OCT embedding matrix (12678646; Thermo Scientific) overnight at 4°C. The kidneys were embedded in the same mixture (30% sucrose/PBS/OCT) followed by being frozen on dry ice. The kidneys were cut at 12 µm using a Leica cryostat CM 3050S. Cryosections were transferred on to polysine coated slides (1255015; Fisher) and were air-dried for an hour. The slides were used directly for IHC or kept in a slide storage case filled with desiccants at -20°C.

2.11.2 IHC on cryosections

Cryosections were permeabilized in 0.1% Triton X-100 in 1xPBS (TPBS) for 20 min. Primary antibodies (Table 2-1) in TPBS were applied to the sections overnight at 4°C. Then, the sections were rinsed in TPBS at RT for 30 min. Secondary antibodies (Table 2-1) in TPBS were also applied overnight at 4°C followed by washing in TPBS for 30 min.

2.12 Cell culture

Cell lines that used in this thesis are raTAL (rat thick ascending limb), 6TA2, Six5N6, and L929. raTAL cells were kindly given by Nicholas R. Ferreri (Department of Pharmacology, New York Medical College, US).

The details of isolation and characterisation of raTAL cells are described by Carroll et al. (Carroll et al., 2003). raTAL cells were cultured in renal epithelial basal medium (REBM)

(CC-3191; LONZA) supplemented with renal epithelial growth medium (REGM) (CC-4127; LONZA). REGM consists of rhEGF, insulin, hydrocortisone, GA-1000 (gentamycin sulphate and amphotericin B), FBS, epinephrine, T3 (triiodothronine), and transferrin. The medium was changed every 3-4 days. For raTAL cell passage, the culture medium was aspirated from a flask and the cells were rinsed with 1xPBS (P4417-100TAB; Sigma) to remove remaining culture medium. The cells were detached from the flask by adding 1xTrypsin/EDTA (TE) (T4174; Sigma) diluted in RPMI 1640 (BE12-167F; LONZA) and incubated for 2-3 at 37°, 5% CO_2. TE was quenched in RPMI 1640 with 10% FBS. The cells were centrifuged at 1,000 rpm for 5 min. The supernatant was discarded and 30% of the cells were re-suspended in the fresh culture medium and seeded in a new flask.

The details of producing and maintaining 6TA2 and Six5N6 cells are described by Tai et al. (Tai et al., 2012). Both cell lines were cultured in DMEM-F12 (D8437; Sigma) with 10% FBS (10108165; Invitrogen), 1x ITS (insulin, transferrin, selenium) (I3146; Sigma), 1x antioxidant (A1345; Sigma), and 1x penicillin/streptomycin-glutamine mix (10378016; Invitrogen). The medium was changed every 3 days. Passage was carried out as described above.

L929 cells (CCL-1™; ATCC) were cultured in MEM supplemented with 10% FBS and 1x p/s and the medium was changed every 3 days. Passage was performed as described above.

2.13 Cell migration assay

2.13.1 General protocol for cell migration assay

The cell migration assay was performed as described in Transwell Permeable Supports introductions (CORNING) and Transwell Migration Assay (Science Protocols.org).

raTAL cells were harvested by 1xTE and quenched in RPMI 1640 with 10% FBS. The cells were re-suspended in fresh medium and counted using a haemocytometer. An optimised density (3×10^4 cells/insert) of raTAL in 300 µl of the culture medium was added to the upper side of a FluoroBlok insert (08772142; BD) and incubated at 37°C, 5% CO_2 overnight. FluoroBlok (pore size; 8µm) was chosen to use since it has a fluorescence-blocking membrane (light between 490-700nm will be interfered from cells on the top), so fluorescently labelled cells from the bottom membrane can be detected. At the same time,

the same density of cells (6TA2, Six5N6, or L929) or 6TA2-conditioned medium was added to a lower 24-well plate (353504; BD) and incubated overnight. The medium volume in each well in the lower plate did not exceed 700 µl. The next day, the inserts were transferred into the plate and incubated at 37°C, 5% CO_2 for 4h.

2.13.2 Heparin-binding assay in 6TA2 conditioned medium

6TA2-conditioned medium (6TA2 cond) was obtained from overnight incubation of 6TA2 cells (3×10^4 cells/insert) in REBM containing REGM (culture medium for raTAL).

For Heparin-binding protein (HBP) removal from 6TA2 cond, 300 µl (Ligand density: 5 mg heparin/ml) of Heparin-Separopore resin (HSr) (20181013-2; bioWORLD) per well were washed in 1 ml of REBM (w/o serum) several times. HSr was added to 700 µl of 6TA2 cond and mixed by rotation overnight in 4°C cold room. The HSr-beads were centrifuged at 1000rpm for 5 min and the supernatant was used in the migration assay.

For the migration assay of raTAL towards HBP, HSr in 6TA2 cond experiment was repeated as described above. The HSr-beads were centrifuged and the supernatant was discarded. 1.5 ml of REBM with 2.5M NaCl was mixed with the HSr-beads for 1h. The beads were centrifuged and the supernatant (9ml from 6 wells) was collected and transferred to a dialysis tube (Scientific Instrument Centre Ltd), which was prepared and rinsed in warm distilled water. The dialysis bag was then dialysed against an excess (100ml) of REBM overnight to get rid of salts. HBP were highly concentrated by removing water (8ml) after adding poly (ethylene oxide) powder (82110; Sigma) around the dialysis bag for 4-5h. HBP in medium was aspirated by a syringe and transferred to 1 ml tube. 300 µl of isolated HBP in medium was added to a well for a migration assay.

2.13.3 Quantification of migrated cells

Since FluoroBlok (pore size; 8µm, the largest available) did not permit trans-filter migration of the nuclei of raTAL cells but only cytoplasm, I decided to quantify number of pores that cytoplasm of raTAL cells penetrated. After the cell migration assay, inserts were rinsed in 1x PBS. Cells on the bottom of the insert were fixed with 4% PFA for 15min at RT. Cells were rinsed in 1xPBS for 10 min and permeabilised with 0.1% Triton X-100 (T8532; Sigma) in 1xPBS (TPBS) for 5 min at RT. Then cells were stained with FITC-Phalloidin (P5282;

Sigma) for 1h at RT and rinsed twice in TPBS for 10 min at RT. For nuclear staining in a control image showing there was no migrated nuclear of cells, cells were stained with 1 in 3000 of propidium iodide (1.0mg/ml) (P3566; Molecular Probe) for 5 min at RT and rinsed with TPBS for 5 min at RT. The insert was placed on a glass slide and imaged by ZEISS observer. D1 inverted microscope. 7 fields per each insert were captured. Pores covered by raTAL cytoplasm were counted by Image J Cell counter.

2.14 Statistical analysis

In order to compare the mean of two groups, a two-tailed t test was performed, and the p value less than 0.05 was considered as a significant difference. For analysing data from more than two groups, one way analysis of variance (ANOVA) was used. If the p value from one way ANOVA was <0.05 (statistically significant), post hoc tests were then performed. In case of the same sample size in each data groups, Tukey's honest significant difference (HSD) post hoc test was used. If each data groups had the different sample size, Scheffe post hoc test was used. These statistical analyses were performed using IBM SPSS Statistics 21.

To show the reliability of the percentage data, 95% confidence interval was used. The formula is t=z´x SQR(p(1-p)/n) (z´; standard normal distribution, x; mean, SQR; square root, p; possible sample size/population of size, n; sample number) (Bremer, 2010).

3 Chapter 3 Anatomy of Henle's loop in the developing mouse kidney

3.1 Introduction

The aim of this chapter is to make careful observation on the natural orientations of Henle's loop (LoH) in developing mouse kidneys. This step was essential for later tests of how the LoH orientation navigates by guidance cue(s). In general, typical orientation of the LoH has been naturally illustrated and accepted as its alignment at the corticomedullary axis when matures, yet no study has been made of any quantitative measurement on the orientation of the developing LoH (Davidson, 2008, Dressler, 2009, Costantini and Kopan, 2010, Little and McMahon, 2012). Therefore, I carefully observed natural features of the LoH and quantified the natural arrangement of developing LoH as evidence to confirm or improve current knowledge of the LoH orientation. By quantification of the developing LoH orientation, I sought any possible pattern that might be an important step to show the possibility of being any cue(s) driving LoH directional growth.

Most of details pertinent to LoH structure and development have been described in Chapter 1. However, it is necessary to briefly account for some important points in this section.

The adult kidney comprises hundreds of thousands of nephrons in human and thousands of nephrons in mouse (Sariola, 2003). The nephron is subdivided into the glomerulus, the proximal tubule, the LoH, and the distal tubule. Finally, the nephron components join the collecting duct system via the connecting tubule. Among these, the LoH, a hair-pin shaped tubule, is the mid-segment that connects the proximal and the distal tubule. The LoH forms in the cortex and crosses the cortical-medullary boundary. This occurs in a repetitive manner; new nephrons (including the LoH) form repeatedly in the outer cortex during the kidney development.

There are two types of nephrons (short and long) as distinguished by the location of the LoH bend (refer to 1.5.1). The short LoH originate from the outer cortex and have a bend in the outer medulla, going no deeper. The short LoH have short length of thin descending limbs. The long LoH begin to form from the juxtamedullary cortex. The long LoH comprise thin-ascending limbs, thin descending limbs, and thick ascending limbs. Unlike the short LoH, the long LoH have their bend within the inner medulla.

Development of the long LoH can be split into three stages (anlage, primitive, and immature) based on morphology and position within the mouse kidney sections (Nakai et al., 2003)

(Figure 3-1). All can be seen at E16.5 (Nakai et al., 2003). The anlage is the earliest stage of the LoH. The anlage LoH has a short U-shape and no straight limbs are distinguishable at this stage (Nakai et al., 2003) (Figure 3-1). The anlage LoH has a close contact with immature glomeruli and is located near the peripheral region of the kidney (Figure 3-1). Compared to the anlage LoH, the primitive LoH has a straight elongated descending and ascending looped tubule (Figure 3-1). From this stage, the apex of LoH starts to reach the medulla of the kidney (Figure 3-1). As the primitive LoH matures, it differentiates into the immature LoH. The immature LoH can be divided into three distinct portions: thin-limbs, thick-limbs and the apex (Figure 3-1). Thin epithelium, characteristics of LoH, can be formed in the deep medulla and even near the tip of the papilla (Huber, 1905, Neiss, 1982) (Figure 3-1).

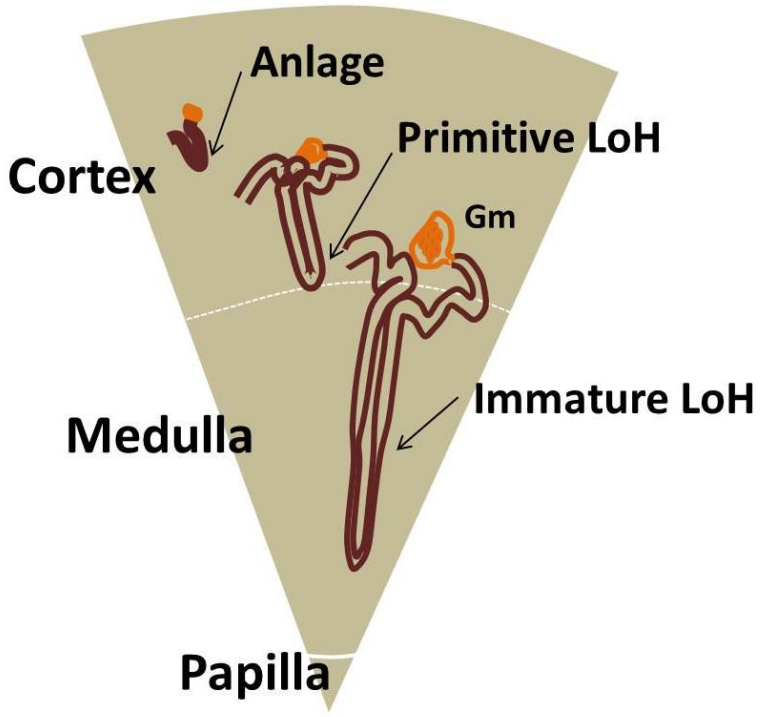

Figure 3-1 A schematic diagram showing the anlage, primitive and immature loop of Henle (modified from Nakai et al., 2003). The anlage LoH resides at the peripheral region of the kidney. No straight limbs are observed at this stage but the LoH has a close contact with the immature glomerulus (Gm). At the primitive LoH stage, the LoH apex begins to reach the medulla. A straight descending and ascending limb of the LoH are observed. As the primitive LoH matures into the immature LoH, some of the immature LoH appears to reach the papillary tip. Distinct portions of thin-limbs, thick-limbs, and the bend are observed at this stage of the LoH.

While Nakai et al. distinguished three stages of the developing LoH from developing mouse kidney sections (Nakai et al., 2003), later Little et al. distinguished only two (primitive and immature LoH) (Little et al., 2007). Little et al. tied the anlage and primitive LoH into merely the primitive LoH (Little et al., 2007). Ontologically, they separated LoH development into a cortical (primitive) and a cortical-medullary (immature) LoH (Little et al., 2007). Since Little et al.-style classification is more recent, and it has been used as the basis of the Edinburgh Mouse Atlas (www.emouseatlas.org) and of GUDMAP (www.gudmap.org) in describing the developing LoH, I have used their nomenclature in this chapter.

Prior to setting up experimental methods to investigate LoH guidance, it was necessary to characterize morphology, marker gene expression, and timing of the U-shaped LoH development *in vivo*. This information could then be used for comparison with LoH being manipulated experimentally. Therefore, I first made careful observations on the morphological features of the LoH. Then, I assessed timing of expression of a known marker; Tamm-Horsfall protein (THP) (Tamm and Horsfall, 1950, Muchmore and Decker, 1985). Additionally, cadherin-6, also known to be expressed in the LoH and proximal tubules, was tested (Cho et al., 1998). Then, the timing of the LoH formation was investigated since knowing the timing information *in vivo* would be critical to determine whether it might be possible to study LoH guidance in an *ex vivo* culture system. If the LoH formed too late *in vivo*, it would be difficult to recapitulate it in an *ex vivo* culture system. More importantly, combined with timing information of the LoH and its final orientation, the question of whether the U-shaped tubule of the LoH orients centripetally from its beginning or forms randomly and then changes its arrangement can be answered. These results can then form the criteria against which to investigate LoH guidance *ex vivo*.

3.2 Results

3.2.1 Characteristics of the loop of Henle in E14.5, E15.5, and E16.5 kidneys

In order to study morphological features of the LoH *in vivo*, serial stages of embryonic kidneys were used. Although all the distinct stages (primitive, and immature stages) of the LoH can be seen at E16.5 (Nakai et al., 2003), a range of E14.5 to E16.5 was chosen to investigate the LoH from different stages of the kidney. Transverse cryosections of kidneys were immunostained to reveal the LoH structure. Anti-laminin antibody was used to mark the general basement membrane of epithelium and anti-Tamm-Horsfall Protein (THP) antibody was used as a molecular marker for the LoH (Tamm and Horsfall, 1950, Pennica et al., 1987). The expression of THP begins from the primitive (= anlage) LoH (Nakai et al., 2003) a little after the LoH forms. To see LoH before this, cadherin-6 was used to mark LoH, although cadherin-6 is also expressed by proximal tubules. However, as will be shown in this and the next chapters, the LoH has a unique morphology, a U-shape, which can be clearly defined by laminin staining.

Primitive LoH (n=8) were observed in transverse cryosections of E14.5 kidneys (n=5) (Figure 3-2). The kidneys were sectioned at 12 µm thickness, but not many sections showed the entire morphology of the LoH. The primitive LoH has a short U-shaped structure and resides in the cortex having its bend orientated toward the medulla (Figure 3-2). At E14.5, the primitive LoH from 8 E14.5 kidneys expressed neither THP nor cadherin-6 (Figure 3-2). However, as described in the paragraph above, the LoH shown in Figure 3-2 were clearly distinguishable by the use of laminin staining which also showed the close co-localisation with the glomerulus as well as cadherin-6 expression in the proximal tubule connecting to the LoH.

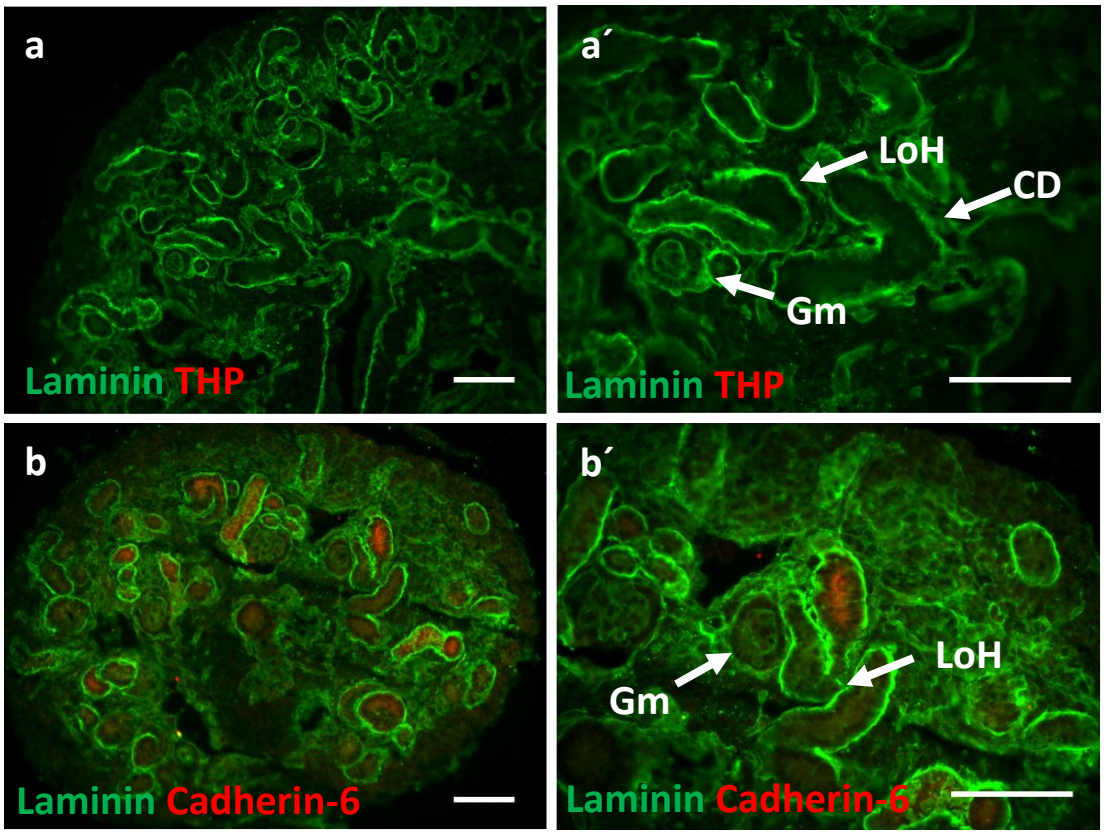

Figure 3-2 The primitive loop of Henle (LoH) from E14.5 kidneys. E14.5 kidneys (n=5) were cryosectioned (transversely) at 12 µm thickness and immunostained to visualise LoH. (a) A low-power view of laminin (general basement membrane; green) and Tamm-Horsfall protein (THP) (LoH; red)-stained cryosections. (a´) A high-power view of (a). THP expression in the LoH was absent at this stage. Gm (glomerulus), CD (collecting duct) and LoH are shown and indicated by the arrows. (b) A low-power view of a laminin and cadherin-6 stained cryosection. As alternative marker for LoH and proximal tubules, cadherin-6 was used. (b´) A high-power view of (b). However, cadherin-6 expression was only observed in the proximal tubule. The scale bar = 100 µm.

More defined straight limbs of the immature LoH (n=9), than those shown at E14.5, were observed at E15.5. THP started to be expressed in the apex of the LoH from this stage of the kidney (Figure 3-3).

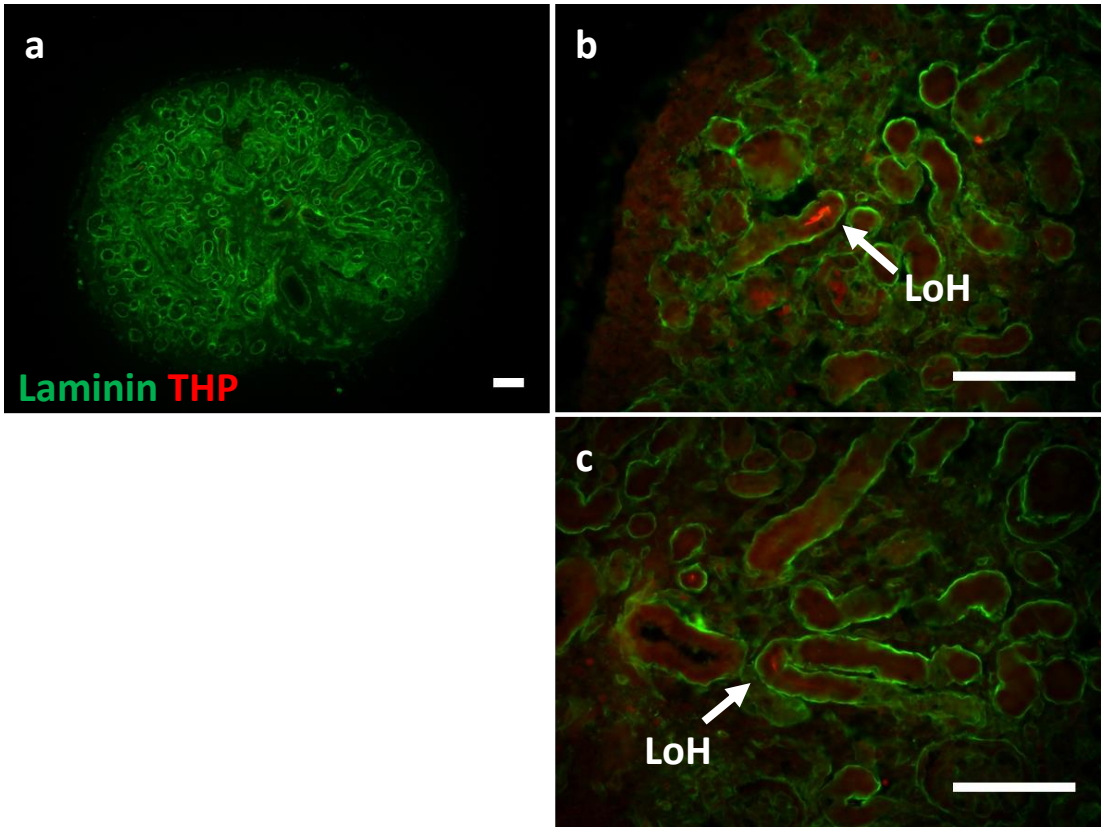

Figure 3-3 The immature loop of Henle (LoH) from E15.5 kidneys. E15.5 kidneys (n=9) were cryosectioned (transverse) at 12 µm thickness, and immunolabled with anti-laminin (general basement membrane; green) and anti-THP (loop of Henle; red) antibody. (a) THP expression was not detected in the low-power view. (b), (c) A high-power view of (a). THP expression in the LoH is indicated by arrows. The scale bar = 100 µm.

Immature LoH from E16.5 kidneys (n=9) also showed defined straight limbs and a U-shaped bend (Figure 3-4). Additional primitive LoH were also observed at this stage (Figure 3-4). Similar to the LoH from E15.5, adluminal THP expression resided in the apex of the LoH (Figure 3-4). THP expression in collecting ducts, weaker than that of the LoH, was also observed. Some immature LoH reached the innermost region of the medulla (Figure 3-4).

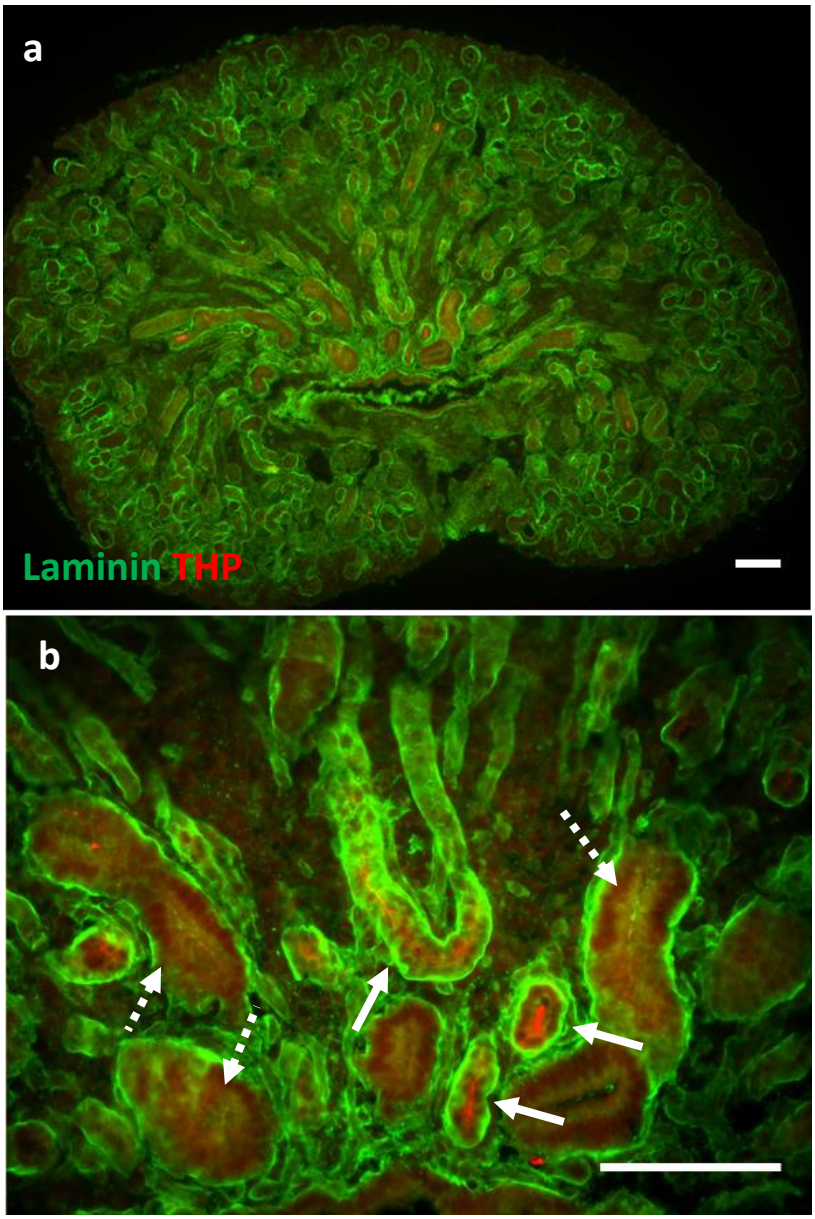

Figure 3-4 The immature loop of Henle (LoH) from E16.5 kidneys. E16.5 kidneys (n=9) were cryosectioned (transverse) at 12 µm, and immunolabled with anti-laminin (general basement membrane; green) and anti-THP (loop of Henle; red) antibody. (a) A low-power view of E16.5 kidney cryosection. (b) A high-power view of (a). Defined U-shaped LoH were shown with THP expression (arrows). Collecting ducts also expressed THP weakly. The scale bar = 100 µm.

3.2.2 The loop of Henle shows a radial orientation in developing kidneys

Confirming a pattern of natural LoH arrangement was critical to studying and manipulating guidance cues of LoH in further experiments. To test whether the LoH head in a preferred (non-random) orientation, I quantified the angles of the LoH direction towards the kidney centre. In E14.5 (n=5), E15.5 (n=9), and E16.5 (n=9) kidneys, only LoH showing a clear apex and a U-shaped tubule were collected for directional quantification. Directions were recorded as an 'error angle', being the difference between the LoH direction and a direct line to the centre of the kidney. The error angles of the LoH were measured between the two lines (Figure 3-5). One line was extended along the LoH axis, and the other connected the apex of the LoH and the centre of the kidney (Figure 3-5). The centre of the kidney was determined by the Image J Centroid tool after designating the outline of the kidney section (Figure 3-5). The Centroid is the centre point of the region of interest (ROI), which is the outline of the kidney sections in this case, and it is determined by averaging the x and y coordinates of all pixels of the ROI. This computer-based approach was used in preference to subjective judgement about where the centre of the kidney was, to avoid inadvertent use of LoH convergence to bias a human's perception of where the centre would be.

The mean ± SEM error angles of LoH were 24.4±2.7°, 25±1.1°, and 18±0.7° from E14.5 (8 LoH from 5 kidneys), E15.5 (15 LoH from 9 kidneys), and E16.5 (22 LoH from 9 kidneys) respectively (Figure 3-5). There was no significant difference of error angles of the LoH between different stages of the kidneys (P value = 0.43 from a one way ANOVA). (Figure 3-5).

To assess the properties of LoH that were orientated centripetally, I classified any LoH with an error angle less than 45° as a 'centripetal LoH'. 85% of total LoH shown in sections were centripetal LoH.

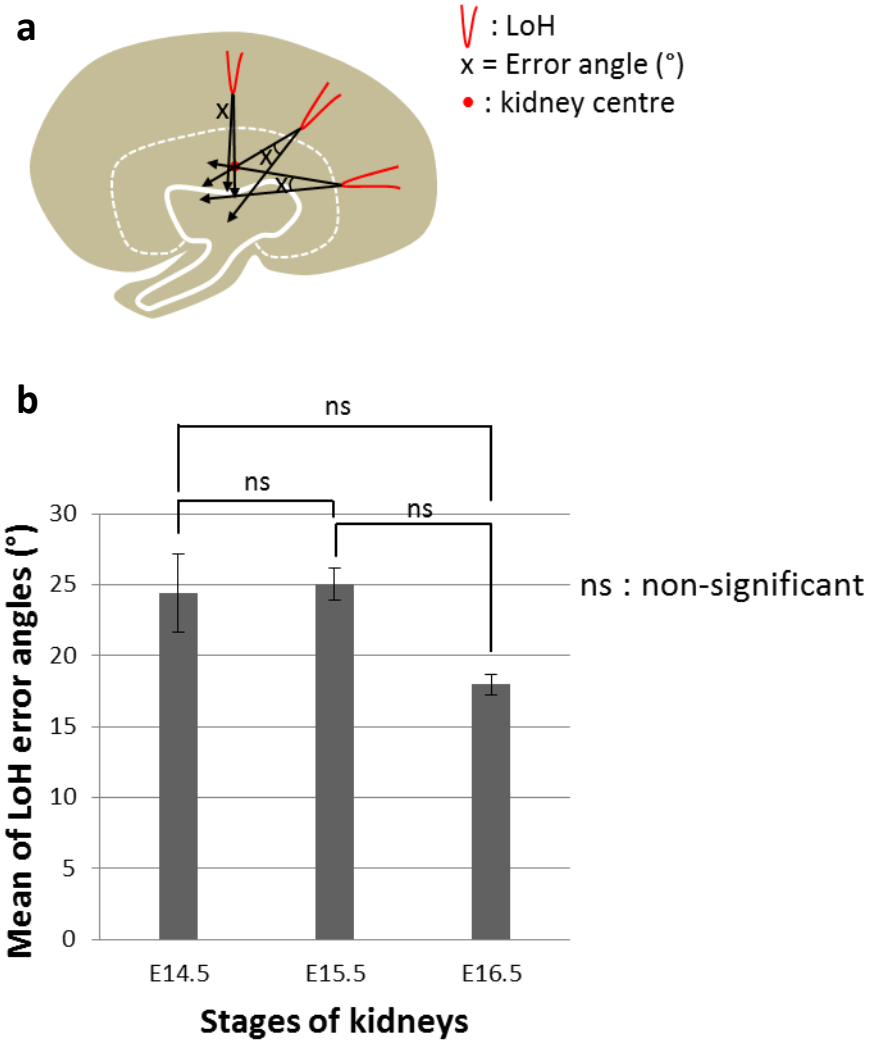

Figure 3-5 Quantification of the radial arrangement of the Henle's loop (LoH) from developing kidneys. (a) A schematic drawing shows the method to quantify the error angles of the LoH from developing kidneys. The error angles were measured between two lines (one extended line that extended the axis of the LoH, and the other line connecting the apex of the LoH and the kidney centre as determined by the Image J Centroid). The angles were measured using AxioVision Rel. 4.8 software. (b) The mean ± SEM error angles from E14.5 (8 LoH from 5 kidneys), E15.5 (15 LoH from 9 kidneys) and E16.5 (22 LoH from 9 kidneys) are 24.4±2.8 (E14.5), 25±1.1 (E15.5), and 18±0.7 (E16.5) respectively. Error bars indicate SEM. Comparisons between groups are analysed by a one way analysis (ANOVA) and the P value is 0.43 (the P value > 0.05 is considered as non-significant differences between groups).

Subsequently, I assessed whether LoH head centripetally from the beginning of showing their U-shape or whether the young U-shapes are randomly oriented and later find their way towards the centre. As nephrogenesis proceeded repetitively by forming new nephrons at the peripheral region of the cortex throughout kidney development (reviewed by Saxén, 1987, Little and McMahon, 2012), in addition to an error angle of each LoH, its distance from outline of the kidney sections was quantified (Figure 3-6). The location of the LoH was quantified by measuring the distance between the LoH apex and the crossing point of the LoH axis and the outline of the kidney section (Figure 3-6). For an objective view on the result, horizontal and vertical diameters were measured in each stage of kidney sections (Figure 3-6). This was to interpret the location of the LoH relative to the size of the kidney.

In E14.5, all the LoH (8 LoH from 5 kidneys) were located in between 200 to 300 μm of distance from the outline of the kidney sections and their error angles varied from 1.41° to 57.76° (Figure 3-6). However, a linear graph (E14.5) indicated that the LoH closer to the outer region of the kidney (newly formed) appeared to orient more centripetally (<45°) (A positive linear relationship) (Figure 3-6). The data of E15.5 LoH (15 LoH from 9 kidneys) showed that most LoH oriented centripetally regardless of their location (No linear relationship) (Figure 3-6). At E16.5, a notable pattern was shown in their orientation. LoH (22 LoH from 9 kidneys) in the outer region of the kidney showed more variable orientation whilst the LoH located close the centre orientated more centripetally (Figure 3-6). The closer to the kidney centre, the more centripetally orientated were the LoH (A negative relationship) (Figure 3-6).

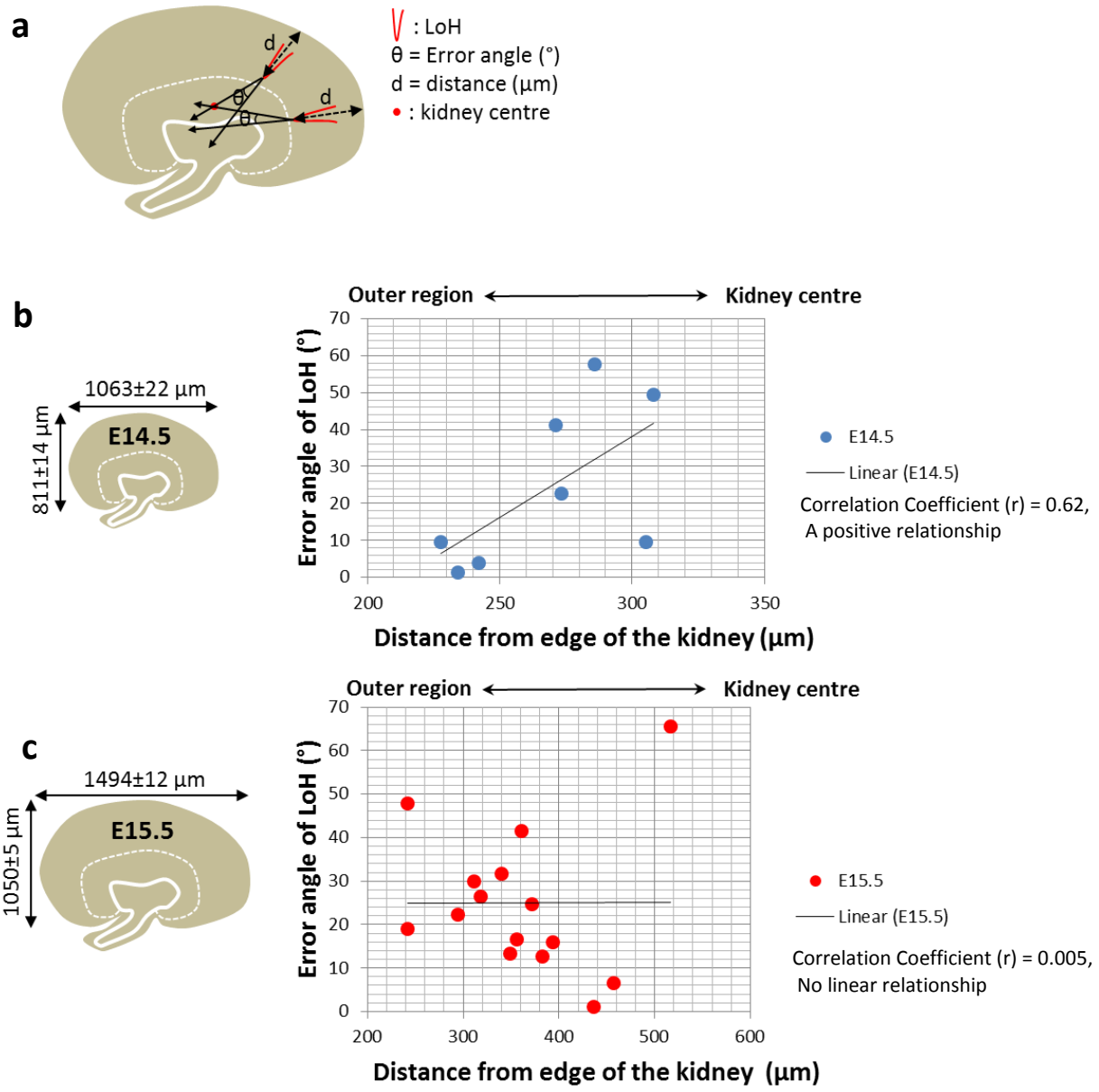
a
d
θ
d
θ
: LoH
θ = Error angle (°)
d = distance (µm)
: kidney centre
b
1063±22 µm
811±14 µm
E14.5
Outer region
Kidney centre
Error angle of LoH (°)
70
60
50
40
30
20
10
0
200
250
300
350
Distance from edge of the kidney (µm)
E14.5
Linear (E14.5)
Correlation Coefficient (r) = 0.62,
A positive relationship
c
1494±12 µm
1050±5 µm
E15.5
Outer region
Kidney centre
Error angle of LoH (°)
70
60
50
40
30
20
10
0
200
300
400
500
600
Distance from edge of the kidney (µm)
E15.5
Linear (E15.5)
Correlation Coefficient (r) = 0.005,
No linear relationship

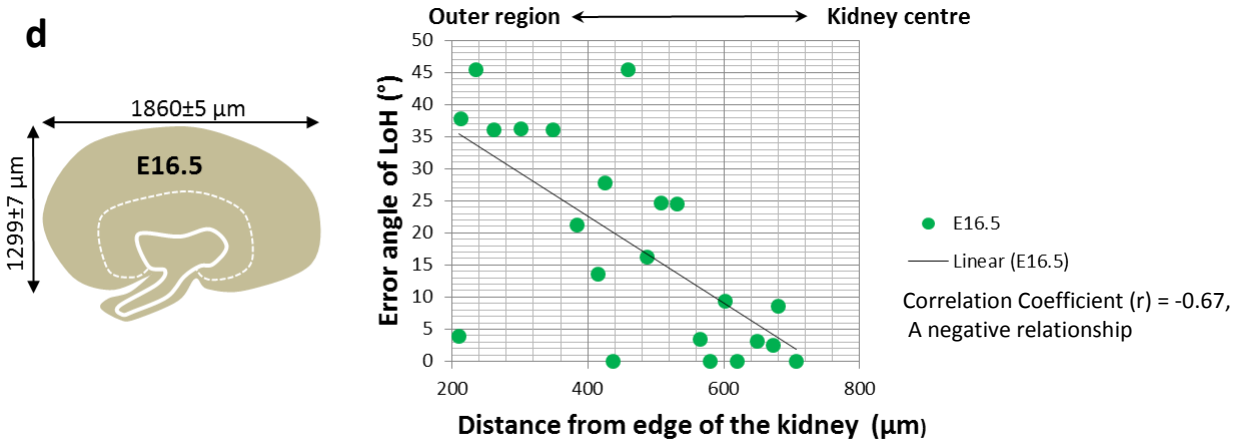

Figure 3-6 Quantification of Henle's loop orientation according to location in developing kidneys. (a) A schematic drawing shows the method to quantify the error angles and locations of the LoH in E14.5 (n=5), E15.5 (n=9), and E16.5 (n=9) kidney. The error angle was measured between one line crossing the LoH axis and the other line connecting the LoH apex and the kidney centre. The location of the LoH was measured by the distance between the LoH apex and a crossing point (the LoH axis and the outline of the kidney). (b, c, d) Mean ± SEM of horizontal and vertical diameters of E14.5 (b), E15.5 (c), and E16.5 (d) kidney sections were measured using AxioVision Rel. 4.8 software to compare locations of the LoH independently in each kidney stage. The error angles and locations of LoH in each stage of E14.5 (b), E15.5 (c), and E16.5 (d) are plotted in scatter charts. Correlation Coefficient (r) between distance and error angles in each groups are 0.62 (b), 0.005 (c), and -0.67 (d) and these are calculated in Excel (r value between +0.50 and +0.70 is considered as a moderate uphill (positive) linear relationship, between -0.50 and -0.70 is considered as a moderate downhill (negative) relationship, and the value close to 0 is considered as no linear relationship).

One issue might arise from interpreting the result shown in Figure 3-6. For instance, when two different LoH aligned in the same axis but at different proximity to the kidney centre, an error angle from the LoH (closer to the centre) would be bigger than one from the other LoH (farther to the centre) (Figure 3-7). This effect might give rise to incorrect interpretation of the LoH arrangement along their location in the kidney. To avoid this problem, I additionally quantified 'absolute error' of each LoH (Figure 3-7). The absolute error is the distance between the kidney centre and the point where the extended line of the LoH axis meets the perpendicular line crossing the kidney centre (Figure 3-7). The absolute error (α) was obtained by the formula; $\alpha = \sin(\text{error angle}) \times \text{distance}$ (between the LoH apex and the kidney centre). Therefore, the smaller the absolute error is close to 0, the more the LoH were centripetally orientated (Figure 3-7).

The absolute error from the LoH in each stage of the kidneys (E14.5, E15.5, and E16.5) also plotted according to the LoH location from the kidney edge as well as the kidney centre as shown in Figure 3-6 (Figure 3-7). The data still showed the pattern that the closer the LoH are to the kidney centre (or away from the kidney edge), the more obviously the LoH are centripetal (Figure 3-7). The result resolved the error angle issue.

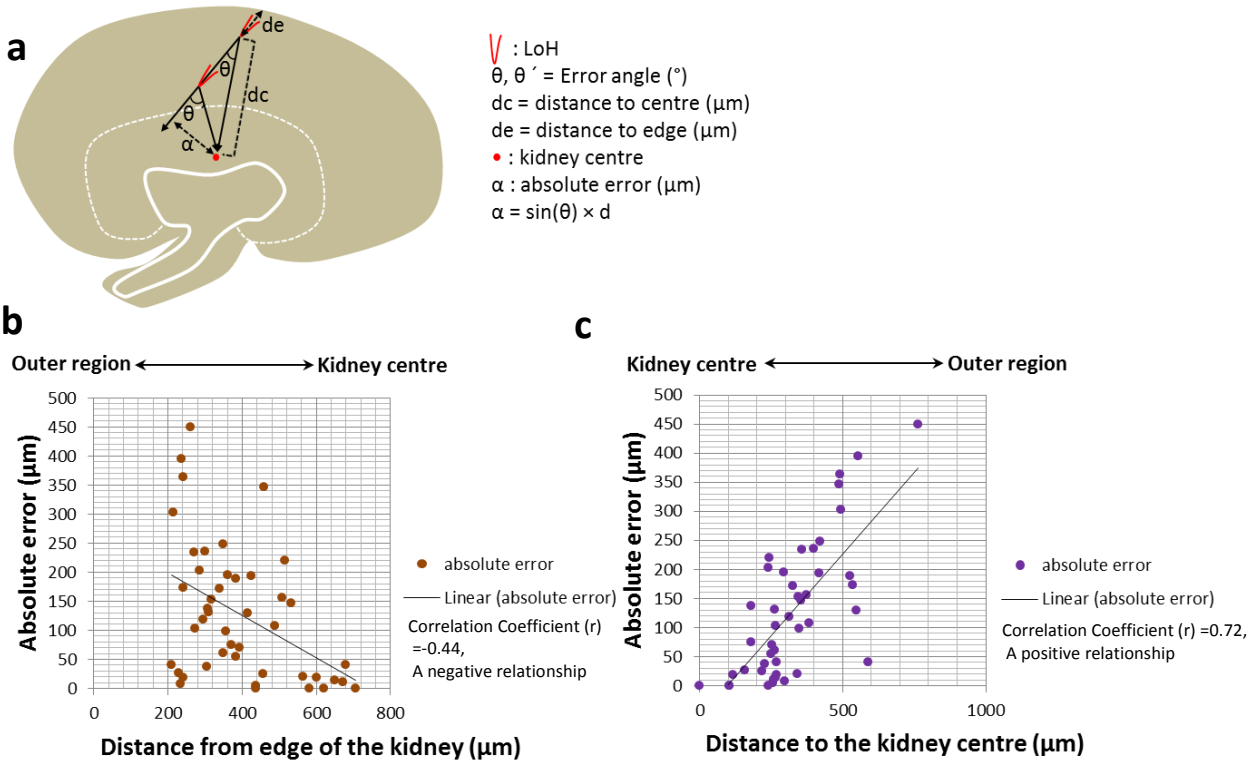

Figure 3-7 Absolute errors of the Henle's loop orientation along their location in developing kidneys. (a) A drawing illustrates that inaccurate interpretation can arise from the error angles. Although two LoH are in the same axis, the error angle (x´) from the LoH closer to the centre is bigger than the error angle (x) from the LoH farther from the centre. To avoid this, I quantified the absolute error (α) to the kidney centre that shows an unbiased value if the LoH align in the same axis. The absolute error (α) was obtained by the formula; α = sin(error angle) × d (distance between the LoH apex and the kidney centre). (b) The absolute error of each LoH was plotted along the distance from the kidney edge (de). (c) The absolute error was also plotted according to the distance from the kidney centre (dc). The distance and angles was measured using AxioVision Rel. 4.8 software. Correlation Coefficient (r) between distance and absolute errors in (b) and (c) are -0.44 and 0.72 respectively. These are calculated in Excel (r value between +0.70 and +1.00 is considered as a strong uphill (positive) linear relationship, between -0.30 and -0.50 is considered as a weak downhill (negative) relationship).

3.3 Chapter discussion

3.3.1 Characterization of Henle's loop

Features of the LoH in the developing kidney have been observed in this chapter. Morphological characteristics of the LoH *in vivo* were assessed by cryosectioning and immunostaining of the serial stages of kidney development. From the results using THP/Umod as LoH markers, it was noted that there were some THP-negative primitive LoH. Those non THP-expressing LoH might be newly formed LoH even before the anlage stage since Nakai et al. mentioned that THP is initially expressed in the anlage LoH (Nakai et al., 2003). Therefore, I propose extra stages of the anlage LoH; type a anlage (THP-negative) and type b anlage (THP-positive).

The absence of THP/Umod expression in E14.5 LoH from the result also corresponded with the microarray expression profile from the GUDMAP (GenitoUrinary Developmental Molecular Anatomy Project) database www.gudmap.org (McMahon et al., 2008, Harding et al., 2011). The expression profile is displayed by heatmap (red; If the log2 RMA (robust-array average) values are bigger than the median value of each row, blue; If the values are smaller than the median value, black; if the values are close to the median) (www.gudmap.org). Although the expression profile of E14.5 was gained from whole organ (kidney) excision and of E15.5 was gained by laser captured from LoH (www.gudmap.org), the heatmap showed that the Umod expression at E14.5 (black) is weaker than E15.5 (red) (Figure 3-8). This was indirectly comparable although E14.5 profile gained the values from whole kidney which is still weaker than E15.5 profile gained from the LoH (Figure 3-8). This also suggests that the use of the marker gene (THP) cannot be an absolute marker for demonstrating the LoH of developing kidneys. Therefore, the unique morphology of the LoH by anti-laminin staining would be mostly employed to show the LoH. THP and Cadherin6 expression would not be sufficient, but would be helpful to demonstrate the LoH in further chapters.

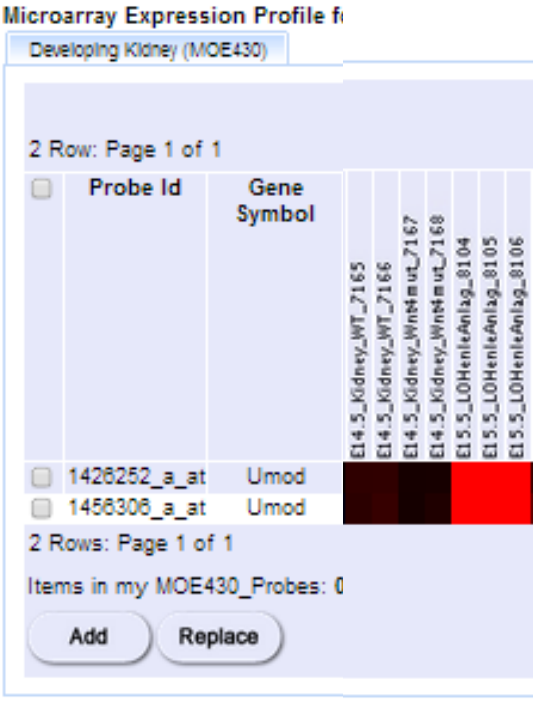

Figure 3-8 Umod microarray expression profile from GUDMAP database (The profile heat map was captured and modified from www.gudmap.org; E14.5 data are originally from Andrew P McMahon's group, E15.5 data are from Steve Potter's group). The THP (Umod) expression profile is displayed by heatmap (red; If the log2 RMA (robust-array average) values are bigger than the media value of each row, black; If the values are close the media value of each row, blue; If the values are smaller than the media value of each row). The Umod expression (black) of E14.5 is achieved by whole organ excision and the Umod expression (red) of E15.5 is achieved by laser captured.

3.3.2 The loop of Henle shows increasing centripetal orientation while maturing

Subsequent to study morphological and molecular properties of the developing LoH, I quantified the LoH orientation in the kidney. I began with quantifying and comparing the LoH orientation by measuring the mean error angle from each stage (E14.5 to E16.5). The result shows that most of the LoH orientated centripetally and there was no significant difference of the mean error angles of the LoH between different stages of kidneys.

In order to find any pattern of the LoH orientation whether the LoH initially forms centripetal orientation or they initially head randomly and steer to the kidney centre, the error angles as well as the absolute errors of the LoH according to their location in the kidney were plotted. Interestingly, both the error angles and the absolute error quantification indicate that the LoH orientates more centripetally while they mature. This also strongly suggests that any guidance cue(s) might steer the LoH orientation during the kidney development.

Taken together, in this chapter natural features of the LoH were characterised and assessed. Since the quantitative analysis on the LoH orientation suggests that study of the LoH guidance cue(s) may be helpful, more precise and manipulative study will be carried out on the LoH in an *ex vivo* culture system. Hence, the results from this chapter will also serve as criteria for further experiments.

4 Chapter 4 Developing an appropriate culture system to test whether the loop of Henle moves

4.1 Introduction

The anatomy of natural development of the loop of Henle (LoH) in embryonic kidneys *in vivo* was described in Chapter 3. There was a stereotyped (centripetal) arrangement of LoH along the corticomedullary axis. The next question is how the LoH elongates towards the deep medulla and what guidance cue(s) it follows. This question seems not to have been investigated. An answer should expand our understanding of nephron development.

To answer the above question, setting up a reliable technique to study the LoH was essential. I chose to use an *ex vivo* culture system to investigate the LoH, as imaging and manipulating the LoH in the culture would be much easier compared to the LoH *in vivo*. A reliable culture system therefore needed to be established to achieve well-developed LoH. The aim of this chapter is to describe a new organ culture method to investigate LoH development.

As embryonic kidneys can grow and recapitulate development of renal structures at least up to a point, organ culture has been widely used to study renal development (Rienhoff, 1922, Grobstein, 1953a, Grobstein, 1953b, Grobstein, 1956, Gluecksohn-Waelsch and Rota, 1963, Saxén and Lehtonen, 1987). In 1922, Reinhoff cultured little pieces from the mesonephros and metanephros of chick embryos (8d to 10d) in a hanging drop culture (Rienhoff, 1922). In the hanging drop tissue culture technique, a tissue can be inoculated into a small amount (drop) of culture media which placed on a culture dish lid. In this manner, the drop containing the tissue can be suspended by its surface tension and this allows the specimens grow. A different kind of the organ culture technique, a grafting technique, has been first used to study metanephric anlagen from 7d chick embryos by Atterbury (Atterbury, 1923). She dissected and grafted whole metanephric anlage on the chorioallantoic membrane (CAM) resulting in fine development of epithelial tubules and vascularised glomeruli (Atterbury, 1923). Other than the CAM, various regions such as the omentum (Waterman, 1940) and the intraocular region (Runner, 1946) in allogeneic hosts have been used as grafting sites to study renal development.

In the 1950s, Grobstein adopted Borghese's organ culture method of mouse salivary gland to his E11 mouse embryonic kidney studies (Grobstein, 1953a, Grobstein, 1955, Saxén, 1987). Then, Saxén modified it further by using a Trowell-type screen made of stainless steel to support a piece of a filter (Saxén, 1962, Saxén et al., 1968, Saxén, 1987). In the Saxén system, the embryonic kidney is grown on the filter at the air-medium interface, and the early stages of development such as ureteric bud (UB) branching, and formation of comma-

and S-shaped nephrons, take place. LoH development is, however, hardly seen. Moreover, in the Saxén system, it is difficult to image specimens in bright-field due to light scatter from the filter.

In 2010, Sebinger at al. presented a novel organ culture method, the so called low-volume (LV) culture, named after the small amount of medium that is used (Sebinger et al., 2010). This culture system allowed many mature tubules to form: these included 'hairpin' structures morphologically similar to LoH, and the organ showed a cortico-medullary difference (Sebinger et al., 2010). It also provided far higher resolution of bright field imaging, since the kidney is grown directly on glass. Therefore, I used this new culture method to form, image, and manipulate LoH.

Optimising and improving the current LV system was essential to improve its reliability in generating well-developed kidneys because the reliability of the original LV system is highly sensitive to a medium volume. After adjustment of the culture system, I assessed the molecular and morphological features of the LoH by the methods described for the *in vivo* LoH (Chapter 3). For the molecular features, I investigated marker gene expression of the LoH in the culture system to confirm the loop-like tubules that I observed in the culture were indeed the LoH, rather than other parts of the nephron such as convoluted proximal or distal tubules. As a marker for the LoH, Tamm-Horsfall protein (THP), a known marker gene that is expressed in the ascending limb of the LoH, was used (Tamm and Horsfall, 1950, Muchmore and Decker, 1985). In addition, cadherin-6 expression, known to be localised to LoH and proximal tubules, was also tested (Cho et al., 1998). For visualization of the morphological features of the LoH, immunofluorescence for laminin was used since laminin localises in the basement membrane of all epithelia.

A time-course study was performed to determine the onset of LoH formation during LV culture. This was necessary to ensure that any measurement and manipulation could be performed, in subsequent experiments, before the loops started to elongate.

The subject of LoH elongation during renal development raises the general problem of guidance cue(s) for the loop. A loop initially forms in the outer region of the kidney and its apex appears to be reaching into the deep medulla (Kriz and Koepsell, 1974). This orientation of the loop seems critical and the apex mostly ends up heading towards the kidney centre. It might suggest that the apex extends towards the medulla by guidance cue(s). It might alternatively be that the apex merely remains in its original place and the other parts of the kidney grow away from it, such as by collecting duct (CD) expansion (Cebrian et al.,

2004, Costantini and Kopan, 2010, Costantini, 2012) (Figure 4-1). If the latter were the case, there would not be guidance cue(s) on the loop to be studied. Hence, it was important that the movements of the LoH apex were measured in relation to other kidney structures to check the apex does move. Two different types of studies were carried out. As a direct measurement of the apex, I directly measured the average length of the loops, and the distance between the apex and the first branching point of the CD. As a second study, time-lapse imaging of Lgr5-EGFP kidneys was performed to trace an individual loop during its elongation. Lgr5-EGFP was used because Lgr5 is known to be expressed in ascending thick limb of LoH and convoluted distal tubules in the developing kidney (Barker et al., 2012).

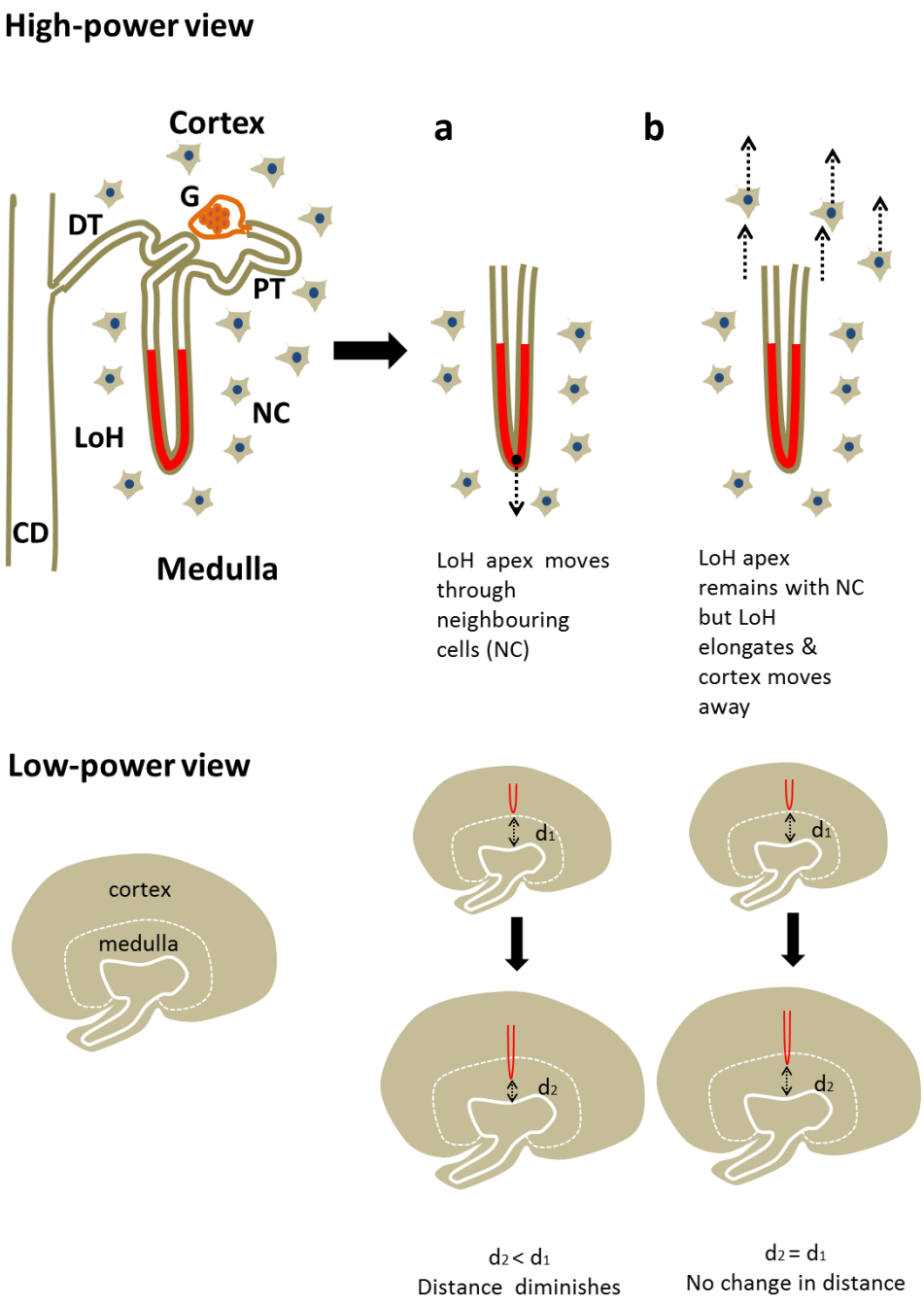

Figure 4-1 Schematic diagram of possible ways that Henle's loop (LoH) can elongate. Possibility (a) is that the apex may elongate through the neighbouring cells (NC) to the medulla, in which case the distance between the apex and the first bifurcated point should decrease. In (b), the apex may be left behind with the NC but the loop elongates and the cortex moves away so the distance from apex to the centre is unchanged. This would not make guidance of the LoH apex (CD; collecting duct, DT; distal tubule, G; glomerulus, PT; proximal tubule, LoH; loop of Henle, NC; neighbouring cells). Movement is indicated by the dotted arrows.

4.2 Results

4.2.1 Improved low-volume culture conditions increase reliability

I made several improvements to the LV system as used by Sebinger et al. (2010) to increase its reliability. When I set up the culture with 85 µl of medium, as specified by Sebinger et al., some kidneys just remained rounded and did not grow (Figure 4-3). To resolve this, I decreased the medium volume from 85 µl to 82 µl (a volume determined empirically) for the initial two days and increased to 85 µl afterward. The low volume in the initial culture days was critical because a kidney has to be firmly attached on the glass for further development: if it is not, it shows abnormal development (Figure 4-3).

I also found that the kidney sometimes detached from the glass because of drying of the medium, made worse by the low amount of medium (82 µl) during the initial two days (Figure 4-3). Therefore, using a 60 × 15 mm culture dish instead of using the 35 × 10 mm dish improved the culture conditions by holding more PBS to provide more humidity (Figure 4-2, 4-3). The silicon ring inserts were placed on a lid of the 35 × 10 mm dish to be isolated from PBS (Figure 4-2). This prevented loss of some cultures by PBS coming into the ring. After the optimized medium volume and the improved culture inserts, the percentage of well-grown kidneys markedly increased from approximately 54 % to 82 % (Figure 4-3). Well-grown kidneys were defined by a clear cortico-medullary difference and an even adherence of the peripheral area of the kidney to the glass.

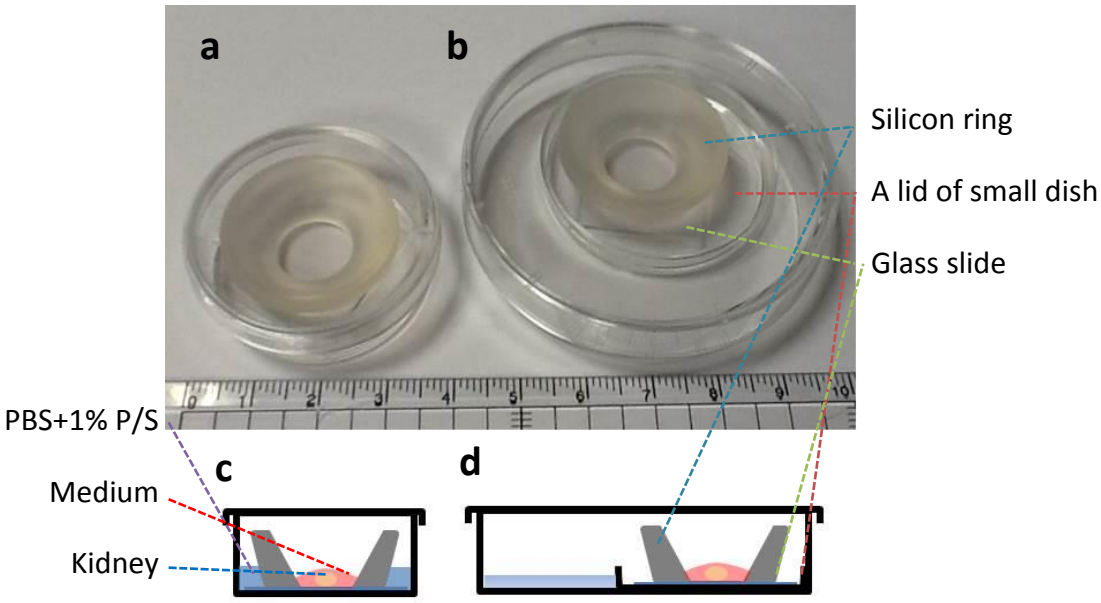

Figure 4-2 Previous (a, c) and improved (b, d) low-volume culture systems (modified from Sebinger et al., 2010). (a, b) shows a LV culture complex of a top view. (c, d) shows schematic images of a side view of the culture complex. In the improved culture, inserts consist of a larger culture dish (60 × 15 mm) and a lid of smaller dish (35 × 15 mm) showed in (b, d). The ruler scale = cm.

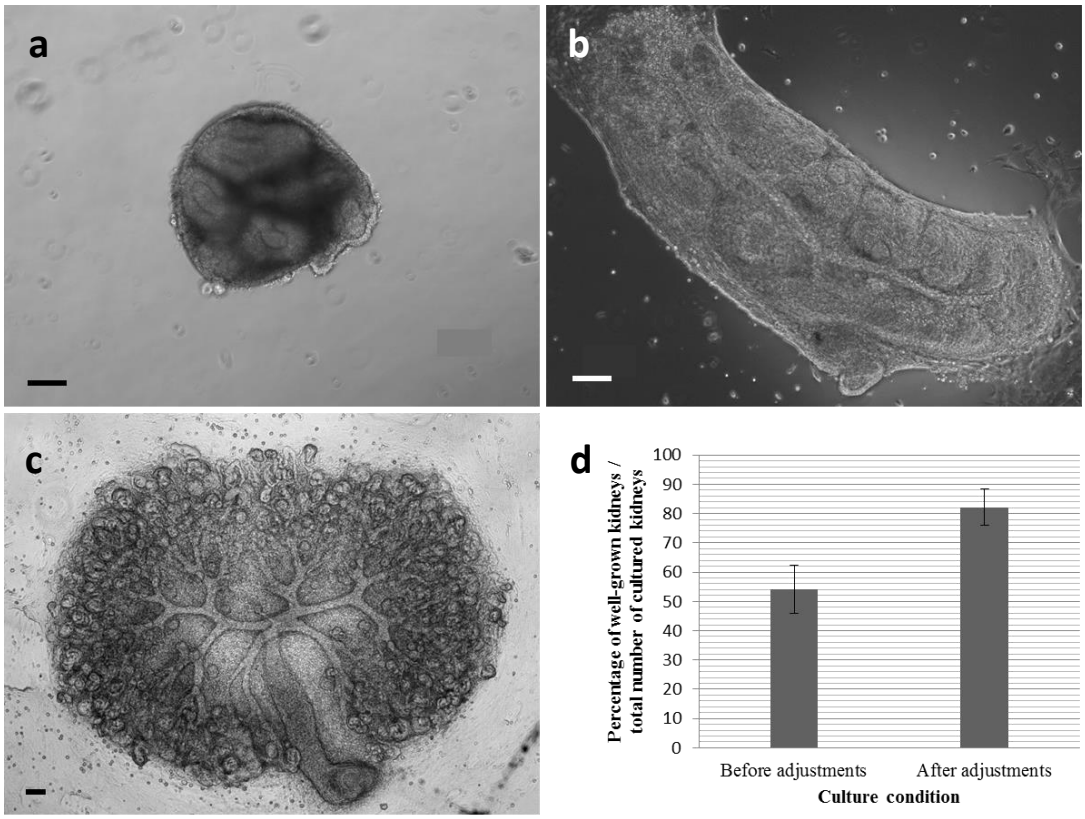

Figure 4-3 Optimized medium volume and improved culture inserts increases the reliability of a low-volume culture system. (a) Phase contrast image of an E11.5 kidney culture for 2-days with 85 µl of medium: it remained rounded and did not grow afterward. (b) Incomplete attachment of the kidney on the glass caused abnormal development. (c) A 7-day cultured E11.5 kidney makes an organotypic tree-like structure in the optimised culture conditions. (d) Comparison of percentages before and after adjustment of the culture conditions. The percentage = the well-grown kidneys / total number of kidneys that were set up × 100 (the error bars show 95% confidence interval, the formula is t=z´x SQR(p(1-p)/n) (z´; standard normal distribution, x; mean, SQR; square root, p; possible sample size/population of size, n; sample number) (Bremer, 2010). The scale bar = 100µm.

4.2.2 Demonstration of Henle's loop in a low-volume culture by marker expression in addition to morphology

In order to confirm the identity of the LoH, the marker expression of loops in a LV system was assessed. Tamm-Horsfall glycoprotein (THP), also called uromodulin, is produced and secreted by ascending limb of LoH (Tamm and Horsfall, 1950, Muchmore and Decker, 1985). Because THP has been well known 'anchor gene' in the sense of Thiagarajan et al. (2011) for LoH, I examined THP expression in low-volume cultured kidneys to test that the loops seen really were LoH. Mostly THP was clearly expressed in the apex of loops of E11.5 + 10d kidney (E11.5 kidney incubated for 10 days) cultures (Figure 4-4). Although not all nephrons showed THP expression (Figure 4-4), I confirmed that U-shaped tubules formed in LV culture did express it so were indeed LoH. In addition to testing THP expression, cadherin-6 expression was examined since cadherin-6 is known to be expressed in LoH and also proximal tubules (Cho et al., 1998) (Figure 4-5).

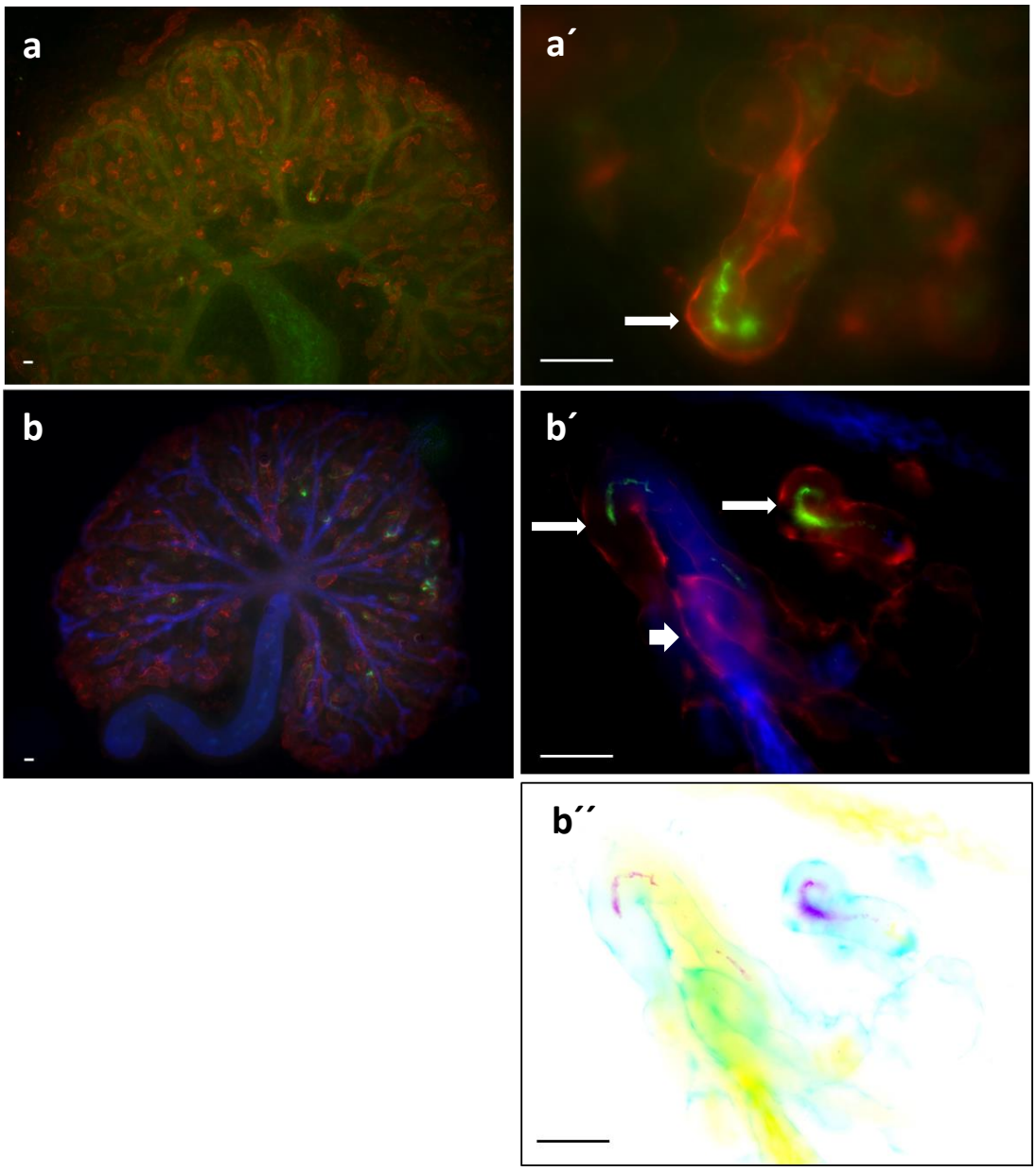

Figure 4-4 THP expression demonstrates Henle's loops in a 10-day cultured E11.5 kidney in the low-volume culture system. Immunofluorescence of THP (green) with laminin (red) was shown in a low power (a) and high power (a´) view. Laminin (red), THP (green), and cytokeratin (blue) expressions in the kidney were shown in a low power (b) and high power (b´) view. A non THP-expressed loop was indicated by short arrow (b´, b´´). Laminin expression (red) revealed the general basement membrane and cytokeratin expression (blue) indicated the collecting duct tree to distinguish it from loops. (b´´) An inverted colour version of (b´) in shown for better viewing on printed paper. The scale bar = 50µm.

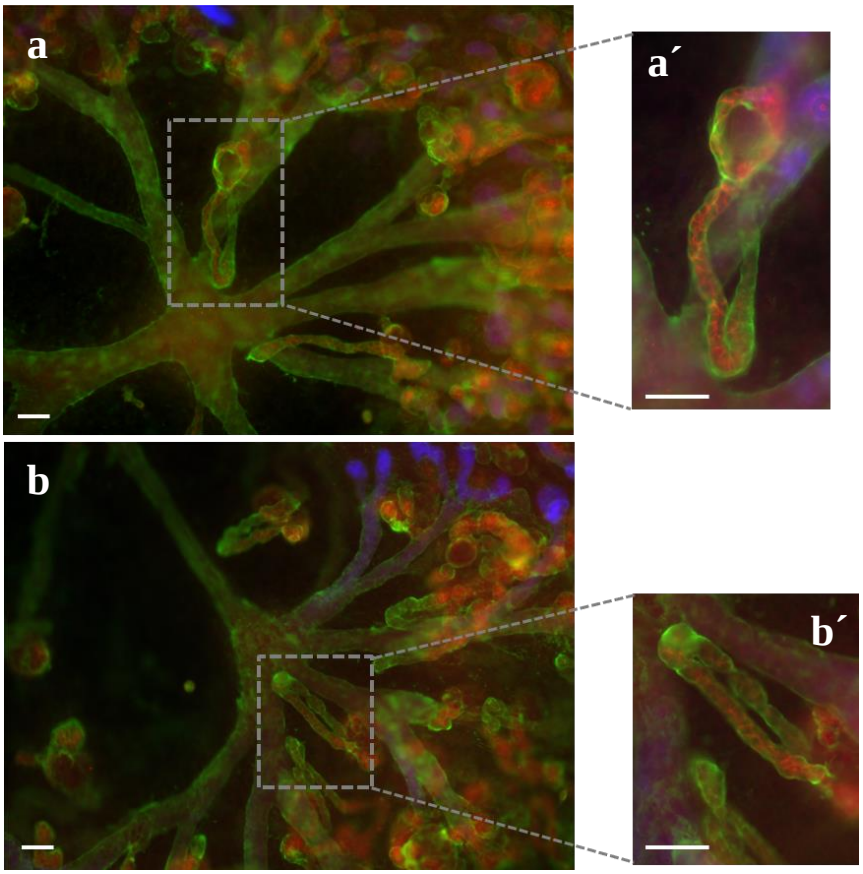

Figure 4-5 Localisation of cadherin-6 expression in Henle's loop in the cultures. An E11.5 kidney was cultured in the low-volume system for 10 days. Cadherin-6 (red) was localised in the loops and proximal tubules. Laminin (green) expression visualised the general basement membrane of epithelium, calbindin (blue) was expressed in ureteric buds. (a, b) are lower power views and (a´, b´) are high power views. The scale bar = 100µm.

4.2.3 Thick and thin limb of Henle's loop can be observed in the low-volume culture

Whilst confirming the identity of the loops by staining for THP and cadherin-6 expression on LV cultures, I made observations on the morphological characteristic of the loops via laminin expression. This was not only to examine the anatomical features of the cultured loops but also to compare the morphological resemblance between loops formed *ex vivo* and *in vivo*. Notably, a 12-day low-volume cultured E12.5 kidney showed both the thick and thin limbs of LoH, resembling those *in vivo* (Figure 4-6). The diameters of the thin and thick limbs are approximately 14 µm and 37 µm respectively (Figure 4-6).

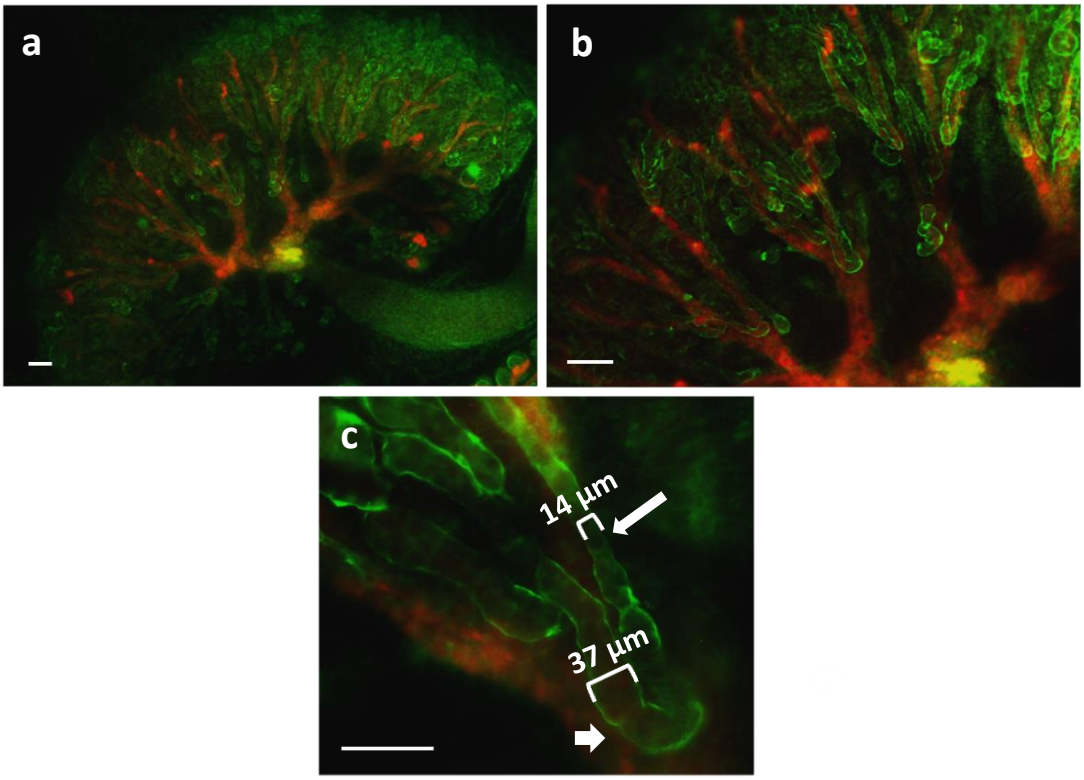

Figure 4-6 A low-volume cultured mouse embryonic kidney forms thin and thick ascending limbs of Henle's loop. E12.5 embryonic kidney was cultured for 12-days. (a, b) shows low power views and (c) shows a high power view. The thin loop is indicated by a longer arrow and the thick limb is indicated by a shorter arrow (c). Laminin expression (green) was used to visualise the outline of the general basement membrane of the entire kidney, and calbindin expression (red) showed the ureteric buds. The diameters of both limbs were measured by AxioVision Rel. 4.8. The scale bar = 100µm.

4.2.4 Loops of Henle start to form after 7-day culture of E11.5 kidneys in the low-volume system

To manipulate directional growth of LoH in further experiments, it was important to know the timing of development in LV cultures. Essentially, determining the onset of LoH formation in the LV system was useful to set the time point to perform experimental manipulations that I will describe in Chapter 6.

I therefore collected the cultures at a range of time points from E11.5 + 4d (E11.5 kidney incubated for 4 days) and identified LoH by immunofluorescence. I found that until E11.5 + 6d, defined structure of LoH was hardly observed (Figure 4-7). LoH mostly began to form from near E11.5 + 7d and kidneys can be incubated until E11.5 + 12d (Figure 4-7).

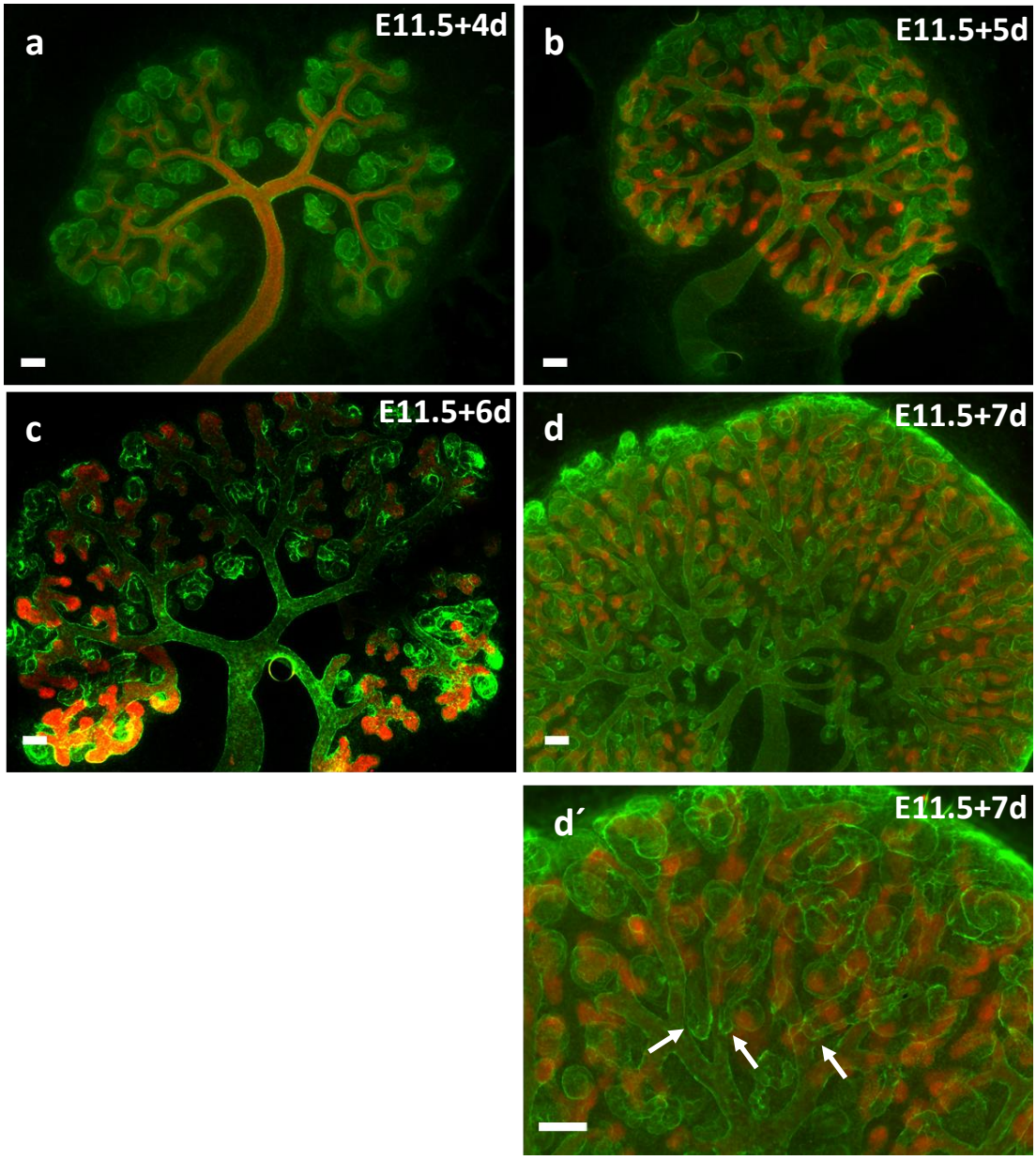

Figure 4-7 Time-course images of an E11.5 kidney in the low-volume system. (a) An E11.5 kidney was cultured for 4-days (a), 5-days (b), 6-days (c), and 7-days (d, d´). (d´) A high power view of (d). The loops start to show from the 7-day cultured kidney and those are indicated by arrows. Laminin (green) is expressed in the general basement membrane and cytokeratin (red, a) is expressed in the collecting ducts and ureteric buds. Calbindin (red, b, c, d, and d´) is expressed in the ureteric buds only. The scale bar = 100μm.

4.2.5 The loop of Henle elongates, but measurement of the distance between the apex and the kidney centre did not indicate a conclusive result about relative motion

After I recognized that LoH started to form from E11.5 + 7d, I investigated how the loop elongates: specifically, to determine whether the apex of the loop actually moves. Otherwise, there would be no guidance cue(s) to be investigated. Possible ways that the loops can elongate were established: its apex could migrate through the neighbouring cells, or developmental events elsewhere in the kidney could give rise to apparently directional loop elongation as an illusion (Figure 4-1).

I measured the average length of the loop in 7-day and in 10-day cultured kidneys. To detect the actual apex movements, I have measured the average distance between the apex and the centre of the kidney. I first tried to define the centre of the kidney by drawing the extended lines on the loops so that I could find the place where those lines converged (Figure 4-8). The lines did not, however, converge at one point, so I used as a notional centre-point, the first bifurcated point of the CD (which most of the lines closely or directly crossed) (Figure 4-8). Figure 4-8 showed that the loops indeed elongated. The calculated distance between the apex of the loops and the centre of the kidney did not, however, show a decisive evidence of the apex movements (Figure 4-8).

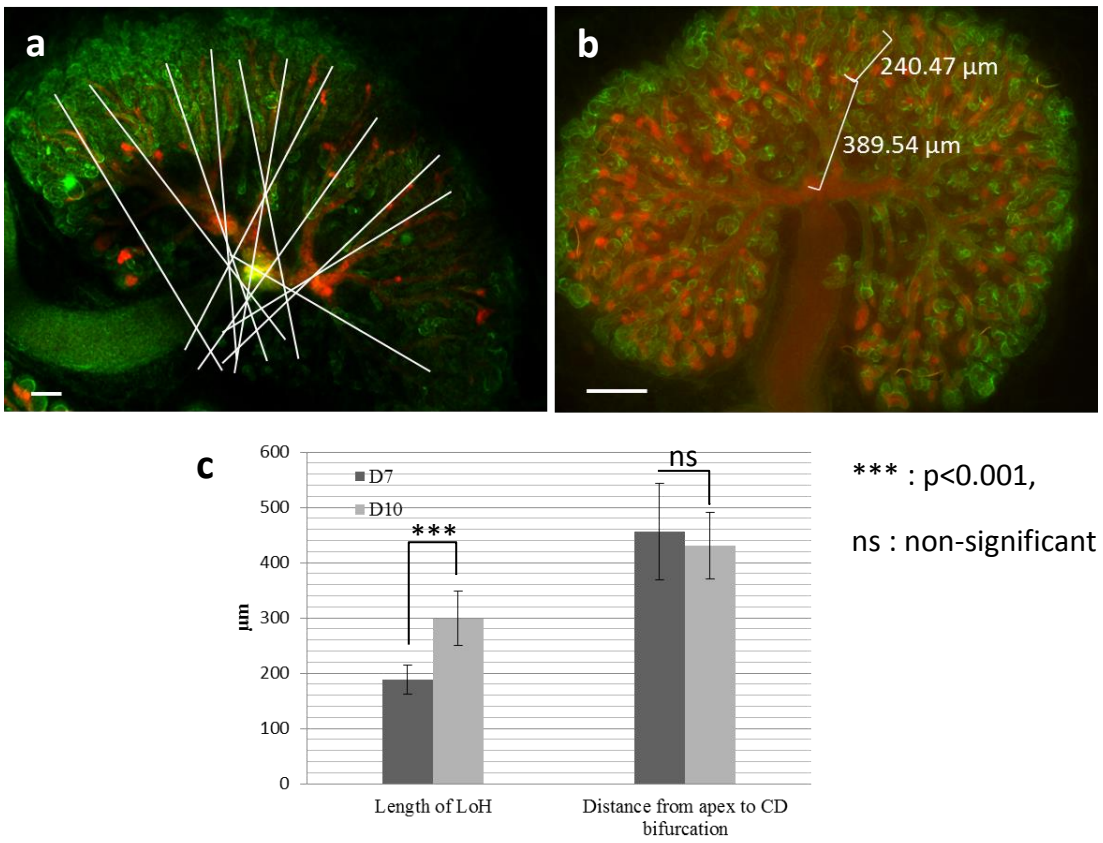

Figure 4-8 Measurement of the length of Henle's loop and distance between the apex and the first bifurcated point of the collecting duct. (a) The lines were drawn on the LoH to determine the point on which the loops converged. The lines did not converge precisely but all did cross somewhere near the first branching point of the collecting duct (CD). Laminin (green) was expressed in the general basement membrane and calbindin (red) was expressed in the ureteric buds. (b, c) Ten 7-days and 10-days cultured kidneys were collected, and the mean of the loop length and the distance between its apex and the first branching point of the CD, were measured by AxioVision Rel. 4.8. Data were represented by Mean ± SEM, and the distance p value (0.325) and length p value (0.01×10^{-3}) were made by Student's unpaired *t* tests. The scale bar = 200µm.

4.2.6 Demonstration of Henle's loop elongating toward the medulla by time-lapse imaging

The result from the measurements in previous section was inconclusive with respect to apex movements. I therefore did a more precise test to demonstrate the apex movements by following individual loops.

Time-lapse imaging was employed using embryos that carried on Lgr5-EGFP transgene. The Lgr5-EGFP carrying embryos were used because Lgr5 is known to be expressed in ascending thick limb in the developing kidney (Barker et al., 2012). Images were taken by a Lumascope (Model 500; etaluma), in-incubator microscope for 57h from E11.5 + 7d (Figure 4-9). Three representative images (the first; E11.7+7d, the middle; E11.5+8d+4h, and the last; E11.5+9d+9h) are shown in Figure 4-9.

Notably, the loop elongated toward the nearest branching point of the CD tree, moving relative to the fixed reference frame of the glass (which was permanently on the in-incubator microscope). The cortex did not expand significantly during 36 h of time-lapse imaging (Figure 4-9). This result suggests the apex of the LoH does move and allows the possibility that guidance cue(s) may govern the directional growth of the apex.

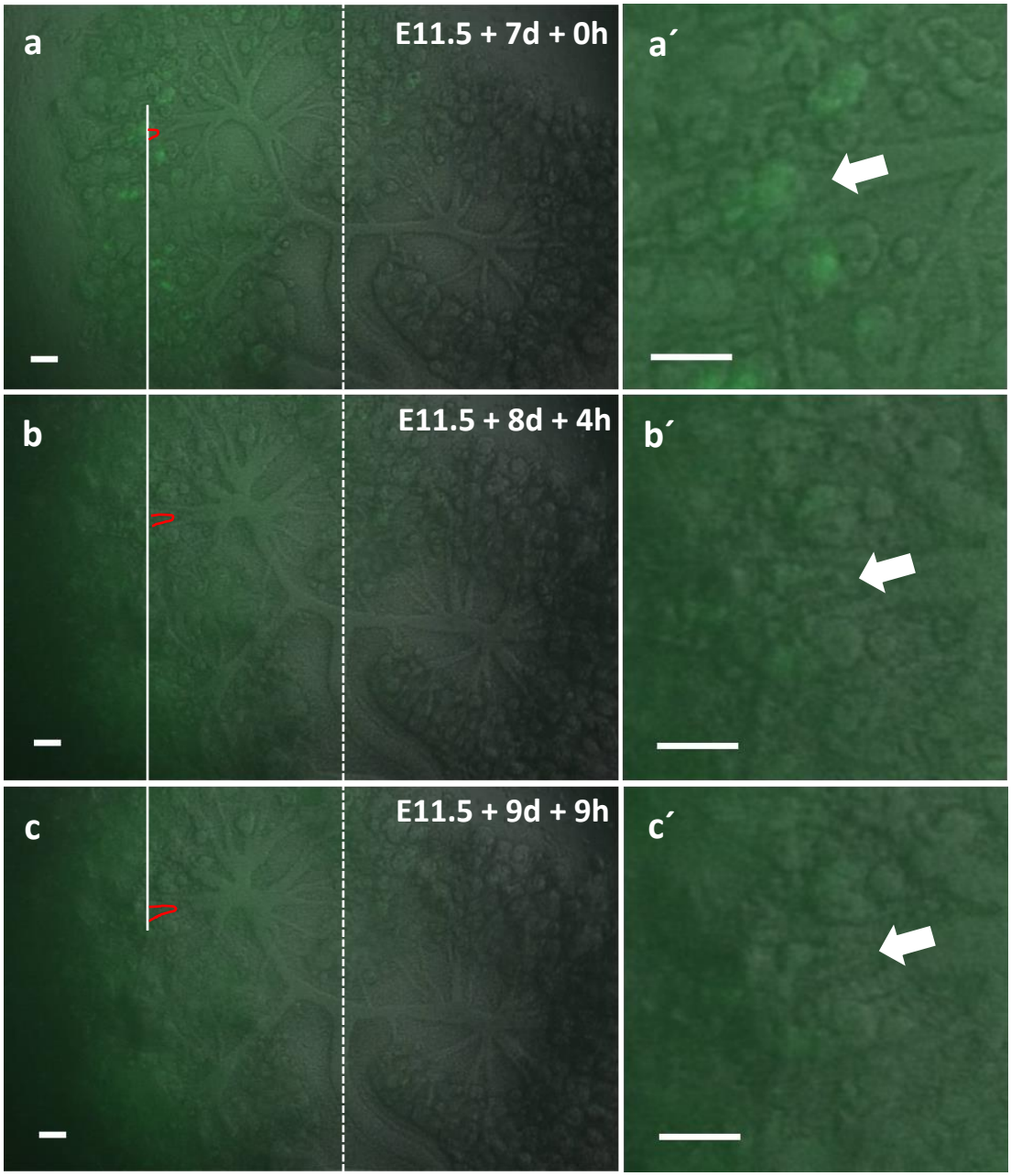

Figure 4-9 Time-lapse imaging of an Lgr5-EGFP kidney showing Henle's loop elongation in the reference frame of the culture dish. Time-lapse imaging was performed between E11.5+7d and E11.5+9d+9h (total 57h, 15 min/image). The first (a, a´), middle (b, b´), and last (c, c´) captured images were selected and shown here to present significant elongation toward a CD branching point. (a, b, c) The loops were emphasized by red (Lumascope (in-incubator microscope) weakly detects EGFP signals but bright-field images showed the LoH outline) and start point was marked by white line over the images. The dotted white line along the first branching point of the CD shows the photos are lined up properly. (a´, b´, c´) High power views of loops were indicated by arrows. The scale bar = 100μm.

4.3 Chapter discussion

4.3.1 Optimising a useful culture system to form later stage nephrons

Having a reliable culture method is a powerful tool to investigate development. Although a LV method had already been published method as a system that allowed LoH development (Sebinger et al., 2010), I had to adjust this system to increase the viability of embryonic kidneys. Optimising medium volume and making improvements on culture inserts gave rise to more reliable culture conditions to form LoH. Moreover, the culture system allowed LoH to be subdivided into thin and thick limb which resembled the *in vivo* characteristics of LoH (Dieterich et al., 1975, Burg, 1982).

4.3.2 Demonstrating Henle's loop elongation and its apex movement

In this chapter, developing a reliable organ culture system was the first step for investigating movement of the Henle's loop. Next was to assess whether the apex of the LoH does move, otherwise there would be no guiding cue(s) to navigate the LoH. This was first investigated by averaging position of many loops, but that resulted in error bars too large to prove the apex movement. Therefore, imaging individual loops by time-lapse was carried out and showed that the apex really does move. The result raised the possibility that the LoH apex might be reaching its final destination by guidance cue(s).

5 Chapter 5 The loop of Henle formed in engineered kidneys shows similar characteristics to those formed in the intact kidney cultures

The main findings of this chapter have been published

CHANG, C. H. & DAVIES, J. A. 2012. An improved method of renal tissue engineering, by combining renal dissociation and reaggregation with a low-volume culture technique, results in development of engineered kidneys complete with loops of henle. ***Nephron Exp Nephrol,*** **121, 7.**

5.1 Introduction

Having optimized the low-volume (LV) culture method so that the loop of Henle (LoH) formed reliably (Chapter 4), I combined the LV system with a recent technique for renal tissue engineering. This engineering technique allows the construction of chimeric tissues and also allows the use of siRNA to block specific gene functions (Unbekandt and Davies, 2010, Siegel et al., 2010). It was, therefore, speculated that this engineering technique may be a useful tool to manipulate, or block, candidate genes involved in the guidance(s) of the LoH.

I first studied engineered kidneys cultured by the LV system to investigate whether loops would be produced in engineered kidneys and whether their orientations were normal. Second, I compared the intact and engineered kidneys in the Saxén and LV culture systems. This confirmed the reliability of the LV system for investigating LoH guidance.

In 2010, Unbekandt and Davies presented a technique of making the immature stages of renal structures from renal cell suspension (Unbekandt and Davies, 2010). This tissue engineering technique was termed the 'dissociation and reaggregation' method since E11.5 kidneys were enzymatically dissociated and reaggregated by centrifugation (Unbekandt and Davies, 2010). After the disturbance by 'dissociation and reaggregation' of the kidney, multitudes of small ureteric cysts (UC) and nephrons were formed in the Saxén culture system (Figure 5-1, 5-2). Although this technique allowed the reaggregate to form the basic structures of the kidney, little sign of LoH was shown in this system, and too many UC formed rather than forming one single collecting duct (CD) tree (Figure 5-2).

In order to have a single CD tree in the reaggregates, Geneva et al. advanced the technique to a serial dissociation and reaggregation system (Ganeva et al., 2011). From the first dissociation and reaggregation, they isolated a UC and combined it with freshly dissociated and reaggregated metanephric mesenchyme (MM) from E11.5 kidneys (Figure 5-3). In this manner, the engineered kidney reproduced a single collecting duct tree resembling the intact kidney (Figure 5-3).

I therefore combined the idea of the LV system (Sebinger et al., 2010) and the serial reaggregation system (Ganeva et al., 2011) to investigate the features of LoH in the engineered kidney (Figure 5-1).

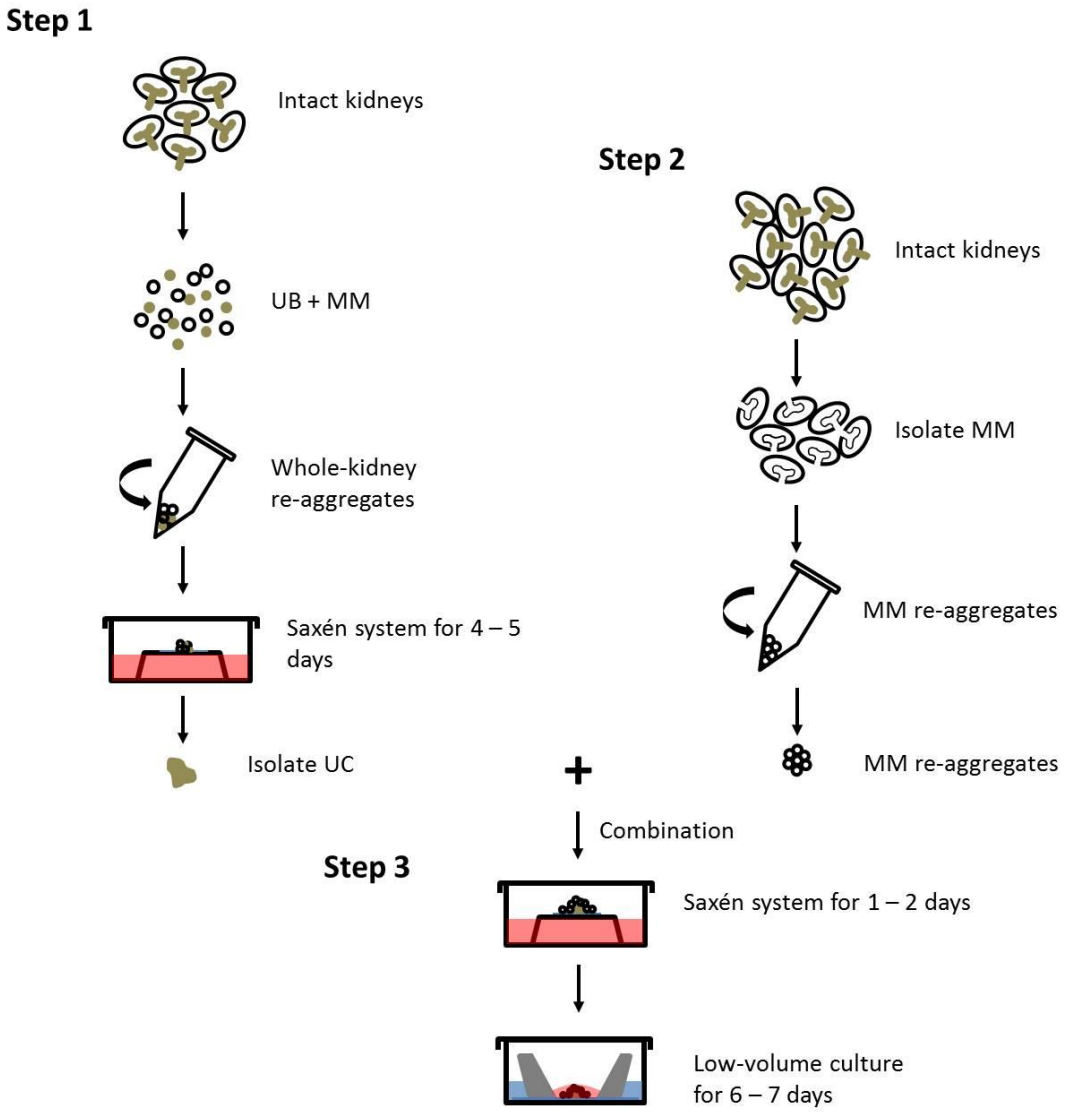

Figure 5-1 Schematic description of the method to culture engineered kidneys by serial reaggregation in low-volume culture (modified from Ganeva et al., 2011). Step 1 describes the process to achieve a ureteric cyst (UC) by the original reaggregation method (Unbekandt and Davies, 2010). **Step 2** shows the process of isolating metanephric mesenchyme (MM) from fresh E11.5 kidneys. **Step 3** illustrates how the combined reaggregates of the UC and MM are pre-cultured in the Saxén system for 1-2 days followed by in LV system for 6-7 days.

5.2 Results

5.2.1 Kidneys engineered by serial dissociation-reaggregation need to be pre-cultured in the Saxén system prior to transfer to the low-volume system.

The Unbekandt- and Davies-style engineering method (single dissociation-reaggregation) does not produce LoH or a single collecting duct (CD) (Figure 5-2). The Ganeva et al.-style advanced method (serial reaggregation) is able to produce a single CD by combining an ureteric cyst (UC), isolated from the Unbekandt and Davies style engineered reaggregates, with freshly reaggregated mesenchymes. This system is, however, insufficient to form LoH in the Saxén system (Figure 5-3). Thus, I combined the Ganeva et al. system and the LV culture system to investigate characteristics of the LoH formed in the engineered kidneys, and to demonstrate the reliability of the LV culture system. Additionally this combined system would later allow further manipulations of possible LoH guidance cue(s).

In order reliably to culture the engineered kidney in the LV system, the engineered kidney had to be rigid enough to be cultured in the LV system. The specimen in the LV system is settled in its position by the pressure of the low volume of the culture medium allowing the culture to grow flat on the glass (Figure 4-2). Under this pressure, the fragile engineered kidney cells could disperse (Figure 5-4). Therefore, I pre-incubated the engineered kidney for 1-2 days, rendering it solid enough to be transferred to the LV system (Figure 5-1, 5-4).

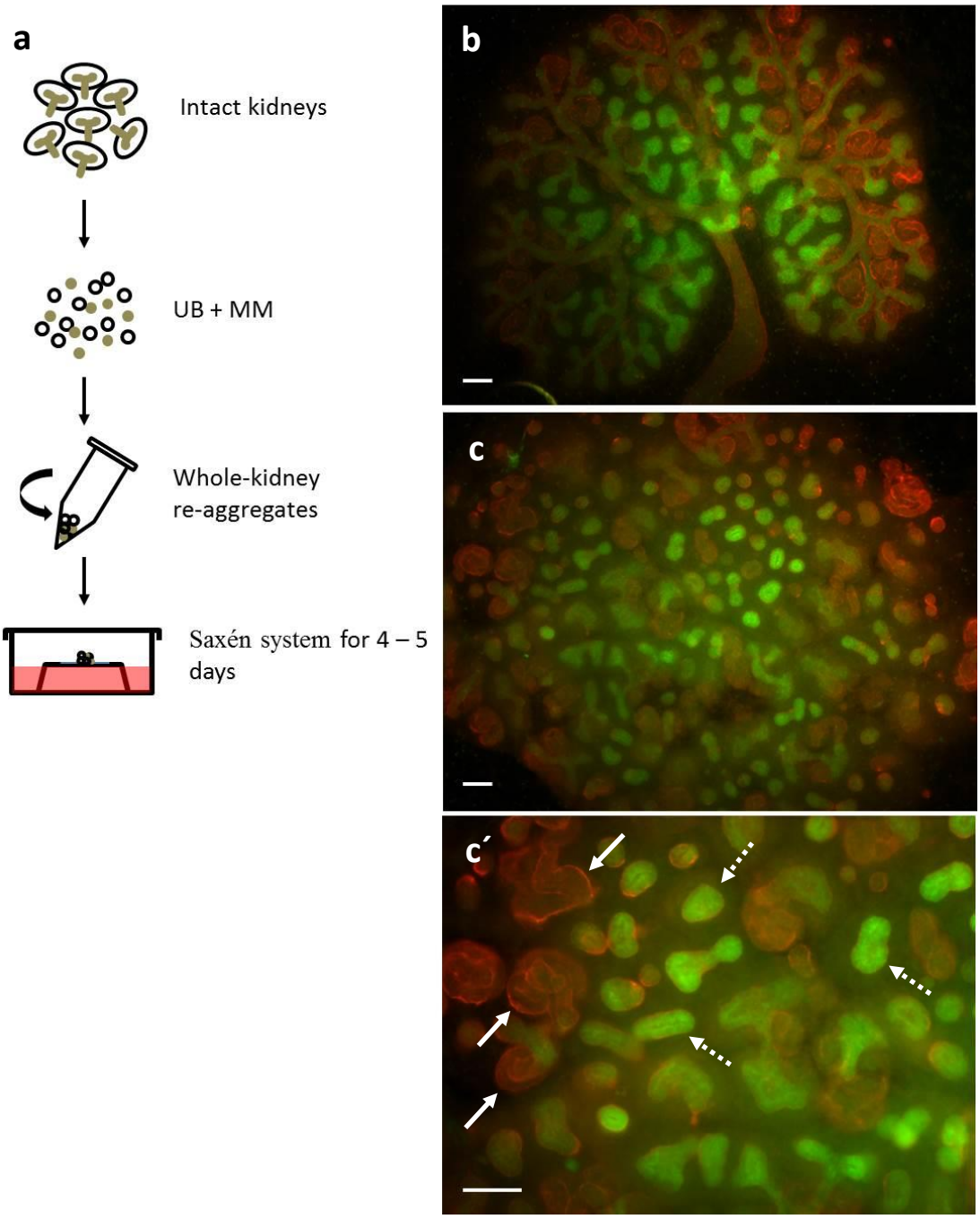

Figure 5-2 The original method to make the engineered kidney from a renal cell suspension by single dissociation-reaggregation (Unbekandt and Davies, 2010). (a) Schematic diagram of the method to make renal reaggregates (modified from Ganeva et al., 2011). (b) An intact kidney in the Saxén system is shown as a control. (c) A low power view of a reaggregate comprising nephrons (laminin; red) and ureteric buds (calbindin; green). (c´) A high power view of (c). Nephrons are indicated by white arrows and ureteric buds are indicated by dotted arrows. The scale bar = 100µm

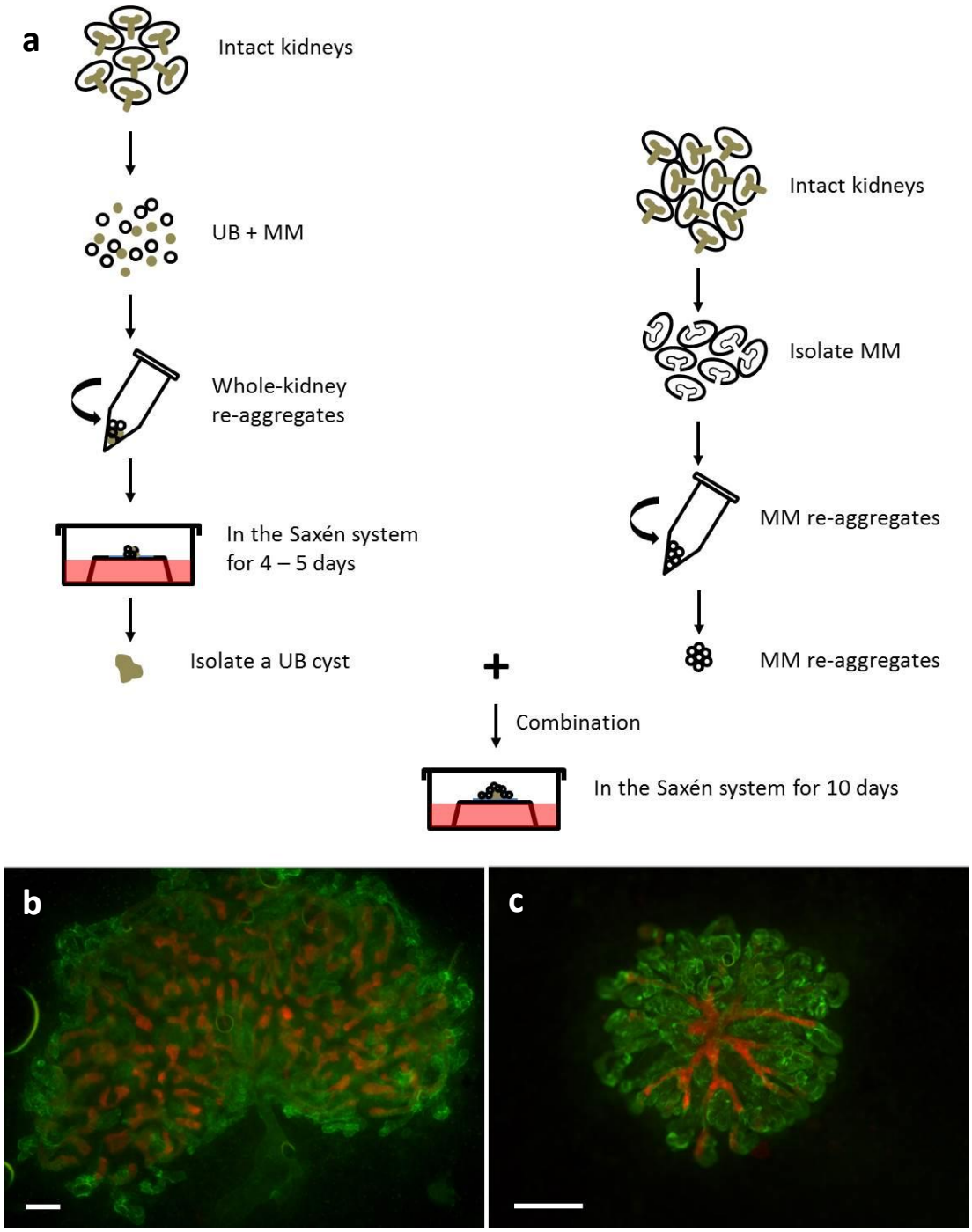

Figure 5-3 The Ganeva et al. style renal engineering method. (a) A diagram describes the process to make an engineered kidney by serial dissociation-reaggregation method (modified from Ganeva et al. 2011). A ureteric bud cyst is isolated from a reaggregate from 6 dissociated kidneys (E11.5) and combined with freshly isolated and reaggregated metanephric mesenchyme (MM) from 10 intact kidneys (E11.5). The combined engineered kidney is cultured in the Saxén system for 10-days (a, c). (b) Intact kidney (E11.5) cultured in the Saxén system for 10-days is shown. Laminin (green) is expressed in the general basement membrane and calbindin (red) is expressed in the CD and UB. The scale bar = 200μm.

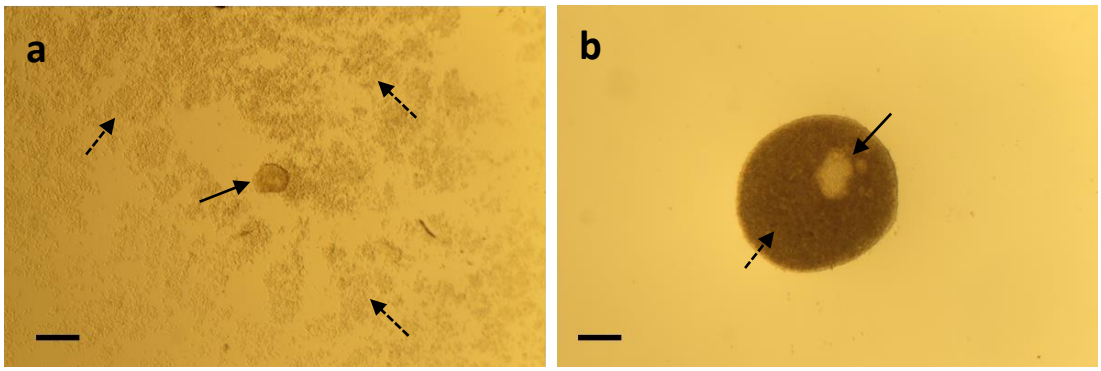

Figure 5-4 Bright field images of a ureteric cyst (UC) with reaggregated metanephric mesenchyme (MM) in the low-volume system without and with pre-incubation. (a) A UC combined with MM is directly placed in the LV system without pre-incubation. MM dispersed immediately after being placed in the LV system. Arrows indicate UC and dotted arrows indicate dispersed MM. (b) Combined reaggregates are pre-incubated in the Saxén system for 1 day and placed in the LV system. MM firmly encloses the UC. The scale bar = 200μm.

5.2.2 Combining the serial dissociation-reaggregation method and the low-volume culture system results in an organotypic engineered kidney with Henle's loops

To advance the current kidney engineering technique with the optimized LV system, I combined those methods to investigate the LoH guidance cue(s). To address this, I firstly found the way of placing the engineered kidney in the LV system after 1-2 days of pre-incubation in the Saxén system. Next, I investigated whether transferring reaggregates to the LV system advanced LoH formation. The LoH were identified by immunohistochemistry (Figure 5-5). By anti-laminin staining of the general basement membrane, many LoH were observed in the engineered kidney cultured in the LV system (Figure 5-5), whilst the engineered kidney cultured in the Saxén system showed hardly any loops (Figure 5-3, 5-5). Unlike the intact kidney, there was no entry point of the collecting duct in the engineered kidney because origin was the reaggregated cyst rather than the ureteric bud (Figure 5-4).

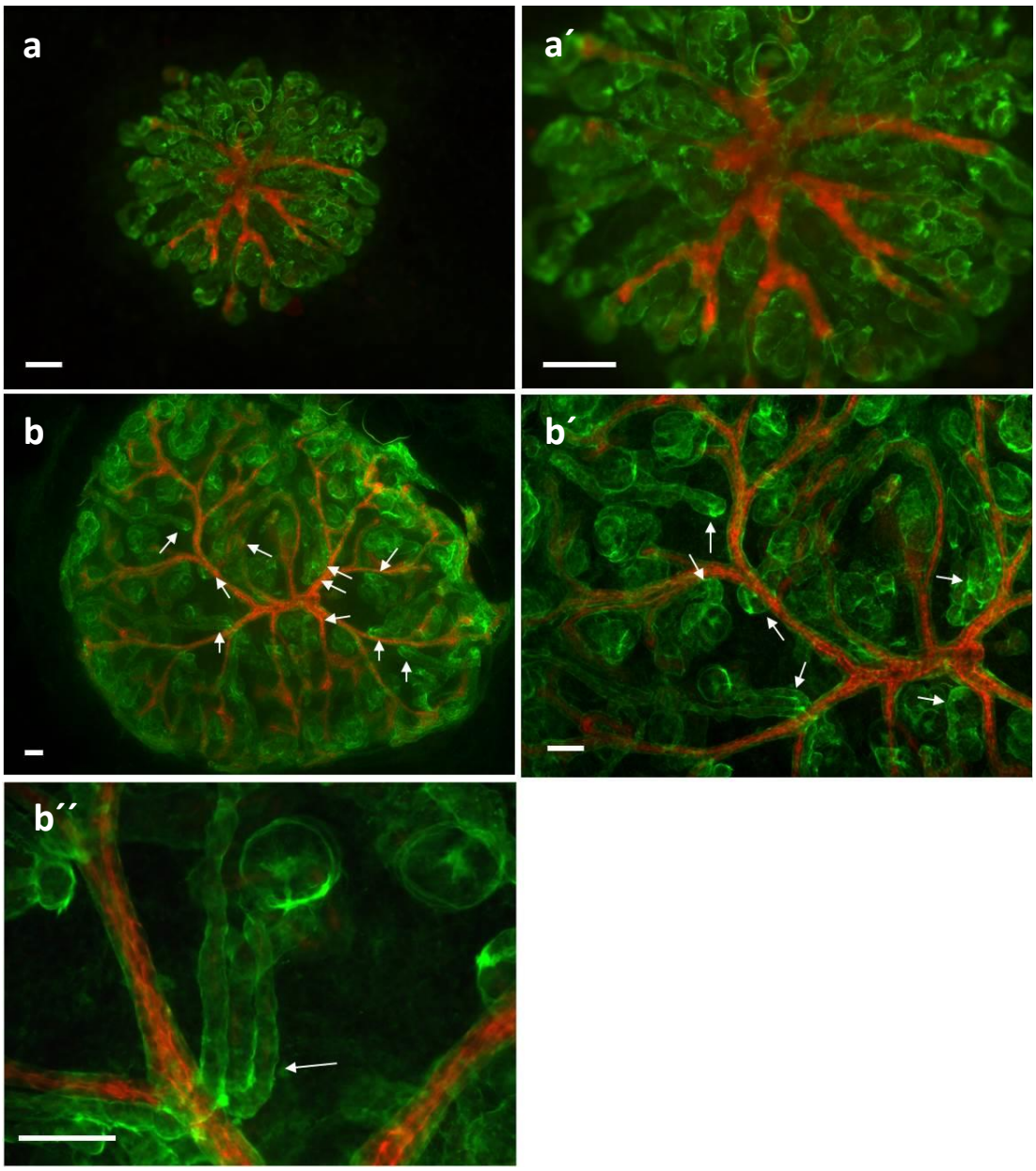

Figure 5-5 Kidneys engineered by serial reaggregation cultured in the Saxén (a, a´) and low-volume (b, b´, b´´) system. (a) A low-power view of the engineered kidney in the Saxén system shows no LoH. (a´) A high-power view of (a). (b) A low-power view of the engineered kidney in the LV system. The arrows indicate the LoH. (b´) A high-power view of (b). (b´´) A high-power view of LoH is clearly shown and indicated by an arrow. Laminin (green) is expressed in the general basement membrane and calbindin (red) is expressed in the collecting ducts and ureteric buds. The scale bar = 100µm.

5.2.3 Identification of marker expression (THP) for the Henle's loop formed in the engineered kidney

To confirm that the LoH formed in engineered kidneys were actual LoH, I examined Tamm-Horsfall protein (THP) expression as a marker for LoH. The result was that specific expression of THP was adlumnially localised in the U-shaped loops in the engineered kidney (Figure 5-6). THP expression was especially strong in the apex of the loops in both intact and engineered kidney (Figure 5-6). Similar to the intact kidney (n=13) (refer to Figure 4-4), the engineered kidney (n=12) also showed some THP-negative loops (Figure 5-6). The mean number of THP positive loops in the intact and engineered kidney in the LV system were similar (p value of a test of difference = 0.90 by two-tailed t test) (Figure 5-6).

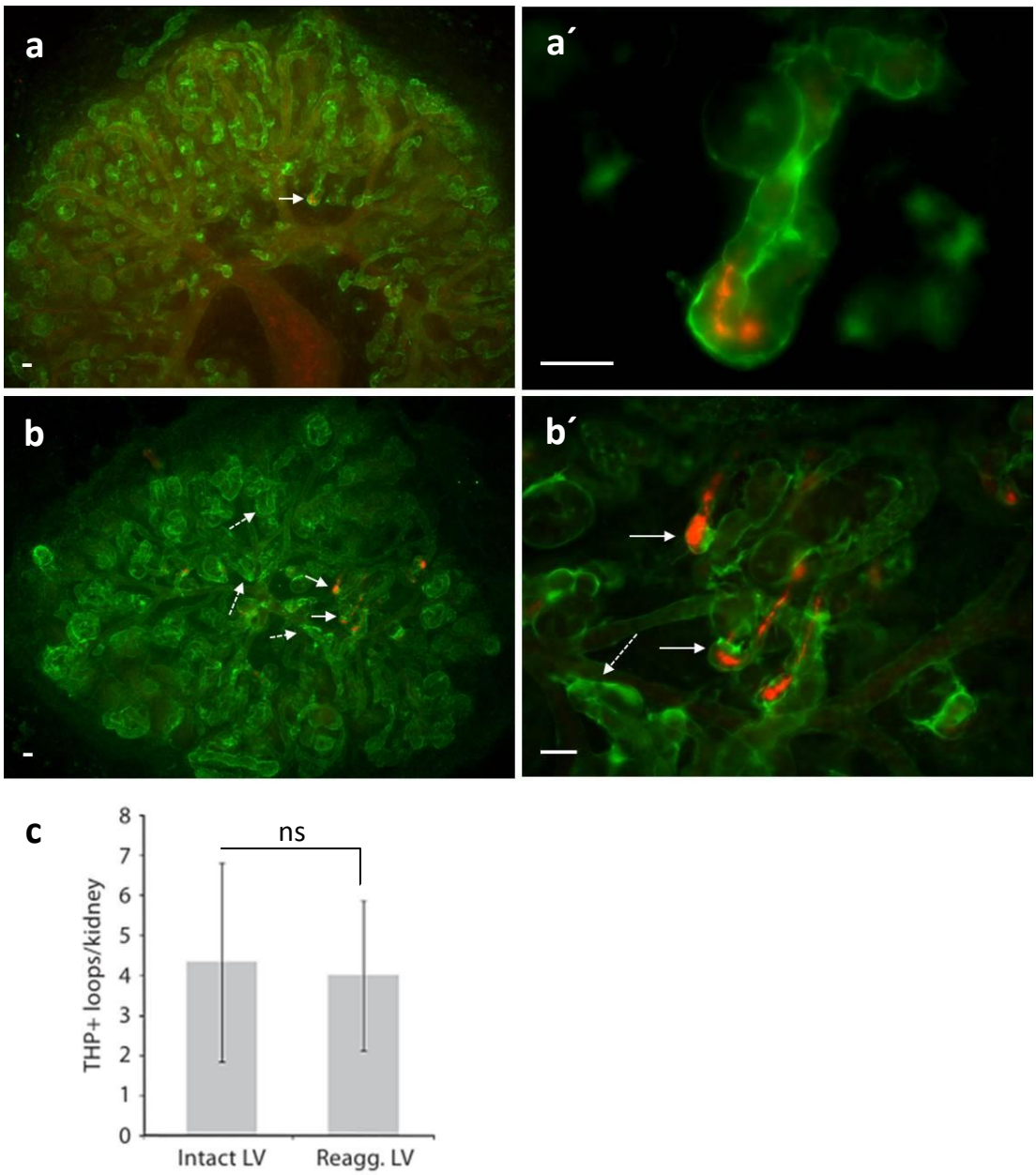

Figure 5-6 THP-expressing loops form in the intact and engineered kidneys in the low-volume (LV) system. (a, b) Low-power views of an intact (n=13) and an engineered kidney (n=12) (Reagg.) expressing THP (red) positive loops (arrows). Laminin (green) is expressed in the general basement membrane. The low-power views are shown to demonstrate the specificity of THP expression in the loops. (a´, b´) High-power views of the THP positive loops of the intact and engineered kidney are shown respectively. THP-negative loops are indicated by the dotted arrows. (c) The mean number of THP-expressed loops per kidney in the LV system (The error bars = standard error of the mean, p value = 0.90 (ns = non-significant) by two-tailed t test). The intact kidneys were cultured for 9 days and engineered kidney was pre-incubated in the Saxén system for 2 days followed by the LV system for 6 days. The scale bar = 100µm.

5.2.4 Engineered kidneys show a similar number and orientation of Henle's loops as the intact kidney does in the low-volume system

The number and orientations of the LoH in the engineered kidney were quantified and compared to the intact kidney from different culture methods. Even after the dissociation-reaggregation, similar numbers of the loops as those seen in the intact kidney were observed (Figure 5-7). The total number of loops formed in the engineered kidney by the LV system was significantly increased compared to those intact kidneys (p value = 0.0003), and those engineered kidneys (p value = 0.0001) cultured in the Saxén system (Figure 5-7). Encouragingly, the average number of total loops between the engineered and intact kidneys cultured in the LV system were not significantly different (p value = 0.41) (Figure5-7).

Furthermore, the orientations of the loops were investigated in the engineered kidneys (Figure 5-7). To measure this, two lines, one on the axis of the loop and the other running between the apex of the loop and the first branching point of the kidney (which I defined as 'centre of the kidney') were drawn (Figure 5-7). An angle of less than 45° between the two lines was determined as a centripetal orientation (Figure 5-7). Nearly 97% of those loops that formed in the engineered kidneys and 95% of those loops that formed in the intact kidneys were centripetally orientated. There was also no significant difference (p value = 0.23) between the average number of the centripetal loops in the engineered kidneys and intact kidneys in the LV system, whilst the engineered kidneys in the LV system showed a conspicuous difference compared to intact (p value = 0.0001) and engineered (p value = 0.001) kidneys in the Saxén system (Figure 5-7). Therefore, the behaviour of the loops that formed in the engineered kidney cultured in the LV system resembled that of those in intact kidneys cultured in a similar manner.

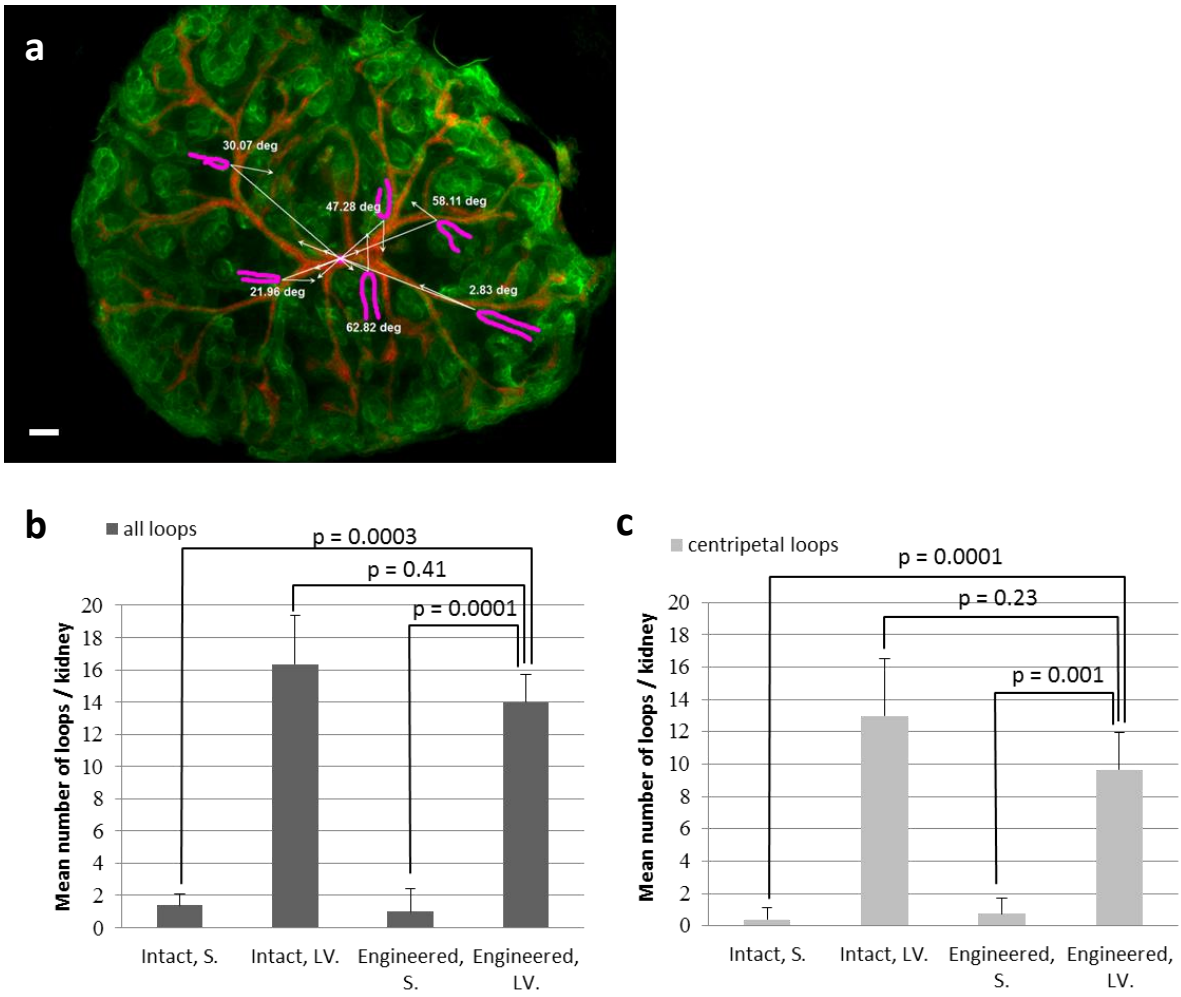

Figure 5-7 The mean number of total and centripetal loops per intact and engineered kidney in low-volume (LV) system. (a) The manner of measuring direction of the loops is shown by drawing lines on the image of the engineered kidney (Laminin; green, Calbindin; red). The angle between two lines (one extended line is crossing the axis of the loop and the other, 'radius line', is connecting the apex of the loop and the kidney centre which I determined as the first branching point) are shown. Angles of less than 45° are defined as 'centripetal'. Five example loops are highlighted here by pink lines. The angle was measured using AxioVision Rel. 4.8. (b, c) Mean numbers of total loops (b) and centripetal loops (c) formed in the intact and engineered kidneys cultured by different methods (Saxén system; S., low-volume system; LV.) were compared. The error bars indicate standard deviations. The p values are estimated by post hoc Scheffe test after examining one way ANOVA was significant ((b);p value = 0.0006, (c);p value = 0.00013). According to the Bonferroni correction, p value between each two groups less than 0.0125 (0.05/number of groups) was considered as significantly different. The scale bar = 100μm.

5.3 Chapter discussion

5.3.1 The morphological and molecular features of the Henle's loop formed in the engineered kidney mimic those of the loops of the intact kidney

The underlying idea of combining the best existing kidney engineering technique with the low-volume culture system was to improve the capability of the engineered kidney to produce the LoH with correct orientations. The engineered kidney produced by serial reaggregation resulted in similar numbers of loops as those seen in the intact kidneys. More importantly, their orientation resembled the intact loop by showing centripetal orientation. This suggests that the natural features of the LoH develop even after the severe disruption caused by 'dissociation-reaggregation' of progenitor cells. These results also confirm that the LV system is a reliable system to recapitulate and investigate the LoH. Additionally, the finding might provide useful tips in constructing functional kidneys as a perspective of renal regenerative medicine (Davies and Chang, 2013).

5.3.2 Practical uses of combining renal engineering and the low-volume culture system

The combining of these two methods would be useful to investigate guidance cue(s) of LoH after identifying the guidance molecule(s). Delivering of siRNA to silence target gene(s), or the application of function blocking antibodies, would presumably be more efficient in those kidneys engineered rather than those intact as tissue accessibility should be improved (Unbekandt and Davies, 2010). In addition to this, the engineering technique allows exogenous cells to mix with dissociated renal cells to make a chimeric kidney (Unbekandt and Davies, 2010, Siegel et al., 2010). These advantages might be useful to study the LoH guidance cue(s).

6 Chapter 6 Experimental manipulations suggest that the loop of Henle navigates towards the ureteric bud / collecting duct system

6.1 Introduction

In Chapters 4 and 5, I have shown that the low-volume (LV) culture system is a reliable method to recapitulate natural development of LoH *ex vivo*. Moreover, I confirmed that the apex of the LoH does move during the culture period, which suggests that the morphology of the LoH might be due to guidance cue(s). Mainly, the LoH formed both *in vivo* and *ex vivo* show directional bias towards the kidney centre. Therefore, this chapter will present the next step, which identifies the source of possible guidance cue(s) by experimental manipulations.

The 'cutting and pasting' technique is a way of systematically studying experimental embryology (reviewed by Schoenwolf, 2001). 'Cutting' is ablation or reduction of a cue from a specific region, and 'pasting' is positioning it ectopically. Combinations of these techniques are capable of identifying sources of developmental cues. Keynes and Stern showed a great example of using the cut-and paste technique to study axon migration from the neural tube to the anterior of each somite in the chick embryos (Keynes and Stern, 1984). They cut a part of the neural tube and pasted it back with a 180° antero-posterior rotation resulting in undisturbed migration of axons through the anterior somite (Keynes and Stern, 1984). On the other hand, when a somite was given a 180° rotation, the point of emergence of axon from the neural tube altered to the ectopic location of the anterior somite. The technique has been used in another study of the neural patterning in the chick embryo. Yamada et al. demonstrated regulatory roles of the notochord and floor plate in patterning the dorsal-to-ventral axis of the chick neural tube by cutting and pasting the notochord or floor plate in ectopic positions (Yamada et al., 1991). Based on these practical uses of it, the cut-and-paste technique was chosen and employed as a tool for experimental manipulations to identify potential source of LoH guidance cue(s).

To begin with, I tested whether the directional growth of the LoH is guided by repulsion from the cortex (local cue) or attracted to the medulla (distant cue). To test this, a part of cortex in which S-shaped bodies were presumably located was removed and pasted in the opposite orientation. Subsequently, the 'cutting only' experiment was carried out to confirm the result from the cut-and-paste experiment.

The mechanical manipulations on specific kidney regions resulted in the LoH heading towards the UB branching point. Thus, I decided to inhibit UB development but maintain the LoH development as an 'ablation of attracting substances' strategy. I intended to see how the

LoH would arrange itself when the UB undergoes inhibition. Furthermore, by having inhibited UB development, it would resolve the issue that the LoH heading towards the UB branching point might be just a random event with a high stochastic chance for the LoH meeting the UB since there are many UB branches in the way where the LoH head. Davies and his colleagues found that sodium chlorate , which is a specific inhibitor of sulphation, can reversibly inhibit UB development, but maintain nephron induction and maturation (Davies et al., 1995). Hence, sodium chlorate was added to the kidney culture medium (KCM) during the LV culture period, and the directional growth of the LoH was observed.

In this chapter, a combination of mechanical manipulations and drug treatment were employed in the LV cultures to elucidate and understand the LoH guidance by the UB.

6.2 Results

6.2.1 The loop of Henle from the cortex cut and pasted in ectopic direction shows the directional orientation towards the medulla.

I first tested whether the cortex contains local directional cue(s) to guide the LoH. In order to address this, a putative region of the cortex in which immature nephrons resided was surgically cut and pasted back to the same region in a different orientation (180° rotated) (Figure 6-1). Cut-and-paste was performed on E11.5 + 7d when the LoH begins to form (as shown in section 4.2.4) and the cut-and-pasted culture was incubated for 3 further days. Since it was not possible to see the LoH within the cortex in bright-field images (Figure 6-1), anti-laminin staining was used to mark all the basement membranes including the LoH. The rotated cortex region was verified by cytokeratin staining to show that it was clearly cut and pasted in the opposite orientation (Figure 6-2).

The LoH in the direction-rotated cortex pointed towards the global medulla even after its local manipulation (Figure 6-2). Among total LoH, 'centripetal' LoH (average angle = 14°, σ = 10) were defined as having an angle of less than 45° as before (Figure 6-2). The angle was measured between two lines; one line crosses along the LoH axis and the other connects the apex of the LoH and the first branching point of the collecting duct (Figure 6-2). Measuring angles were achieved by AxioVision Rel. 4.8 software. As described in previous chapters (chapter 4, 5), the first branching point of the collecting duct was determined as a criterion to measure the error angles of the LoH towards the kidney centre (medulla). The number of those medulla-heading LoH from the rotated cortex (n=7) were quantified (Figure 6-2). 95% of the LoH appeared to point at the medulla among total LoH (n=19) in the rotated cortex (Figure 6-2).

From the findings in this section, rotating the cortex did not prevent the directional arrangement of the LoH towards the medulla. This strongly suggests that the LoH is guided more by distant cue(s) from the medulla than by cue(s) local to the cortex.

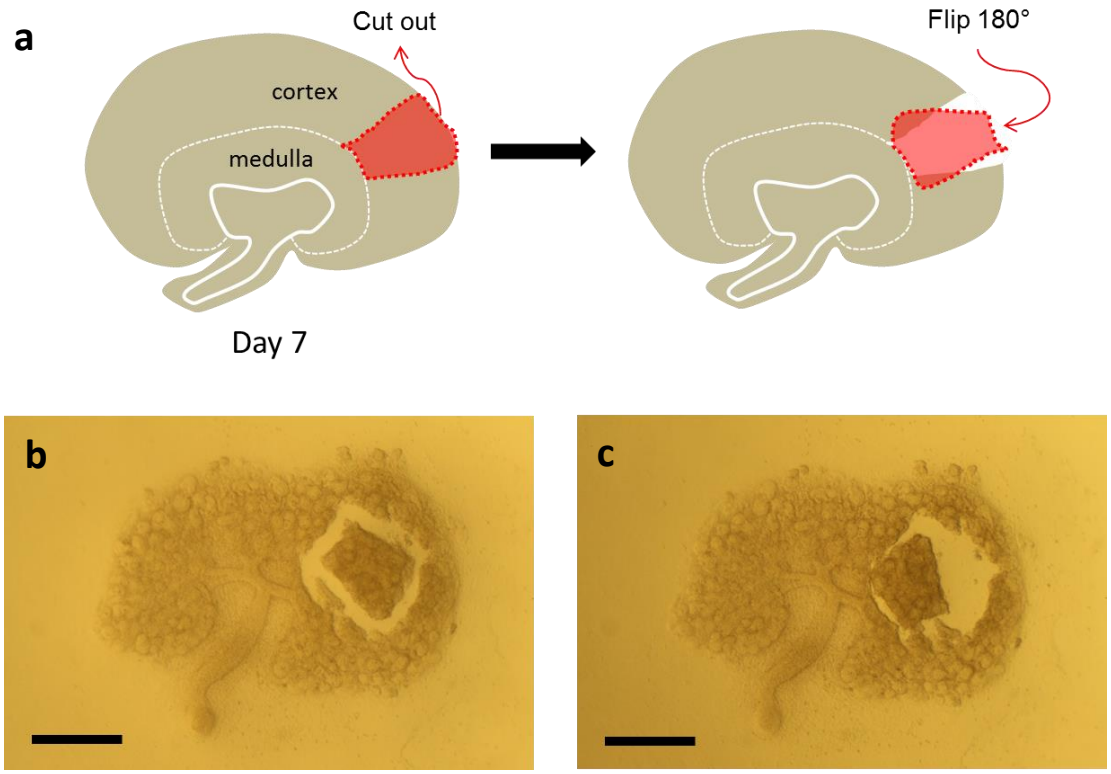

Figure 6-1 Cutting the cortex and pasting it in an ectopic direction to manipulate its LoH direction. (a) Diagram of cut-and-paste experiment. An E11.5 kidney was pre-incubated for 7-days and a section of cortex in which early LoH were presumably located was cut and pasted in an opposite orientation. The cut-and-paste kidney was then cultured for 2-3 days. (b) A bright-field image of the E11.5 + 7d kidney after its cortex fragment was cut. (c) The kidney immediately after ectopic pasting of the cortex section. The scale bar = 500µm.

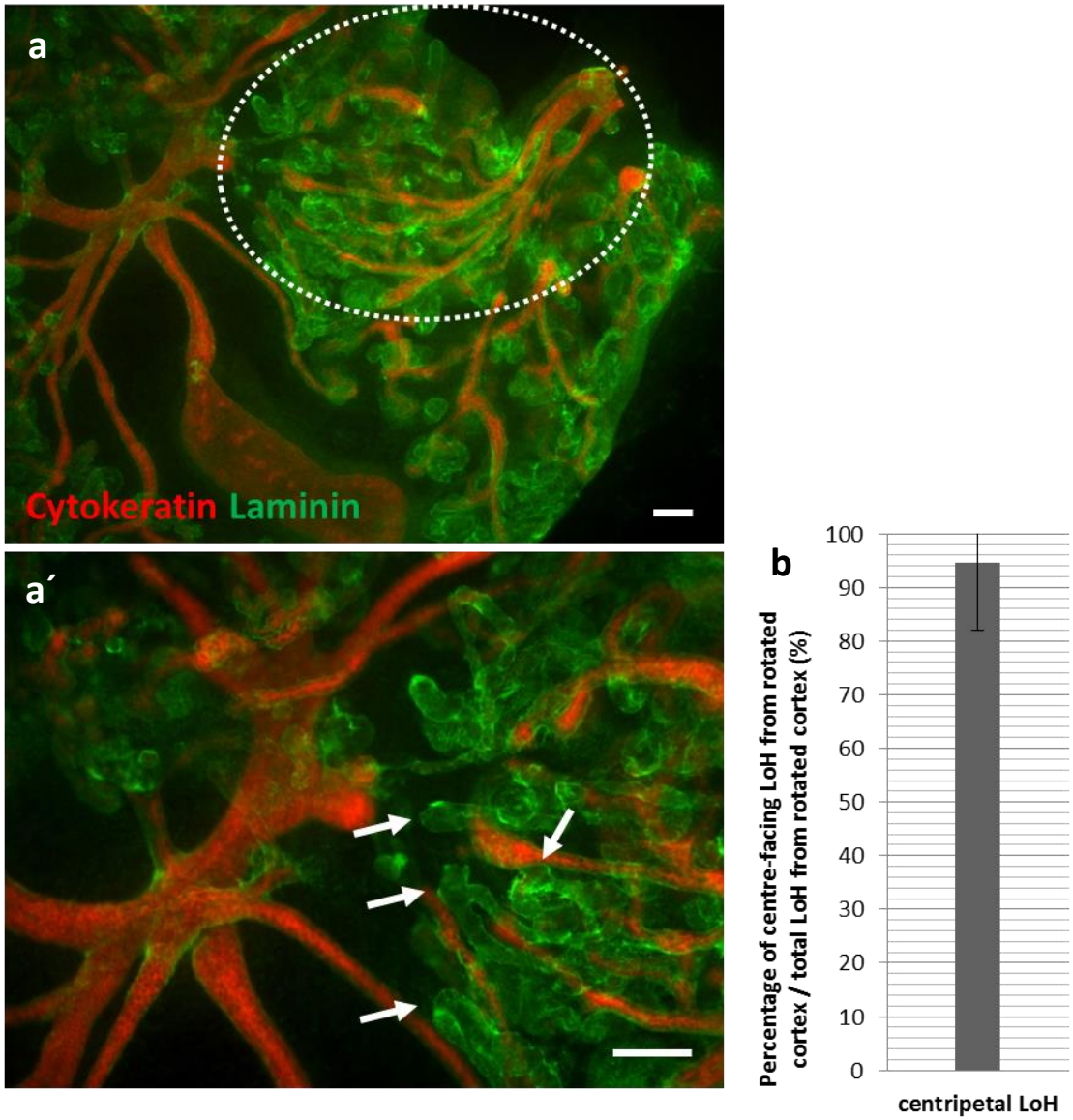

Figure 6-2 The LoH orientates towards the medulla after 'cut-and paste'. (a) E11.5 + 10d kidney after rotation of the cortex at E11.5+7d. The dotted circle indicates the region of the cut cortex and it was pasted in an opposite direction. Laminin (green) was expressed in the general basement membrane and cytokeratin (red) was expressed in the collecting duct. (a´) A high magnification view of (a). The arrows point the LoH that point at the centre of the kidney. (b) 95 % of the LoH (n=18) residing in the rotated cortex headed towards the kidney centre (the first branching point of the collecting duct) among the total LoH (n=19) from the rotated cortex (the error bar indicates 95% confidence interval (13), the formula is t= z' x SQR(p(1-p)/n) (z´; standard normal distribution, x; mean, SQR; square root, p; possible sample size/population of size, n; sample number) (Bremer, 2010). The centripetal LoH were defined as having an angle of less than 45° between two lines (one extended line along the axis of the LoH, and the other connecting the apex of the LoH and the kidney centre) using AxioVision Rel. 4.8. The scale bar = 400μm.

6.2.2 The loop of Henle orientated towards a remaining branching point of the ureteric buds after removal of the medulla.

In the cut-and-paste (cortex region) experiment, most of the LoH in the rotated cortex became oriented towards the medulla (Figure 6-8). This suggests that the directional arrangement of the LoH may not be guided by any local cues in the cortex but by cues from the medulla. In addition, it is unlikely but possible that the LoH prefer to grow towards the less crowded space, since there was always some space between the cut-and-pasted cortex and the rest of the culture (Figure 6-2).

In order to address whether the medulla is the region causing the centripetal arrangement of the LoH, the entire medulla was removed and then the LoH arrangement was observed. With this experiment, it was also possible to test whether the LoH prefers to grow towards free space. The medulla was surgically removed from E11.5 + 7d kidney in the LV system and the medulla-removed kidney was cultured for 3 further days (Figure 6-3). The medulla was defined as the region near the first branching point of the collecting duct (CD) that does not contain any nephrons (Figure 6-3). Due to the invisibility of the LoH in the cortex in bright-field images, anti-laminin staining was performed to outline the basement membrane of the LoH epithelium and other tubules (Figure 6-4). Anti-cadherin-6 staining was performed to mark the LoH and proximal tubules as well (Figure 6-4). Finally, anti-calbindin staining was performed to mark the UB (Figure 6-4).

After the medulla was removed, the LoH did not show an arrangement towards the region where medulla used to be. Notably, the LoH instead converged on the oldest branching point of the UB that remained in the cortex (Figure 6-4). Specifically, many LoH directed their apices towards the UB junction.

For quantification of the LoH arrangement towards the UB, the error angle (in other words, the angle between the line along the LoH axis, and the line connecting the apex of the LoH and the UB junction) was measured from 64 LoH of 6 medulla-removed kidneys (Figure 6-4). For precise quantification, all the LoH and the UB junctions were marked by colours using Image J software (Figure 6-4). 94% of total LoH converging on the UB junction were arranged within an error angle of less than 45° (95% confidence interval = 7°) (Bremer, 2010) (Figure 6-4).

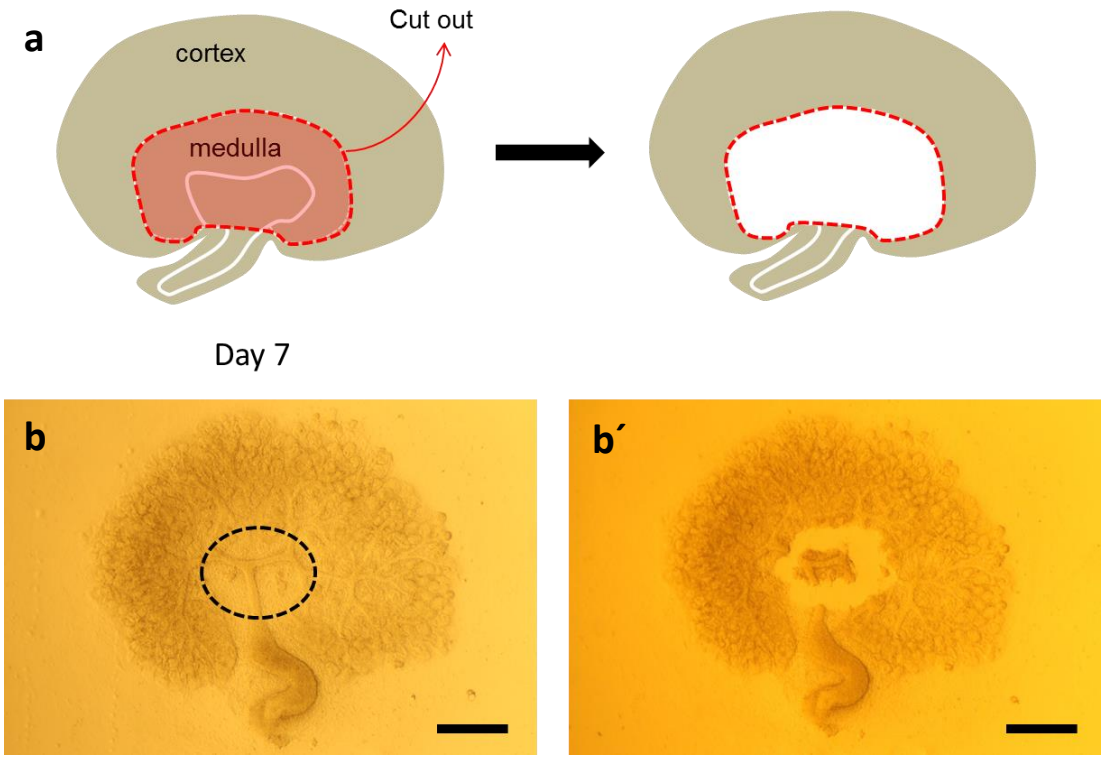

Figure 6-3 Experimental removal of the medulla. (a) The diagram describes how the medulla was cut out. The medulla was cut out at 7d and cultured for 3-days. (b) An E11.5 + 7d kidney in LV system is shown in a bright-field. The medulla was determined by the first branching point of the collecting duct and no nephrons reside. The dotted circle indicates the medulla. (b´) The image immediately after the medulla was cut. The scale bar = 500 µm.

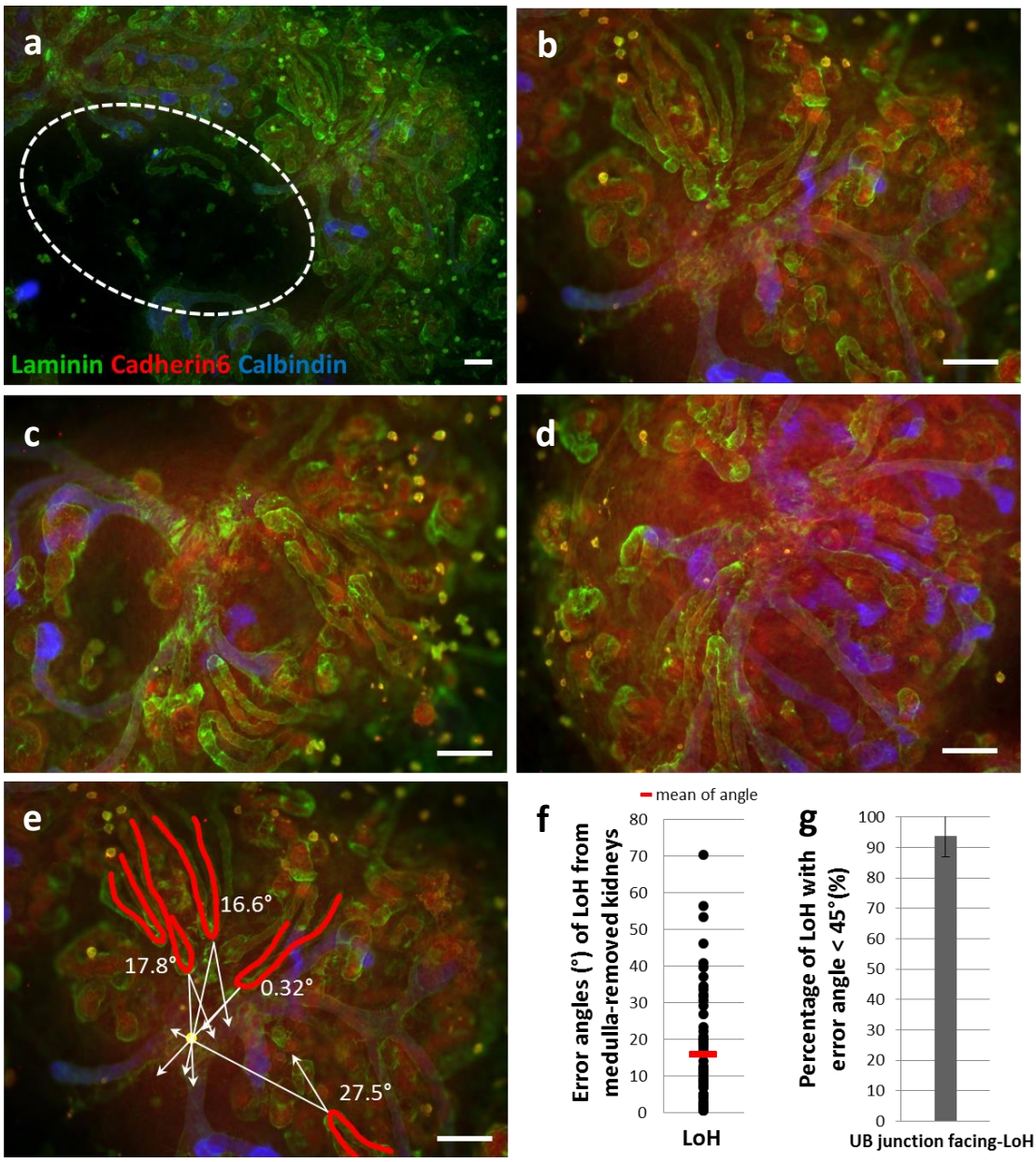

Figure 6-4 The LoH migrate toward the nearest major branching point of the ureteric bud (UB). (a) The medulla was removed from E11.5+7d and the culture was incubated for 3 further days. The dotted circle indicates the region that the medulla was cut. Laminin (green) is expressed in the general basement membrane of the epithelium, cadherine6 (red) is expressed in the LoH and proximal tubules, and calbindin (blue) is expressed in the UB. (b, c, d) High magnification views from (a). Three different regions of the medulla-removed kidney show that the LoH converges towards the largest remaining branching part of the UB. (e) A representative image showing how error angles between the line crossing the LoH axis and the other line connecting the LoH apex and the UB junction were measured. The LoH (red) and the UB junction (yellow) were marked by Image J software. The error angles were measured using AxioVision Rel. 4.8 software. (f) Error angles from the LoH (n=64) were plotted in a scatter chart (Mean = 15.8°, σ = 15.3°). (g) 94% of total LoH (n=64) converged on the UB junction and the error bar indicates 95% confidence interval (=7), the formula is t= z' x SQR(p(1-p)/n) (z´; standard normal distribution, x; mean, SQR; square root, p; possible sample size/population of size, n; sample number) (Bremer, 2010). The scale bar = 400μm.

To support the result that the LoH migrate towards the branching point of the UB rather than simply migrating into free space, an additional surgical experiment was performed. In fact, some LoH heading towards the free surrounding area of the kidney culture were observed in the cultures (Figure 6-5). However, these only occurred in the peripheral area of the cultures with several LoH (Figure 6-5). Thus, I tested where the LoH would choose to head if they closely encounter both free space and the branching point of UB. Free spaces close the LoH, in which the LoH might be able to grow, were provided by surgically removing not the part of the cortex where the LoH might reside but rest of the parts and culturing it (Figure 6-6).

Similar to the medulla-removal experiment, the LoH from the partial cortex produced an orientation towards the nearest UB branching point even though there were plenty of free spaces that the LoH could have grown towards (Figure 6-6). The result strongly suggested that the branching point of the UB or a region near it might be the source of the target molecule(s) or cue(s) that attract the LoH.

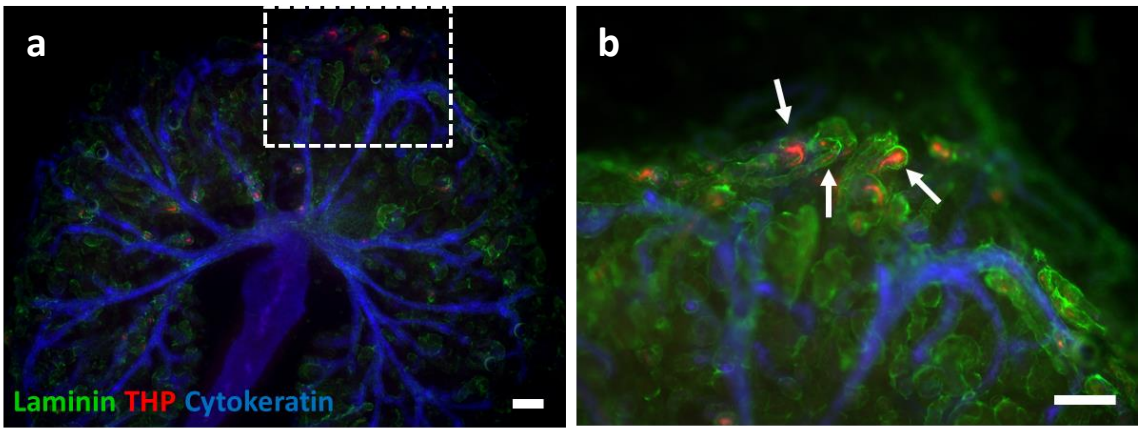

Figure 6-5 The LoH oriented towards the free space in the surrounding kidney. (a) An E11.5 + 10d kidney cultured in the LV system. Laminin (green) is expressed in the general basement membrane of the epithelium, THP (red) is expressed in the LoH, and cytokeratin (blue) is expressed in the UBs. (b) High magnification views of a dotted square in (a). The white arrows indicate the outward LoH. The scale bar = 400μm.

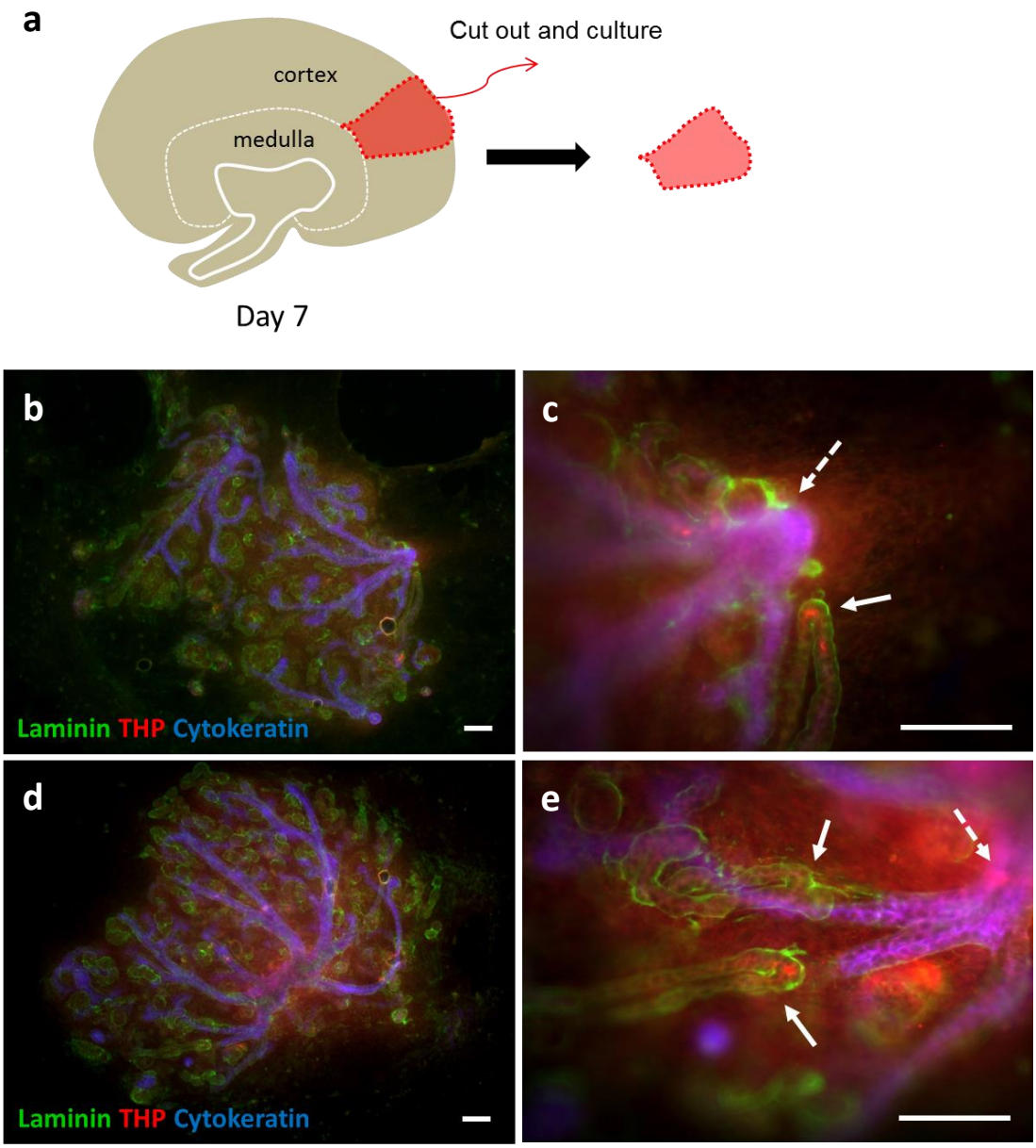

Figure 6-6 The LoH in a piece of isolated cortex still orient towards a UB branching point. (a) A part of a cortex was excised from E11.5+7d kidney and cultured for 3 days. (b, d) Two different regions of the cortex from different kidneys are shown. Laminin (green) is expressed in the general basement membrane of the epithelium, THP (red) is expressed in the LoH, and cytokeratin (blue) is expressed in the UBs. (c, e) High magnification views of (b, d) respectively. The white arrows indicate the LoH and the dotted arrows indicate the branching point of UB. The scale bar = 200μm.

6.2.3 The LoH still orientate towards the collecting duct in $NaClO_3$-treated cultures

Both 'cut-and-paste' (cortex) and 'cut' (medulla, cortex) experiments resulted in a directional arrangement of the LoH towards the UB branching point. As another method of demonstrating that the UB junctions are the target region to which the LoH are attracted, UB development was inhibited and subsequent LoH orientation was observed. By inhibition of UB development, it was also possible to test whether the LoH orientation towards the UB is actually only the effect of random collision since there are many UB branches in a normal kidney.

The inhibition was achieved using the drug, sodium chlorate ($NaClO_3$). Sodium chlorate is a specific sulphation inhibitor that inhibits collecting duct development whilst maintaining nephron development (Davies et al., 1995). As previously described (Davies et al., 1995), 30mM Sodium chlorate was added in kidney culture medium (KCM) during the culture period. To begin with, correct timing of sodium chlorate treatment had to be tested, since the culture system (LV system) used in this section was different from what Davies et al. 1995 used (Saxén system). Thus, each kidney was cultured in KCM, and then supplemented with 30mM Sodium chlorate at different time points (from 0d, 2d, and 4d) for 3 further days (Figure 6-7). Kidneys cultured in KCM with sodium chlorate added from 0d and 2d could not be reliably maintained in the LV system. They remained rounded and floated in KCM after adding sodium chlorate (Figure 6-7). However, a kidney (E11.5 + 7d) in KCM with sodium chlorate added from 4d could develop under chlorate treatment for at least 3 more days. Thus, E11.5 + 4d was chosen as a start point to add Sodium chlorate in KCM (Figure 6-7).

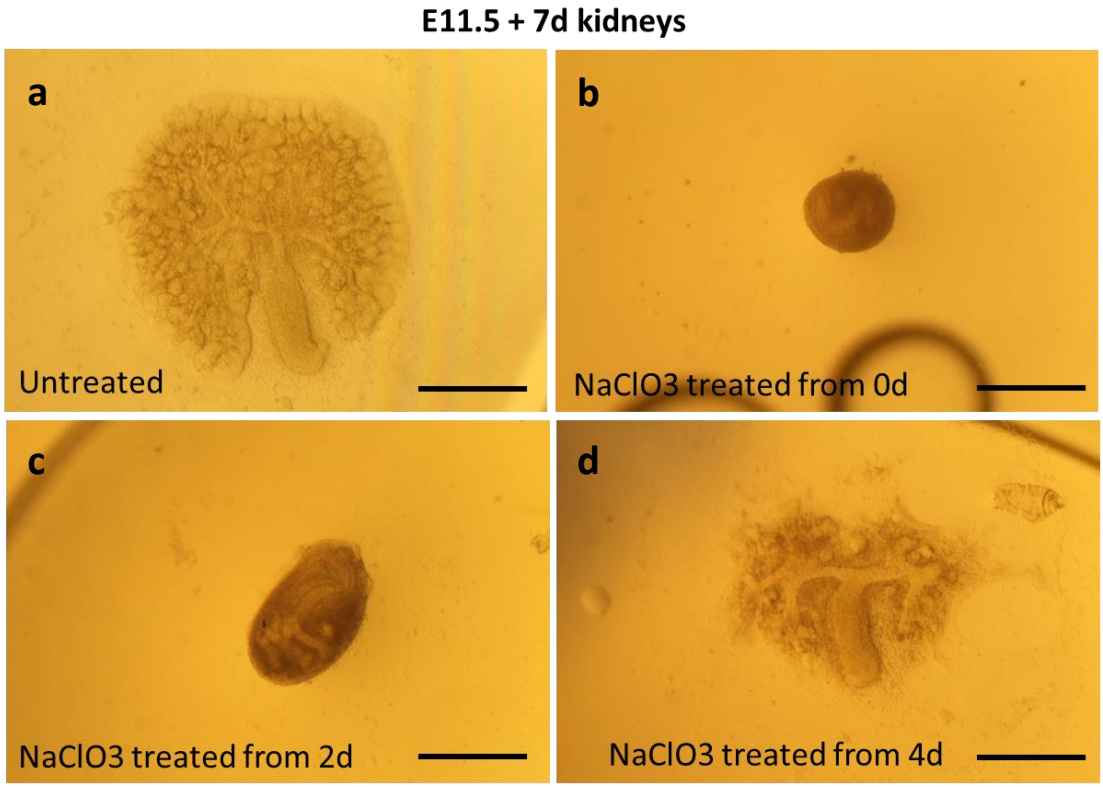

Figure 6-7 Treatment of kidneys cultured in LV system with $NaClO_3$. (a) An untreated E11.5 +7d kidney in the LV system is shown as a control. (b, c, d) The kidney treated with 30mM $NaClO_3$ from 0d (b), 2d (c), and 4d (d), and cultured for a total of 7 days. The scale bar = 500 µm.

E11.5 kidneys were pre-incubated in plain KCM for 4 days, and were then supplemented with 30mM sodium chlorate for a 5 further days (Figure 6-8). Since sodium chlorate was added in the culture after the kidney had developed normally for 4 days, the morphogenesis of the collecting duct was not entirely blocked (Figure 6-8). However, the chlorate-treated kidneys showed a less branched collecting duct compared to the untreated kidney (Figure 6-8). In particular, in the peripheral region of the chlorate-treated kidneys, UB development was clearly inhibited (Figure 6-8). However, many nephrons formed and some of them were still linked to the UB (Figure 6-8). Markedly, the LoH were still oriented towards the inhibited UB even though it was now a small target (Figure 6-8). Specifically, the LoH oriented towards the shaft of less branched UB suggesting that the UB in general, not necessarily a branching point of it, attracts the LoH (Figure 6-8).

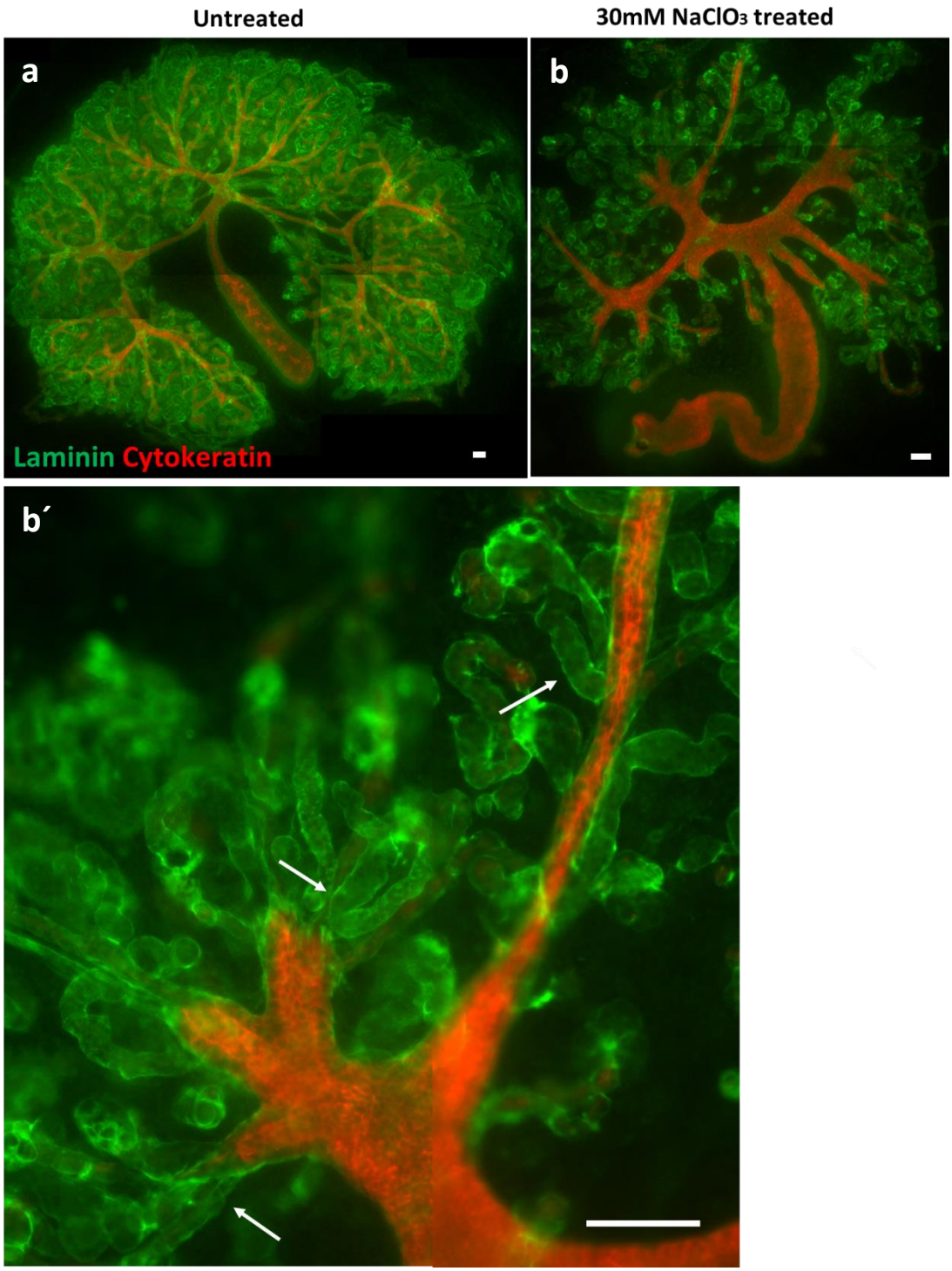

Figure 6-8 The LoH head towards the nearest ureteric bud (UB) of the kidney cultured in 30mM sodium chlorate. (a) The untreated E11.5 + 9d kidney cultured in the LV system is shown as a control. Anti-laminin (green) stained the general basement membrane of epithelia and anti-cytokeratin (red) stained the collecting duct. (b) The E11.5 + 9d kidney cultured in 30mM sodium chlorate in KCM for 5 days from E11.5+4d. Compared to the control kidney, there is less extensive development of the UB system. (b´) High magnification views of (b). The arrows indicate UB-heading LoH. The scale bar = 200µm.

6.3 Discussion

6.3.1 The ureteric bud / collecting duct system as a source to navigate the loop of Henle orientation

In this chapter, I studied LoH guidance(s) using the cut-and-paste technique. One of the main findings is that the LoH converged on the branching point of the remaining UB in the cortex in the medulla-removed culture.

As reviewed in Chapter 1, the UB initiate outgrowth from the Wolffian duct followed by developing into tip and stalk regions (reviewed in Davies and Davey, 1999, Costantini and Kopan, 2010). As the UB enters the branching phase, UB cells proliferate predominantly at the tip region by increasing the size of it, thereby forming new branches to have a fractal-like structure during development (Michael and Davies, 2004, Watanabe and Costantini, 2004). While the cortex comprises many thin UB branches, the medulla consists of thicker CD (Knepper et al., 1977).

Several important points can be discussed from the finding to precisely account for the LoH guidance cue(s) related to the UB/CD anatomy. One point is that the LoH can be guided to the UB residing in the cortex not necessarily to it in the medulla when the medulla was removed. Specifically, regardless of the location of the UB in the kidney, the LoH might follow the oldest region of the UB. This is also supported by the result achieved from the cortex rotating experiment that the LoH heading towards the medulla which was actually the first bifurcated region of the collecting duct. In fact, according to Fick's first law of diffusion, the concentration of a substance (a guiding molecule in this case) varies as distance^{-2}, in terms of distance to the source. Thus, if all UB cells produce the same amount of guiding molecules, a nearby younger UB branch would be more attractive than a further distant one. Therefore, the data actually suggest that, while all UB produce guiding molecules, older regions of the UB / CD system secrete much more.

It is also possible to speculate that the junction of the UB surely has more populations of UB cells which possibly secrete more quantity of guiding molecule(s) compared to those secreted from the thin UB shaft, thereby attracts the LoH. However, if there is no UB junction near LoH, the LoH showed its arrangement towards the nearest UB shaft. This was observed in the chlorate-treated culture.

Pertinent to this, another important point from the result is that the actual target region in the UB for guiding the LoH is probably not the UB tip region but the stalk including the junction. This finding would provide instrumental information to exclude molecules unrelated to the LoH guidance. For instance, Wnt-11 is restrictedly expressed in the UB tip rather than stalk region (Kispert et al., 1996, Vainio et al., 1999), so is thereby excluded from the possible candidates. However, it is also completely not sure that the source of guiding LoH is UB cells since the thin sheath of mesenchyme surrounds the UB / CD system.

6.3.2 Inhibition of sulphated glycosaminoglycan (GAG) does not interfere the loop of Henle guidance

Linked to the result from the cut-and-paste experiment, I tested how the LoH would orientate if the UB development is inhibited. In agreement with the previous study (Davies et al., 1995), the branching and development of UB was inhibited but the nephron formation and development was maintained. Although not many LoH were observed, the result still showed the LoH orientation towards the UB. As described in the previous section, the result showed that the LoH can be navigated to the UB shaft not necessarily to UB junction. The result might also suggest that candidate signaling(s) attract the LoH by GAG-sulphation-independent manner.

To sum, I demonstrated, using the cut-and-paste technique, that the typical orientation of the LoH can be altered and the LoH can be guided towards the UB, probably by GAG-sulphation-independent manner. The next step is to try to identify guiding molecule(s).

7 Chapter 7 Experimental manipulations to guide identification of Henle's loop guidance molecules

7.1 Introduction

In the previous chapter, I showed that the ureteric bud (UB) /collecting duct (CD) system appears to attract Henle's loop (LoH). In this chapter, I tried to screen possible LoH guiding molecule(s).

Correctly guessing correct molecule(s) from numerous possible candidates would be unlikely succeeded. The UB/CD system expresses more than a hundred molecules having functions of ligand and/or cytokine (www.informatics.jax.org). Thus, I began with a broad strategy for screening candidate molecule(s) such as targeting major signaling pathways which might possibly related to the LoH guidance.

Major signaling pathways implicated in renal development include sonic hedgehog (SHH), the transforming growth factor beta (TGFβ) superfamily, the canonical wingless-related integration site (Wnt) signaling, glial cell derived neurotropic factor (GDNF), fibroblast growth factor (FGF), vascular endothelial growth factor (VEGF) and Notch pathways (reviewed in Reidy and Rosenblum, 2009, Woolf, 2010). These have been shown to act as guidance cues in different systems; for instance, guiding growth cones in neural development, SHH (Charron et al., 2003), BMP (Butler and Dodd, 2003), and Wnt (Lyuksyutova et al., 2003, Yoshikawa et al., 2003) signaling pathways have been found to be implicated. With respect to signaling pathways that underlie a tube guidance, migration of angiogenic sprouts provide a great example, and are directed by VEGF and Delta-Notch pathways from the leading tip cells (Hellstrom et al., 2007, Gerhardt, 2008). Therefore, I investigated the LoH guidance by linking it with current understanding of major pathways driving solitary cell and collective migrations since in conceptual aspects, mechanisms steering individual cells migration and collective migration are not completely mutually exclusive (see chapter 1).

To begin with, I chose to use embryonic spinal cord to broadly screen the candidates. The embryonic spinal cord is known to secrete signalling molecules such as Wnt and SHH (reviewed in Ulloa and Marti, 2010). The spinal cord has also been used as a robust renal tubule inducer, demonstrated in early studies of tubule induction from metanephric mesenchyme (Saxén, 1987, Grobstein, 1956). I placed a piece of spinal cord next to a kidney culture to test whether centripetal arrangement of LoH was manipulated by interfering in endogenous guidance cue(s) of LoH in the kidney culture. Since the co-culture with spinal cord gave rise to altered directional arrangement of some LoH, a more precise manner of

experiment was carried out to screen guiding molecule(s). In embryonic spinal cord, different kinds of Wnt are expressed along the dorsal-ventral axis; Wnt-1, Wnt-3, and Wnt-3a are expressed from dorsal spinal cord, and Wnt-7a and Wnt-7b are expressed from ventral spinal cord (Figure 7-1). Wnt-4 is expressed in dorsal and floor plate of ventral spinal cord (Parr et al., 1993) (Figure 7-1). Hence, different parts (dorsal or ventral) of spinal cord were surgically isolated and placed next to kidney cultures to determine which Wnt were involved in LoH guidance cue(s). However, both parts altered of centripetal arrangement of LoH.

SHH is expressed in a gradient in the spinal cord (Ericson et al., 1997, Wilson and Maden, 2005, Ulloa and Marti, 2010) (Figure 7-1). More importantly, SHH is expressed from the medullary collecting duct in the kidney (Yu et al., 2002, Jenkins et al., 2007). Linked to this, the previous chapter 6 showed that the LoH heads towards the UB/CD and this chapter showed that the LoH oriented towards the spinal cord, SHH was a reasonable target to investigate as a guiding molecule. Therefore, I tested the LoH orientation in the kidney under the condition of blocking SHH signalling pathway. SHH signalling was inhibited by an inhibitor, cyclopamine (Cooper et al., 1998) by direct binding of cyclopamine to smoothened (Smo) (Chen et al., 2002). However, cyclopamine did not prevent typical orientation of the LoH.

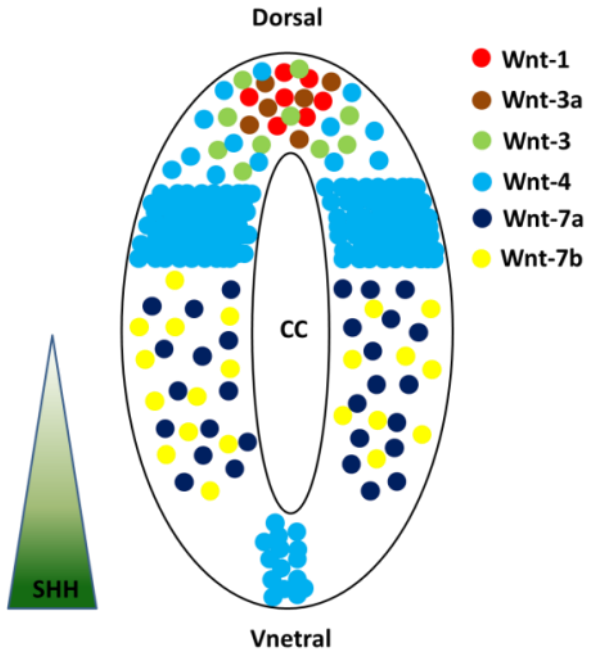

Figure 7-1 Diagram of Wnt and SHH spatial expression in a transverse section of the embryonic spinal cord (modified from Parr et al., 1993, Wilson and Maden, 2005). Wnt-1, Wnt-3a, and Wnt-3 are expressed dorsally and wnt-7a and wnt-7b are expressed ventrally in the spinal cord. Wnt-4 is expressed in both dorsal and floor plate region of the spinal cord. SHH is expressed in a gradient in ventral spinal cord.

7.2 Results

7.2.1 The typical orientation of the loop of Henle can be altered by adjacent co-culture with a fragment of spinal cord.

As the natural arrangement of the LoH seen in *in vivo* and *ex vivo* cultures appeared to be centripetal, manipulations that alter this orientation might be used as screen processes to identify the guidance cue(s). By disturbing endogenous guidance cues in kidney cultures, I hoped to alter typical (centripetal) orientation of the LoH.

In order to interfere with endogenous guidance cues of the LoH in kidney cultures, embryonic spinal cord was used since it secretes numerous signalling molecules (reviewed in Ulloa and Marti, 2010). Spinal cord was surgically isolated from E11.5 embryos and cut in pieces. E11.5 kidneys were pre-cultured for 7 days in the LV system to allow LoH formation. The piece of spinal cord was juxtaposed to the kidney culture in close contact and co-cultured for 3 further days (Figure 7-2).

The result, notably, was that the LoH residing near the spinal cord orientated towards the spinal cord rather than towards the kidney centre (Figure 7-3). Based on the maturity of the LoH heading towards the spinal cord, those might have arisen from nephrons that already formed before the incubation with the spinal cord, since it takes at least 120h for the spinal cord to induce nephron tubules from the mesenchyme (Figure 7-3) (Saxén, 1987, Davies and Garrod, 1995, Vainio et al., 1999). Some LoH even penetrates into the spinal cord, suggesting that the spinal cord may have robust capability to attract the LoH (Figure 7-3).

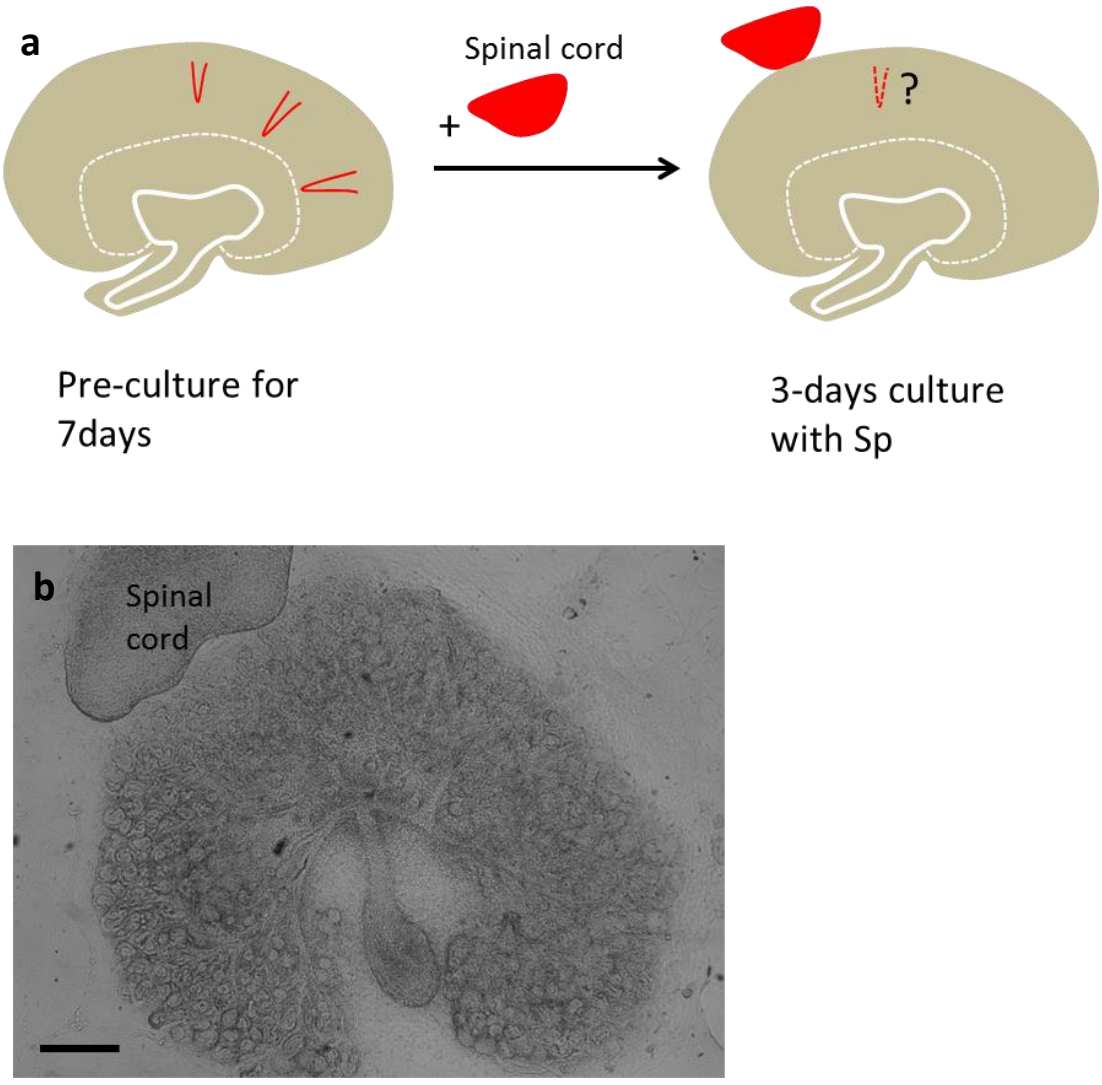

Figure 7-2 Experimental set-up of spinal cord co-culture. (a) An E11.5 kidney was pre-cultured for 7 days in the LV system to form LoH and a spinal cord piece was placed next to the kidney for 3 further days also in the LV culture. (b) A bright-field image of the spinal cord next to the kidney after 3-days of co-culture. The scale bar = 400µm.

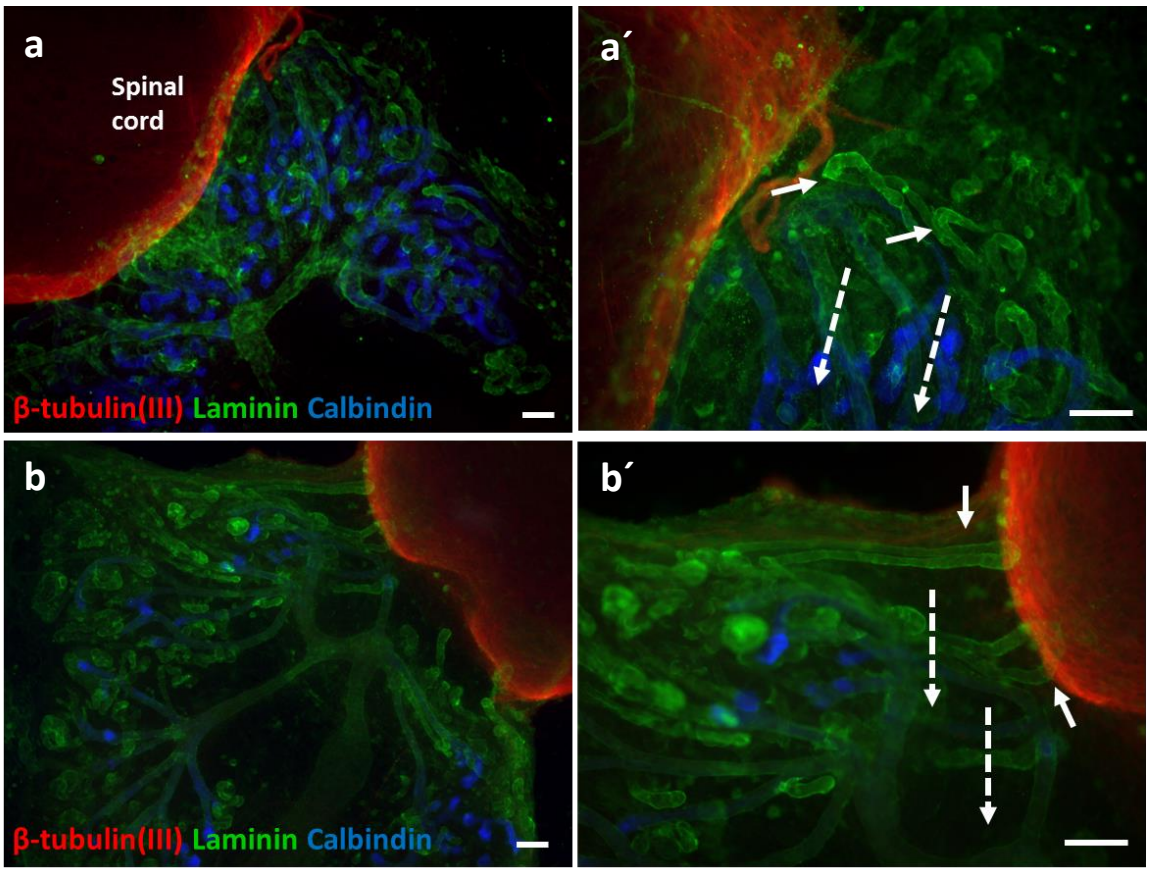

Figure 7-3 The LoH arranged towards a piece of spinal cord in the LV culture. (a), (b) Low-magnification views of co-cultures of the spinal cord and kidney. A 7-days pre-cultured kidney (E11.5 + d7) was co-cultured with the spinal cord for another 3 days in the LV system. The spinal cord was marked by β-tubulin III (red) expression. The general basement membrane of epithelia and the ureteric buds were marked by laminin (green) and calbindin (blue) respectively. (a´), (b´) High-power views of (a), (b) respectively. The short white arrows indicate the spinal cord-heading LoH and long dotted arrows indicate the direction toward the kidney centre. The scale bar = 200μm.

To quantitatively test whether co-culture with spinal cord interfered with the typical orientation of LoH, directional arrangement of LoH were quantified. LoH orientations were measured by error angles between two lines (one line crossing LoH axis and the other line connecting the LoH apex and the first branching point of a collecting duct). As controls, a culture without any exogenous tissue, and a co-culture with adrenal gland chosen as a probably irrelevant tissue were set up. A piece of adrenal gland was obtained from E15.5 embryos and it was used as a comparative exogenous tissue to spinal cord.

Mean ± SEM of error angles of LoH from each conditions are 28.1±0.2° (kidney), 21.7±2.9° (kidney+adrenal gland), 77.8±1.6° (kidney+spinal cord) (Figure 7-4). There was no significant difference between the two control groups (p =0.822, kidney vs kidney+adrenal

gland) (Figure 7-4). However, the mean error angle of LoH from co-culture with spinal cord were significantly high compared to those in kidney only (p=0.0006) and those in co-culture with adrenal gland (p=0.00001) (Figure 7-4). The result indicated that the spinal cord might be secreting molecule(s) that are capable of disturbing typical orientation of LoH.

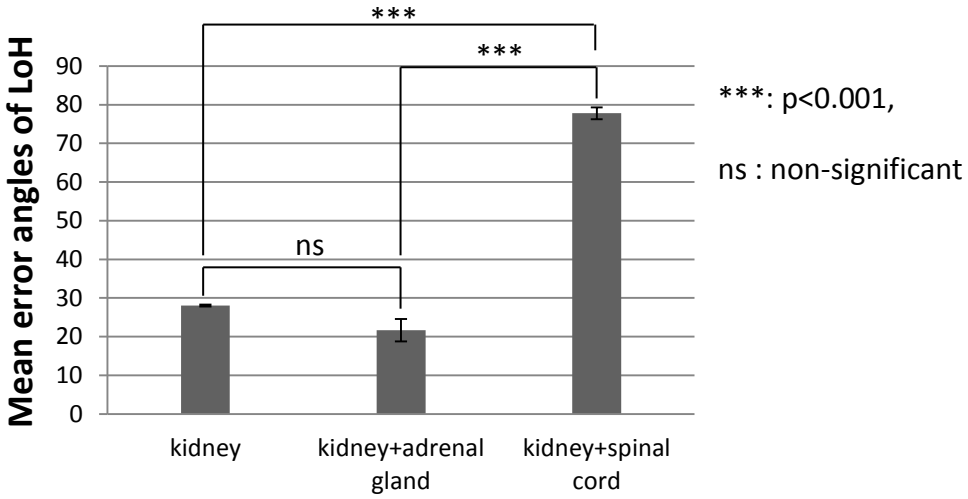

Figure 7-4 Co-culture with spinal cord alters orientation of the LoH. LoH orientation was determined by the error angle between one line crossing the LoH axis and the other line connecting the LoH apex and the first branching point of collecting duct. As controls to LoH from co-culture with spinal cord, LoH from kidney only and co-culture with adrenal gland were quantified. Error angles were measured by AxioVision Rel. 4.8. software. Mean ± SEM of error angles from each conditions are 28.1±0.2° (kidney), 21.7±2.9° (kidney+adrenal gland), 77.8±1.6° (kidney+spinal cord). p value in one way ANOVA is 0.0004 considered as significant. Thus, post hoc Scheffe test is performed to compare each two groups and p values are 0.822 (kidney vs kidney+adrenal gland), 0.0006 (kidney vs kidney+spinal cord), and 0.00001 (kidney+adrenal gland vs kidney+spinal cord). Based on the Bonferroni correction, p values obtained from post hoc t-tests less than 0.017 (0.05/number of sample groups) are considered as statistically significant.

7.2.2 Both dorsal and ventral spinal cords attract loops of Henle

The result form co-culture with a piece of spinal cord gave rise to some of the LoH directional growth towards the spinal cord (Figure 7-3). Moreover, several LoH closely located to the spinal cord even penetrated into the spinal cord. As the spinal cord secretes many signaling molecules, I strove to narrow target gene(s)/region down by additional co-culture experiments with different regions of the spinal cord; ventral and dorsal spinal cord. This was because the ventral and dorsal spinal cords are known to express different Wnt along the dorsal-ventral axis; Wnt-1, Wnt-3, and Wnt-3a are expressed from dorsal spinal cord, and Wnt-7a, and Wnt-7b are expressed from ventral spinal cord (Parr et al., 1993) (Figure 7-1). In addition to Wnt, SHH is also expressed in a gradient from ventral spinal cord (Ericson et al., 1997, Wilson and Maden, 2005, Ulloa and Marti, 2010).

E11.5 kidneys (n=10) were pre-incubated for 7 days, and 5 pieces of either dorsal or ventral spinal cords were located next to the kidneys and cultured for 3 further days. Only LoH located less than 500 μm from the spinal cord were counted. The mean number of either dorsal or ventral spinal cord-heading LoH were measured (Figure 7-5). However, there was no significant difference ($p = 0.94$) between the mean ± SEM number of the dorsal spinal cord-heading (2.8±0.3, n=11) and ventral spinal cord-heading (2.7±0.5, n=8) LoH (Figure 7-5).

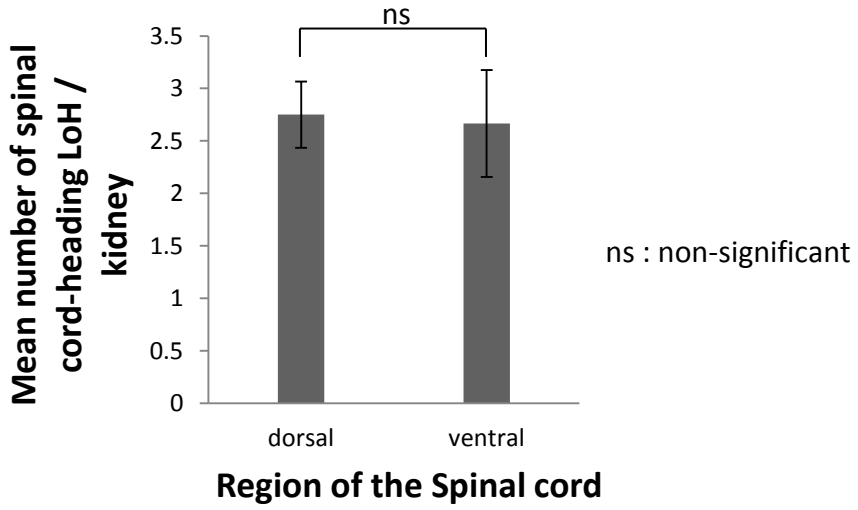

Figure 7-5 Comparison of the mean number of the LoH that orient towards different regions (dorsal and ventral) of the spinal cord. Each E11.5 + 7d kidney in the LV system was juxtaposed with either a dorsal (n=5) or a ventral (n=5) piece of embryonic spinal cord and cultured for 3 days. Only LoH close (<500μm) to the spinal cord were counted. Mean ± SEM number of dorsal-heading LoH is 2.8±0.3 (n=11) and ventral-heading LoH is 2.7±0.5 (n=8). The error bars indicates SEM. There was no significant difference (p = 0.94) between the mean number of dorsal- and ventral-heading LoH. The p value was assessed by two-tailed t-test.

7.2.3 Inhibition of the SHH signaling pathway could not prevent centripetal orientation of the LoH in LV system

As shown in the co-culture experiment with the spinal cord, it seemed that the spinal cord could attract the LoH. In addition to Wnt, SHH is one of major molecules expressed in ventral spinal cord (Ericson et al., 1997, Wilson and Maden, 2005, Ulloa and Marti, 2010). Also, SHH is expressed from the medullary collecting duct in the kidney (Yu et al., 2002). Therefore, SHH was a possible candidate to investigate as a target molecule involved in the LoH guidance.

In order to test how SHH affects the LoH orientation, I blocked SHH signaling pathway. Cyclopamine is an inhibitor that is known to block the SHH signaling pathway (Cooper et al., 1998). By adding cyclopamine to the kidney culture medium (KCM), I tested whether the LoH showed different orientation rather than their typical direction towards the kidney centre (Figure 7-6). E11.5 kidneys (n=4) were pre-incubated in the LV system with normal KCM for 7 days to form LoH. The E11.5+7d kidneys were then cultured in KCM supplemented with 5 μM cyclopamine for 3 further days (Figure 7-6). LoH orientation was

measured by error angles between the line crossing the LoH axis and the other line connecting the apex of the LoH and the first branching point of the collecting duct. As described in the previous chapter 4, the first branching point of the collecting duct was determined as the kidney centre. The mean ± SEM number of the LoH error angles in the untreated kidneys is 23.8±1.9° and it in the cyclopamine treated kidneys is 24.6±0.8°. There was no significant difference (p value = 0.92) of LoH orientation between untreated and cyclopamine treated kidneys (Figure 7-6).

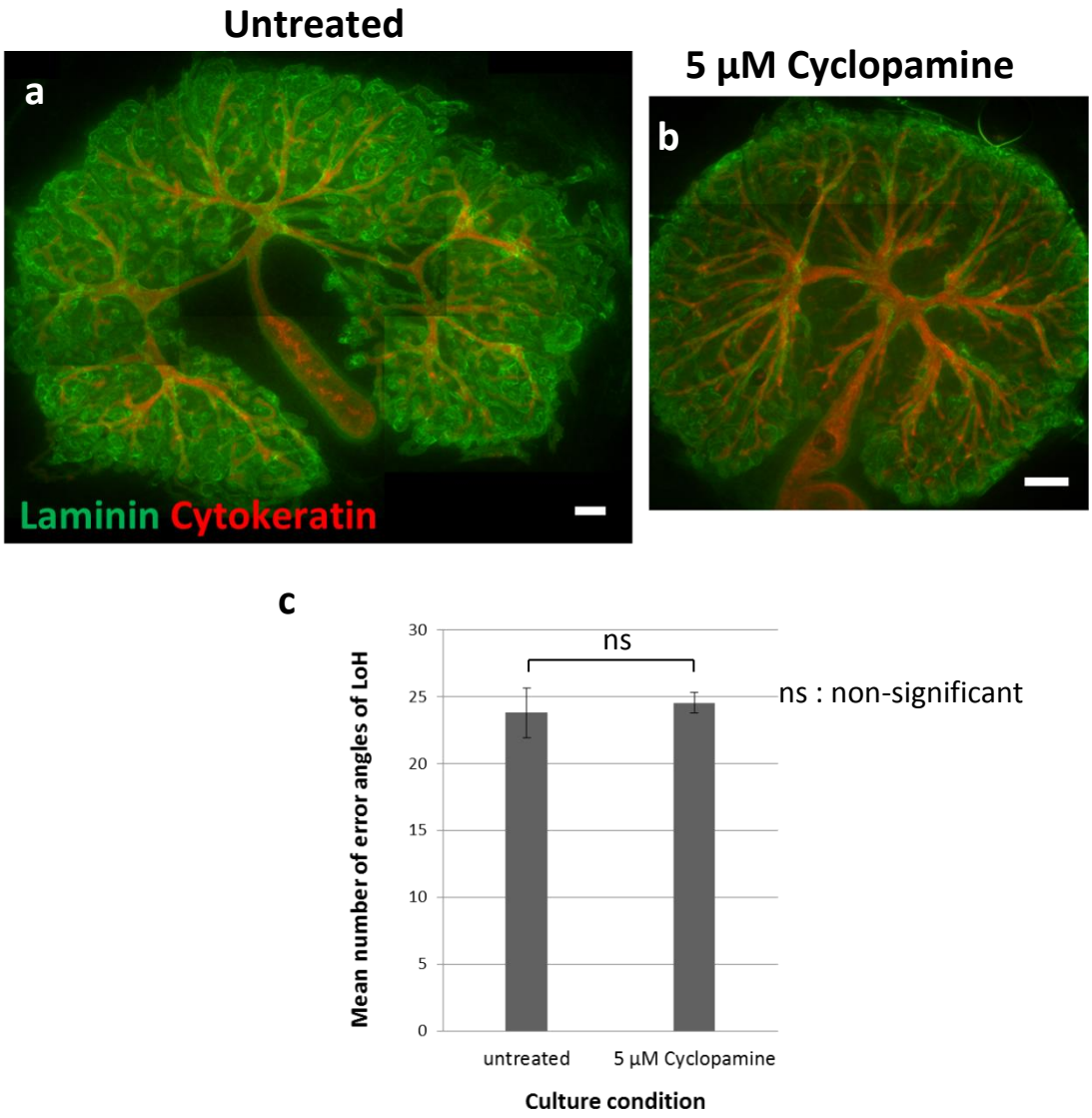

Figure 7-6 Comparison of the untreated kidney and cyclopamine-treated kidney. (a) The E11.5 + 10d kidney cultured in LV system with normal kidney culture medium (KCM) is shown as a control. (b) The E11.5 + 7d kidney was cultured in KCM with 5 µM of cyclopamine and cultured for 3 days. Anti-laminin (green) stains the general basement membrane of epithelia and cytokeratin (red) stains the ureteric buds. (c) The error angles of LoH (n=27) from cyclopamine-treated kidneys was compared to those (n=11) from the untreated kidney. The error angles were measured between one line crossing the LoH axis and the other line connecting the LoH apex and the first branching point of the collecting duct. The mean ± SEM number of the LoH error angle from untreated kidneys is 23.8±1.9 and those from 5 µM cyclopamine-treated kidney is 24.6±0.8. The error bars indicate SEM. The p-value (0.92) was measured by two-tailed t test. The scale bar = 400 µm

7.3 Chapter discussion

7.3.1 Embryonic spinal cord, as well as the ureteric bud (Chapter 6), as a possible source of candidate molecule(s) to guide the loop of Henle

The spinal cord has been extensively studied as a robust surrogate of the UB for renal tubule induction from the metanephric mesenchyme (Grobstein, 1955, Grobstein, 1956, Saxén, 1987, Vainio et al., 1999). In addition to this, I propose another ability of the embryonic spinal cord, guiding the LoH. I demonstrated that the typical orientation of the LoH driven by endogenous cue(s) in the developing kidney can be interfered by co-culture with the spinal cord. Markedly, the apex of LoH even penetrated into the spinal cord. I speculated that this might be the effect of uncontrolled secretion of candidate substance(s) from the spinal cord rather than regulated secretion of those from the kidney.

Both the co-culture experiment with the embryonic spinal cord and the cut-and-paste experiments gave rise to attraction of the LoH towards the embryonic spinal cord (this chapter) or the maturing UB (Chapter 6). This suggests that candidate(s) attracting the LoH is substance(s) that made and secreted by both the spinal cord and the UB.

There are several possible candidates (ligands) that might mediate LoH guidance, based on the results in this chapter and the previous chapter. They are listed in Table 7-1. Those molecules were chosen only relying on the findings that directional bias of the LoH towards the spinal cord or the UB. Possible candidates defined as gene functions, receptor binding (ligand) or growth factor activity (cytokine), were screened by Gene Expression Data tool in Mouse Genome Informatics (MGI) (www.informatics.jax.org). Expression level of each gene was also checked by searching it in GenitoUrinary Molecular Anatomy Project (GUDMAP) Expression Database (www.gudmap.org).

Gene ID	Gene Symbol	Gene Name
MGI:103302	Bmp7	bone morphogenetic protein 7
MGI:106643	Efna4	ephrin A4
MGI:1095416	Jag1	jagged 1
MGI:96974	Kitl	kit ligand
MGI:96949	Mdk	midkine
MGI:1859631	Pdgfc	platelet-derived growth factor, C polypeptide
MGI:1099818	Pkd2	polycystic kidney disease 2
MGI:97804	Ptn	pleiotrophin
MGI:1337026	Sdcbp	syndecan binding protein
MGI:107557	Sema3c	sema domain, immunoglobulin domain (Ig), short basic domain, secreted, (semaphorin) 3C
MGI:107556	Sema5a	sema domain, seven thrombospondin repeats (type 1 and type 1-like), transmembrane domain (TM) and short cytoplasmic domain, (semaphorin) 5A
MGI:1315205	Slit2	slit homolog 2 (Drosophila)
MGI:98957	Wnt4	wingless-related MMTV integration site 4
MGI:98962	Wnt7b	wingless-related MMTV integration site 7B

Table 7-1 Examples of possible candidates (ligands) expressed in the spinal cord and UB for guiding the LoH. Genes were searched by Mouse Genome Informatics (MGI) (www.informatics.jax.org) and expression levels were checked by GUDMAP (www.gudmap.org).

Because developing spinal cord is major source of Wnt and Shh (reviewed in Ulloa and Marti, 2010) and these are also expressed by the UB (Vainio et al., 1999, Schmidt-Ott et al., 2005, Yu et al., 2002) during renal development, these molecules were the most intriguing. Among spatial expression of Wnt along dorsal-ventral axis of spinal cord (Parr et al., 1993) and the UB (www.gudmap.org), Wnt-4 and Wnt-7b were candidate molecules. Besides their regional expression pattern, both Wnt-4 (Tanigawa et al., 2011) and Wnt-7b (Yu et al., 2009) are required for nephron formation. Especially, it was shown that Wnt-7b-mediated pathway regulates coordinated elongation of the LoH (Yu et al., 2009). Thus, I speculate that Wnt-4 and Wnt-7b can be possible candidates to guide directional orientation of the LoH in addition to their already proven roles in nephrogenesis.

Among BMP, Bmp7 is mutually expressed by the spinal cord (Magdaleno et al., 2006), the UB (www.gudmap.org), and the mesenchyme surrounding collecting duct (Davies and Davey, 1999). Bmp-7 is also known to play important role for nephrogenesis as well as normal arborisation of the UB (Vukicevic et al., 1996, Davies and Davey, 1999). Due to the requirement of Bmp-7 in collecting duct branching, Bmp-7 can also be one of candidate molecules regarding the result that the LoH converged on the branching point of the UB.

Midkine (Mdk) is also in relation to promote target cells growth, survival, and migration (Muramatsu, 2010). Structurally related to Mdk, Pleiotrophin (Ptn) has approximately 50% sequence similarity with Mdk (Muramatsu, 2010). As another neurite outgrowth-promoting factor in rat brain (Rauvala and Pihlaskari, 1987), Ptn can be added as one of candidate molecules.

In human retinal pigment epithelial (RPE) cells, platelet-derived growth factor, C polypeptide (PDGFC) is known to mediate those cells' proliferation and migration (Li et al., 2007). Additionally, PDGFC has also been studied as crucial regulators for cell migration, survival, cell death, and transformation in the breast carcinoma cell line MCF7 (Hurst et al., 2012).

Semaphorins have extensively been documented proteins that act as a regulator of axonal growth cone guidance (Nakamura et al., 2000). Although semaphorins primarily mediates axonal guidance as a repellent (Tessier-Lavigne and Goodman, 1996), semaphorin3C (Sema3c) has been investigated that it promotes the breast cancer cells' migration (Esselens et al., 2010).

As a pair to the ligand list above, molecules with a receptor activity function known to be in the developing LoH can also be listed (Table 7-2). Although there was no matched ligand-receptor pair from those lists, the ligands from the list can still be possible candidates owing to orphan receptors and other unknown receptors in the LoH suggesting more screening processes for searching for guiding molecule(s) are necessary.

Gene ID	Gene Symbol	Gene Name
MGI:1351351	Casr	calcium-sensing receptor
MGI:109175	Dab2	disabled 2, mitogen-responsive phosphoprotein
MGI:95276	Epha7	Eph receptor A7
MGI:1917943	Gpr125	G protein-coupled receptor 125
MGI:2685858	Gpr176	G protein-coupled receptor 176
MGI:1917605	Gprc5c	G protein-coupled receptor, family C, group 5, member C
MGI:95794	Lrp2	low density lipoprotein receptor-related protein 2

Table 7-2 Examples of receptors localised in the loop of Henle (LoH). Genes were searched by Mouse Genome Informatics (MGI) (www.informatics.jax.org) and expression levels in the developing LoH were checked by GUDMAP (www.gudmap.org).

Taken together, not all molecules listed in Table 7-1 are highly implicated with cell migration and gene searching for ligand-receptor pairs from MGI (www.informatics.jax.org) and GUDMAP (www.gudmap.org) was inconclusive. Therefore, development of a high-throughput assay for searching target molecule(s) was necessary.

8 Chapter 8 Development of a high-throughput assay for loop of Henle guidance molecules

8.1 Introduction

Having confirmed the directional growth of the Henle's loop (LoH) towards the ureteric bud (UB) (Chapter 6) and shown that unknown molecule(s) from the spinal cord can probably guide the LoH (Chapter 7), the next step was to identify candidate molecule(s) or at least study characteristics of those molecule(s) implicated in guiding the LoH. In order to address this, development of a high throughput assay system was essential. Therefore, I will search guiding molecule(s) for the LoH using combination of high throughput screening methods in this chapter.

Mechanisms that direct cell migration can be divided into five types; contact guidance, durotaxis (mechanotaxis), galvanotaxis (electrotaxis), haptotaxis, and chemotaxis (reveiwed by Petrie et al., 2009, Lara Rodriguez and Schneider, 2013). As reviewed in Chapter 1, these cues drive cell migration in respond to topographical control of the extracellular matrix (ECM) (contact guidance) (Curtis and Wilkinson, 1997), increased stiffness (durotaxis) (Lo et al., 2000), an electrical potential gradient (galvanotaxis) (Sato et al., 2009), a gradient of a factor bound to substratum (haptotaxis) (Carter, 1967) and diffusible factors (chemotaxis) (Devreotes and Zigmond, 1988, Rappel et al., 2002). Among these cues, chemotaxis is strongly suggested as one of guiding cues for the LoH based on the results discussed in the previous chapters. Such chemotactic movements can be studied by cell migration assay.

Cell migration assays provide straightforward advantages to studying certain functions of cells such as migration, absorption and secretion (Kramer et al., 2013). In the 1950s, Grobstein showed that membrane filters could be used as cell growth substrates for the study of metanephric induction (Grobstein, 1953a, Grobstein, 1953b, Grobstein, 1956). Since then, many kinds of permeable supports have been developed and manufactured to study various aspects of cell biology. One of those supports is the Boyden chamber initially developed by Boyden to study leukocyte chemotaxis (Boyden, 1962). In this system, there are two chambers (upper and lower) separated by a membrane filter having an appropriate size of pores. In general, cells of interest are seeded in the upper chamber and a factor (attractant) can be added to the medium placed in the lower chamber. The number of migrated cells through the filter is used as the parameter to measure the cell motility. In addition to chemotaxis, many alterations can also be made to the Boyden chamber-based cell migration assay to study haptotaxis by coating a filter with ECM and chemokinesis (random migration) by adding equal concentrations of factors in the upper and lower chambers (Chen, 2005).

I chose to use FluoroBlok (commercially available) cell culture inserts for a migration assay. Since the FluoroBlok membrane blocks 490-700nm of light transmission (www.bdbiosciences.com), only the migrated cells on the bottom of the membrane are detected after fluorescently labelling cells. Using this insert, removing cells on the upper membrane, that do not migrate through the membrane, is not required. The insert provided a convenient and efficient way of testing the motility of cells.

In the migration assay that used in this chapter, the rat thick ascending limb (raTAL) of LoH cell line was employed (Eng et al., 2007). Regarding the idea that the apex is probably the region leading the directional growth of the LoH, I wanted to choose a cell line representing the bend region of the LoH in developing kidneys. Although such localisation occurs restrictedly in developing kidneys, the choice of using an apex-localised cell line would be reasonable to study LoH guidance, since this project focused on developing kidneys. In addition, the *in vivo* (Chapter 3) and *ex vivo* (Chapter 4, 5) experiments have shown that the LoH apex expresses Tamm-Horsfall protein (THP), a marker for TAL (Hoyer et al., 1979, Bachmann et al., 1990). Depending on the context above, as a surrogate for the apex, raTAL of LoH cell line was employed in the assay. raTAL is long-term cell line that retains the characteristics of TAL cells (Eng et al., 2007). The details of generating and characterising the cells are described in Carroll et al. (Carroll et al., 2003).

Based on the previous result that the LoH might be attracted towards the UB, specifically the region of ureteric stalk, I first test whether raTAL cells are attracted to a UB cell line in a cell migration assay. As surrogate for the UB, I chose to use 6TA2 cell line derived from UBs from E11.5 kidneys of 'immortomice' (Tai et al., 2012, Tai et al., 2013). 6TA2 cells are known to express the ureteric stalk-specific markers, collagen 18 (Lin et al., 2001) and Wnt9b (Qian et al., 2003) as described in Tai et al. (Tai et al., 2013). Thus, I tested raTAL cells' motility towards 6TA2 cells (Figure 7-1).

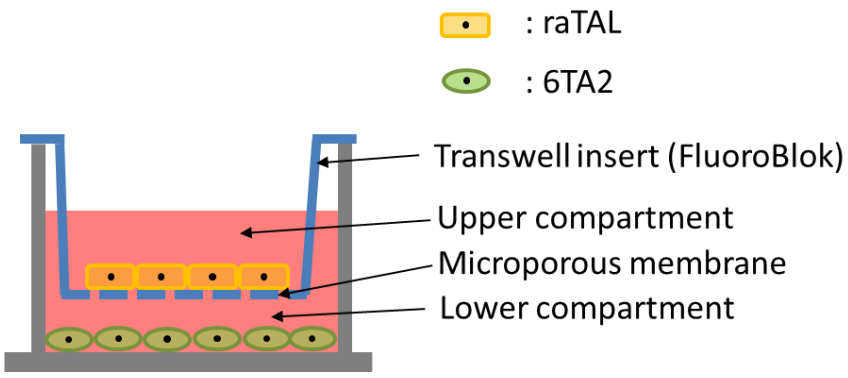

Figure 8-1 Cell migration of raTAL towards 6TA2 (Image adopted and modified from www.bdbiosciences.com). raTAL are seeded in an upper insert and 6TA2 are seeded in a lower well (24-well plate).

Then, the experiment leaded to broadly investigating candidate molecule(s) involved with attractive activity of raTAL. Since isolating key molecule(s) among numerous numbers of other signalling molecules is difficult and time-consuming process, I broadly approached to target candidate(s) by testing one of biochemical features of growth factors. As one of striking features of many growth factors is heparin-binding (Conrad, 1998), I chose to use this feature to categorise the candidate molecule(s). In addition, once the candidates(s) are verified as heparin-binding proteins, it would be useful purify these molecules by simply eluting them.

In this chapter, I aim to develop a useful high-throughput assay for searching for and studying LoH guiding molecules.

8.2 Results

8.2.1 Characterisation of raTAL and 6TA2 cell lines for migration assays

Investigating the attraction of LoH towards UB at the cellular level is another way of dissecting LoH guidance cue(s). Therefore, I performed migration assays between two cell lines; raTAL (rat thick ascending limb of LoH) and 6TA2 (mouse embryonic ureteric bud).

To begin with, I used markers to confirm molecular characteristics of raTAL and 6TA2 cell lines prior to performing migration assays. Tamm-Horsfall protein (THP), a marker of TAL of LoH (Tamm and Horsfall, 1950, Pennica et al., 1987, Hoyer et al., 1979), was employed to confirm raTAL as TAL cells (Figure 8-2). Collagen 18α1, one of the marker genes for ureteric stalks (Lin et al., 2001), was employed to demonstrate that 6TA2 cells were ureteric bud cells (Figure 8-2). Cytoplasmic localizations of both THP (green) and collagen 18α1 (red) expressions were observed in raTAL and 6TA2 cells respectively (Figure 8-2).

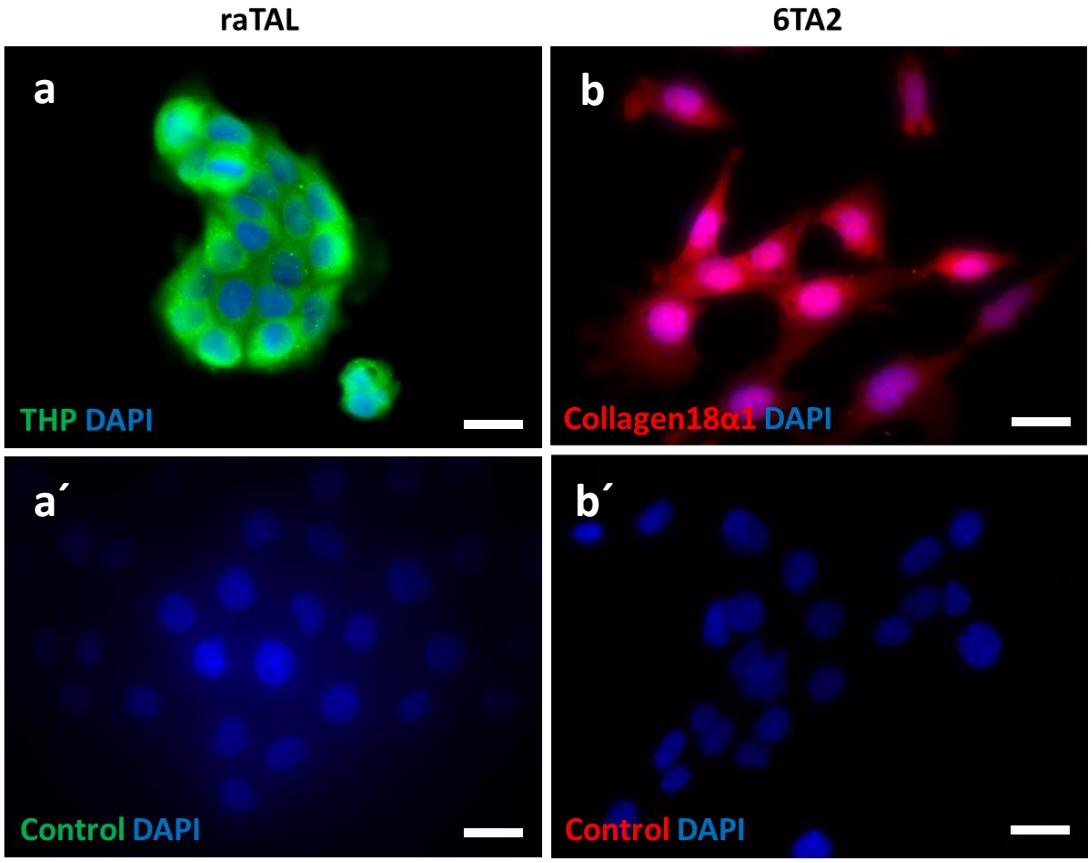

Figure 8-2 Characterisation of raTAL and 6TA2 cell lines. (a) raTAL cells express a marker for LoH (thick ascending limb), THP (green). (b) 6TA2 cells express one of stalk markers, collagen 18α1 (red). DAPI was for nuclear staining in both cell lines. Negative controls (secondary antibody used only) are shown in (a´) and (b´). The scale bar = 50µm.

8.2.2 An alternative method to quantify motility of raTAL in cell migration assays

One direct method to study the chemotactic activity between a cell line and chemoattractant(s) /chemorepellent(s), is to use a cell migration assay. After confirming marker gene expression in raTAL and 6TA2 cells, a migration assay was carried out to determine whether raTAL cells were attracted to 6TA2 cells. For the assay, appropriate pore size of Transwell inserts and cell density were carefully chosen. I chose to use of Fluoroblock™ Transwell (8μm pore size, 6.5 mm diameter) inserts, since they can block a wide range (490 – 700 nm) of light. Thus, only fluorescence from the underside of the well, to which migrated cells would relocate, will be visible and will not be confused by cells remaining on the top of the filter. Using a Fluoroblock™ Transwell, scraping the upper side of the membrane to eliminate resident cells was therefore not required. Regarding the diameter of an insert and cell growth, 3×10^4 cells per insert were determined as the optimal seeding density. raTAL cells were seeded and pre-incubated in the insert (upper compartment) overnight. At the same time, 6TA2 cells were also seeded and pre-incubated in an empty plate (lower compartment) overnight. The insert was then placed in the well of the 6TA2-seeded plate and the migration assay was carried out for 4h. The Transwell membrane was then fixed in 4% PFA followed by staining, and fluorescent cells were counted.

In conventional cell migration assays using Transwell membranes, chemotactic activity of target cells (upper insert seeded cells) is quantified by counting the number of membrane-crossing cells. These cells on the bottom of the membrane are detected by nuclear staining since counting migrated cells is generally considered as a criterion to measure chemotactic activity of cells. However, it was found that the Transwell insert with the largest pore size of 8μm (at the moment) did not permit raTAL cells to migrate through the pores. This was confirmed by propidium iodide (PI) staining for nucleic acids (Figure 8-3). No PI expression was detected (Figure 8-3). This might be due to a size of raTAL cells, a lot larger than the pore size (refer to Figure 8-2). Thus, an alternative method of quantifying membrane-crossing cells had to be developed. Rather than counting cells by nuclear staining, pores that were covered by cytoplasm of raTAL, which can be revealed by phalloidin (actin filament) staining, were counted (Figure 8-3). In this manner, the attempted motility of raTAL cells towards 6TA2 cells was measured.

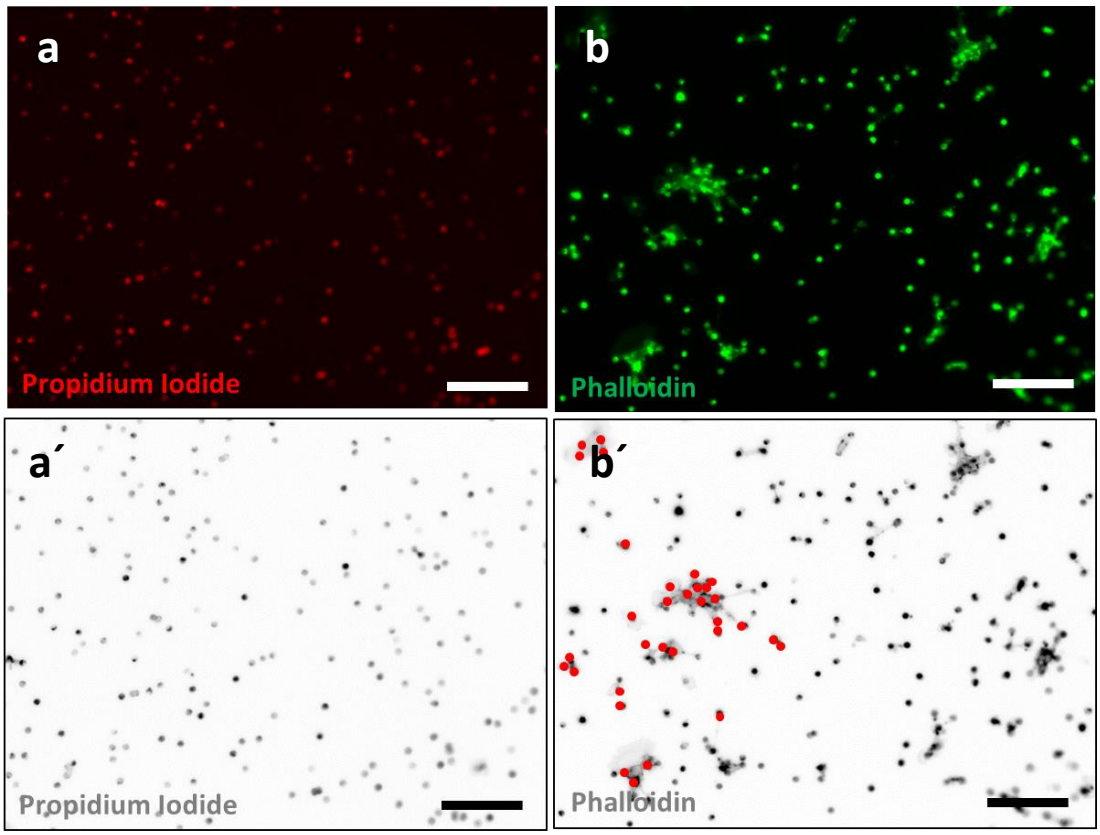

Figure 8-3 Motility of raTAL can be quantified by counting number of pores crossed by cytoplasm of raTAL. raTAL cells (3×10^4) were seeded and pre-incubated in a Fluoroblock™ Transwell insert (8µm pore size, 6.5mm diameter) overnight and placed in a 24-well plate, in which 6TA2 cells were also seeded and pre-incubated overnight. After 4h of cell migration assay, the bottom of Transwell insert was fixed in 4% PFA and stained with (a) propidium iodide (PI, nucleic acids) or (b) FITC phalloidin (filamentous actin). A black and white version of images is shown in (a´) and (b´) for easier viewing on a printed paper. In a panel (b´), some pores that are covered by phalloidin-stained cytoplasm have been marked by red dots to show how crossing raTAL cells were counted. The scale bar = 100µm

8.2.3 raTAL cells show chemotactic motility towards 6TA2 cells

Using already-optimized conditions for the cell migration assay, the motility of raTAL cells to 6TA2 cells was assessed. The initial assay aimed to test whether this is a higher attractive motility of raTAL cells towards 6TA2 cells compared to raTAL towards other cell lines. As a comparison to 6TA2 cells, Six5N6 (a metanephric mesenchymal cell line) (Tai et al., 2012) or L929 (a fibroblast cell line) (CCL-1™; ATCC) were employed. As a negative control (ctrl), culture medium alone was used. raTAL cells were pre-incubated in inserts overnight, and culture medium, 6TA2, Six5N6, and L929 cells were also pre-incubated in 24-well

plates overnight at the same time. After the pre-incubation, the inserts were placed in the wells and the migration assay was carried out for 4h. The inserts were fixed in PFA and stained with phalloidin. Seven fields of the bottom of each membrane were captured at 10× magnification in the inverted microscope.

Mean numbers of pores that raTAL cytoplasm crossed against culture medium (ctrl), 6TA2, Six5N6, L929 cells were counted (Figure 8-4). The mean numbers±SEM were 31.3±0.3 (ctrl), 161.7±1.9 (6TA2), 35.3±0.9 (Six5N6), and 26.6±1.2 (L929) (Figure 8-4). raTAL cell showed highly motility towards 6TA2 cells compared to culture medium, reflected in a low p-value (0.0007)(Figure 8-4). raTAL cells did not show significant motility towards Six5N6 (p=0.984) and L929 cells (p=0.982) compared to raTAL towards culture medium (Figure 8-4). The result strongly suggests that raTAL cells showed more attractive motility towards 6TA2 cells than those towards culture medium, Six5N6, or L929 cells.

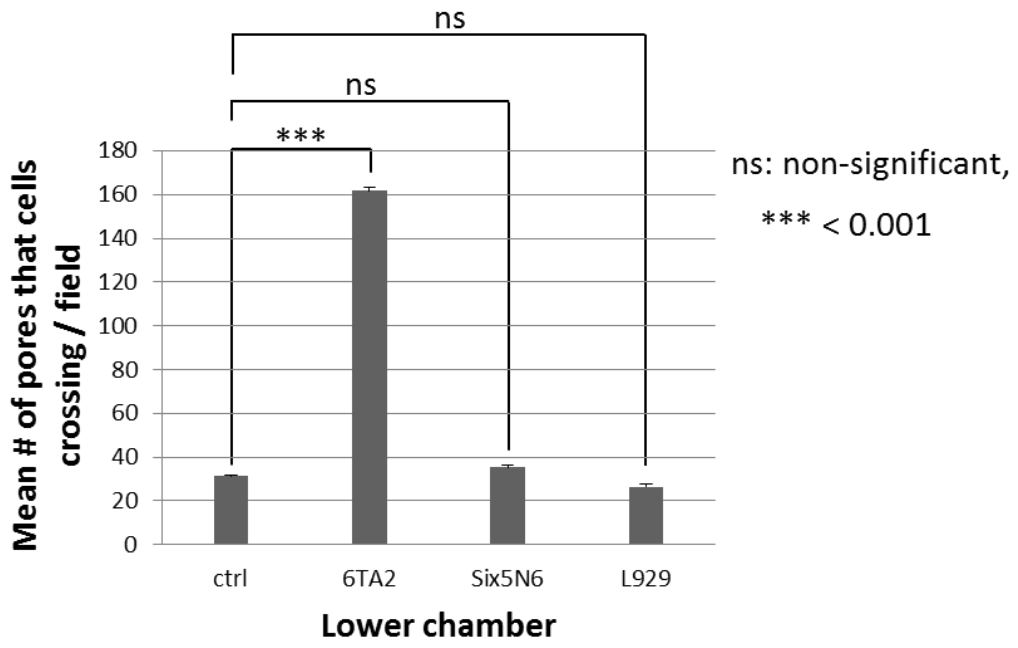

Figure 8-4 Attractive activity of raTAL towards 6TA2 cells. Cell migration assays between raTAL cells versus 6TA2 cell, Six5N6, and L929 cells are shown. raTAL cells were seeded in upper chambers (inserts) and culture medium (ctrl; control), 6TA2, Six5N6 (metanephric mesenchymal cells), and L929 (fibroblasts) were placed or seeded in the lower chambers (24-well plate). The migration assay duration was 4h and stained using FITC-phalloidin. Seven fields for each insert were captured by inverted microscope. The result shows mean numbers ±SEM of pores (ctrl=31.3±0.3, 6TA2=161.7±1.9, Six5N6=35.3±0.9, and L929=26.6±1.2) that raTAL cells crossed per field (the file names of images were randomised before counting to avoid bias). Data are analysed by one way ANOVA and significant p value (0.00023) was obtained. Post hoc Scheffe test were then introduced to compare each two groups, and p values were 0.0007 (ctrl vs 6TA2), 0.984 (ctrl vs Six5N6), and 0.982 (ctrl vs L929). According to the Bonferroni correction, p values less than 0.0125 (0.05/number of groups) were considered as statistically significant.

To test whether molecules secreted from 6TA2 cells were long-lived enough for conditioned medium to be an effective attractant, I performed the migration assay between raTAL cells and 6TA2-conditioned medium. To obtain 6TA2-conditioned medium, 6TA2 cells were pre-incubated overnight at the same density as previous experiments. The 6TA2-conditioned medium was harvested and filtered to remove any remaining 6TA2 cells. The conditioned medium was then used in the assay.

Mean numbers±SEM of pores that raTAL crossed were 22.5±0.5 (ctrl), 102±1.2 (6TA2), and 125.5±2.1 (6TA2-conditioned medium) (Figure 8-5). As shown in the previous result, raTAL cells showed attractive motility towards 6TA2 compared to those towards culture medium (p=0.0002) (Figure 8-5). Notably, raTAL cells also showed chemotactic activity towards 6TA2-conditioned medium, and this chemotactic activity was significantly higher than the activity of raTAL towards culture medium (p=0.0003) (Figure 8-5). Moreover, there was no significant difference between motility of raTAL cells towards 6TA2 cells and that of raTAL cells towards 6TA2-conditioned medium (p=0.078) (Figure 8-5).

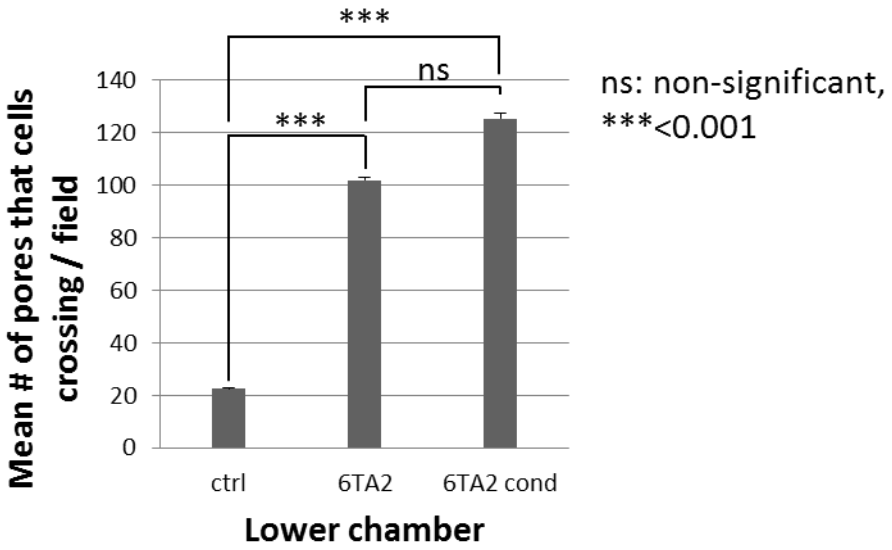

Figure 8-5 Attractive activity of raTAL towards 6TA2-conditioned medium. Cell migration assays between raTAL cells versus 6TA2-conditioned medium (6TA2 cond) are shown. 6TA2-cond was obtained from incubation of 6TA2 cells in a 24-well plate overnight. raTAL cells were seeded in upper chambers (inserts) and culture medium (ctrl; control) and 6TA2 cond were placed in the lower chambers of a 24-well plate to perform migration assay. The migration assay was carried out for 4h and stained using FITC-phalloidin. Seven fields for each insert were captured using an inverted microscope. The result shows mean numbers±SEM of pores (ctrl=22.6±0.5, 6TA2=102±1.2, 6TA2 cond=125.5±2.1) that raTAL cells crossed per field (the file names of images were randomised before counting to avoid bias). P-value from one way ANOVA was 0.0005 (Significant). P-values from Post hoc Tukey HSD test were p=0.0002 (ctrl vs 6TA2), 0.0003 (ctrl vs 6TA2 condition), and 0.078 (6TA2 vs 6TA2 cond). According to the Bonferroni correction, p values less than 0.0167 (0.05/number of groups) were considered as significant.

8.2.4 The motility of raTAL towards 6TA2-conditioned medium diminishes when heparin-binding proteins in the conditioned medium are removed.

In the previous section, the result showed that the motility of raTAL towards 6TA2-conditioned medium (6TA2 cond) increased compared to that towards ctrl. This strongly suggested that the 6TA2 cells were secreting molecule(s) into the medium that might be guiding/attracting raTAL cells. It was therefore imperative to investigate those molecule(s).

Among so many growth factors, it would be almost impossible to directly select target molecule(s) which are implicated in the LoH guidance cue(s). However, it is possible to categorize the molecule(s) by their biochemical characteristics. One of major features of many growth factors is their ability to bind heparin (Conrad, 1998). Therefore, I chose to use the characteristic of heparin-binding for investigating raTAL attracting molecule(s) from 6TA2 cond.

To test whether the molecule(s) to increase the motility of raTAL towards 6TA2 is heparin-binding, I combined a heparin-binding assay with a migration assay. Commercially available Heparin-Separopore Agarose 4B was used. 6TA2 cond was prepared as described in the previous section. 6TA2 cond was incubated with Heprain-Separopore resin (HSr) on a rotator overnight at 4°C. HSr was removed from 6TA2 cond by centrifugation and filtration. HSr-removed 6TA2 cond was used in a migration assay (Figure 8-6). In the migration assay, raTAL culture medium was used as control (ctrl) (Figure 8-5). In addition, Separopore 4B without heparin attached (Matrix; Mt) was incubated in ctrl and 6TA2 cond as a further control (Figure 8-6). The motility of raTAL towards different conditions of medium was evaluated as described in the previous section (Figure 8-6).

Mean numbers of pores ± SEM in each condition were 29.4±1.6 (ctrl), 29.6±1.5 (ctrl-Mt), 27.4±1.2 (ctrl-HSr), 69.7±1.7 (6TA2 cond), 64.7±0.4 (6TA2 cond-Mt), and 37.9±1.5 (6TA2 cond-HSr) (Figure 8-6). There was no significant difference between the motility of raTAL towards ctrl and ctrl-Mt ($p=0.98$) or ctrl-HSr ($p=0.99$) (Figure 8-6). As shown in the previous section, raTAL showed significantly increased motility towards 6TA2 cond compared to ctrl ($p=0.0003$) (Figure 8-6). raTAL motility towards 6TA2 cond-Mt showed a similar result to 6TA2 cond ($p=0.93$) (Figure 8-6). Markedly, the motility of raTAL towards 6TA2 cond-HSr significantly decreased compared to 6TA2 cond ($p=0.0008$) (Figure 8-6). The result indicates that the molecule(s) from 6TA2 cond that attracts raTAL is heparin binding.

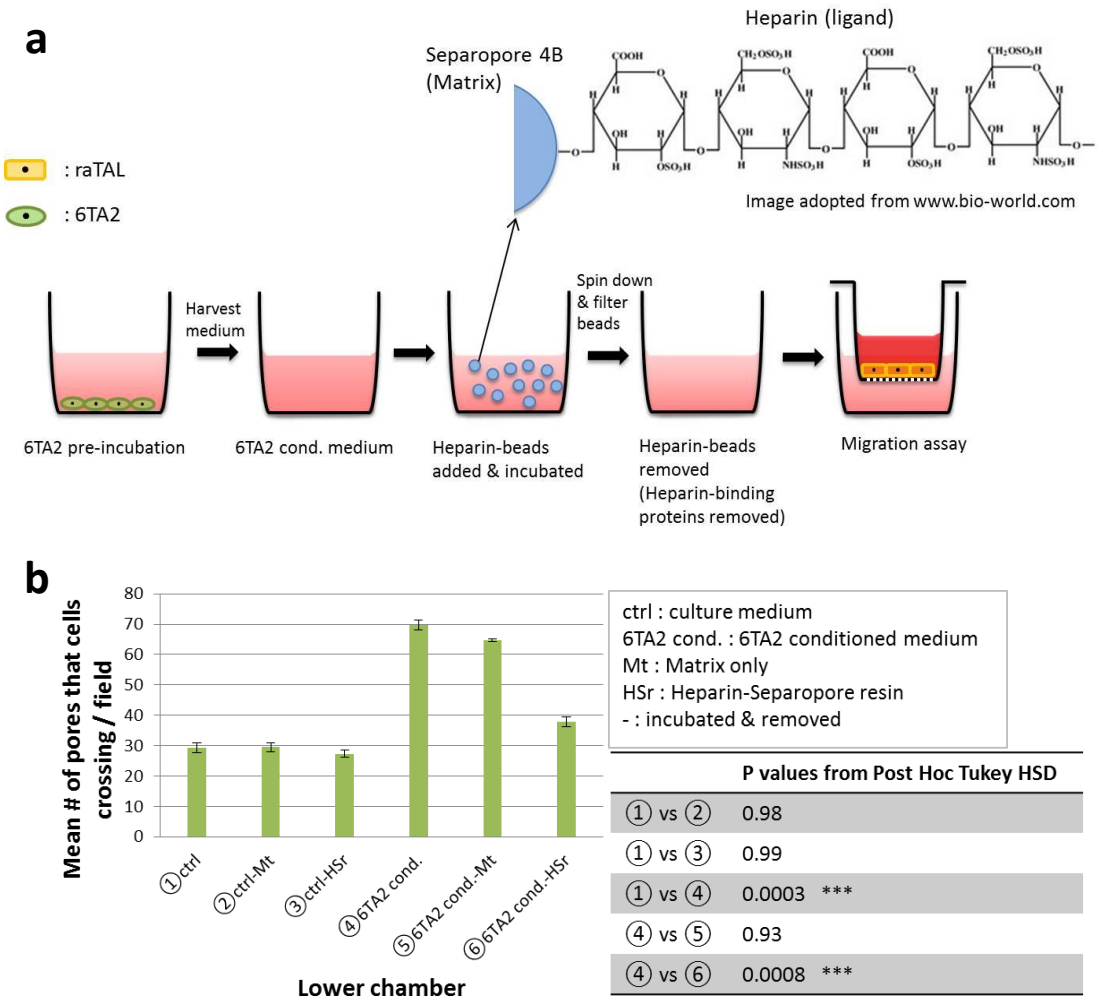

Figure 8-6 raTAL cells are guided by a heparin-binding molecule(s) in 6TA2-conditioned medium. (a) A schematic diagram shows how the heparin-binding assay and migration assay were combined to test whether raTAL-attracting molecule(s) in 6TA2 conditioned medium (6TA2 cond) is heparin binding. 6TA2 cells were pre-incubated overnight and 6TA2 cond was filtered and transferred to a new well. 6TA2 cond was incubated with Heparin-Separopore resin (HSr) and mixed by rotation overnight at 4°C. HSr in 6TA2 cond was removed by centrifugation and filtration. 6TA2 cond with heparin-binding proteins removed was used for migration assay. (b) Mean numbers of pores that raTAL cells crossed towards different conditions were quantified. For ctrl, culture medium for raTAL cells was used. As a control to HSr, Separopore resin (without heparin attached) was employed (shown as Mt; Matrix only). Mean numbers ± SEM are 29.4±1.6 (①), 29.6±1.5 (②), 27.4±1.2 (③), 69.7±1.7 (④), 64.7±0.4 (⑤), and 37.9±1.5 (⑥). P-value from one way ANOVA was 0.0004 (Significant). P-values between each two groups from Post hoc Tukey HSD test were shown in (b) According to the Bonferroni correction, p values less than 0.0083 (0.05/number of groups) were considered as significant.

8.2.5 Heparin-binding proteins isolated from 6TA2-conditioned medium do not increase the attractive motility of raTAL

In the previous section, it was demonstrated that the attractive activity of raTAL towards 6TA2-conditioned medium (6TA2 cond) was decreased when heparin-binding proteins (HBP) were removed. In the inverse way, I tried to confirm that heparin-binding proteins from 6TA2 are sufficient to attract raTAL cells. Instead of removing HBP from 6TA2 cond, HBPs were isolated and added into the lower compartment of migration unit to assess whether raTAL cells still show attractive activity.

To test this, 6TA2 cond was obtained as described before, and it was incubated with Heparin-Separopore resin (HSr) in a rotator overnight (4°C). HSr were centrifuged and the supernatant was removed (Figure 8-7). HSr were placed into a plain medium containing 2.5M NaCl in order to elute HBP from HSr (Figure 8-7). HSr were centrifuged and the supernatant was dialysed against excess of a plain medium to get rid of salts overnight (Figure 8-7). The medium containing HBP was used in a migration assay. As a control, fresh HSr that were not incubated in 6TA2 cond but instead fresh medium were processed in the same way as HSr incubated with 6TA2 cond. In the result, HBP eluted from HSr incubated with 6TA2 cond was named as cHBP and HBP eluted from fresh HSr incubated with fresh medium was named as mHBP (Figure 8-7).

The motility of raTAL towards the lower chamber was quantified by mean number of pores across which 6TA2 cells migrated as described in the previous sections. Migration assays of raTAL towards ctrl (culture medium), ctrl+mHBP, and ctrl+cHBP were carried out (Figure 8-7). The mean numbers ± SEM are 73.4±4.3 (ctrl), 98±4.9 (ctrl+mHBP), and 99.3±3.8 (ctrl+cHBP) (Figure 8-7). However, there were no differences of raTAL motility between any two groups (p value = 0.23 from one way ANOVA) (Figure 8-7).

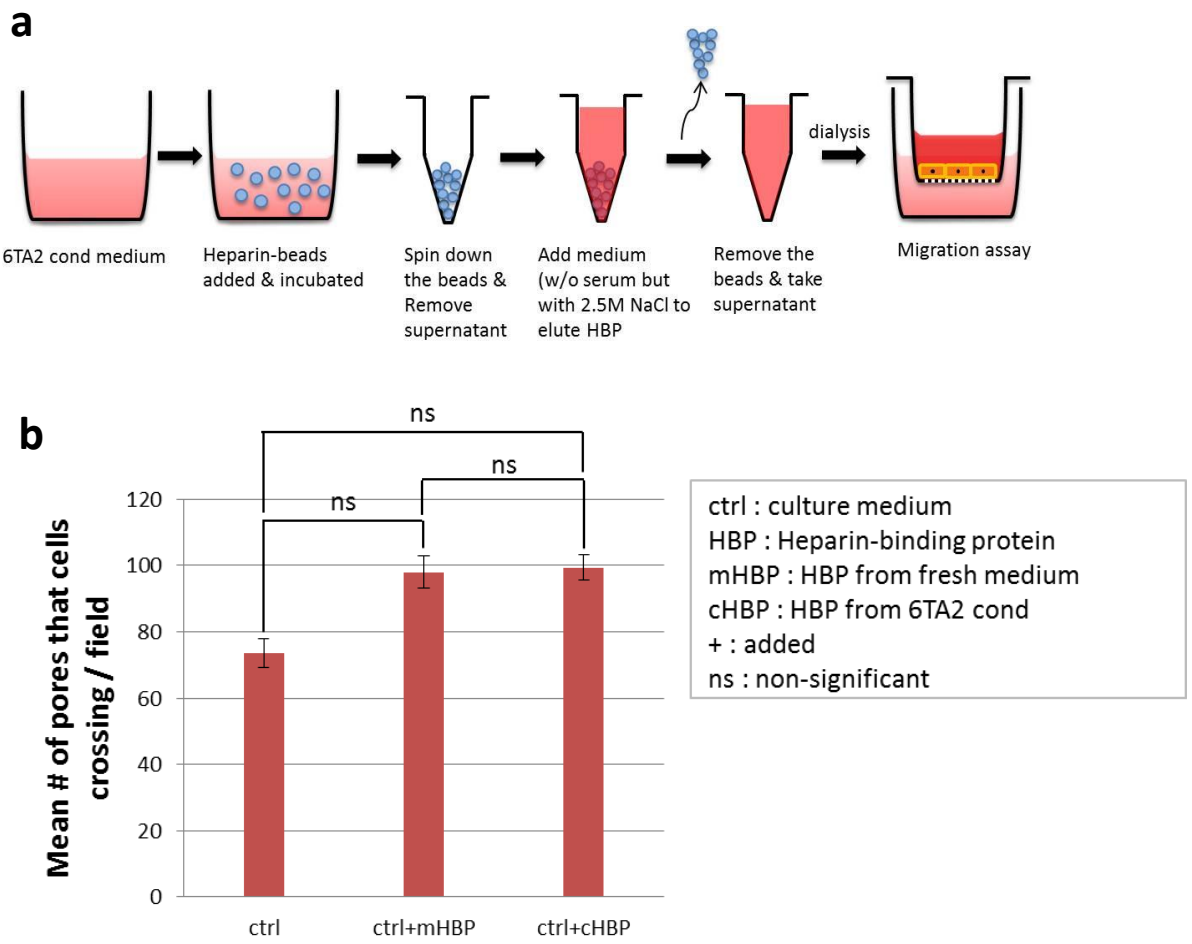

Figure 8-7 Heparin-binding protein (HBP) from 6TA2 conditioned medium did not increase the motility of raTAL. (a) Schematic illustration explains how HBP was isolated from 6TA2 cond. 6TA2 cond was obtained from overnight incubation of 6TA2 cells. 6TA2 cond was incubated with HSr (Heparin-Separopore resin) at a rotator overnight (4°C). HSr was centrifuged and supernatant was removed. Fresh plain medium (without serum) with 2.5M NaCl was added to HSr to isolate HBP. HSr was removed and the medium containing HBP was dialysed overnight against an excess of plain medium to remove salt. Migration assay of raTAL towards culture medium with HBP added was performed and the motility of raTAL was quantified as described in the previous section. (b) As a control to culture medium with HBP added, HSr that was not incubated in 6TA2 cond but rather in fresh medium was used and HBP were isolated as named by mHBP. cHBP indicates HBP isolated from 6TA2 cond. Mean numbers ±SEM are 73.4±4.3 (ctrl), 98±4.9 (ctrl+mHBP), and 99.3±3.8 (ctrl+cHBP). There were no significant differences between groups due to p value (0.23) from one way ANOVA was >0.05.

8.3 Chapter discussion

Whereas there are a number of studies on the cell migration mediated by complex and elaborate cues, cues that navigate the developing LoH towards their destination during renal development are unknown. In Chapter 6 and 7, I showed that unidentified molecule(s) secreted by the UB and the embryonic spinal cord attracted directional growth of the LoH, and I stressed the need of a high-throughput assay for searching for guiding molecule(s). In this chapter, I showed that the cell line representing the developing LoH apex displayed increased motility (chemotactic activity) towards the cell line representing the UB as if the LoH attracted towards the UB at a tissue level. Finally, I showed that one of LoH-guiding molecules is heparin binding.

8.3.1 A new method to quantify cell motility in cell migration assays

The transwell membrane with the largest pore size (8 μm) did not allow raTAL cells to completely cross the membrane. raTAL cells have a enormous size (>40μm) or/and have a growing pattern that proliferates as a group and later construct dome formation (Eng et al., 2007), and thereby hindered their complete migration through the membrane pores. Hence, I decided to count the number of pores across which the cytoplasm of raTAL crossed rather than the number of cell nuclei. The cytoplasm was visualized by phalloidin staining, which stains F-actins. Regarding the manner of quantifying cell motility by its cytoplasm, this method might provide a more accurate way of measuring cell motility, since one of mechanisms of cell migration can be described by actin polymerization in the leading edge of cells (Mitchison and Cramer, 1996, Pollard and Borisy, 2003). Therefore, this method is a useful alternative when one is unable to visualize the cell nucleus after the cell migration assay. However, it should not be ignored that actual movements of the cytoplasm could be an effect of raTAL chemokinesis. For accurate results, the transwell membrane with larger pore size (>8 μm) might resolve this issue.

8.3.2 Heparin-binding molecule(s) from 6TA2-conditioned medium is required to attract raTAL cells

To test whether raTAL cells showed attractive activity towards 6TA2 cells, cell migration assays were carried out using raTAL and 6TA2 cell lines. The motility of raTAL towards 6TA2-conditioned medium (6TA2 cond) was similar to motility towards 6TA2. In other words, raTAL motility can respond to soluble secreted molecule(s) from 6TA2 cells and these molecules are long-lived. Therefore, the next step was to study those secreted molecules.

Isolating candidate molecule(s) from hundreds of thousands of other molecules at once is almost impossible. However, it was possible to classify candidate molecule(s) in groups based on their biochemical properties. One of the biochemical features of a candidate molecule could be whether it can bind to heparin. In fact, many growth factors (cytokines) are heparin-binding (Conrad, 1998). Conversely, there are also non heparin-binding growth factors that can be excluded from growth factors secreted by the UB and the spinal cord (Table 8-1).

Gene symbol	Gene Name	Non Heparin-binding (references)
EGF	Epidermal growth factor	(Zhao et al., 2010)
GM-CSF	Granulocyte macrophage colony-stimulating factor	(Gordon et al., 1989)
IGF-I	Insulin like growth factor I	(Liekens et al., 2001)
TGF-α	Transforming growth factor alpha	(Higashiyama et al., 1993)
TGF-β3	Transforming growth factor beta 3	(Lyon et al., 1997)
$VEGF_{121}$	Vascular endothelial growth factor 121	(Houck et al., 1992)

Table 8-1 Examples of non-heparin-binding growth factors.

By applying a heparin-binding assay to a cell migration assay, I tested whether key molecule(s) causing increased motility of raTAL were heparin-binding. Eliminating heparin-binding proteins (HBP) from 6TA2 cond resulted in lower motility of raTAL compared to raTAL towards normal 6TA2 cond, suggesting that the candidates have a heparin-binding domain. Thus, I selected heparin-binding proteins from the candidates listed in Table 7-1 (Table 8-2). Some candidates including Bmp-7, Wnt-4, and Wnt7b are listed as having affinity with heparin (Table 8-2).

Gene Symbol	Gene Name	Heparin-binding (references)
Bmp7	bone morphogenetic protein 7	Yes (Gandhi and Mancera, 2012)
Efna4	ephrin A4	Unknown
Jag1	jagged 1	Unknown
Kitl	kit ligand	Unknown
Mdk	midkine	Yes (Muramatsu, 2010)
Pdgfc	platelet-derived growth factor, C polypeptide	Yes (Ori et al., 2009)
Pkd2	polycystic kidney disease 2	Unknown
Ptn	pleiotrophin	Yes (Singh and Srivastava, 2012)
Sdcbp	syndecan binding protein	Unknown but probable
Sema3c	sema domain, immunoglobulin domain (Ig), short basic domain, secreted, (semaphorin) 3C	Yes (Esselens et al., 2010)
Sema5a	sema domain, seven thrombospondin repeats (type 1 and type 1-like), transmembrane domain (TM) and short cytoplasmic domain, (semaphorin) 5A	Unknown but possible
Slit2	slit homolog 2 (Drosophila)	Yes (Seiradake et al., 2009)
Wnt4	wingless-related MMTV integration site 4	Yes (Zhong et al., 2007)
Wnt7b	wingless-related MMTV integration site 7B	Yes (Zhong et al., 2007)

Table 8-2 Examples of candidate molecules with a heparin-binding property. The candidates can bind to heparin are coloured by yellow.

Given that molecule(s) increase the raTAL motility can bind to heparin, it should have been possible to elute them. However, raTAL did not show any increased motility towards HBP added medium compared to raTAL towards the same medium without HBP added. This might suggest that attraction of raTAL might be driven by the combined action of more than one molecule secreted by 6TA2 cells, but not all of these molecules bind heparin (Figure 8-8). It is also possible that the molecule was damaged (conformationally) by the high-salt elution wash, or that it was a very small peptide, small enough to be lost during dialysis. The apparent range of spatially, from the medulla to the cortex, does suggest that a small peptide is a reasonable candidate.

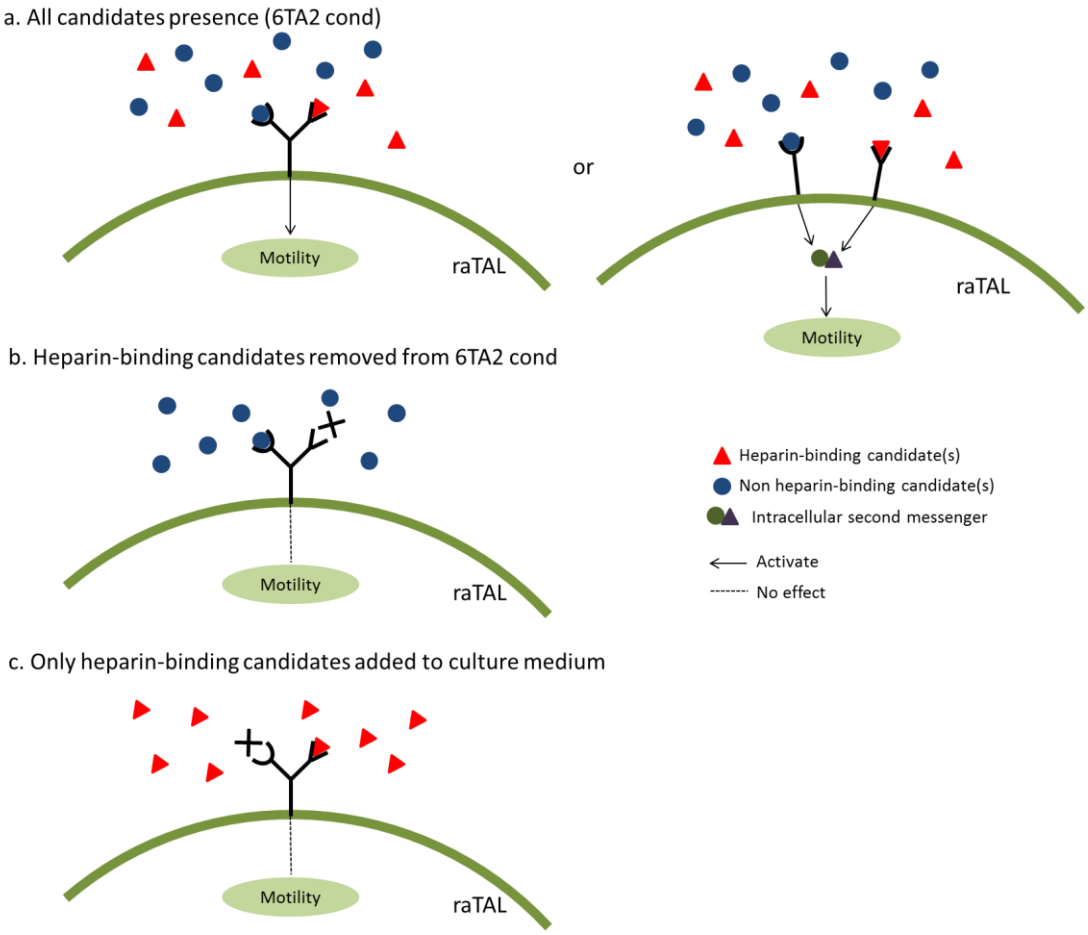

Figure 8-8 The candidate attractant for raTAL might consist of more than one molecule. The results from cell migration assays were simply described in diagrams. (a) Two possible signalling pathways were simply described. The first case is to have one receptor for two different ligands to activate the motility. The second case is to have two different receptors and their second messenger molecules act as a cofactor to activate the motility. (b) Removal of heparin-binding candidates resulted in no effect on raTAL motility. (c) raTAL did not show increased motility towards the culture medium having heparin-binding candidates.

9 Chapter 9 Overall conclusions

9.1 Conclusions

The results in each of the chapters have been discussed at the end of each chapter. The aim of this chapter is to briefly tie these results together to consider what more general conclusions can be made.

In order for the kidney to operate normally, each segment of each nephron has to localise to its correct position. Among a number of guiding processes that take place during renal development, I focused on loop of Henle (LoH) guidance to address how the middle of a bent tube navigates. This problem arose from the fact that, while mechanisms that underlie guidance of the end of tubes (e.g. angiogenesis) are well studied, how an apex of a U-shaped tube navigates is not understood. As the LoH has a hairpin structure, I chose the LoH to address this question. In order to understand the cue(s) to direct orientating the LoH, both *in vivo* and *ex vivo* studies were performed and their major findings are listed below.

- LoH become more centripetal as they mature *in vivo*.
- The low-volume system is a reliable culture method to study LoH.
- The ureteric bud / collecting duct system as well as the embryonic spinal cord are possible sources of molecules that can guide LoH orientation.
- One of guiding molecules to attract raTAL is heparin-binding.

9.1.1 The loop of Henle navigates by chemotaxis

There are several types of guidance cues to direct solitary / collective cell migration as discussed in section 1.2.2 and 1.2.3. Among those cues, I propose that chemotaxis probably controls the LoH orientation. This conclusion is supported by the result obtained from a cell migration assay. In the assay, I confirmed that the loops cells (raTAL) are attracted to diffusible and long-lived molecules secreted by the ureteric bud / collecting duct cells (6TA2) as shown in chapter 8. Moreover, the cut-and-paste experiment stresses the LoH is orientated by chemotaxis. The LoH was still attracted towards the medulla although there was a gap between the LoH and the medulla caused by the cutting and pasting the cortex (see chapter 6).

Although I have not ruled out any other cues for the LoH guidance, it is possible that more than one cue orientate the LoH. In general, multiple cues simultaneously direct cells' migration and these cues often increase efficiency for cells to move (Lara Rodriguez and Schneider, 2013). Endothelial cells' migration during angiogenesis is a great example of multiple cues directing tube locomotion (Lamalice et al., 2007). In addition to chemotaxis, haptotaxis and durotaxis also regulate endothelial cell's migration during angiogenesis (Lamalice et al., 2007). Similarly, I speculate that other cues accompanying chemotaxis might navigate the LoH.

9.1.2 Maturing collecting duct as a source to guide Henle's loops?

One of important findings in this thesis is that the LoH orientate towards developing ureteric bud / collecting duct system in cultures. Based on another critical finding that one of cues to navigate the LoH orientation is chemotaxis, I suggest two possible ways for maturing collecting duct system to guide the LoH. The first is that both the ureteric stalk and the collecting duct secrete the same kind of LoH guiding molecules but the most maturing collecting duct produces them much more. Thus, the LoH are attracted to the oldest collecting duct. Secondly, it is also possible that not the collecting duct but the mesenchyme surrounding it is the source to secrete LoH guiding molecules to navigate the LoH orientation. However, this case less possibly occur since Six5N6 (mesenchymal cell line) did not seem to attract raTAL as shown in chapter 8.

Therefore, guiding molecules are probably expressed in a gradient along the collecting duct. For instance, Wnt-7b can be a candidate since it satisfies several requirements as LoH guiding molecules. Firstly, Wnt-7b expressed in a gradient (more strongly expressed in the medullary collecting duct than the cortical collecting duct) along the collecting duct (Yu et al., 2009) (www.gudmap.org). Secondly, Wnt-7b is also expressed by the embryonic spinal cord (Parr et al., 1993, Ulloa and Marti, 2010) that I found it as an alternative source to attract the LoH (chapter 7). Third, Wnt-7b is known as a heparin-binding protein (Zhong et al., 2007). More importantly, Yu el al. demonstrated Wnt-7b as an essential factor for the LoH elongation using Wnt-7b lacking mutant mice (Yu et al., 2009). Thus, I postulate that Wnt-7b also plays direction-finding role in the LoH in addition to its role in elongation. This orientating LoH process by Wnt-7b might be mediated by orientated cell division as if the cortico-medullary axis is established by a Wnt7b-related pathway acting on the orientated

cell division (Yu et al., 2009). Therefore, it would be interesting to test a role of Wnt-7b in the LoH orientation.

9.2 Future prospects

9.2.1 Further studies on analyzing the candidate molecules

As discussed in the previous section, it would be interesting to assess whether Wnt-7b acts in LoH orientation. To test if Wnt-7b is required for LoH orientation, Wnt-7b can be blocked by siRNA or function blocking antibodies after the LoH form in cultures.

If Wnt-7b does not turn out to be the LoH guiding molecules, there would be more work in identifying candidates that attract raTAL for future research. In order to test whether the candidates are destroyed during the salt-based elution step or whether both HBP and non-HBP are required to attract raTAL, it would be interesting to mix HBP (derived from 6TA2-conditioned medium) and the supernatant (HBP-removed 6TA2-conditioned medium). If the mixed solution attracts raTAL, the candidates are indeed consists of HBP and non-HBP and both are required for raTAL attraction. If the mix still does not attract raTAL, HBP are destroyed or are small peptides that can easily be lost during the elution or dialysis.

Subsequently, protein sequencing (e.g. mass spectrometry) of molecules eluted from heparin-binding molecules would provide a list of candidates. In addition to this, since I showed that excreted molecules from 6TA2 cells can attract raTAL cells but that molecules from other cell lines (Six5N6, L929) cannot, two-dimensional gel electrophoresis (2DE) can be used here. For instance, 6TA2 cells are labelled with ^{3}H amino acids, and Six5N6 or L929 cells are labelled with ^{35}S amino acids. Then, run a 2DE of the mix of the conditioned media and find spots that correspond to ^{3}H. As an alternative method, aliquots of 6TA2-conditioned medium can be analysed by the size fractionation technique such as size-exclusion chromatography. In these ways, useful information such as molecular weight and/or isoelectric point of the candidates (the bioactive molecules) can be determined.

Inversely, raTAL receptors that recognise ligands secreted by 6TA2 but not by other cells can be investigated after performing cell migration assays. This can be done by detecting phosphorylated receptors. For instance, dual staining methods using an anti-target antibody and a phospho-specific antibody can be used.

Once LoH guiding molecules are found, it would be interesting to test the function of those molecules in a culture system. By inhibiting target molecules using a small interference RNA technique and function blocking antibodies, it would be possible to confirm that the molecules actually guide the LoH orientation.

9.2.2 Tracing cell proliferation in the developing loop of Henle

It is also intriguing to assess cell proliferation of the developing LoH. In fact, there is a lack of study defining the growth region of the developing LoH although Cha et al. showed that the corticomedullary junction is the growth zone of the LoH in rat pups (Cha et al., 2001). Therefore, detection of cell proliferation such as 5-bromo-2'-deoxy-uridine (BrdU) labeling might be a key experiment to check the correlation between the LoH direction and their elongation.

In this thesis, I have studied the guidance cues of developing LoH. Although some of the findings might lead to the idea that guidance cue(s) that direct the LoH orientation are more complicated than expected, this thesis demonstrates that the LoH is an excellent model to study guidance cues of the middle of a U-shaped tube. In addition, the findings will provide useful information in our understanding of orientating LoH, which is one of the essential components for renal function.

10 Chapter 10 References

ABRAHAMSON, D. R. 2009. Development of kidney glomerular endothelial cells and their role in basement membrane assembly. *Organogenesis,* 5**,** 275-87.

AMAN, A. & PIOTROWSKI, T. 2010. Cell migration during morphogenesis. *Developmental biology,* 341**,** 20-33.

ANDREWS, W. D., BARBER, M. & PARNAVELAS, J. G. 2007. Slit-Robo interactions during cortical development. *Journal of anatomy,* 211**,** 188-98.

ARIMA, S., NISHIYAMA, K., KO, T., ARIMA, Y., HAKOZAKI, Y., SUGIHARA, K., KOSEKI, H., UCHIJIMA, Y., KURIHARA, Y. & KURIHARA, H. 2011. Angiogenic morphogenesis driven by dynamic and heterogeneous collective endothelial cell movement. *Development,* 138**,** 4763-76.

ATTERBURY, R. R. 1923. Development of the metanephric anlage of chick in allantoic grafts. *American Journal of Anatomy,* 31**,** 409-437.

AUSPRUNK, D. H. & FOLKMAN, J. 1977. Migration and proliferation of endothelial cells in preformed and newly formed blood vessels during tumor angiogenesis. *Microvascular research,* 14**,** 53-65.

BACHMANN, S., METZGER, R. & BUNNEMANN, B. 1990. Tamm-Horsfall protein-mRNA synthesis is localized to the thick ascending limb of Henle's loop in rat kidney. *Histochemistry,* 94**,** 517-23.

BADERCA, F., LIGHEZAN, R., DEMA, A., ALEXA, A. & RAICA, M. 2006. Immunohistochemical expression of VEGF in normal human renal parenchyma. *Romanian journal of morphology and embryology = Revue roumaine de morphologie et embryologie,* 47**,** 315-22.

BAGNARD, D., THOMASSET, N., LOHRUM, M., PUSCHEL, A. W. & BOLZ, J. 2000. Spatial distributions of guidance molecules regulate chemorepulsion and chemoattraction of growth cones. *The Journal of neuroscience : the official journal of the Society for Neuroscience,* 20**,** 1030-5.

BARKER, N., ROOKMAAKER, M. B., KUJALA, P., NG, A., LEUSHACKE, M., SNIPPERT, H., VAN DE WETERING, M., TAN, S., VAN ES, J. H., HUCH, M., POULSOM, R., VERHAAR, M. C., PETERS, P. J. & CLEVERS, H. 2012. Lgr5(+ve) stem/progenitor cells contribute to nephron formation during kidney development. *Cell reports,* 2**,** 540-52.

BARKER, N., VAN ES, J. H., KUIPERS, J., KUJALA, P., VAN DEN BORN, M., COZIJNSEN, M., HAEGEBARTH, A., KORVING, J., BEGTHEL, H., PETERS, P. J. & CLEVERS, H. 2007. Identification of stem cells in small intestine and colon by marker gene Lgr5. *Nature,* 449**,** 1003-7.

BASSON, M. A., AKBULUT, S., WATSON-JOHNSON, J., SIMON, R., CARROLL, T. J., SHAKYA, R., GROSS, I., MARTIN, G. R., LUFKIN, T., MCMAHON, A. P., WILSON, P. D., COSTANTINI, F. D., MASON, I. J. & LICHT, J. D. 2005. Sprouty1 is a critical regulator of GDNF/RET-mediated kidney induction. *Developmental cell,* 8**,** 229-39.

BASSON, M. A., WATSON-JOHNSON, J., SHAKYA, R., AKBULUT, S., HYINK, D., COSTANTINI, F. D., WILSON, P. D., MASON, I. J. & LICHT, J. D. 2006. Branching morphogenesis of the ureteric epithelium during kidney development is coordinated by the opposing functions of GDNF and Sprouty1. *Developmental biology,* 299**,** 466-77.

BATTYE, R., STEVENS, A. & JACOBS, J. R. 1999. Axon repulsion from the midline of the Drosophila CNS requires slit function. *Development,* 126**,** 2475-81.

BOSGRAAF, L., RUSSCHER, H., SMITH, J. L., WESSELS, D., SOLL, D. R. & VAN HAASTERT, P. J. 2002. A novel cGMP signalling pathway mediating myosin phosphorylation and chemotaxis in Dictyostelium. *The EMBO journal,* 21**,** 4560-70.

BOYDEN, S. 1962. The chemotactic effect of mixtures of antibody and antigen on polymorphonuclear leucocytes. *The Journal of experimental medicine,* 115**,** 453-66.

BRAVO-CORDERO, J. J., MAGALHAES, M. A., EDDY, R. J., HODGSON, L. & CONDEELIS, J. 2013. Functions of cofilin in cell locomotion and invasion. *Nature reviews. Molecular cell biology,* 14**,** 405-15.

BREIER, G., ALBRECHT, U., STERRER, S. & RISAU, W. 1992. Expression of vascular endothelial growth factor during embryonic angiogenesis and endothelial cell differentiation. *Development,* 114**,** 521-32.

BREMER, M. 2010. *Statistics at the bench : a step-by-step handbook for biologists*, Cold Spring Harbor Laboratory Press.

BULGER, R. E., CRONIN, R. E. & DOBYAN, D. C. 1979. Survey of the morphology of the dog kidney. *The Anatomical record,* 194**,** 41-65.

BURG, M. B. 1982. Thick ascending limb of Henle's loop. *Kidney international,* 22**,** 454-64.

BUTLER, S. J. & DODD, J. 2003. A role for BMP heterodimers in roof plate-mediated repulsion of commissural axons. *Neuron,* 38**,** 389-401.

CARROLL, M. A., MCGIFF, J. C. & FERRERI, N. R. 2003. Products of arachidonic acid metabolism. *Methods in molecular medicine,* 86**,** 385-97.

CARROLL, T. J., PARK, J. S., HAYASHI, S., MAJUMDAR, A. & MCMAHON, A. P. 2005. Wnt9b plays a central role in the regulation of mesenchymal to epithelial transitions underlying organogenesis of the mammalian urogenital system. *Developmental cell,* 9**,** 283-92.

CARTER, S. B. 1967. Haptotaxis and the mechanism of cell motility. *Nature,* 213**,** 256-60.

CAWSTON, T. E. & YOUNG, D. A. 2010. Proteinases involved in matrix turnover during cartilage and bone breakdown. *Cell and tissue research,* 339**,** 221-35.

CEBRIAN, C., BORODO, K., CHARLES, N. & HERZLINGER, D. A. 2004. Morphometric index of the developing murine kidney. *Developmental dynamics : an official publication of the American Association of Anatomists,* 231**,** 601-8.

CHA, J. H., KIM, Y. H., JUNG, J. Y., HAN, K. H., MADSEN, K. M. & KIM, J. 2001. Cell proliferation in the loop of henle in the developing rat kidney. *Journal of the American Society of Nephrology : JASN,* 12**,** 1410-21.

CHANG, P. C., SULIK, G. I., SOONG, H. K. & PARKINSON, W. C. 1996. Galvanotropic and galvanotaxic responses of corneal endothelial cells. *Journal of the Formosan Medical Association = Taiwan yi zhi,* 95**,** 623-7.

CHAREST, P. G. & FIRTEL, R. A. 2010. "TORCing" neutrophil chemotaxis. *Developmental cell,* 19**,** 795-6.

CHARRON, F., STEIN, E., JEONG, J., MCMAHON, A. P. & TESSIER-LAVIGNE, M. 2003. The morphogen sonic hedgehog is an axonal chemoattractant that collaborates with netrin-1 in midline axon guidance. *Cell,* 113**,** 11-23.

CHEN, H. C. 2005. Boyden chamber assay. *Methods in molecular biology,* 294**,** 15-22.

CHEN, J. K., TAIPALE, J., COOPER, M. K. & BEACHY, P. A. 2002. Inhibition of Hedgehog signaling by direct binding of cyclopamine to Smoothened. *Genes & development,* 16**,** 2743-8.

CHENG, H. T., KIM, M., VALERIUS, M. T., SURENDRAN, K., SCHUSTER-GOSSLER, K., GOSSLER, A., MCMAHON, A. P. & KOPAN, R. 2007. Notch2, but not Notch1, is required for proximal fate acquisition in the mammalian nephron. *Development,* 134**,** 801-11.

CHENG, H. T., MINER, J. H., LIN, M., TANSEY, M. G., ROTH, K. & KOPAN, R. 2003. Gamma-secretase activity is dispensable for mesenchyme-to-epithelium transition but required for podocyte and proximal tubule formation in developing mouse kidney. *Development,* 130**,** 5031-42.

CHO, E. A., PATTERSON, L. T., BROOKHISER, W. T., MAH, S., KINTNER, C. & DRESSLER, G. R. 1998. Differential expression and function of cadherin-6 during renal epithelium development. *Development,* 125**,** 803-12.

CHO, E. A. D., G. R. 2003. Formation and Development of Nephrons. *In:* PETER D. VIZE, A. S. W., JONATHAN B.L. BARD (ed.) *The Kideny: From Normal Development to Congenital Disease.* Elsevier Inc.

CHRISTENSEN, E. I. & GBUREK, J. 2004. Protein reabsorption in renal proximal tubule-function and dysfunction in kidney pathophysiology. *Pediatric nephrology,* 19**,** 714-21.

CLUZEL, C., SALTEL, F., LUSSI, J., PAULHE, F., IMHOF, B. A. & WEHRLE-HALLER, B. 2005. The mechanisms and dynamics of (alpha)v(beta)3 integrin clustering in living cells. *The Journal of cell biology,* 171**,** 383-92.

CONDEELIS, J. 1993. Life at the leading edge: the formation of cell protrusions. *Annual review of cell biology,* 9**,** 411-44.

CONRAD, H. E. 1998. *Heparin-binding proteins [electronic resource] / H. Edward Conrad*, San Diego : Academic Press, [1998], ©1998.

COOPER, J. A. 2013. Cell biology in neuroscience: mechanisms of cell migration in the nervous system. *The Journal of cell biology,* 202**,** 725-34.

COOPER, J. A. & SEPT, D. 2008. New insights into mechanism and regulation of actin capping protein. *International review of cell and molecular biology,* 267**,** 183-206.

COOPER, M. K., PORTER, J. A., YOUNG, K. E. & BEACHY, P. A. 1998. Teratogen-mediated inhibition of target tissue response to Shh signaling. *Science,* 280**,** 1603-7.

COOPER, M. S. & KELLER, R. E. 1984. Perpendicular orientation and directional migration of amphibian neural crest cells in dc electrical fields. *Proceedings of the National Academy of Sciences of the United States of America,* 81**,** 160-4.

COSTANTINI, F. 2010. GDNF/Ret signaling and renal branching morphogenesis: From mesenchymal signals to epithelial cell behaviors. *Organogenesis,* 6**,** 252-62.

COSTANTINI, F. 2012. Genetic controls and cellular behaviors in branching morphogenesis of the renal collecting system. *Wiley interdisciplinary reviews. Developmental biology,* 1**,** 693-713.

COSTANTINI, F. & KOPAN, R. 2010. Patterning a complex organ: branching morphogenesis and nephron segmentation in kidney development. *Developmental cell,* 18**,** 698-712.

CRAMER, L. P. 2013. Mechanism of cell rear retraction in migrating cells. *Current opinion in cell biology,* 25**,** 591-9.

CURTIS, A. & WILKINSON, C. 1997. Topographical control of cells. *Biomaterials,* 18**,** 1573-83.

DAVIDSON, A. J. 2008. Mouse kidney development. *StemBook.* Cambridge (MA).

DAVIES, J., LYON, M., GALLAGHER, J. & GARROD, D. 1995. Sulphated proteoglycan is required for collecting duct growth and branching but not nephron formation during kidney development. *Development,* 121**,** 1507-17.

DAVIES, J. A. 2010. The embryonic kidney: isolation, organ culture, immunostaining and RNA interference. *Methods in molecular biology,* 633**,** 57-69.

DAVIES, J. A. 2013a. Guidance by Chemotaxis. *Mecahnisms of Morphogenesis.* Second ed.: Elsevier Ltd.

DAVIES, J. A. 2013b. Guidance by Contact. *Mechanisms of Morphogenesis.* Second ed.: Elsevier Ltd.

DAVIES, J. A. & CHANG, C. H. 2013. Engineering kidneys from simple cell suspensions: an exercise in self-organization. *Pediatric nephrology*.

DAVIES, J. A. & DAVEY, M. G. 1999. Collecting duct morphogenesis. *Pediatric nephrology,* 13**,** 535-41.

DAVIES, J. A. & GARROD, D. R. 1995. Induction of early stages of kidney tubule differentiation by lithium ions. *Developmental biology,* 167**,** 50-60.

DEVREOTES, P. N. & ZIGMOND, S. H. 1988. Chemotaxis in eukaryotic cells: a focus on leukocytes and Dictyostelium. *Annual review of cell biology,* 4**,** 649-86.

DIETERICH, H. J., BARRETT, J. M., KRIZ, W. & BULHOFF, J. P. 1975. The ultrastructure of the thin loop limbs of the mouse kidney. *Anatomy and embryology,* 147**,** 1-18.

DRESSLER, G. R. 2009. Advances in early kidney specification, development and patterning. *Development,* 136**,** 3863-74.

EDWARDS, D. C., SANDERS, L. C., BOKOCH, G. M. & GILL, G. N. 1999. Activation of LIM-kinase by Pak1 couples Rac/Cdc42 GTPase signalling to actin cytoskeletal dynamics. *Nature cell biology,* 1**,** 253-9.

ENG, B., MUKHOPADHYAY, S., VIO, C. P., PEDRAZA, P. L., HAO, S., BATTULA, S., SEHGAL, P. B., MCGIFF, J. C. & FERRERI, N. R. 2007. Characterization of a long-term rat mTAL cell line. *American journal of physiology. Renal physiology,* 293**,** F1413-22.

ERICSON, J., BRISCOE, J., RASHBASS, P., VAN HEYNINGEN, V. & JESSELL, T. M. 1997. Graded sonic hedgehog signaling and the specification of cell fate in the ventral neural tube. *Cold Spring Harbor symposia on quantitative biology,* 62**,** 451-66.

ESSELENS, C., MALAPEIRA, J., COLOME, N., CASAL, C., RODRIGUEZ-MANZANEQUE, J. C., CANALS, F. & ARRIBAS, J. 2010. The cleavage of semaphorin 3C induced by ADAMTS1 promotes cell migration. *The Journal of biological chemistry,* 285**,** 2463-73.

FENTON, R. A. & KNEPPER, M. A. 2007. Urea and renal function in the 21st century: insights from knockout mice. *Journal of the American Society of Nephrology : JASN,* 18**,** 679-88.

FORSYTHE, J. A., JIANG, B. H., IYER, N. V., AGANI, F., LEUNG, S. W., KOOS, R. D. & SEMENZA, G. L. 1996. Activation of vascular endothelial growth factor gene transcription by hypoxia-inducible factor 1. *Molecular and cellular biology,* 16**,** 4604-13.

FRIEDL, P. & GILMOUR, D. 2009. Collective cell migration in morphogenesis, regeneration and cancer. *Nature reviews. Molecular cell biology,* 10**,** 445-57.

FRIEDL, P. & WEIGELIN, B. 2008. Interstitial leukocyte migration and immune function. *Nature immunology,* 9**,** 960-9.

FUNAMOTO, S., MEILI, R., LEE, S., PARRY, L. & FIRTEL, R. A. 2002. Spatial and temporal regulation of 3-phosphoinositides by PI 3-kinase and PTEN mediates chemotaxis. *Cell,* 109**,** 611-23.

GANDHI, N. S. & MANCERA, R. L. 2012. Prediction of heparin binding sites in bone morphogenetic proteins (BMPs). *Biochimica et biophysica acta,* 1824**,** 1374-81.

GANEVA, V., UNBEKANDT, M. & DAVIES, J. A. 2011. An improved kidney dissociation and reaggregation culture system results in nephrons arranged organotypically around a single collecting duct system. *Organogenesis,* 7**,** 83-7.

GEORGAS, K., RUMBALLE, B., VALERIUS, M. T., CHIU, H. S., THIAGARAJAN, R. D., LESIEUR, E., ARONOW, B. J., BRUNSKILL, E. W., COMBES, A. N., TANG, D., TAYLOR, D., GRIMMOND, S. M., POTTER, S. S., MCMAHON, A. P. & LITTLE, M. H. 2009. Analysis of early nephron patterning reveals a role for distal RV proliferation in fusion to the ureteric tip via a cap mesenchyme-derived connecting segment. *Developmental biology,* 332**,** 273-86.

GERHARDT, H. 2008. VEGF and endothelial guidance in angiogenic sprouting. *Organogenesis,* 4**,** 241-6.

GERHARDT, H., GOLDING, M., FRUTTIGER, M., RUHRBERG, C., LUNDKVIST, A., ABRAMSSON, A., JELTSCH, M., MITCHELL, C., ALITALO, K., SHIMA, D. & BETSHOLTZ, C. 2003. VEGF

guides angiogenic sprouting utilizing endothelial tip cell filopodia. *The Journal of cell biology,* 161**,** 1163-77.

GHYSEN, A. & DAMBLY-CHAUDIERE, C. 2007. The lateral line microcosmos. *Genes & development,* 21**,** 2118-30.

GILBERT, S. F. 2013. *Developmental Biology*, Sinauer Associates Inc., U. S.

GLUECKSOHN-WAELSCH, S. & ROTA, T. R. 1963. Development in organ tissue culture of kidney rudiments from mutant mouse embryos. *Developmental biology,* 6**,** 432-44.

GORDON, M. Y., BEARPARK, A. D., CLARKE, D. & HEALY, L. E. 1989. Matrix Glycoproteins May Regulate the Local Concentrations of Different Hemopoietic Growth Factors. *In:* BAUM, S. J., DICKE, K. A., LOTZOVÁ, E. & PLUZNIK, D. H. (eds.) *Experimental Hematology Today—1988.* Springer New York.

GRIESHAMMER, U., LE, M., PLUMP, A. S., WANG, F., TESSIER-LAVIGNE, M. & MARTIN, G. R. 2004. SLIT2-mediated ROBO2 signaling restricts kidney induction to a single site. *Developmental cell,* 6**,** 709-17.

GROBSTEIN, C. 1953a. Inductive epitheliomesenchymal interaction in cultured organ rudiments of the mouse. *Science,* 118**,** 52-5.

GROBSTEIN, C. 1953b. Morphogenetic interaction between embryonic mouse tissues separated by a membrane filter. *Nature,* 172**,** 869-70.

GROBSTEIN, C. 1955. Inductive interaction in the development of the mouse metanephros. *Journal of Experimental Zoology,* 130**,** 319-339.

GROBSTEIN, C. 1956. Trans-filter induction of tubules in mouse metanephrogenic mesenchyme. *Experimental cell research,* 10**,** 424-40.

HALLGRIMSSON, B., BENEDIKTSSON, H., AND VIZE, P. D. 2003. Anatomy and Histology of the Human Urinary System. *In:* VIZE, C., WOOLF, A. S, AND BARD, J. B. L. (ed.) *The Kidney: From normal development to congenital disease.* Elsevier Inc.

HARDING, S. D., ARMIT, C., ARMSTRONG, J., BRENNAN, J., CHENG, Y., HAGGARTY, B., HOUGHTON, D., LLOYD-MACGILP, S., PI, X., ROOCHUN, Y., SHARGHI, M., TINDAL, C., MCMAHON, A. P., GOTTESMAN, B., LITTLE, M. H., GEORGAS, K., ARONOW, B. J., POTTER, S. S., BRUNSKILL, E. W., SOUTHARD-SMITH, E. M., MENDELSOHN, C., BALDOCK, R. A., DAVIES, J. A. & DAVIDSON, D. 2011. The GUDMAP database--an online resource for genitourinary research. *Development,* 138**,** 2845-53.

HEASMAN, S. J. & RIDLEY, A. J. 2008. Mammalian Rho GTPases: new insights into their functions from in vivo studies. *Nature reviews. Molecular cell biology,* 9**,** 690-701.

HELLMICH, H. L., KOS, L., CHO, E. S., MAHON, K. A. & ZIMMER, A. 1996. Embryonic expression of glial cell-line derived neurotrophic factor (GDNF) suggests multiple developmental roles in neural differentiation and epithelial-mesenchymal interactions. *Mechanisms of development,* 54**,** 95-105.

HELLSTROM, M., PHNG, L. K., HOFMANN, J. J., WALLGARD, E., COULTAS, L., LINDBLOM, P., ALVA, J., NILSSON, A. K., KARLSSON, L., GAIANO, N., YOON, K., ROSSANT, J., IRUELA-ARISPE, M. L., KALEN, M., GERHARDT, H. & BETSHOLTZ, C. 2007. Dll4 signalling through Notch1 regulates formation of tip cells during angiogenesis. *Nature,* 445**,** 776-80.

HERZLINGER, D., KOSEKI, C., MIKAWA, T. & AL-AWQATI, Q. 1992. Metanephric mesenchyme contains multipotent stem cells whose fate is restricted after induction. *Development,* 114**,** 565-72.

HIGASHIYAMA, S., ABRAHAM, J. A. & KLAGSBRUN, M. 1993. Heparin-binding EGF-like growth factor stimulation of smooth muscle cell migration: dependence on interactions with cell surface heparan sulfate. *The Journal of cell biology,* 122**,** 933-40.

HOUCK, K. A., LEUNG, D. W., ROWLAND, A. M., WINER, J. & FERRARA, N. 1992. Dual regulation of vascular endothelial growth factor bioavailability by genetic and proteolytic mechanisms. *The Journal of biological chemistry,* 267**,** 26031-7.

HOYER, J. R., SISSON, S. P. & VERNIER, R. L. 1979. Tamm-Horsfall glycoprotein: ultrastructural immunoperoxidase localization in rat kidney. *Laboratory investigation; a journal of technical methods and pathology,* 41**,** 168-73.

HU, H., MARTON, T. F. & GOODMAN, C. S. 2001. Plexin B mediates axon guidance in Drosophila by simultaneously inhibiting active Rac and enhancing RhoA signaling. *Neuron,* 32**,** 39-51.

HU, K., JI, L., APPLEGATE, K. T., DANUSER, G. & WATERMAN-STORER, C. M. 2007. Differential Transmission of Actin Motion Within Focal Adhesions. *Science,* 315**,** 111-115.

HUBER, G. C. 1905. On the development and shape of human uriniferous tubules of certain higher mammals. *American Journal of Anatomy,* 4**,** 1-98.

HURST, N. J., JR., NAJY, A. J., USTACH, C. V., MOVILLA, L. & KIM, H. R. 2012. Platelet-derived growth factor-C (PDGF-C) activation by serine proteases: implications for breast cancer progression. *The Biochemical journal,* 441**,** 909-18.

IIJIMA, M. & DEVREOTES, P. 2002. Tumor suppressor PTEN mediates sensing of chemoattractant gradients. *Cell,* 109**,** 599-610.

IIJIMA, M., HUANG, Y. E., LUO, H. R., VAZQUEZ, F. & DEVREOTES, P. N. 2004. Novel mechanism of PTEN regulation by its phosphatidylinositol 4,5-bisphosphate binding motif is critical for chemotaxis. *The Journal of biological chemistry,* 279**,** 16606-13.

ILINA, O. & FRIEDL, P. 2009. Mechanisms of collective cell migration at a glance. *Journal of Cell Science,* 122**,** 3203-8.

IVASKA, J. 2012. Unanchoring integrins in focal adhesions. *Nature cell biology,* 14**,** 981-3.

JAFFE, A. B. & HALL, A. 2005. Rho GTPases: biochemistry and biology. *Annual review of cell and developmental biology,* 21**,** 247-69.

JAIN, S. 2009. The many faces of RET dysfunction in kidney. *Organogenesis,* 5**,** 177-90.

JENKINS, D., WINYARD, P. J. & WOOLF, A. S. 2007. Immunohistochemical analysis of Sonic hedgehog signalling in normal human urinary tract development. *Journal of anatomy,* 211**,** 620-9.

JIN, Z. & STRITTMATTER, S. M. 1997. Rac1 mediates collapsin-1-induced growth cone collapse. *The Journal of neuroscience : the official journal of the Society for Neuroscience,* 17**,** 6256-63.

JING, S., WEN, D., YU, Y., HOLST, P. L., LUO, Y., FANG, M., TAMIR, R., ANTONIO, L., HU, Z., CUPPLES, R., LOUIS, J. C., HU, S., ALTROCK, B. W. & FOX, G. M. 1996. GDNF-induced activation of the ret protein tyrosine kinase is mediated by GDNFR-alpha, a novel receptor for GDNF. *Cell,* 85**,** 1113-24.

JORGENSEN, P. L. 1976. The function of (Na+, K+)-ATPase in the thick ascending limb of Henles loop. *Current problems in clinical biochemistry,* 6**,** 190-9.

JUNG, A. C., DENHOLM, B., SKAER, H. & AFFOLTER, M. 2005. Renal tubule development in Drosophila: a closer look at the cellular level. *Journal of the American Society of Nephrology : JASN,* 16**,** 322-8.

KAISSLING, B. & KRIZ, W. 1979. Structural analysis of the rabbit kidney. *Advances in anatomy, embryology, and cell biology,* 56**,** 1-123.

KAPLAN, M. R., PLOTKIN, M. D., LEE, W. S., XU, Z. C., LYTTON, J. & HEBERT, S. C. 1996. Apical localization of the Na-K-Cl cotransporter, rBSC1, on rat thick ascending limbs. *Kidney international,* 49**,** 40-7.

KEYNES, R. J. & STERN, C. D. 1984. Segmentation in the vertebrate nervous system. *Nature,* 310**,** 786-9.

KIM, D. & DRESSLER, G. R. 2007. PTEN modulates GDNF/RET mediated chemotaxis and branching morphogenesis in the developing kidney. *Developmental biology,* 307**,** 290-9.

KISPERT, A., VAINIO, S., SHEN, L., ROWITCH, D. H. & MCMAHON, A. P. 1996. Proteoglycans are required for maintenance of Wnt-11 expression in the ureter tips. *Development,* 122**,** 3627-37.

KITAMOTO, Y., TOKUNAGA, H. & TOMITA, K. 1997. Vascular endothelial growth factor is an essential molecule for mouse kidney development: glomerulogenesis and nephrogenesis. *The Journal of clinical investigation,* 99**,** 2351-7.

KNEPPER, M. A., DANIELSON, R. A., SAIDEL, G. M. & POST, R. S. 1977. Quantitative analysis of renal medullary anatomy in rats and rabbits. *Kidney international,* 12**,** 313-23.

KOBAYASHI, A., KWAN, K. M., CARROLL, T. J., MCMAHON, A. P., MENDELSOHN, C. L. & BEHRINGER, R. R. 2005. Distinct and sequential tissue-specific activities of the LIM-class homeobox gene Lim1 for tubular morphogenesis during kidney development. *Development,* 132**,** 2809-23.

KOBAYASHI, A., VALERIUS, M. T., MUGFORD, J. W., CARROLL, T. J., SELF, M., OLIVER, G. & MCMAHON, A. P. 2008. Six2 defines and regulates a multipotent self-renewing nephron progenitor population throughout mammalian kidney development. *Cell stem cell,* 3**,** 169-81.

KOLODKIN, A. L., LEVENGOOD, D. V., ROWE, E. G., TAI, Y. T., GIGER, R. J. & GINTY, D. D. 1997. Neuropilin is a semaphorin III receptor. *Cell,* 90**,** 753-62.

KRAMER, N., WALZL, A., UNGER, C., ROSNER, M., KRUPITZA, G., HENGSTSCHLAGER, M. & DOLZNIG, H. 2013. In vitro cell migration and invasion assays. *Mutation research,* 752**,** 10-24.

KRAUSE, M., DENT, E. W., BEAR, J. E., LOUREIRO, J. J. & GERTLER, F. B. 2003. Ena/VASP proteins: regulators of the actin cytoskeleton and cell migration. *Annual review of cell and developmental biology,* 19**,** 541-64.

KRIZ, W. 1967. [The architectonic and functional structure of the rat kidney]. *Zeitschrift fur Zellforschung und mikroskopische Anatomie,* 82**,** 495-535.

KRIZ, W. & BANKIR, L. 1988. A standard nomenclature for structure of the kidney. The Renal Commission of the International Union of Physiological Sciences(IUPS). *Anatomy and embryology,* 178**,** N1-8.

KRIZ, W. & KOEPSELL, H. 1974. The structural organization of the mouse kidney. *Zeitschrift fur Anatomie und Entwicklungsgeschichte,* 144**,** 137-163.

KRUGMANN, S., JORDENS, I., GEVAERT, K., DRIESSENS, M., VANDEKERCKHOVE, J. & HALL, A. 2001. Cdc42 induces filopodia by promoting the formation of an IRSp53:Mena complex. *Current biology : CB,* 11**,** 1645-55.

KUNWAR, P. S., SIEKHAUS, D. E. & LEHMANN, R. 2006. In vivo migration: a germ cell perspective. *Annual review of cell and developmental biology,* 22**,** 237-65.

KUROSAKA, S. & KASHINA, A. 2008. Cell biology of embryonic migration. *Birth defects research. Part C, Embryo today : reviews,* 84**,** 102-22.

KUURE, S., CEBRIAN, C., MACHINGO, Q., LU, B. C., CHI, X., HYINK, D., D'AGATI, V., GURNIAK, C., WITKE, W. & COSTANTINI, F. 2010. Actin depolymerizing factors cofilin1 and destrin are required for ureteric bud branching morphogenesis. *PLoS genetics,* 6**,** e1001176.

LAMALICE, L., LE BOEUF, F. & HUOT, J. 2007. Endothelial cell migration during angiogenesis. *Circulation research,* 100**,** 782-94.

LARA RODRIGUEZ, L. & SCHNEIDER, I. C. 2013. Directed cell migration in multi-cue environments. *Integrative Biology,* 5**,** 1306-1323.

LE CLAINCHE, C. & CARLIER, M. F. 2008. Regulation of actin assembly associated with protrusion and adhesion in cell migration. *Physiological reviews,* 88**,** 489-513.

LEONG, H. S., CHAMBERS, A. F. & LEWIS, J. D. 2012. Assessing cancer cell migration and metastatic growth in vivo in the chick embryo using fluorescence intravital imaging. *Methods in molecular biology,* 872**,** 1-14.

LI, R., MAMINISHKIS, A., WANG, F. E. & MILLER, S. S. 2007. PDGF-C and -D induced proliferation/migration of human RPE is abolished by inflammatory cytokines. *Investigative ophthalmology & visual science,* 48**,** 5722-32.

LI, X. & KOLEGA, J. 2002. Effects of direct current electric fields on cell migration and actin filament distribution in bovine vascular endothelial cells. *Journal of vascular research,* 39**,** 391-404.

LIEKENS, S., DE CLERCQ, E. & NEYTS, J. 2001. Angiogenesis: regulators and clinical applications. *Biochemical pharmacology,* 61**,** 253-70.

LIN, Y., ZHANG, S., REHN, M., ITARANTA, P., TUUKKANEN, J., HELJASVAARA, R., PELTOKETO, H., PIHLAJANIEMI, T. & VAINIO, S. 2001. Induced repatterning of type XVIII collagen expression in ureter bud from kidney to lung type: association with sonic hedgehog and ectopic surfactant protein C. *Development,* 128**,** 1573-85.

LINDSTROM, N. O., HOHENSTEIN, P. & DAVIES, J. A. 2013. Nephrons require Rho-kinase for proximal-distal polarity development. *Scientific reports,* 3**,** 2692.

LITTLE, M. H., BRENNAN, J., GEORGAS, K., DAVIES, J. A., DAVIDSON, D. R., BALDOCK, R. A., BEVERDAM, A., BERTRAM, J. F., CAPEL, B., CHIU, H. S., CLEMENTS, D., CULLEN-MCEWEN, L., FLEMING, J., GILBERT, T., HERZLINGER, D., HOUGHTON, D., KAUFMAN, M. H., KLEYMENOVA, E., KOOPMAN, P. A., LEWIS, A. G., MCMAHON, A. P., MENDELSOHN, C. L., MITCHELL, E. K., RUMBALLE, B. A., SWEENEY, D. E., VALERIUS, M. T., YAMADA, G., YANG, Y. & YU, J. 2007. A high-resolution anatomical ontology of the developing murine genitourinary tract. *Gene expression patterns : GEP,* 7**,** 680-99.

LITTLE, M. H. & MCMAHON, A. P. 2012. Mammalian kidney development: principles, progress, and projections. *Cold Spring Harbor perspectives in biology,* 4.

LIU, Y., COX, S. R., MORITA, T. & KOUREMBANAS, S. 1995. Hypoxia regulates vascular endothelial growth factor gene expression in endothelial cells. Identification of a 5' enhancer. *Circulation research,* 77**,** 638-43.

LO, C. M., WANG, H. B., DEMBO, M. & WANG, Y. L. 2000. Cell movement is guided by the rigidity of the substrate. *Biophysical journal,* 79**,** 144-52.

LU, P., TAKAI, K., WEAVER, V. M. & WERB, Z. 2011. Extracellular matrix degradation and remodeling in development and disease. *Cold Spring Harbor perspectives in biology,* 3.

LYON, M., RUSHTON, G. & GALLAGHER, J. T. 1997. The Interaction of the Transforming Growth Factor-βs with Heparin/Heparan Sulfate Is Isoform-specific. *Journal of Biological Chemistry,* 272**,** 18000-18006.

LYUKSYUTOVA, A. I., LU, C. C., MILANESIO, N., KING, L. A., GUO, N., WANG, Y., NATHANS, J., TESSIER-LAVIGNE, M. & ZOU, Y. 2003. Anterior-posterior guidance of commissural axons by Wnt-frizzled signaling. *Science,* 302**,** 1984-8.

MAGDALENO, S., JENSEN, P., BRUMWELL, C. L., SEAL, A., LEHMAN, K., ASBURY, A., CHEUNG, T., CORNELIUS, T., BATTEN, D. M., EDEN, C., NORLAND, S. M., RICE, D. S., DOSOOYE, N., SHAKYA, S., MEHTA, P. & CURRAN, T. 2006. BGEM: an in situ hybridization database of gene expression in the embryonic and adult mouse nervous system. *PLoS biology,* 4**,** e86.

MAISONPIERRE, P. C., SURI, C., JONES, P. F., BARTUNKOVA, S., WIEGAND, S. J., RADZIEJEWSKI, C., COMPTON, D., MCCLAIN, J., ALDRICH, T. H., PAPADOPOULOS, N., DALY, T. J., DAVIS, S., SATO, T. N. & YANCOPOULOS, G. D. 1997. Angiopoietin-2, a natural antagonist for Tie2 that disrupts in vivo angiogenesis. *Science,* 277**,** 55-60.

MAJUMDAR, A., VAINIO, S., KISPERT, A., MCMAHON, J. & MCMAHON, A. P. 2003. Wnt11 and Ret/Gdnf pathways cooperate in regulating ureteric branching during metanephric kidney development. *Development,* 130**,** 3175-85.

MATTILA, P. K. & LAPPALAINEN, P. 2008. Filopodia: molecular architecture and cellular functions. *Nature reviews. Molecular cell biology,* 9**,** 446-454.

MCMAHON, A. P., ARONOW, B. J., DAVIDSON, D. R., DAVIES, J. A., GAIDO, K. W., GRIMMOND, S., LESSARD, J. L., LITTLE, M. H., POTTER, S. S., WILDER, E. L. & ZHANG, P. 2008. GUDMAP: the genitourinary developmental molecular anatomy project. *Journal of the American Society of Nephrology : JASN,* 19**,** 667-71.

MEJILLANO, M. R., KOJIMA, S., APPLEWHITE, D. A., GERTLER, F. B., SVITKINA, T. M. & BORISY, G. G. 2004. Lamellipodial versus filopodial mode of the actin nanomachinery: pivotal role of the filament barbed end. *Cell,* 118**,** 363-73.

MENG, W. & TAKEICHI, M. 2009. Adherens junction: molecular architecture and regulation. *Cold Spring Harbor perspectives in biology,* 1**,** a002899.

MICHAEL, L. & DAVIES, J. A. 2004. Pattern and regulation of cell proliferation during murine ureteric bud development. *Journal of anatomy,* 204**,** 241-55.

MICHOS, O., GONCALVES, A., LOPEZ-RIOS, J., TIECKE, E., NAILLAT, F., BEIER, K., GALLI, A., VAINIO, S. & ZELLER, R. 2007. Reduction of BMP4 activity by gremlin 1 enables ureteric bud outgrowth and GDNF/WNT11 feedback signalling during kidney branching morphogenesis. *Development,* 134**,** 2397-405.

MITCHISON, T. J. & CRAMER, L. P. 1996. Actin-based cell motility and cell locomotion. *Cell,* 84**,** 371-9.

MOGILNER, A. & OSTER, G. 1996. Cell motility driven by actin polymerization. *Biophysical journal,* 71**,** 3030-45.

MSEKA, T. & CRAMER, L. P. 2011. Actin depolymerization-based force retracts the cell rear in polarizing and migrating cells. *Current biology : CB,* 21**,** 2085-91.

MUCHMORE & DECKER 1985. Uromodulin: a unique 85-kilodalton immunosuppressive glycoprotein isolated from urine of pregnant women. *Science,* 229**,** 479-81.

MUGFORD, J. W., SIPILA, P., MCMAHON, J. A. & MCMAHON, A. P. 2008. Osr1 expression demarcates a multi-potent population of intermediate mesoderm that undergoes progressive restriction to an Osr1-dependent nephron progenitor compartment within the mammalian kidney. *Developmental biology,* 324**,** 88-98.

MURAMATSU, T. 2010. Midkine, a heparin-binding cytokine with multiple roles in development, repair and diseases. *Proceedings of the Japan Academy. Series B, Physical and biological sciences,* 86**,** 410-25.

MYCIELSKA, M. E. & DJAMGOZ, M. B. 2004. Cellular mechanisms of direct-current electric field effects: galvanotaxis and metastatic disease. *Journal of Cell Science,* 117**,** 1631-9.

NAKAI, S., SUGITANI, Y., SATO, H., ITO, S., MIURA, Y., OGAWA, M., NISHI, M., JISHAGE, K., MINOWA, O. & NODA, T. 2003. Crucial roles of Brn1 in distal tubule formation and function in mouse kidney. *Development,* 130**,** 4751-9.

NAKAMURA, F., KALB, R. G. & STRITTMATTER, S. M. 2000. Molecular basis of semaphorin-mediated axon guidance. *Journal of neurobiology,* 44**,** 219-29.

NAKATSUJI, N. & JOHNSON, K. E. 1982. Cell locomotion in vitro by Xenopus laevis gastrula mesodermal cells. *Cell motility,* 2**,** 149-61.

NARLIS, M., GROTE, D., GAITAN, Y., BOUALIA, S. K. & BOUCHARD, M. 2007. Pax2 and pax8 regulate branching morphogenesis and nephron differentiation in the developing kidney. *Journal of the American Society of Nephrology : JASN,* 18**,** 1121-9.

NEISS, W. F. 1982. Histogenesis of the loop of Henle in the rat kidney. *Anatomy and embryology,* 164**,** 315-30.

NEWELL, P. C., EUROPE-FINNER, G. N., LIU, G., GAMMON, B. & WOOD, C. A. 1990. Signal transduction for chemotaxis in Dictyostelium amoebae. *Seminars in cell biology,* 1**,** 105-13.

NG, Y.-S. 2008. The Biology of Vascular Endothelial Cell Growth Factor Isoforms. *VEGF in Development.* Springer New York.

NGUYEN BA-CHARVET, K. T., BROSE, K., MARILLAT, V., KIDD, T., GOODMAN, C. S., TESSIER-LAVIGNE, M., SOTELO, C. & CHEDOTAL, A. 1999. Slit2-Mediated chemorepulsion and collapse of developing forebrain axons. *Neuron,* 22**,** 463-73.

NIELSEN, S., CHOU, C. L., MARPLES, D., CHRISTENSEN, E. I., KISHORE, B. K. & KNEPPER, M. A. 1995. Vasopressin increases water permeability of kidney collecting duct by inducing translocation of aquaporin-CD water channels to plasma membrane. *Proceedings of the National Academy of Sciences of the United States of America,* 92**,** 1013-7.

NIELSEN, S., FROKIAER, J., MARPLES, D., KWON, T. H., AGRE, P. & KNEPPER, M. A. 2002. Aquaporins in the kidney: from molecules to medicine. *Physiological reviews,* 82**,** 205-44.

NOBES, C. D. & HALL, A. 1995. Rho, rac, and cdc42 GTPases regulate the assembly of multimolecular focal complexes associated with actin stress fibers, lamellipodia, and filopodia. *Cell,* 81**,** 53-62.

OBARA-ISHIHARA, T., KUHLMAN, J., NISWANDER, L. & HERZLINGER, D. 1999. The surface ectoderm is essential for nephric duct formation in intermediate mesoderm. *Development,* 126**,** 1103-8.

ONUMA, E. K. & HUI, S. W. 1988. Electric field-directed cell shape changes, displacement, and cytoskeletal reorganization are calcium dependent. *The Journal of cell biology,* 106**,** 2067-75.

ORI, A., FREE, P., COURTY, J., WILKINSON, M. C. & FERNIG, D. G. 2009. Identification of heparin-binding sites in proteins by selective labeling. *Molecular & cellular proteomics : MCP,* 8**,** 2256-65.

OSAFUNE, K., TAKASATO, M., KISPERT, A., ASASHIMA, M. & NISHINAKAMURA, R. 2006. Identification of multipotent progenitors in the embryonic mouse kidney by a novel colony-forming assay. *Development,* 133**,** 151-61.

PACHNIS, V., MANKOO, B. & COSTANTINI, F. 1993. Expression of the c-ret proto-oncogene during mouse embryogenesis. *Development,* 119**,** 1005-17.

PALLONE, T. L., TURNER, M. R., EDWARDS, A. & JAMISON, R. L. 2003. Countercurrent exchange in the renal medulla. *American journal of physiology. Regulatory, integrative and comparative physiology,* 284**,** R1153-75.

PANNABECKER, T. L. 2012. Structure and function of the thin limbs of the loop of Henle. *Comprehensive Physiology,* 2**,** 2063-86.

PARENT, C. A., BLACKLOCK, B. J., FROEHLICH, W. M., MURPHY, D. B. & DEVREOTES, P. N. 1998. G protein signaling events are activated at the leading edge of chemotactic cells. *Cell,* 95**,** 81-91.

PARR, B. A., SHEA, M. J., VASSILEVA, G. & MCMAHON, A. P. 1993. Mouse Wnt genes exhibit discrete domains of expression in the early embryonic CNS and limb buds. *Development,* 119**,** 247-61.

PATAN, S. 2004. Vasculogenesis and angiogenesis. *Cancer treatment and research,* 117**,** 3-32.

PAVLOV, D., MUHLRAD, A., COOPER, J., WEAR, M. & REISLER, E. 2007. Actin filament severing by cofilin. *Journal of molecular biology,* 365**,** 1350-8.

PENNICA, D., KOHR, W. J., KUANG, W. J., GLAISTER, D., AGGARWAL, B. B., CHEN, E. Y. & GOEDDEL, D. V. 1987. Identification of human uromodulin as the Tamm-Horsfall urinary glycoprotein. *Science,* 236**,** 83-8.

PEPICELLI, C. V., KISPERT, A., ROWITCH, D. H. & MCMAHON, A. P. 1997. GDNF induces branching and increased cell proliferation in the ureter of the mouse. *Developmental biology,* 192**,** 193-8.

PETRIE, R. J., DOYLE, A. D. & YAMADA, K. M. 2009. Random versus directionally persistent cell migration. *Nature reviews. Molecular cell biology,* 10**,** 538-49.

POLE, R. J., QI, B. Q. & BEASLEY, S. W. 2002. Patterns of apoptosis during degeneration of the pronephros and mesonephros. *The Journal of urology,* 167**,** 269-71.

POLLARD, T. D. & BORISY, G. G. 2003. Cellular motility driven by assembly and disassembly of actin filaments. *Cell,* 112**,** 453-65.

POUKKULA, M., CLIFFE, A., CHANGEDE, R. & RORTH, P. 2011. Cell behaviors regulated by guidance cues in collective migration of border cells. *The Journal of cell biology,* 192**,** 513-24.

PUSCHEL, A. W., ADAMS, R. H. & BETZ, H. 1995. Murine semaphorin D/collapsin is a member of a diverse gene family and creates domains inhibitory for axonal extension. *Neuron,* 14**,** 941-8.

QIAN, J., JIANG, Z., LI, M., HEAPHY, P., LIU, Y. H. & SHACKLEFORD, G. M. 2003. Mouse Wnt9b transforming activity, tissue-specific expression, and evolution. *Genomics,* 81**,** 34-46.

QUAGGIN, S. E. & KREIDBERG, J. A. 2008. Development of the renal glomerulus: good neighbors and good fences. *Development,* 135**,** 609-20.

RAFTOPOULOU, M. & HALL, A. 2004. Cell migration: Rho GTPases lead the way. *Developmental biology,* 265**,** 23-32.

RAJNICEK, A., BRITLAND, S. & MCCAIG, C. 1997. Contact guidance of CNS neurites on grooved quartz: influence of groove dimensions, neuronal age and cell type. *Journal of Cell Science,* 110 (Pt 23)**,** 2905-13.

RAPPEL, W. J., THOMAS, P. J., LEVINE, H. & LOOMIS, W. F. 2002. Establishing direction during chemotaxis in eukaryotic cells. *Biophysical journal,* 83**,** 1361-7.

RAUVALA, H. & PIHLASKARI, R. 1987. Isolation and some characteristics of an adhesive factor of brain that enhances neurite outgrowth in central neurons. *The Journal of biological chemistry,* 262**,** 16625-35.

RAZ, E. & MAHABALESHWAR, H. 2009. Chemokine signaling in embryonic cell migration: a fisheye view. *Development,* 136**,** 1223-9.

REIDY, K. J. & ROSENBLUM, N. D. 2009. Cell and molecular biology of kidney development. *Seminars in nephrology,* 29**,** 321-37.

REILLY, R. F. & ELLISON, D. H. 2000. Mammalian distal tubule: physiology, pathophysiology, and molecular anatomy. *Physiological reviews,* 80**,** 277-313.

RIDLEY, A. J. 2001. Rho GTPases and cell migration. *Journal of Cell Science,* 114**,** 2713-22.

RIDLEY, A. J., SCHWARTZ, M. A., BURRIDGE, K., FIRTEL, R. A., GINSBERG, M. H., BORISY, G., PARSONS, J. T. & HORWITZ, A. R. 2003. Cell migration: integrating signals from front to back. *Science,* 302**,** 1704-9.

RIENHOFF, W. F. 1922. Development and growth of the metanephros or permanent kidney in chick embryos. *Johns Hopkins Hosp. Bull.,* 33**,** 392-406.

ROBERT, B. & ABRAHAMSON, D. R. 2001. Control of glomerular capillary development by growth factor/receptor kinases. *Pediatric nephrology,* 16**,** 294-301.

ROBERT, B., ST JOHN, P. L. & ABRAHAMSON, D. R. 1998. Direct visualization of renal vascular morphogenesis in Flk1 heterozygous mutant mice. *The American journal of physiology,* 275**,** F164-72.

ROHM, B., OTTEMEYER, A., LOHRUM, M. & PUSCHEL, A. W. 2000. Plexin/neuropilin complexes mediate repulsion by the axonal guidance signal semaphorin 3A. *Mechanisms of development,* 93**,** 95-104.

RORTH, P. 2009. Collective cell migration. *Annual review of cell and developmental biology,* 25**,** 407-29.

RORTH, P. 2011. Whence directionality: guidance mechanisms in solitary and collective cell migration. *Developmental cell,* 20**,** 9-18.

ROTHBERG, J. M., JACOBS, J. R., GOODMAN, C. S. & ARTAVANIS-TSAKONAS, S. 1990. slit: an extracellular protein necessary for development of midline glia and commissural axon pathways contains both EGF and LRR domains. *Genes & development,* 4**,** 2169-87.

RUNNER, M. N. 1946. The development of the mesonephros of the albino rat in intraocular grafts. *Journal of Experimental Zoology,* 103**,** 305-319.

SAEZ, A., GHIBAUDO, M., BUGUIN, A., SILBERZAN, P. & LADOUX, B. 2007. Rigidity-driven growth and migration of epithelial cells on microstructured anisotropic substrates. *Proceedings of the National Academy of Sciences of the United States of America,* 104**,** 8281-6.

SAINIO, K. 2003. Development of the mesonephric kidney. *In:* VIZE, C., WOOLF, A. S, AND BARD, J. B. L. (ed.) *The kidney. From normal development to congenital disease.* London: Academic Press.

SANDS, J. M. 2012. Urine concentrating and diluting ability during aging. *The journals of gerontology. Series A, Biological sciences and medical sciences,* 67**,** 1352-7.

SANDS, J. M., BLOUNT, M. A. & KLEIN, J. D. 2011. Regulation of renal urea transport by vasopressin. *Transactions of the American Clinical and Climatological Association,* 122**,** 82-92.

SANDS, J. M. & LAYTON, H. E. 2009. The physiology of urinary concentration: an update. *Seminars in nephrology,* 29**,** 178-95.

SARIOLA, H., SAINIO, K., AND BARD, J. B.L. 2003. Fates of the metanephric mesenchyme. *In:* PETER D. VIZE, A. S. W., JONATHAN B.L. BARD (ed.) *The Kidney: From Normal Development to Congenital Disease.* London: Academic Press, Inc.

SATO, M. J., KUWAYAMA, H., VAN EGMOND, W. N., TAKAYAMA, A. L., TAKAGI, H., VAN HAASTERT, P. J., YANAGIDA, T. & UEDA, M. 2009. Switching direction in electric-signal-induced cell migration by cyclic guanosine monophosphate and phosphatidylinositol signaling. *Proceedings of the National Academy of Sciences of the United States of America,* 106**,** 6667-72.

SAXE, C. L., 3RD, JOHNSON, R., DEVREOTES, P. N. & KIMMEL, A. R. 1991. Multiple genes for cell surface cAMP receptors in Dictyostelium discoideum. *Developmental genetics,* 12**,** 6-13.

SAXÉN, L. 1987. *Organogenesis of the Kidney*, Cambridge University Press.

SAXÉN, L., KOSKIMIES, O., LAHTI, A., MIETTINEN, H., RAPOLA, J. & WARTIOVAARA, J. 1968. Differentiation of kidney mesenchyme in an experimental model system. *Advances in morphogenesis,* 7**,** 251-93.

SAXÉN, L. & LEHTONEN, E. 1987. Embryonic kidney in organ culture. *Differentiation,* 36**,** 2-11.

SAXÉN, L. T. S. 1962. *Primary embryonic induction,* [London, Logos Press.

SCHMIDT-OTT, K. M., YANG, J., CHEN, X., WANG, H., PARAGAS, N., MORI, K., LI, J. Y., LU, B., COSTANTINI, F., SCHIFFER, M., BOTTINGER, E. & BARASCH, J. 2005. Novel regulators

of kidney development from the tips of the ureteric bud. *Journal of the American Society of Nephrology : JASN,* 16**,** 1993-2002.

SCHOENWOLF, G. C. 2001. Cutting, pasting and painting: experimental embryology and neural development. *Nature reviews. Neuroscience,* 2**,** 763-71.

SEBINGER, D. D. R., UNBEKANDT, M., GANEVA, V. V., OFENBAUER, A., WERNER, C. & DAVIES, J. A. 2010. A Novel, Low-Volume Method for Organ Culture of Embryonic Kidneys That Allows Development of Cortico-Medullary Anatomical Organization. *PLoS ONE,* 5**,** e10550.

SEIRADAKE, E., VON PHILIPSBORN, A. C., HENRY, M., FRITZ, M., LORTAT-JACOB, H., JAMIN, M., HEMRIKA, W., BASTMEYER, M., CUSACK, S. & MCCARTHY, A. A. 2009. Structure and functional relevance of the Slit2 homodimerization domain. *EMBO reports,* 10**,** 736-41.

SHERIDAN, D. M., ISSEROFF, R. R. & NUCCITELLI, R. 1996. Imposition of a physiologic DC electric field alters the migratory response of human keratinocytes on extracellular matrix molecules. *The Journal of investigative dermatology,* 106**,** 642-6.

SHIMABUKURO, K., NODA, N., STEWART, M. & ROBERTS, T. M. 2011. Reconstitution of amoeboid motility in vitro identifies a motor-independent mechanism for cell body retraction. *Current biology : CB,* 21**,** 1727-31.

SIEGEL, N., ROSNER, M., UNBEKANDT, M., FUCHS, C., SLABINA, N., DOLZNIG, H., DAVIES, J. A., LUBEC, G. & HENGSTSCHLAGER, M. 2010. Contribution of human amniotic fluid stem cells to renal tissue formation depends on mTOR. *Human molecular genetics,* 19**,** 3320-31.

SINGH, P. K. & SRIVASTAVA, V. 2012. Recombinant expression and purification of heparin binding proteins: midkine and pleiotrophin from Escherichia coli. *Protein expression and purification,* 85**,** 181-6.

SINGH, S. R., LIU, W. & HOU, S. X. 2007. The adult Drosophila malpighian tubules are maintained by multipotent stem cells. *Cell stem cell,* 1**,** 191-203.

SKAER, H. 2003. Development of Malpighian Tubules in *Drosophila Melanogaster*. *In:* PETER D. VIZE, A. S. W., AND JONATHAN B.L. BARD (ed.) *The Kidney: From Normal Development to Congenital Disease.*

SMITH, C. & MACKAY, S. 1991. Morphological development and fate of the mouse mesonephros. *Journal of anatomy,* 174**,** 171-84.

SOKER, S., TAKASHIMA, S., MIAO, H. Q., NEUFELD, G. & KLAGSBRUN, M. 1998. Neuropilin-1 is expressed by endothelial and tumor cells as an isoform-specific receptor for vascular endothelial growth factor. *Cell,* 92**,** 735-45.

SONG, R., EL-DAHR, S. S. & YOSYPIV, I. V. 2011. Receptor Tyrosine Kinases in Kidney Development. *Journal of Signal Transduction,* 2011.

STAHL, A., CONNOR, K. M., SAPIEHA, P., CHEN, J., DENNISON, R. J., KRAH, N. M., SEAWARD, M. R., WILLETT, K. L., ADERMAN, C. M., GUERIN, K. I., HUA, J., LÖFQVIST, C., HELLSTRÖM, A. & SMITH, L. E. H. 2010. The Mouse Retina as an Angiogenesis Model. *Investigative ophthalmology & visual science,* 51**,** 2813-2826.

SUDARSAN, V., PASALODOS-SANCHEZ, S., WAN, S., GAMPEL, A. & SKAER, H. 2002. A genetic hierarchy establishes mitogenic signalling and mitotic competence in the renal tubules of Drosophila. *Development,* 129**,** 935-44.

SUTER, D. M., ERRANTE, L. D., BELOTSERKOVSKY, V. & FORSCHER, P. 1998. The Ig superfamily cell adhesion molecule, apCAM, mediates growth cone steering by substrate-cytoskeletal coupling. *The Journal of cell biology,* 141**,** 227-40.

TAI, G., HOHENSTEIN, P. & DAVIES, J. A. 2012. Making immortalized cell lines from embryonic mouse kidney. *Methods in molecular biology,* 886**,** 165-71.

TAI, G., HOHENSTEIN, P. & DAVIES, J. A. 2013. FAK-Src signalling is important to renal collecting duct morphogenesis: discovery using a hierarchical screening technique. *Biology open,* 2**,** 416-23.

TAIPALE, J., CHEN, J. K., COOPER, M. K., WANG, B., MANN, R. K., MILENKOVIC, L., SCOTT, M. P. & BEACHY, P. A. 2000. Effects of oncogenic mutations in Smoothened and Patched can be reversed by cyclopamine. *Nature,* 406**,** 1005-9.

TAMM, I. & HORSFALL, F. L., JR. 1950. Characterization and separation of an inhibitor of viral hemagglutination present in urine. *Proceedings of the Society for Experimental Biology and Medicine. Society for Experimental Biology and Medicine,* 74**,** 106-8.

TANG, M. J., CAI, Y., TSAI, S. J., WANG, Y. K. & DRESSLER, G. R. 2002. Ureteric bud outgrowth in response to RET activation is mediated by phosphatidylinositol 3-kinase. *Developmental biology,* 243**,** 128-36.

TANG, M. J., WORLEY, D., SANICOLA, M. & DRESSLER, G. R. 1998. The RET-glial cell-derived neurotrophic factor (GDNF) pathway stimulates migration and chemoattraction of epithelial cells. *The Journal of cell biology,* 142**,** 1337-45.

TANIGAWA, S., WANG, H., YANG, Y., SHARMA, N., TARASOVA, N., AJIMA, R., YAMAGUCHI, T. P., RODRIGUEZ, L. G. & PERANTONI, A. O. 2011. Wnt4 induces nephronic tubules in metanephric mesenchyme by a non-canonical mechanism. *Developmental biology,* 352**,** 58-69.

TANSEY, M. G., WORD, R. A., HIDAKA, H., SINGER, H. A., SCHWORER, C. M., KAMM, K. E. & STULL, J. T. 1992. Phosphorylation of myosin light chain kinase by the multifunctional calmodulin-dependent protein kinase II in smooth muscle cells. *The Journal of biological chemistry,* 267**,** 12511-6.

TESSIER-LAVIGNE, M. & GOODMAN, C. S. 1996. The molecular biology of axon guidance. *Science,* 274**,** 1123-33.

THEVENEAU, E. & MAYOR, R. 2012. Neural crest delamination and migration: from epithelium-to-mesenchyme transition to collective cell migration. *Developmental biology,* 366**,** 34-54.

TSE, J. R. & ENGLER, A. J. 2011. Stiffness Gradients Mimicking <italic>In Vivo</italic> Tissue Variation Regulate Mesenchymal Stem Cell Fate. *PLoS ONE,* 6**,** e15978.

UEMURA, A., KUSUHARA, S., KATSUTA, H. & NISHIKAWA, S. 2006. Angiogenesis in the mouse retina: a model system for experimental manipulation. *Experimental cell research,* 312**,** 676-83.

ULLOA, F. & MARTI, E. 2010. Wnt won the war: antagonistic role of Wnt over Shh controls dorso-ventral patterning of the vertebrate neural tube. *Developmental dynamics : an official publication of the American Association of Anatomists,* 239**,** 69-76.

UNBEKANDT, M. & DAVIES, J. A. 2010. Dissociation of embryonic kidneys followed by reaggregation allows the formation of renal tissues. *Kidney international,* 77**,** 407-16.

UNWIN, R., CAPASSO, G. & GIEBISCH, G. 1994. Potassium and sodium transport along the loop of Henle: effects of altered dietary potassium intake. *Kidney international,* 46**,** 1092-9.

VAINIO, S. J., ITARANTA, P. V., PERASAARI, J. P. & UUSITALO, M. S. 1999. Wnts as kidney tubule inducing factors. *The International journal of developmental biology,* 43**,** 419-23.

VAN HAASTERT, P. J. 2010. Chemotaxis: insights from the extending pseudopod. *Journal of Cell Science,* 123**,** 3031-7.

VAN VACTOR, D. V. & LORENZ, L. J. 1999. Neural development: The semantics of axon guidance. *Current biology : CB,* 9**,** R201-4.

VELTMAN, D. M., KEIZER-GUNNIK, I. & VAN HAASTERT, P. J. 2008. Four key signaling pathways mediating chemotaxis in Dictyostelium discoideum. *The Journal of cell biology,* 180**,** 747-53.

VESTWEBER, D. 2008. VE-cadherin: the major endothelial adhesion molecule controlling cellular junctions and blood vessel formation. *Arteriosclerosis, thrombosis, and vascular biology,* 28**,** 223-32.

VETTER, M. R. & GIBLEY, C. W., JR. 1966. Morphogenesis and histochemistry of the developing mouse kidney. *Journal of morphology,* 120**,** 135-55.

VICENTE-MANZANARES, M., CHOI, C. K. & HORWITZ, A. R. 2009. Integrins in cell migration--the actin connection. *Journal of Cell Science,* 122**,** 199-206.

VICKER, M. G. & GRUTSCH, J. F. 2008. Dual chemotaxis signalling regulates Dictyostelium development: intercellular cyclic AMP pulses and intracellular F-actin disassembly waves induce each other. *European journal of cell biology,* 87**,** 845-61.

VIGNJEVIC, D., KOJIMA, S., ARATYN, Y., DANCIU, O., SVITKINA, T. & BORISY, G. G. 2006. Role of fascin in filopodial protrusion. *The Journal of cell biology,* 174**,** 863-75.

VIKIS, H. G., LI, W., HE, Z. & GUAN, K. L. 2000. The semaphorin receptor plexin-B1 specifically interacts with active Rac in a ligand-dependent manner. *Proceedings of the National Academy of Sciences of the United States of America,* 97**,** 12457-62.

VIZE, P. D., WOOLF, A. S. & BARD, J. B. L. 2003. *The kidney : from normal development to congenital abnormalities / edited by Peter D. Vize, Adrian S. Woolf, Jonathan B.L. Bard*, San Diego, Calif. ; London : Academic, 2003.

VUKICEVIC, S., KOPP, J. B., LUYTEN, F. P. & SAMPATH, T. K. 1996. Induction of nephrogenic mesenchyme by osteogenic protein 1 (bone morphogenetic protein 7). *Proceedings of the National Academy of Sciences of the United States of America,* 93**,** 9021-6.

WANG, Y., CHEN, C.-L. & IIJIMA, M. 2011. Signaling mechanisms for chemotaxis. *Development, Growth & Differentiation,* 53**,** 495-502.

WATANABE, T. & COSTANTINI, F. 2004. Real-time analysis of ureteric bud branching morphogenesis in vitro. *Developmental biology,* 271**,** 98-108.

WATERMAN, A. J. 1940. Growth and differentiation of kidney tissue of the rabbit embryo in omental grafts. *Journal of morphology,* 67**,** 369-385.

WEAVERS, H. & SKAER, H. 2013. Tip cells act as dynamic cellular anchors in the morphogenesis of looped renal tubules in Drosophila. *Developmental cell,* 27**,** 331-44.

WEIJER, C. J. 2009. Collective cell migration in development. *Journal of Cell Science,* 122**,** 3215-23.

WELCH, M. D. & MULLINS, R. D. 2002. Cellular control of actin nucleation. *Annual review of cell and developmental biology,* 18**,** 247-88.

WELLS, A. (ed.) 2006. *Cell Motility in Cancer Invasion and Metastasis*: Spinger.

WILSON, L. & MADEN, M. 2005. The mechanisms of dorsoventral patterning in the vertebrate neural tube. *Developmental biology,* 282**,** 1-13.

WIMMER, R., CSEH, B., MAIER, B., SCHERRER, K. & BACCARINI, M. 2012. Angiogenic sprouting requires the fine tuning of endothelial cell cohesion by the Raf-1/Rok-alpha complex. *Developmental cell,* 22**,** 158-71.

WITKE, W. 2004. The role of profilin complexes in cell motility and other cellular processes. *Trends in cell biology,* 14**,** 461-9.

WITZENBICHLER, B., MAISONPIERRE, P. C., JONES, P., YANCOPOULOS, G. D. & ISNER, J. M. 1998. Chemotactic properties of angiopoietin-1 and -2, ligands for the endothelial-

specific receptor tyrosine kinase Tie2. *The Journal of biological chemistry,* 273**,** 18514-21.

WONG, K., REN, X. R., HUANG, Y. Z., XIE, Y., LIU, G., SAITO, H., TANG, H., WEN, L., BRADY-KALNAY, S. M., MEI, L., WU, J. Y., XIONG, W. C. & RAO, Y. 2001. Signal transduction in neuronal migration: roles of GTPase activating proteins and the small GTPase Cdc42 in the Slit-Robo pathway. *Cell,* 107**,** 209-21.

WOOLF, A. S. 2010. Angiopoietins: vascular growth factors looking for roles in glomeruli. *Current opinion in nephrology and hypertension,* 19**,** 20-5.

WOOLF, A. S., GNUDI, L. & LONG, D. A. 2009. Roles of angiopoietins in kidney development and disease. *Journal of the American Society of Nephrology : JASN,* 20**,** 239-44.

WOOLF, A. S. & YUAN, H. T. 2001. Angiopoietin growth factors and Tie receptor tyrosine kinases in renal vascular development. *Pediatric nephrology,* 16**,** 177-84.

WOOLF, A. S. Y., H. T. 2003. Development of Kidney Blood Vessels. *In:* PETER D. VIZE, A. S. W., JONATHAN B.L. BARD (ed.) *The Kidney: From Normal Development to Congenital Disease.* Academic Press.

WRIGHT, D. E., WAGERS, A. J., GULATI, A. P., JOHNSON, F. L. & WEISSMAN, I. L. 2001. Physiological migration of hematopoietic stem and progenitor cells. *Science,* 294**,** 1933-6.

YAMADA, T., PLACZEK, M., TANAKA, H., DODD, J. & JESSELL, T. M. 1991. Control of cell pattern in the developing nervous system: polarizing activity of the floor plate and notochord. *Cell,* 64**,** 635-47.

YOSHIKAWA, S., MCKINNON, R. D., KOKEL, M. & THOMAS, J. B. 2003. Wnt-mediated axon guidance via the Drosophila Derailed receptor. *Nature,* 422**,** 583-8.

YU, J., CARROLL, T. J. & MCMAHON, A. P. 2002. Sonic hedgehog regulates proliferation and differentiation of mesenchymal cells in the mouse metanephric kidney. *Development,* 129**,** 5301-12.

YU, J., CARROLL, T. J., RAJAGOPAL, J., KOBAYASHI, A., REN, Q. & MCMAHON, A. P. 2009. A Wnt7b-dependent pathway regulates the orientation of epithelial cell division and establishes the cortico-medullary axis of the mammalian kidney. *Development,* 136**,** 161-71.

YUAN, H. T., SURI, C., YANCOPOULOS, G. D. & WOOLF, A. S. 1999. Expression of angiopoietin-1, angiopoietin-2, and the Tie-2 receptor tyrosine kinase during mouse kidney maturation. *Journal of the American Society of Nephrology : JASN,* 10**,** 1722-36.

ZENG, G., TAYLOR, S. M., MCCOLM, J. R., KAPPAS, N. C., KEARNEY, J. B., WILLIAMS, L. H., HARTNETT, M. E. & BAUTCH, V. L. 2007. Orientation of endothelial cell division is regulated by VEGF signaling during blood vessel formation. *Blood,* 109**,** 1345-52.

ZHAI, X. Y., FENTON, R. A., ANDREASEN, A., THOMSEN, J. S. & CHRISTENSEN, E. I. 2007. Aquaporin-1 is not expressed in descending thin limbs of short-loop nephrons. *Journal of the American Society of Nephrology : JASN,* 18**,** 2937-44.

ZHAI, X. Y., THOMSEN, J. S., BIRN, H., KRISTOFFERSEN, I. B., ANDREASEN, A. & CHRISTENSEN, E. I. 2006. Three-dimensional reconstruction of the mouse nephron. *Journal of the American Society of Nephrology : JASN,* 17**,** 77-88.

ZHAO, B., ZHANG, C., FORSTEN-WILLIAMS, K., ZHANG, J. & FANNON, M. 2010. Endothelial Cell Capture of Heparin-Binding Growth Factors under Flow. *PLoS Comput Biol,* 6**,** e1000971.

ZHAO, M., BAI, H., WANG, E., FORRESTER, J. V. & MCCAIG, C. D. 2004. Electrical stimulation directly induces pre-angiogenic responses in vascular endothelial cells by signaling through VEGF receptors. *Journal of Cell Science,* 117**,** 397-405.

ZHONG, X., DESILVA, T., LIN, L., BODINE, P., BHAT, R. A., PRESMAN, E., POCAS, J., STAHL, M. & KRIZ, R. 2007. Regulation of secreted Frizzled-related protein-1 by heparin. *The Journal of biological chemistry,* 282**,** 20523-33.

ZIGMOND, S. H. 1996. Signal transduction and actin filament organization. *Current opinion in cell biology,* 8**,** 66-73.

11 Appendix I: Publications

Original Paper

nephron
Experimental
Nephrology

Nephron Exp Nephrol 2012;121:e79–e85
DOI: 10.1159/000345514

Received: May 15, 2012
Accepted: October 23, 2012
Published online: December 7, 2012

An Improved Method of Renal Tissue Engineering, by Combining Renal Dissociation and Reaggregation with a Low-Volume Culture Technique, Results in Development of Engineered Kidneys Complete with Loops of Henle

C-Hong Chang Jamie A. Davies

University of Edinburgh Centre for Integrative Physiology, Edinburgh, UK

Key Words
Embryonic kidney · Reaggregates · Tissue engineering · Low-volume culture · Loop of Henle

Abstract
Background: Tissue engineering of functional kidney tissue is an important goal for clinical restoration of renal function in patients damaged by infectious, toxicological, or genetic disease. One promising approach is the use of the self-organizing abilities of embryonic kidney cells to arrange themselves, from a simply reaggregated cell suspension, into engineered organs similar to fetal kidneys. The previous state-of-the-art method for this results in the formation of a branched collecting duct tree, immature nephrons (S-shaped bodies) beside and connected to it, and supportive stroma. It does not, though, result in the significant formation of morphologically detectable loops of Henle – anatomical features of the nephron that are critical to physiological function. ***Methods:*** We have combined the best existing technique for renal tissue engineering from cell suspensions with a low-volume culture technique that allows intact kidney rudiments to make loops of Henle to test whether engineered kidneys can produce these loops. ***Results:*** The result is the formation of loops of Henle in engineered cultured 'fetal kidneys', very similar in both morphology and in number to those formed by intact organ rudiments. ***Conclusion:*** This brings the engineering technique one important step closer to production of a fully realistic organ.

Introduction

The primary goal of renal tissue engineering is to construct an organ that resembles the natural kidney as closely as possible [1–4]. One strategy for achieving this is to exploit the capacity of renal cells for self-organization.

Two years ago, Unbekandt and Davies [5] invented a method to recapitulate the early stages of organotypic renal structure from simple suspensions of isolated embryonic renal cells. Because the cell suspension was obtained by dissociation of early (E11.5, 'T-bud stage') embryonic mouse kidneys, the method was called the 'dissociation-reaggregation technique'. In its basic form, it produced immature nephrons arranged around ureteric bud tissue, but the ureteric bud cells were arranged as a multitude of small ureteric buds/collecting duct trees rather than as one single coherent collecting duct tree system, and there-

KARGER

Fax +41 61 306 12 34
E-Mail karger@karger.ch
www.karger.com

1660–2129/12/1214–0079$38.00/0

Accessible online at:
www.karger.com/nee

C.-Hong Chang
University of Edinburgh Centre for Integrative Physiology
Hugh Robson Building
Edinburgh EH8 9XB (UK)
E-Mail c.chang-19@sms.ed.ac.uk

fore failed to reproduce a key feature of normal renal anatomy [5, 6]. The 'nephrosphere' technique developed by Lusis and colleagues [7] in the same year did not include collecting ducts at all, so suffered from an even more severe version of this problem.

To resolve this limitation, Ganeva et al. [6] developed a serial dissociation and reaggregation system. They first used the original dissociation and reaggregation system to make reaggregates with multiple, small ureteric buds. They then manually isolated one of these small reaggregated ureteric buds and combined it with fresh disaggregated and reaggregated mesenchyme: the result was development of immature nephrons that were arranged around one, highly-branched ureteric bud/collecting duct system. This was a good reflection of the structure of mouse embryonic kidneys at about 13 days' gestation.

As normal kidneys mature, from about 14 days of mouse development [8], they develop distinct cortical and medullary zones. Bowman's capsules, proximal tubules and distal tubules are restricted to the cortex, while the medulla consists of collecting ducts and loops of Henle, elements of the nephron that extend radially inwards from the cortex. This arrangement is vital for normal physiology, particularly the recovery of water (which depends on loops of Henle making the medullary interstitium very hypertonic compared to normal body fluids). Any useful system for renal tissue engineering must therefore be able to reproduce this feature. The standard, Trowell-screen culture methods used for development of existing dissociation-reaggregation methods do not support efficient development of loops of Henle, even when they are used to culture normal, intact kidney rudiments. There is therefore neither positive nor reliable negative evidence about the potential for reaggregated kidneys to organize themselves to produce realistic corticomedullary zonation or loops of Henle.

A recently published novel culture method, based on growing rudiments on silicone-bounded glass slides with extremely low volumes of medium (just tens of microlitres), allows an intact kidney isolated directly from an E11.5 embryo to develop organotypic corticomedullary zonation with loops of Henle over the course of 7–10 days [9]. In this short report, we combine the idea of tissue engineering, from cell suspensions by the serial dissociation-reaggregation method, with the low-volume culture method for corticomedullary zonation. The result is the production, from cell suspensions, of kidneys with distinct cortical and medullary zones and with loops of Henle extending radially inwards. This marks a further step towards engineering a realistic fetal kidney from simple suspensions of cells, and provides a potential path by which renal stem cells could be used to make kidney rudiments for clinical applications.

Materials and Methods

Organ Culture

The main method is depicted diagrammatically in figure 1. Kidney rudiments were obtained from E11.5 CD1 mouse embryos (morning of plug check considered to be E0.5) by manual dissection in Eagle's minimum essential medium (MEM) with Earle's salts (Sigma cat. # M5650). For whole-kidney conventional (Trowell screen) culture, they were placed on a 5-μm Isopore membrane filter (Millipore cat. # TMTP02500) supported by a stainless steel grid in a 3.5-cm culture dish at the gas-medium interface. The medium was Kidney Culture Medium (KCM): Eagle's MEM (Sigma cat. # M5650) with 10% fetal bovine serum (Invitrogen cat. # 10108165) and 1% penicillin/streptomycin (Sigma cat. # P4333), as described by Unbekandt and Davies [5]. For the low-volume culture system, we followed the method described in Sebinger et al. [9]. The cone shape 'A' silicon ring (Sarstedt cat. # 94.6077.434) was attached to a 22 × 22 mm glass coverslip (VWR International cat. # 631-0125) and the reaggregates were placed in the centre of it in 85 μl of KCM.

Tissue Engineering by Reaggregation

E11.5 embryonic kidneys from CD1 mice were dissected in MEM (Sigma cat. # M5650). The kidney rudiments were then dissociated enzymatically and reaggregated exactly as described in Unbekandt and Davies [5]. They were cultured in KCM on Isopore filters supported by metal grids as described above. For the first 24 h, the ROCK inhibitor, 1.25 μM glycyl-H1152-dihydrochloride (Tocris batch # 1A/93503), was added to KCM. This medium was then replaced with drug-free KCM for the remaining 3–4 days of culture, as described [5]. After this first incubation, single ureteric bud cysts were isolated from the whole-kidney reaggregates by manual dissection. Dissociated fresh metanephric mesenchyme was isolated as described by Ganeva et al. [6]; briefly, 10–15 kidneys were incubated in 2× trypsin/EDTA (Sigma cat. # T4174) in MEM for 2 min at 37°C and quenched in KCM. Following this, the mesenchymes were peeled away from the ureteric bud. The mesenchymes were collected in a 500-μl tube, dissociated by gentle pipetting and reaggregated by centrifugation at 3,000 rpm for 2 min in a microcentrifuge. The reaggregated ureteric buds from the dissociation-reaggregation experiment were combined, singly, with reaggregated fresh mesenchymes on a membrane filter in the conventional culture system. They were then cultured for 1–2 days in KCM; during this time, they became solid enough to manipulate. They were removed from their filters and transferred to the low-volume culture system. They were incubated for a further 5–7 days (so to a total of 6–9 days from application of mesenchyme to bud cyst), medium being changed every 2 days.

Immunohistochemistry

Tissues were fixed using cold methanol initially at –20°C and allowed to warm up towards room temperature during the 15-min fixation. They were rinsed in PBS for 30 min at room temperature.

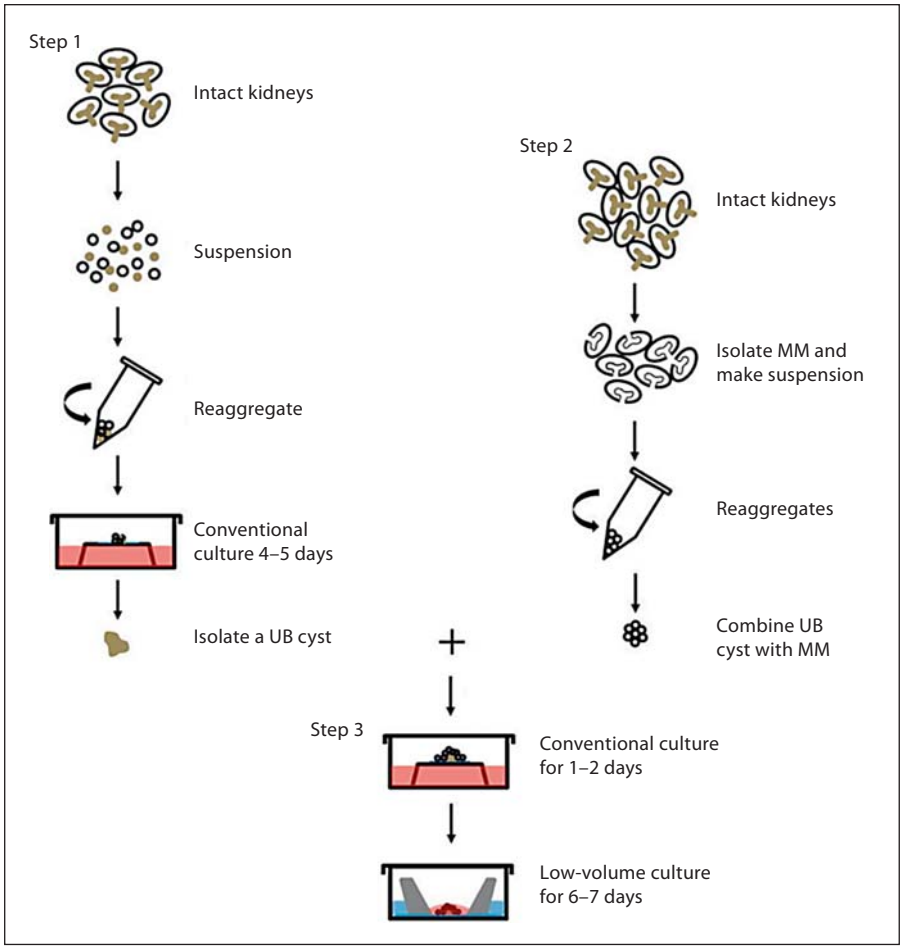

Fig. 1. Schematic description of the method to incubate the reaggregated kidney cells in the conventional and low-volume culture system.

Primary antibodies applied to the tissues were diluted 1:100 in PBS and applied overnight at 4°C; primary antibodies were mouse anti-calbindin (Abcam cat. # ab9481), mouse anti-pan cytokeratin (Sigma cat. # C2562), chicken anti-laminin (Abcam cat. # ab14055), rabbit anti-laminin (Sigma cat. # L9393), and rabbit anti-human Tamm-Horsfall glycoprotein (Bioquote cat. # bt-590). The next day, tissues were washed for a few hours in PBS and secondary antibodies were applied overnight at 4°C. Secondary antibodies were goat FITC anti-chicken (Abcam cat. # ab97134), goat FITC anti-mouse (Sigma cat. # F2012) and goat TRITC anti-rabbit (Sigma cat. # T6778), and were applied at 1/100 in PBS. Finally, tissues were washed in PBS for a few hours. Those grown on filters in Trowell culture were mounted, still on their pieces of filter, between two 22 × 64 mm coverslips that had 22 × 22 mm coverslips sandwiched between them at their ends as spacers, to keep the longer coverslips apart and prevent the samples being crushed: the whole assembly was sealed with nail varnish (Portobello Pink, Rimmel) and mounted loosely on a microscope slide so that the coverslip assembly could be inverted if the filter-and-kidney combination happened to be upside down. These samples were viewed on a Zeiss Axioscope epifluorescence microscope. Organs and reaggregates grown in the low-volume system were viewed using a Zeiss Axiovert epifluorescence microscope.

Identification and Counting of Loops of Henle

Loops of Henle were identified and counted primarily by morphological criteria because the existence of an actual *loop* (rather than mere expression of marker genes, some of which appear in the S-shaped body before real loops form) has greater physiological relevance: see Results and Discussion. Anti-laminin staining (see above) was used to trace the shapes of all tubules. The criterion used to define the presence of an LoH, and to count them, was the existence of a tube that was bent sharply back on itself like a hair grip (US: 'bobby pin'), extending from the mid-portion of a nephron. The straight part of the tube had to be more than a tubule diameter in length before it was considered to be a bona fide loop of Henle (in practice, they were much longer). As an additional test, immunostaining for Tamm-Horsfall glycoprotein was used in some experiments to confirm that the morphologically identified loops do indeed express this loop of Henle marker in the expected manner (they do – see Results and Discussion). Counting was done using a low-power image of the whole kidney and using high-power views to confirm loop morphology as shown in figures 2–4.

We also recorded whether loops of Henle extended towards the middle of the kidney. To do this, two lines were drawn on an image: one ran along the long axis of the loop itself and the other,

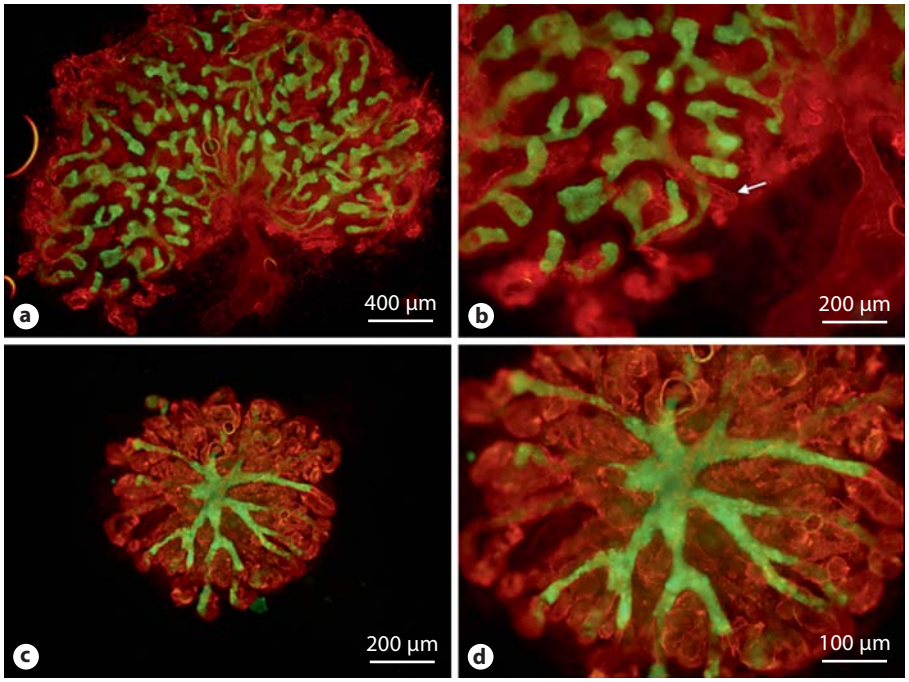

Fig. 2. In 10 days of conventional Trowell-screen culture, both intact kidneys (**a**, **b**) and kidneys engineered (**c**, **d**) through serial reaggregation produce an organotypic arrangement of nephrons around a single collecting duct tree, but there is little sign of development of loops of Henle (one rare example is arrowed in **b**. Green shows the ureteric bud marker, calbindin-D-28k, and red the basement membrane marker, laminin.

radius line, ran from the centre of the kidney to and beyond the tip of the loop ('centre of the kidney' defined as the first branching point of the collecting duct system). The angle between the axis of the loop and the radius line beyond the tip was then measured, to assess how accurately the loop of Henle was orientated radially towards the centre of the kidney: perfect radial alignment would yield an angle of zero. Where the angle was less than 45°, the loop was counted as extending towards the centre ('centripetal').

Results and Discussion

The aim of the work described here is to produce morphologically detectable and correctly positioned loops of Henle. We emphasize development of a proper loop morphology, rather than just presence of early Loop of Henle gene expression markers in the central section of an S-shaped body, because the function of the loop of Henle depends critically on its anatomy: just having marker expression with no extending loop would not be physiologically useful. The principal criterion used to define the presence of a LoH was therefore the existence of a tube, bent sharply back on itself like a hair grip (US: 'bobby pin'), extending from the mid-portion of a nephron. Immunostaining for Tamm-Horsfall glycoprotein was used as an additional confirmation that the criterion for identifying loops of Henle described above does correlate with expression of this marker (see below).

As has been described before [10], intact kidneys in conventional organ culture produced well-branched collecting duct trees that had nephrons developing next to them and connecting with them (fig. 2a, b). Even after 10 days of culture, there was little evidence of morphologically detectable loops of Henle: on average, only a mean of 1.4 ($\sigma = 0.74$) formed per culture, and those that could be found tend to be very short. An example of one of these rare loops is arrowed in figure 2b. Kidneys engineered by serial reaggregation from cell suspensions, by the method in figure 1, and cultured conventionally, also produced nephrons arranged around a well-branched collecting duct system (fig. 2c, d) but, again, loops of Henle were rare, with a mean number per culture of 1.0 ($\sigma = 1.4$). There was no significant difference between the number of these loop rudiments produced in intact and engineered kidneys cultured conventionally on Trowell screens ($p = 0.65$ by two-tailed t test).

To overcome this restriction, we used the low-volume culture method of Sebinger et al. [9]. For intact kidneys, this technique was used exactly as published. For serial reaggregates, the combination of a ureteric bud cyst from the first reaggregation (fig. 1, step 1) with fresh mesenchyme (from fig. 1, step 2) was cultured conventionally for 1–2 days before being transferred to the low-volume culture system (fig. 1, step 3). This period of conventional culture before low-volume culture had to be used be-

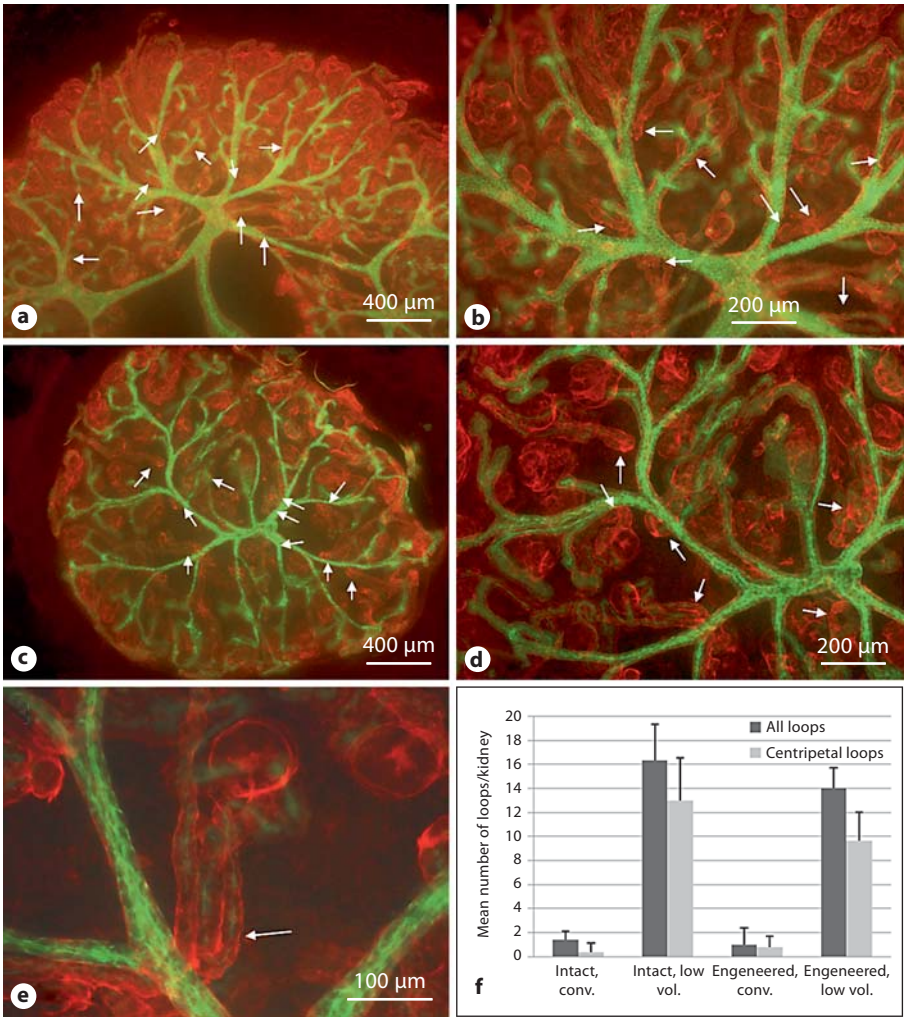

Fig. 3. In low-volume culture, kidneys engineered by series reaggregation form loops of Henle like those formed by intact kidneys in low-volume culture. **a** A low-power view of an intact kidney in low-volume culture. The arrows point to positions of developing loops of Henle, identified by examination of higher magnification images. **b** An example of a higher magnification image, with loops of Henle marked with arrows (the arrows point at the loops and have nothing to do with the orientation of the loops). **c** A low-power view of a kidney engineered by serial reaggregation in low-volume culture. Again, the arrows point to developing loops of Henle, identified by examination of higher magnification images. **d**, **e** Examples of successively higher magnification images, with loops of Henle marked with arrows. **f** The average total number of loops of Henle per kidney formed in each method, and the average number of loops that extend radially inwards (heading towards the first ureteric branch with less than a 45° error): these are called 'centripetal', i.e. centre-seeking, on the graph). Intact kidneys were cultured for 10 days and serial reaggregates for 2 days of conventional culture (from final aggregation of UB cyst with fresh MM) followed by 6 days of low-volume culture. Error bars show standard deviation; p values are given in the main text; the groups contained 8, 6, 4 and 3 cultures, respectively. Green shows the ureteric bud marker, calbindin-D-28k, and red the basement membrane marker, laminin.

cause the low-volume culture method requires an organ rudiment to be placed in a specific place (the centre, where the medium is at its shallowest so that surface tension presses down on the tissue [9]). This accurate placement was not possible until reaggregation had proceeded far enough to make a solid 'tissue' that could be manipulated by pipette.

Intact kidneys behaved in the low-volume culture system exactly as has been described before [9]. The organ rudiments spread over a large area and formed a well-branched collecting duct tree (fig. 3a, b). Under these culture conditions, loops of Henle could be seen; a mean of 16.3 (σ = 3.0) per culture, some long and extended and some shorter but still identifiable: examples of both can be seen, arrowed, in the higher magnification view of the sample of figure 3a that is presented in figure 3b. This increase in loop production was highly significant (p = 0.00004 by a two-tailed t test). Most (95 of 98: 97%) loops extended correctly towards the middle of the kidney ('centripetally', defined for measurement purposes as heading towards the first ureteric branch with an error of less than $\pm$45°).

Kidneys engineered by serial reaggregation, preincubated in conventional culture for 2 days and then transferred to low-volume culture, also spread over a large area and formed a well-branched collecting duct system (fig. 3c, d). Except for the fact that the intact kidneys had an overall polarity arising from the ureteric bud entry point while the engineered ones had no unique entry point and therefore showed radial symmetry, these engineered organs were difficult to distinguish from their intact counterparts (compare fig. 3c with fig. 3a). Importantly, under these culture conditions the engineered kidneys produced morphologically identifiable loops of

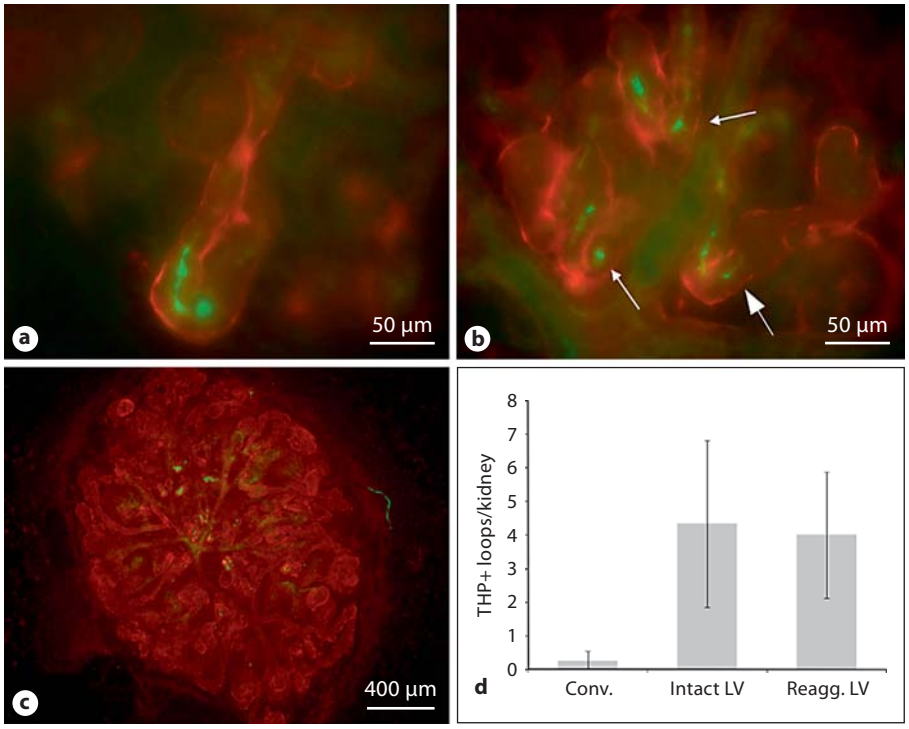

Fig. 4. THP expressed loops were shown in the intact and engineered kidneys in the low-volume system. **a** An intact kidney cultured in the low-volume system, with a loop of Henle (arrow) marked with U-shaped adluminal expression of THP (green), the basement membrane again being stained for laminin (red). **b** A similarly stained image of a serial reaggregate kidney, with several loops visible (arrows; the arrow with the larger head marks a loop, the bend of which can clearly be seen as such in this plane of focus). **c** A low-power view to demonstrate the specificity of anti-THP for loops of Henle (i.e. absence of stain in other parts of the kidney). **d** The average number of THP-expressing loops of Henle per kidney formed in each method (error bars = standard error of the mean). Intact kidneys were cultured for 9 days and serial reaggregates for 2 days of conventional culture followed by 6 days of low-volume culture.

Henle, which can be seen in figure 3c and more easily in the successively higher magnification views, figure 3d and e. Quantitatively, the engineered kidneys produced a mean of 14.0 ($\sigma = 1.73$) morphologically identifiable loops per culture. This was highly significantly different from loop production in conventional culture ($p = 0.0005$ by a two-tailed t test). Encouragingly, it was not significantly different from the performance of intact kidneys in low-volume culture (a two-tailed t test yields $p = 0.19$; no significant difference). Once again, most (40 of 42: 95%) loops were orientated towards the centre of the kidney. The quantitative behaviour of kidneys and engineered kidneys in these culture systems, with respect to Loop of Henle formation, is shown in figure 3f.

To confirm morphological identification of loops of Henle, we examined the expression of Tamm-Horsfall protein (THP), which is expressed strongly in the ascending limb of the mature loop of Henle [11, 12]. In intact kidneys and in serial reaggregates, THP expression could be seen in the growing loops of Henle (fig. 4a–c). It is striking to note that, in these early kidneys (both intact and engineered), THP expression is particularly strong near the bend of the growing loop. THP expression begins a little after loop emergence, which means that some shorter morphologically defined loops did not express THP. Nevertheless, counting only the THP-positive loops shows the same pattern (fig. 4d): very few in conventional culture and significantly more ($p = 0.02$ by two-tailed t test) in low-volume cultures of intact and engineered kidneys. Again, there was no significant difference ($p = 0.90$ by two-tailed t test) between the numbers in intact and engineered.

The development of loops of Henle brings engineered kidneys an important step closer to being properly representative of kidneys that have developed normally in vivo. Essentially, it makes the anatomical development of the epithelial tubules very similar to that found in a normal late-gestation fetal murine kidney. Important remaining steps include the introduction of properly patterned and integrated vascular and nervous systems.

Acknowledgements

We thank David Sebinger, Mathieu Unbekandt, Veronika Ganeva and Peter Hohenstein for helpful advice. This work was funded in part by the NC3Rs.

References

1 Rosines E, Sampogna RV, Johkura K, Vaughn DA, Choi Y, Sakurai H, Shah MM, Nigam SK: Staged in vitro reconstitution and implantation of engineered rat kidney tissue. Proc Natl Acad Sci USA 2007;104:20938–20943.

2 Perin L, Da Sacco S, De Filippo RE: Regenerative medicine of the kidney. Adv Drug Deliv Rev 2011;63:379–387.

3 Davies JA: Self-organization as a tool in mammalian tissue engineering; in Winslet-Gendebien S (ed): Regenerative Medicine. Intech, 2011, pp 261–274.

4 Steer DL, Nigam SK: Developmental approaches to kidney tissue engineering. Am J Physiol Renal Physiol 2004;286:F1–F7.

5 Unbekandt M, Davies JA: Dissociation of embryonic kidneys followed by reaggregation allows the formation of renal tissues. Kidney Int 2010;77:407–416.

6 Ganeva V, Unbekandt M, Davies JA: An improved kidney dissociation and reaggregation culture system results in nephrons arranged organotypically around a single collecting duct system. Organogenesis 2011;7:83–87.

7 Lusis M, Li J, Ineson J, Christensen ME, Rice A, Little MH: Isolation of clonogenic, long-term self-renewing embryonic renal stem cells. Stem Cell Res 2010;5:23–39.

8 Little MH, Brennan J, Georgas K, Davies JA, Davidson DR, Baldock RA, Beverdam A, Bertram JF, Capel B, Chiu HS, Clements D, Cullen-McEwen L, Fleming J, Gilbert T, Herzlinger D, Houghton D, Kaufman MH, Kleymenova E, Koopman PA, Lewis AG, McMahon AP, Mendelsohn CL, Mitchell EK, Rumballe BA, Sweeney DE, Valerius MT, Yamada G, Yang Y, Yu J: A high-resolution anatomical ontology of the developing murine genitourinary tract. Gene Expr Patterns 2007;7:680–699.

9 Sebinger DD, Unbekandt M, Ganeva VV, Ofenbauer A, Werner C, Davies JA: A novel, low-volume method for organ culture of embryonic kidneys that allows development of cortico-medullary anatomical organization. PLoS One 2010;5:e10550.

10 Saxen L: Organogenesis of the Kidney. Cambridge, Cambridge University Press, 1985.

11 Tamm I, Horsfall FL: Characterization and separation of an inhibitor of viral hemagglutination present in urine. Proc Soc Exp Biol Med 1950;74:106–108.

12 Vyletal P, Bleyer AJ, Kmoch S: Uromodulin biology and pathophysiology – an update. Kidney Blood Press Res 2010;33:456–475.

Pediatr Nephrol
DOI 10.1007/s00467-013-2579-4

REVIEW

Engineering kidneys from simple cell suspensions: an exercise in self-organization

Jamie A. Davies · C-Hong Chang

Received: 28 May 2013 / Revised: 28 June 2013 / Accepted: 12 July 2013

Abstract Increasing numbers of people approaching and living with end-stage renal disease and failure of the supply of transplantable kidneys to keep pace has created an urgent need for alternative sources of new organs. One possibility is tissue engineering of new organs from stem cells. Adult kidneys are arguably too large and anatomically complex for direct construction, but engineering immature kidneys, transplanting them, and allowing them to mature within the host may be more feasible. In this review, we describe a technique that begins with a suspension of renogenic stem cells and promotes these cells' self-organization into organ rudiments very similar to foetal kidneys, with a collecting duct tree, nephrons, corticomedullary zonation and extended loops of Henle. The engineered rudiments vascularize when transplanted to appropriate vessel-rich sites in bird eggs or adult animals, and show preliminary evidence for physiological function. We hope that this approach might one day be the basis of a clinically useful technique for renal replacement therapy.

Keywords Tissue engineering · Adaptive self-organization · Transplantation · Angiogenesis · Organ culture

Clinical need for renal tissue engineering

Renal disease is a serious and increasing problem all over the developed world. A combination of congenital kidney diseases, acute chemical damage (including pharmacological), infection and damage from chronic diseases such as diabetes and idiopathic hypertension mean that a large number of people reach end-stage renal disease (ESRD) [1]. Two common treatments exist: dialysis to maintain life and, for more fortunate patients, transplantation of a functional kidney. There is, however, a serious shortage of transplantable kidneys: the waiting list is around 7,000 people in the UK alone. This creates an urgent need for new developments in preventing renal damage in the first place, in regenerating damaged kidney tissue in situ and in engineering new transplantable kidneys when endogenous kidney function cannot be saved. This review focuses on the last of these needs.

A full-scale adult kidney is an anatomically complicated structure that contains >60 cell types [2]. Engineering a new one is therefore unlikely to be easy. Different research groups currently take one of three broad approaches: (1) direct construction by printing, (2) repopulation of decellularised matrix and (3) construction of simple kidney progenitors intended to mature in a host. So far, although the idea of printing a kidney has been talked about within the research community and in more public platforms [3], the spatial resolution and cellular complexity required is beyond existing technologies. Repopulating a decellularised matrix is more promising. It still requires a decellularised donor kidney, but in a postmortem condition, this could be far worse than the minimum required for living transplant. It also requires a source of adult kidney cells to perform the repopulation, so is not exactly a solution to transplant waiting lists, although conceivably a patient's own remaining cells from a damaged kidney may be persuaded to multiply enough to colonize the matrix of a good one. So far, the best experiments with decellularisation have succeeded in at least limited repopulation and better filtration than achieved by decellularised matrix alone [4]. There is still a long way to go from here to acceptable functionality.

The idea of using stem cells to engineer 'foetal kidneys' that can be grafted into a host to grow and mature in situ is the only one of these approaches that needs neither cells nor matrix from an adult kidney. Therefore, it might in principle be a way of escaping the restrictions of waiting lists. This method, too, has a very long way to go before it is clinically

J. A. Davies (✉) · C.-H. Chang
University of Edinburgh, Edinburgh, Scotland, UK
e-mail: jamie.davies@ed.ac.uk

Published online: 30 August 2013

practical, but this approach is the subject of the rest of this review.

Overview of the engineering-then-maturation approach

There are essentially three steps to the 'engineering-then-maturation' approach (Fig. 1). The first is to generate renogenic (kidney-producing) stem cells from a patient's own induced pluripotent stem cells (iPS) cells or some other convenient stem cell source. The second is to engineer a foetal kidney from the simple suspension of stem cells that would be obtained from cultures. The third is to graft the engineered rudiment in a way that promotes its maturation and function. Each of these stages presents quite different problems and requires a different set of skills.

The first problem, that of differentiating embryonic (ES) or iPS cells into renogenic stem cells is often called reprogramming, although the term is poorly chosen because the aim is not to alter the natural developmental programme in the genome, but, rather to move cells to the kidney-producing part of it. Several groups have made progress with this: One approach uses specific exogenous growth factors to mimic the succession of signals that cells would receive in their progress from inner cell mass via mesoderm and intermediate mesoderm to metanephrogenic mesoderm or ureteric bud [5]. Another approach uses culture in a niche. A third approach works by directly transfecting the cells with appropriate transcription factors [6]. Each of these approaches remains a work in progress, but production of stem cells with some apparently renogenic characteristics has been achieved, albeit with low efficiency [6, 7].

Even when the problem of making renogenic stem cells has been solved, a culture of stem cells is not a kidney. A critical step is therefore the development of a technique that enables tissue engineering a small, properly organised kidney. Our work has been directed towards this step, and a technique for performing it is the main focus of the rest of this review. Before discussing this specific step in detail, however, it is worth considering the feasibility of 'downstream' techniques for transplantation of the engineered foetal kidneys into adult hosts. Experiments on grafting embryonic kidneys into adults began in the 1940s and included grafting to the omentum [8], into the eye [9, 10] and subcutaneously [11]. In rats, E15 foetal kidneys transplanted into uninephrectomised or pregnant adult hosts grew and became vascularised; between 17 and 21 days later, it was possible to connect their ureters to that of the host [12]. As these foetal kidneys continued to mature, they produced urine, although with only about 6 % of normal glomerular filtration rate [13]: for comparison, haemodialysis of humans provides the equivalent of about 10 % normal filtration rate. If the remaining adult kidney was removed, the transplants functioned well enough to produce a modest prolongation of host life—not enough to be clinically useful, but perhaps enough to indicate that these existing experiments provide a foundation on which better techniques might be constructed [13].

The hope of the engineering-then-maturation approach is that the three critical steps, each currently being tackled almost in isolation from the other two, can be refined and then connected to complete a pathway from stem cells to functional, transplanted, engineered rudiment.

Development of a renal tissue engineering technique: the stem cell reaggregation approach

Embryonic kidneys develop almost autonomously: even when removed from the rest of the embryo and cultured in simple media, intact organ rudiments will develop essentially organotypically (except for a lack of blood vessels) to produce nephrons arranged around and connected to a branched collecting duct system [14, 15]. When first isolated from the embryo, the organ rudiments consist of two stem cell types—ureteric bud and metanephrogenic mesenchyme—which will each later produce further cell types. Clearly, these cells and the communication loops between them [16] are capable of sufficient adaptive self-organisation [17] to arrange them-

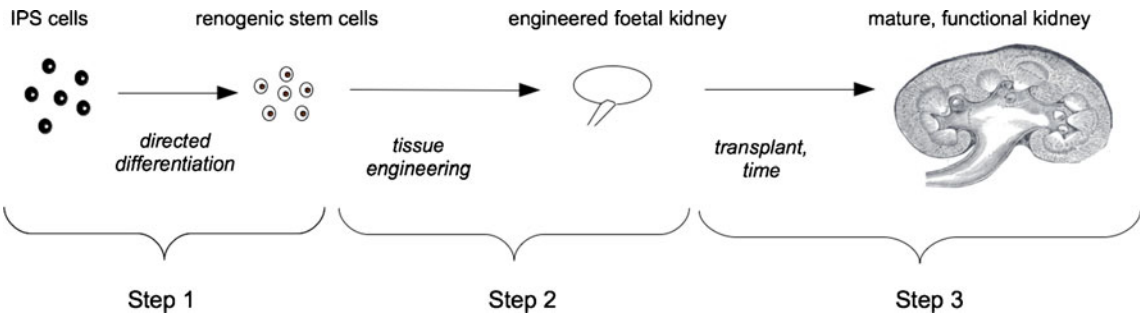

Fig. 1 Overview of the engineering-then-maturation approach. *Step 1* is the production of renogenic stem cells from induced pluripotent stem cells (iPS) cells (or any other stem cell easily obtainable from a patient). *Step 2*, the main topic of this review, is the construction of an engineered foetal kidney from these stem cells. *Step 3* is transplantation of the engineered rudiment and subsequent maturation to physiological maturity in the host

selves into a foetal organ without detailed external signals and even to make an appropriately unusually shaped organ to fit an unusually constrained environment. A trivial example of this plasticity, familiar to many in the field, is the ability of kidneys to grow flat on a filter instead of three-dimensionally in an embryo. Coming from a research background with a theoretical interest in self-organising systems, we reasoned from known communication loops that the self-organising ability of the cells may be sufficiently high to work even when their original anatomical relationships have been erased. This is the abstract basis of the stem cell reaggregation approach.

Because there is so far no reliable way of producing significant numbers of renogenic stem cells as pure populations from ES, iPS or mesenchymal stem cells (MSCs), we began by harvesting E10.5 mouse kidneys and dissociating them into simple cell suspensions. These suspensions are a simulation of what we hope will, one day, be available from a reliable iPS-to-renogenic stem cell process: it has never been our intention to engineer human kidneys for clinical use from suspensions of human fetal cells for obvious ethical reasons.

Simply bringing suspensions of mixed ureteric bud and metanephrogenic mesenchymal cells together by centrifuging them into a random aggregate does not result in development of renal structures: instead, the cells die. This cell death is not surprising: suspending the cells removes them from their natural cell–cell and cell–matrix contacts. In general, when untransformed cells lose these contacts, they die by a type of programmed cell death called anoikis [18], probably a valuable safety mechanism for eliminating cells that are erroneously placed during natural development. A quite different line of research in the laboratory, on the role of the cytoskeleton in ureteric bud branching [19], indicated that inhibiting the rho-dependent-kinase (ROCK) strongly inhibited elective cell death that is a normal feature of metanephric development [20]. Incubation of reaggregated suspensions of renogenic stem cells with ROCK-inhibiting drugs suppressed anoikis and promoted survival but interfered dramatically with subsequent morphogenesis, as might be expected from the effects of ROCK inhibition on intact kidneys [19]. An improved technique, which used ROCK-inhibiting drugs to protect reaggregates for their first 24 h and then replaced them with simple media, was much more successful [21]. Over the next few days, the reaggregates formed many small, branching ureteric bud tree-lets, which induced early nephron formation in the surrounding mesenchyme. By morphology and gene expression, the development of these nephrons was normal, and they connected to the ureteric bud tree-lets (Fig. 2a).

Arranging the kidney around one collecting duct system

The problem with the simple reaggregation system described above is that it produces many small collecting duct tree-lets rather than a single connected tree that could be joined to a ureter. Clearly, a kidney made in this way, even if it could be connected to the blood system, would not be useful because the filtrate would have nowhere to go. Also, at a more subtle level, there would be no clear corticomedullary organisation. Formation of multiple small collecting duct tree-lets is inherent in the manner in which the system is assumed to work, as ureteric bud cells aggregate together to make multiple small clumps that cannot be expected to join because growing ureteric bud branches show mutual repulsion (Davies et al., unpublished data).

A method by which to engineer kidneys arranged around a single collecting duct system was developed by us [22] using a serial culture method. The first step is a basic reaggregation culture to produce a ‘kidney’ with many small ureteric bud

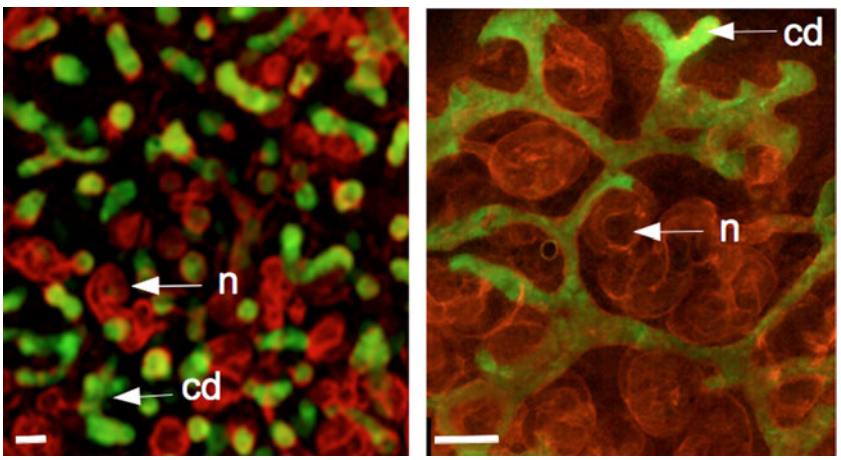

Fig. 2 Engineered renal tissues produced by single (*left panel*) and serial (*right panel*) reaggregation. Each contains nephrons (*n*: *red*) and collecting ducts (*cd*: *green*); in the single reaggregation system, the organ is disorganised because there are many collecting duct tree-lets rather than one tree. The serial reaggregation system generates a kidney organised around a single collecting duct tree. These micrographs are ‘spare’ images from data sets described in our earlier publications [21, 22]

tree-lets, as above. One of these is then isolated and surrounded by a fresh suspension of metanephrogenic mesenchymal cells. The result is ramification of the tree-let into a single collecting duct tree and conversion of metanephrogenic mesenchymal cells into cap mesenchyme, nephrons and stroma in the usual manner, with nephrons connecting to the collecting duct system (Fig. 2b). Under appropriate culture conditions that favour corticomedullary zonation in intact kidney rudiments, these serial reaggregates show a distinct outer cortex and inner medulla and medullary extension of loops of Henle [23].

Connecting to a blood supply

Reaggregated kidneys, as with intact kidney rudiments cultured in incubators filled with 5 % carbon dioxide (CO_2) in air, show little or no development of a vascular system. This is a problem for tissue engineering for the purposes of regenerative medicine, the main physiological function of a kidney is to filter blood: normal adult human kidneys receive about 20 % of cardiac output. Clearly, some way has to be found to connect the nephrons of engineered kidneys to flowing blood.

The metanephrogenic mesenchyme of kidney rudiments contains endogenous endothelial progenitors even though they do not differentiate well in normal culture. Endothelial differentiation can be encouraged by incubation in very low oxygen, but this results in large masses of endothelial cells rather than organised vessels [24]. If a kidney rudiment is cultured with an external source of vessels that are capable of angiogenesis, for example the chorioallantoic membrane (CAM) of a bird egg, it is capable of attracting exogenous blood vessel branches and thereby gaining a blood supply [25, 26]. When such grafts are made from one strain or species into another, it is possible to determine that blood vessels are in fact derived from both graft and host, generally the larger vessels being host-derived and the smaller ones coming from the graft's own mesenchyme [27]. Presumably, the incoming exogenous vessels somehow stimulate differentiation of endogenous endothelial progenitors, though the biology of this is not understood.

Whatever the underlying organising mechanisms, the ability of kidney rudiments to acquire a vascular system when placed near host vessels offers a possible method for equipping cell-derived reaggregate kidneys with a functional blood supply. Grafting them on chick CAM (Fig. 3a) results in ingrowth of host vessels (Fig. 3b) and formation of glomerulus-type structures in the graft (Fig. 3c).

First functional tests

It has been known for some years that foetal kidneys transplanted into adult hosts can organise a blood supply, grow and show some physiological activity [13]. Logically, if the engineered foetal kidneys really are like their natural counterparts, they should behave the same way. We adapted the methods used in foetal kidney transplantations to assess the ability of engineered reaggregated kidneys to function in a mammalian host. Integration with the host vasculature happened efficiently only when the reaggregates were presoaked in vascular endothelial growth factor (VEGF), a known stimulant of angiogenesis [28]. When VEGF was used, however, host vessels entered the grafted engineered kidney. Injected fluorescently labelled albumen crossed from the blood system to enter the urinary space and was recovered by proximal tubule cells [29]. On a positive note, this implies that fluid flow from vessels to urinary space is taking place, presumably through glomeruli, and that at least some proximal reuptake function is normal. On the other hand, a well-constructed glomerulus should not allow major flow of molecules as large as albumin across it. In the system used, quantitative measurement was not possible, so the physiological quality of the engineered, grafted kidneys remains unclear with respect to filtration, recovery or concentration.

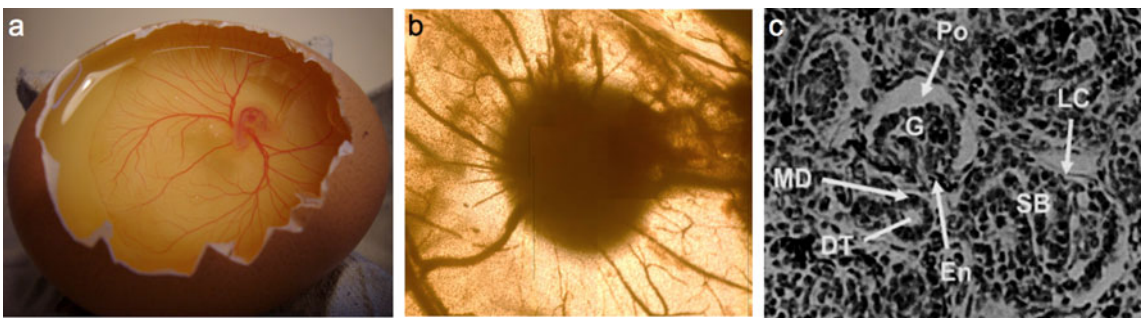

Fig. 3 Vascularisation of engineered kidney rudiments on chick chorioallantoic membrane (*CAM*). **a** The CAM itself. **b** Chick vessels entering an engineered kidney rudiment (the *dark object, centre*). **c** A section through such a kidney: present are S-shaped body-stage (*SB*) nephrons and more mature nephrons that have Bowman's capsules with glomeruli (*G*) and a lower cleft (*LC*) consisting of podocytes (*Po*) and endothelial cells (*En*). As in normal nephrons, the distal tubule (*DT*) approaches the glomerular entrance, where it makes a macula densa (*MD*)

Prospects

From the point of view of tissue engineering with a view to transplantation, the most pressing needs are to: (1) investigate how much engineered kidneys can grow and mature after grafting, (2) establish the physiological parameters of the engineered kidneys and (3) find a way of obtaining renogenic stem cells from a patient (for example, by partly differentiating iPS cells).

Given the similarity between engineered foetal kidneys and real ones, existing programmes of research and development on transplantation of foetal kidneys might be expected to improve the prospects for transplanted kidneys, even if such programmes are not specifically aimed at doing this. There are already some encouraging results from transplantation of foetal kidneys to large animals instead of rodents. E28 pig kidney to adult pig transplants, for example, show growth and production of new nephrons while in the host [30, 31]. Likely areas for development include finding better sites for engraftment, protection of immature kidneys from adult blood pressure (something likely to be a problem in humans, even if it is not in rodents), and possibly developing ways to engraft many kidneys into one host so they can share the physiological load. Identifying humoral changes that take place on unilateral nephrectomy and during pregnancy, both of which are already known to encourage growth of grafted kidney rudiments, may also be useful.

Testing the physiological function of engineered kidneys is difficult in the context of a mammalian host. It may be better to return to the chick CAM system, in which the kidney is plumbed in to a pumped blood supply powered by the chick embryo heart. This system is highly accessible for injection of tracer molecules or drugs into the blood supply and to sampling from the collecting duct system. This would allow measurement of filtration rates, cutoff, concentration of filtrate, osmolarity of the medullary stroma etc.

The problem of obtaining renogenic stem cells may turn out to be the most frustrating, or it may fall quickly. The reaggregate system offers a highly valuable tool for stem cell biologists because it provides a clear test for renogenic activity. In particular, it is possible to mix marked candidate stem cells with the embryo-derived kidney stem cells and then to test whether they contribute to making a chimeric engineered organ [20, 32]. This has already been used to test the abilities of some suspected stem cells with results that are, frankly, disappointing compared with the abilities of cells straight from the kidney-forming part of the embryo [33–36]. Any cells that do pass this test would be highly promising candidates for practical use.

The entire approach of tissue engineering as a means of restoring renal function will not be helpful in all patients with ESRD: it will probably be most suited to diseases involving gradual but unstoppable renal degeneration, which allow time for maturation of a graft in a still healthy body rather than for fast-onset, acute failure. Even if it can be made to work as well as hoped, engineering new organs will probably be just one technique amongst many, including conventional transplantation and, hopefully, stem-cell-based regeneration in situ.

Conflict of Interest The authors declare that they have no personal financial stake in this work or any other conflicting interests.

References

1. Steenkamp R, Castledine C, Feest T, Fogarty D (2011) UK renal registry 13th annual report (December 2010): Chapter 2: UK RRT prevalence in 2009: National and centre-specific analyses. Nephron Clin Pract 119(Suppl 2):c27–52
2. Little MH, Brennan J, Georgas K, Davies JA, Davidson DR, Baldock RA, Beverdam A, Bertram JF, Capel B, Chiu HS, Clements D, Cullen-McEwen L, Fleming J, Gilbert T, Herzlinger D, Houghton D, Kaufman MH, Kleymenova E, Koopman PA, Lewis AG, McMahon AP, Mendelsohn CL, Mitchell EK, Rumballe BA, Sweeney DE, Valerius MT, Yamada G, Yang Y, Yu J (2007) A high-resolution anatomical ontology of the developing murine genitourinary tract. Gene Expr Patterns 7:680–699
3. Atala A (2010) Growing New Organs. TED lecture available at https://www.ted.com/talks/anthony_atala_growing_organs_engineering_tissue.html
4. Song JJ, Guyette JP, Gilpin SE, Gonzalez G, Vacanti JP, Ott HC (2013) Regeneration and experimental orthotopic transplantation of a bioengineered kidney. Nat Med. doi:10.1038/nm.3154
5. Kim D, Dressler GR (2005) Nephrogenic factors promote differentiation of mouse embryonic stem cells into renal epithelia. J Am Soc Nephrol 16(12):3527–3534
6. Hendry CE, Little MH (2012) Reprogramming the kidney: A novel approach for regeneration. Kidney Int 82(2):138–146
7. Harari-Steinberg O, Pleniceanu O, Dekel B (2011) Selecting the optimal cell for kidney regeneration: Fetal, adult or reprogrammed stem cells. Organogenesis 7(2):123–134
8. Waterman AJ (1940) Growth and differentiation of kidney tissue of the rabbit embryo in omental grafts. J Morphol 67:369–385
9. Runner MN (1946) The development of the mesonephros of the albino rat in intraocular grafts. J Exp Zool 103:305–319
10. Grobstein C, Parker G (1958) Epithelial tubule formation by mouse metanephrogenic mesenchyme transplanted in vivo. J Nat Cancer Inst 2:107–119
11. Barakat TI, Harrison RG (1971) The capacity of fetal and neonatal renal tissues to regenerate and differentiate in a heterotopic allogenic subcutaneous tissue site in the rat. J Anat 110:393–407
12. Hammerman MR (2007) Transplantation of renal primordia: renal organogenesis. Pediatr Nephrol 22(12):1991–1998
13. Rogers SA, Lowell JA, Hammerman NA, Hammerman MR (1998) Transplantation of developing metanephroi into adult rats. Kidney Int 54:27–37
14. Rienhoff WF (1922) Development and growth of the metanephros or permanent kidney in chick embryos. Johns Hopkins Hosp Bull 33:392–406
15. Grobstein C (1953) Inductive epithelio-mesenchymal interaction in cultured organ rudiments of the mouse. Science 118:52–55

16. Davies JA, Fisher CE (2002) Genes and proteins in renal development. Exp Nephrol 10:102–113
17. Davies JA (2013) Mechanisms of morphogenesis, 2nd edn. Elsevier Academic Press, London
18. Frisch SM (2000) Anoikis. Methods Enzymol 322:472–479
19. Michael L, Sweeney DE, Davies JA (2005) A role for microfilament-based contraction in branching morphogenesis of the ureteric bud. Kidney Int 68(5):2010–2018
20. Coles HS, Burne JF, Raff MC (1993) Large-scale normal cell death in the developing rat kidney and its reduction by epidermal growth factor. Development 118(3):777–784
21. Unbekandt M, Davies JA (2010) Dissociation of embryonic kidneys followed by reaggregation allows the formation of renal tissues. Kidney Int 77(5):407–416
22. Ganeva V, Unbekandt M, Davies JA (2011) An improved kidney dissociation and reaggregation culture system results in nephrons arranged organotypically around a single collecting duct system. Organogenesis 7(2):83–87
23. Chang CH, Davies JA (2012) An improved method of renal tissue engineering, by combining renal dissociation and reaggregation with a low-volume culture technique, results in development of engineered kidneys complete with loops of henle. Nephron Exp Nephrol 21(3–4):e79–85
24. Loughna S, Yuan HT, Woolf AS (1998) Effects of oxygen on vascular patterning in Tie1/LacZ metanephric kidneys in vitro. Biochem Biophys Res Commun 18;247(2):361–366
25. Atterbury RR (1923) Development of the metanephric anlage of chick in allantoic grafts. Am J Anat 31:409–436
26. Sariola H, Timpl R, von der Mark K, Mayne R, Fitch JM, Linsenmayer TF, Ekblom P (1984) Dual origin of glomerular basement membrane. Dev Biol 101(1):86–96
27. Woolf AS (1998) Loughna S. Origin of glomerular capillaries: Is the verdict in? Exp Nephrol 6:17–21
28. Ferrara N (2009) VEGF-A: A critical regulator of blood vessel growth. Eur Cytokine Netw 20(4):158–163
29. Xinaris C, Benedetti V, Rizzo P, Abbate M, Corna D, Azzollini N, Conti S, Unbekandt M, Davies JA, Morigi M, Benigni A, Remuzzi G (2012) In vivo maturation of functional renal organoids formed from embryonic cell suspensions. J Am Soc Nephrol 23(11):1857–1868
30. Rogers SA, Talcott M, Hammerman MR (2003) Transplantation of pig metanephroi. ASAIO J 49:48–52
31. Hammerman MR (2009) Xenotransplantation of pancreatic and kidney primordia-where do we stand? Transpl Immunol 21(2):93–100
32. Davies JA, Unbekandt M, Ineson J, Lusis M, Little MH (2012) Dissociation of embryonic kidney followed by re-aggregation as a method for chimeric analysis. Methods Mol Biol 886:135–146
33. Siegel N, Rosner M, Unbekandt M, Fuchs C, Slabina N, Dolznig H, Davies JA, Lubec G, Hengstschläger M (2010) Contribution of human amniotic fluid stem cells to renal tissue formation depends on mTOR. Hum Mol Genet 19(17):3320–3331
34. Kuzma-Kuzniarska M, Rak-Raszewska A, Kenny S, Edgar D, Wilm B, Fuente Mora C, Davies JA, Murray P (2012) Integration potential of mouse and human bone marrow-derived mesenchymal stem cells. Differentiation 83(3):128–137
35. Rak-Raszewska A, Wilm B, Edgar D, Kenny S, Woolf AS, Murray P (2012) Development of embryonic stem cells in recombinant kidneys. Organogenesis 8(4):124–136
36. Ranghini E, Mora CF, Edgar D, Kenny SE, Murray P, Wilm B (2013) Stem cells derived from neonatal mouse kidney generate functional proximal tubule-like cells and integrate into developing nephrons in vitro. PLoS One 8(5):e62953